



M Ű E G Y E T E M 1 7 8 2

BUDAPEST UNIVERSITY OF TECHNOLOGY AND ECONOMICS  
DEPARTMENT OF STRUCTURAL MECHANICS

Róbert K. NÉMETH • Attila KOCSIS

# The Hidden Beauty of Structural Dynamics

Budapest, 2013

ISBN 978-963-313-088-9



(Updated version, August 7, 2015)

# Contents

<b>Contents</b>	<b>i</b>
<b>List of figures</b>	<b>iv</b>
<b>List of tables</b>	<b>v</b>
<b>Preface</b>	<b>vii</b>
<b>1 Dynamics of single- and multi-DOF systems</b>	<b>1</b>
1.1 Vibration of SDOF systems . . . . .	1
1.1.1 Derivation of the equation of motion . . . . .	2
1.1.2 General solution of the homogeneous ODE . . . . .	4
1.1.3 Particular solution of the non-homogeneous ODE with harmonic forcing	7
1.1.4 Support vibration of SDOF systems . . . . .	11
1.2 General forcing of SDOF systems . . . . .	13
1.2.1 <i>Duhamel's</i> integral . . . . .	13
1.2.2 Numerical solution of the differential equation . . . . .	15
1.3 Vibration of MDOF systems . . . . .	18
1.3.1 Equation of motion of MDOF systems . . . . .	18
1.3.2 Free vibration of MDOF systems . . . . .	21
1.3.3 Harmonic forcing of MDOF systems . . . . .	24
1.3.4 Approximate solution of the generalized eigenvalue problem (Ritz- Rayleigh's method) . . . . .	31
1.4 Summation theorems . . . . .	39
1.4.1 <i>Dunkerley</i> theorem . . . . .	39
1.4.2 <i>Southwell</i> theorem . . . . .	42
1.4.3 <i>Föppl–Papkovitch</i> theorem . . . . .	44
<b>2 Dynamics of slender continua</b>	<b>46</b>
2.1 Longitudinal vibration of prismatic bars . . . . .	47
2.1.1 Differential equation of motion . . . . .	48
2.1.2 Free longitudinal vibration . . . . .	49
2.1.3 Forced longitudinal vibration: kinematic loading . . . . .	51
2.2 Free torsional vibration of prismatic shafts . . . . .	53

## CONTENTS

---

2.3	Shear vibration of prismatic beams . . . . .	54
2.3.1	Differential equation of motion . . . . .	56
2.3.2	Free vibration of a fixed-free beam . . . . .	57
2.4	Transverse vibration of prismatic beams . . . . .	59
2.4.1	The equation of transverse vibration . . . . .	60
2.4.2	Free vibration of prismatic beams . . . . .	62
2.4.3	Forced vibration of prismatic beams . . . . .	72
<b>3</b>	<b>Dynamics of planar frame structures</b>	<b>80</b>
3.1	Static matrix displacement method . . . . .	81
3.1.1	Nodal decomposition of planar frames . . . . .	81
3.1.2	Global and local reference systems, transformations . . . . .	82
3.1.3	Elementary static stiffness matrix in the local reference system . . . . .	85
3.1.4	Equivalent nodal forces . . . . .	92
3.1.5	Different end conditions of beam members . . . . .	95
3.1.6	Transformation of the elementary stiffness matrix . . . . .	99
3.1.7	Compilation of the total stiffness matrix . . . . .	100
3.1.8	Boundary conditions . . . . .	100
3.2	Dynamic stiffness matrix of frame structures . . . . .	103
3.2.1	Diagonally lumped mass matrix . . . . .	103
3.2.2	Dynamic stiffness matrix . . . . .	104
3.3	Consistent mass matrix . . . . .	112
3.3.1	Different end conditions of beam members . . . . .	113
3.3.2	Accuracy with the consistent mass matrix . . . . .	115
3.3.3	Additional masses . . . . .	116
3.4	Equivalent dynamic nodal loads . . . . .	117
3.5	Support vibration of MDOF systems . . . . .	123
3.5.1	Prescribed motion of DOFs . . . . .	123
3.5.2	Harmonic support vibration . . . . .	124
3.5.3	Support motion due to earthquake . . . . .	126
3.6	Real modal analysis, internal forces . . . . .	127
3.6.1	Real modal analysis . . . . .	127
3.6.2	Internal forces . . . . .	130
3.7	Partial solution of the generalized eigenvalue problem . . . . .	133
3.8	Second order effects . . . . .	141
3.8.1	Rotational inertia . . . . .	141
3.8.2	Static normal force . . . . .	144
<b>4</b>	<b>Damping in structural dynamics</b>	<b>148</b>
4.1	Steady-state vibration of viscously damped systems . . . . .	149
4.1.1	Harmonic excitation of damped MDOF systems . . . . .	149
4.2	Proportional damping . . . . .	152
4.2.1	The <i>Kelvin-Voigt</i> material . . . . .	152
4.2.2	Stiffness of a damped beam made of <i>Kelvin-Voigt</i> material . . . . .	152

## CONTENTS

---

4.2.3	Real modal analysis of proportionally damped systems . . . . .	155
4.3	Rate-independent damping . . . . .	158
4.3.1	Real modal analysis in case of rate-independent damping . . . . .	158
4.3.2	Direct solution of rate-independently damped systems . . . . .	159
4.4	Equivalent rate-independent damping . . . . .	160
4.4.1	Quasi-modal analysis for equivalent rate-independent damping . . . . .	161
4.5	Dynamics of soil . . . . .	161
4.5.1	Differential equation of the equivalent soil bar . . . . .	162
4.5.2	Static stiffness of the soil model . . . . .	163
4.5.3	Dynamic stiffness of the soil model . . . . .	164
4.6	Numerical solution of the matrix differential equation . . . . .	172
4.6.1	Newmark method . . . . .	172
<b>5</b>	<b>Earthquake analysis</b> . . . . .	<b>175</b>
5.1	Introduction to earthquakes . . . . .	175
5.2	Response spectrum of SDOF systems . . . . .	177
5.2.1	Response functions . . . . .	177
5.2.2	Response spectrum . . . . .	180
5.2.3	Design spectrum . . . . .	181
5.3	Response spectrum of MDOF systems . . . . .	183
5.3.1	Modal analysis . . . . .	183
5.4	Earthquake analysis . . . . .	186
5.4.1	Inelastic response of structure . . . . .	186
5.4.2	Time history analysis . . . . .	187
<b>A</b>	<b>Additional derivations and notes</b> . . . . .	<b>190</b>
A.1	Travelling-wave solution for the free vibration of a prismatic bar . . . . .	190
A.2	Static shape functions . . . . .	193
A.3	Stiffness matrices of beam members . . . . .	194
A.4	Elementary dynamical stiffness matrix using purely dynamical shape functions . . . . .	196
A.5	Consistent mass matrices of beam members . . . . .	197
A.6	Few trigonometric identities . . . . .	199
A.7	Damped SDOF system solved with a different approach . . . . .	200
A.7.1	Sine . . . . .	200
A.7.2	Cosine . . . . .	201
A.7.3	Sine and cosine . . . . .	202
A.7.4	Quasi-periodic loading . . . . .	203
A.8	Damped MDOF systems solved using complex algebra . . . . .	205
A.8.1	Inverse of a complex square matrix . . . . .	205
A.8.2	Application forced MDOF systems . . . . .	206

# List of Figures

1.1	Common examples of single-degree-of-freedom structures . . . . .	2
1.2	A mass-spring-damper model . . . . .	3
1.3	Typical time-displacement diagrams of free vibration of a damped, elastic supported SDOF system . . . . .	5
1.4	Responses of a damped SDOF system to a harmonic excitation . . . . .	9
1.5	Support vibration of an undamped mechanical system . . . . .	11
1.6	Response factor of the elongation of the spring as a function of the ratio of the forcing and natural frequencies due to a harmonic support vibration . . . . .	13
1.7	General time-dependent forcing . . . . .	14
1.8	Explanation of the Cauchy-Euler method and the second order Runge-Kutta method . . . . .	16
1.9	Explanation of the finite difference approximation of velocity and acceleration using secant lines . . . . .	17
1.10	Examples of multi-degree-of-freedom structures . . . . .	18
1.11	Free body diagrams of the model shown in Figure 1.10 (c) . . . . .	19
1.12	Two-storey frame structure with rigid floors . . . . .	20
1.13	Vibration of a three-storey frame structure with rigid interstorey girders and flexible columns . . . . .	28
1.14	Mode shapes of the three-storey structure of Fig. 1.13 corresponding to the natural circular frequencies . . . . .	30
1.15	Model of a 10-storey frame structure with rigid interstorey girders and elastic columns . . . . .	34
1.16	Rayleigh quotient of Problem 1.3.1 . . . . .	38
1.17	A clamped rod with its mass concentrated at three points of equal distances . . . . .	41
1.18	Model of a rigid roof supported by a linear spring and by two clamped, massless rods of equal length . . . . .	43
1.19	A straight, massless rod carrying a lumped mass at its free top end, connected to a fixed hinge and a rotational spring at the bottom . . . . .	45
2.1	Sketch of (a) a prismatic bar subjected to a longitudinal distributed load $q_n(x, t)$ . . . . .	48
2.2	Sketch of an inextensional, unbendable prismatic beam subjected to a transverse, distributed load $q_t(x, t)$ . . . . .	55
2.3	Model of an inextensional and unbendable beam which is elastically clamped at one end and free at the other end . . . . .	58

## LIST OF FIGURES

---

2.4	Sketch of a prismatic beam subjected to a transverse, distributed load $q_t(x, t)$	60
2.5	Common types of supporting modes	63
2.6	Sketch of a prismatic beam subjected to an axial compressive force	70
2.7	Prismatic beam subjected to a harmonic exciting force $F \sin(\omega t)$	75
3.1	Comparing discrete models of beam structures	82
3.2	Local and global reference systems	83
3.3	Model of a frame structure	84
3.4	Sketch of the deformed shape of a fixed-fixed beam $ij$ due to a unit translation of end $i$ along axis $y$ , and the corresponding bending moment diagram	86
3.5	Sketch of the deformed shape of a fixed-fixed beam $ij$ due to a unit rotation of end $i$ , and the corresponding bending moment diagram	89
3.6	Beam $ij$ under a transverse, static, distributed load $q_t(x)$	93
3.7	A beam with its ends $0$ and $\ell$ are elastically connected to the coinciding nodes $i$ and $j$ through linearly elastic springs	95
3.8	Elastically supported node	102
3.9	Sketch of the deformed shape of beam $ij$ due to a harmonic translation of unit amplitude of end $i$ along axis $y$ , and the corresponding bending moment diagram	108
3.10	Sketch of a simple planar frame and the mechanical model for the matrix displacement method	118
3.11	The change of the block structure of the matrix equation of motion during the elimination of the prescribed motion of supports.	125
3.12	Sketch of a fixed-fixed beam and the mechanical model for the matrix displacement method (fixed support model)	135
3.13	Sketch of a fixed-fixed beam and the mechanical model for the matrix displacement method (spring model)	138
3.14	Sketch of the deformed shape of beam $ij$ due to a harmonic translation of unit amplitude of end $i$ along axis $y$ , and the corresponding bending moment diagram	141
3.15	Demonstration of the moment caused by the normal force $S$ on a rotated elementary segment of the beam.	145
4.1	Sketch of the deformed shape of a damped beam and the bending moment diagram due to a dynamic vibration of end $i$ along axis $y$ .	153
4.2	Assumed stress propagation in the equivalent soil bar	161
5.1	Solid and surface waves	177
5.2	Response functions	179
5.3	Concept of response spectrum	181
5.4	The function $\beta(T_0)$ of the pseudo-acceleration response vs. the natural period.	182
5.5	Force-deformation diagram of the linear elastic-plastic material model and structure.	187
5.6	Typical envelope functions of artificial earthquake records.	188
A.1	Rod with fixed-free ends with an initial displacement and the travelling waves	192

# List of Tables

1.1	Harmonic forcing of a three-storey structure. Modal loads, coefficients of resonance, and other parameters . . . . .	30
3.1	The first few natural circular frequencies (in rad/s) of the frame and all the six natural circular frequencies of the approximate models (with the consistent the diagonally lumped mass matrices). . . . .	122
3.2	The first six natural circular frequencies of the frame, the projections of the load vector to the modal shape vectors, and the modal participation factors . . .	130
3.3	The natural circular frequencies of the beam with elastic supports for various spring stiffnesses. . . . .	140
4.1	Equivalent spring stiffness $k_{\text{soil}}^{\text{eq}}$ and damping coefficient $c_{\text{soil}}^{\text{eq}}$ of the soil, assuming a homogeneous elastic half space, corresponding to “low” and “high” forcing frequency $\omega$ . Here $E_c$ is the constrained modulus of the soil, $A_0$ is the area of the rigid plate on the soil surface, $c_n = \sqrt{E_c/\varrho}$ with $\varrho$ being the mass density of the soil, while the characteristic depth $f$ is given by (4.43) for a disk. The velocity of the travelling wave $c_{\text{sd}}$ is computed according to (4.51) . . . . .	168

# Preface

This lecture notes of the MSc course Structural Dynamics is devoted for the civil engineering students of the Budapest University of Technology and Economics. The objective of the course is to introduce the basic concepts of the dynamical analysis of engineering structures. The topics that are covered in this course are equations of motion of single- and multi-degree-of-freedom systems, free and steady-state vibrations, analytical and numerical solution techniques, and earthquake loads on structures. Both continuum and discrete mechanical systems are considered.

In civil engineering practice structures are aimed to be in equilibrium. However, due to continuous disturbances (effects of wind, heat, traffic, movement of the foundations, etc.), the structures undergo vibrations. Some of these motions are slow, allowing us to treat them as a *quasi-static* kinematic load, and to neglect the inertial effect of the mass of the structure. But some of them happen fast enough to exert a significant dynamical impact on the structure. Many of these cases are still handled as a quasi-static load with a proper dynamical factor, but other cases really require the engineers to accomplish dynamical analysis. The goal of the semester is to prepare our students for these tasks.

Dynamics play an important role in many fields of structural engineering. Earthquakes, fast moving trains on bridges, urban traffic generated or machine induced vibrations, etc. Modern materials enable the fabrication of lighter, more flexible structures, where the effects of vibrations can be significantly high. Additionally, investment companies desire cost effective structures, which also tends the engineers towards more accurate computations, which implies dynamical analysis, too.

Not only theory is given in this notes, but there are also many problems solved. The authors hope that these examples help our students to comprehend all the introduced concepts. In these problems the calculations are done following the *care your units* approach. It means that we use a *consistent system of units*, which does not require us to carry the units during the operations. Every number is substituted in the formulae in a common system of units, in SI (International System of Units), hence the results are also obtained in SI.

We offer these notes to our readers under a Creative Commons Attribution-NonCommercial-NoDerivs 3.0 Unported License, in the hope it will help them understand the basics of structural dynamics. Please feel free to share your thoughts about it with us.

Budapest, 29<sup>th</sup> August, 2013



# Chapter 1

## Dynamics of single- and multi-degree-of-freedom systems

In this chapter first we repeat the basics of vibration of elastic structures. The motion of continuous structures is often approximated by the displacements of some of its points. In these models the mass of the structure is concentrated into discrete points. The concentrated masses are assumed to be rigid bodies, and the elasticity and the viscoelasticity of the structure is modeled by massless springs and damping elements, respectively. These models are called *mass-spring-damper* systems.

We introduce the *degree-of-freedom* (DOF) as the number of independent variables required to define the displaced positions of all the masses. If there is only one mass, with one direction of displacement, then we talk about a *single-degree-of-freedom* (SDOF) system. If there are more than one masses, or one mass with more than one directions of displacement, then we have a *multi-degree-of-freedom* (MDOF) system. If we try to describe the deformed shape of a continuous structure with the displacements of all of (infinitely many of) its points, then we use a continuum approach, where there are infinitely many degrees of freedom.

In Section 1.1 we start with the free vibration of SDOF systems, then harmonic forced vibration of SDOF systems, and support vibration of SDOF systems are discussed. Then SDOF systems excited by a general force are studied in Section 1.2. Section 1.3 is devoted for the free vibration of MDOF systems. We also present an approximate method capable to solve the generalized eigenvalue problem occurring in the analysis of MDOF systems. At the end of the chapter, in Section 1.4 we present a few summation theorems useful to approximate the first natural frequency of a structure.

### 1.1 Vibration of single-degree-of-freedom systems

Civil engineering structures are intended in general to be in equilibrium. Despite the common requirements, many of the loading situations result in motion of the structures. The most simple motion occurs when we can describe it by one single space variable.

Examples for these type of dynamical systems are horizontal girders with a significant mass (e.g. a machine, where the mass of the girder can be neglected with respect to the mass of the

machine) (Figure 1.1 (a-b)), frame structures with significant mass on the rooftop (Figure 1.1 (c)), chimneys and water towers (Figure 1.1 (d)), etc..

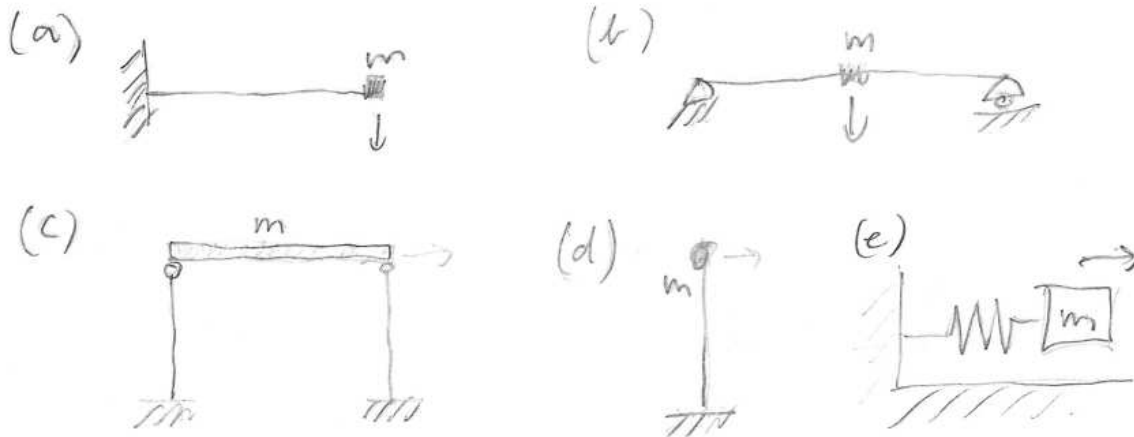


**Figure 1.1:** Common examples of single-degree-of-freedom structures: (a) fixed girder, (b) hinged-hinged girder, (c) single frame with mass on rooftop, (d) chimney or water-tower, and (e) common mechanical model.

The common in the above examples is that any displacement from the equilibrium state results a force pulling the DOF back to the initial state. The simplest mechanical model of this behaviour is the material particle (lumped mass) connected by a linear spring to a rigid wall (Figure 1.1 (e)).

### 1.1.1 Derivation of the equation of motion

If we analyse the motion of a structure caused by a small disturbance, then we can see that in the absence of external forcing the amplitude of the vibration around the original state decreases with the time. This is caused by internal friction in the material and at the connections. Effect of external dampers can be considered as well. The mathematically easiest way to deal with damping is the viscous damping. (In this case the damping force is proportional to the velocity.) The mechanical model of the viscous damping is a *dashpot*. Figure 1.2 (a) shows a damped, elastically supported system with a dashpot of damping coefficient  $c$ , a linear elastic spring of stiffness  $k$ , and a time dependent exciting force  $F(t)$ . Our goal is in general one of the followings:

- to find the displacement function as a function of time
- to find the elongation of the spring as a function of time
- to find the force in the spring or in the dashpot as a function of time
- to find the possible maxima of the above functions

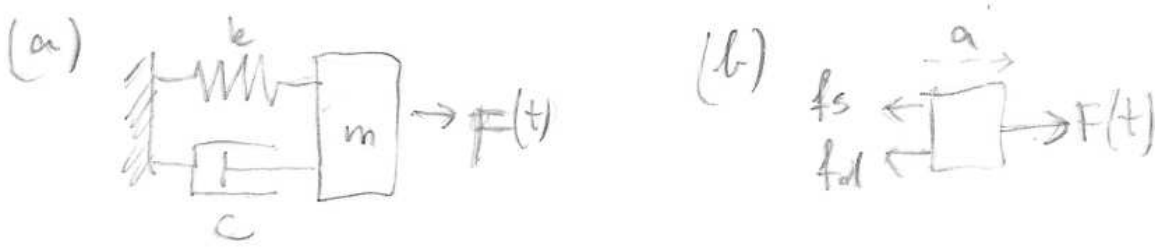


**Figure 1.2:** (a) A mass-spring-damper model: a lumped mass  $m$  is connected to a support through a massless linear spring  $k$  and a massless viscous damper  $c$ . The mass excited by the time dependent force  $F(t)$  undergoing a single-degree-of-freedom vibration. (b) Free body diagram of the mass-spring-damper model.

The free body diagram (FBD) of the mass  $m$  can be seen in Figure 1.2 (b). Newton's second law of motion can be written for the body:

$$F(t) - f_s(t) - f_d(t) = ma(t), \quad (1.1)$$

where  $F(t)$  is the external force,  $f_s(t)$  is the elastic force from the massless spring,  $f_d(t)$  is the damping force from the massless dashpot,  $m$  is the mass and  $a(t)$  is the acceleration. Assuming a linear spring  $f_s(t) = ku(t)$ , where  $k$  is the spring stiffness, and  $u(t)$  is the elongation of the spring. Assuming a viscous damping  $f_d(t) = c\dot{u}(t)$ , where  $c$  is the damping coefficient, and  $\dot{u}(t)$  is the derivative of the elongation  $u(t)$  with respect to time (i.e. it is the elongation-velocity). (The dot over a variable denotes differentiation with respect to time.) The acceleration  $a(t)$  is the second derivative of the displacement of the body with respect to time:  $a(t) = \ddot{x}(t)$ . So the equation of motion is:

$$F(t) - ku(t) - c\dot{u}(t) = m\ddot{x}(t). \quad (1.2)$$

(Note: in many textbook authors write a so called kinetic equilibrium equation using the principle of *d'Alembert* with an inertial force  $f_I = -ma(t)$ . Then, Eq. (1.1) would have the form:  $F(t) - f_s(t) - f_d(t) + f_I(t) = 0$ . In formal calculation it leads to the same result, but during calculations by hand the correct interpretation of the minus sign in the definition of  $f_I$  requires a deep understanding of the concept, at which level writing the classic formula makes no problem. Because of that we will avoid writing kinetic equilibrium equations. )

In most cases we are interested in the internal deformations and the corresponding internal forces of the structures. These are represented in this model by the elongation of the spring, so we have to write the displacement of the body as a function of elongation. If the support is fixed, then these two values are equal ( $x(t) = u(t)$ ) and the same applies to their derivatives ( $\ddot{x}(t) = \ddot{u}(t)$ ). Substituting these into Eq. (1.2) we get:

$$\boxed{m\ddot{u}(t) + c\dot{u}(t) + ku(t) = F(t)}. \quad (1.3)$$

This non-homogeneous, linear, second order ordinary differential equation of constant coefficients describes the motion of the forced vibration of the damped SDOF-system.

For the solution of the differential equation (1.3) we introduce its complementary differential equation:

$$m\ddot{u}(t) + c\dot{u}(t) + ku(t) = 0. \quad (1.4)$$

which is a homogeneous differential equation. The *complete solution* of Eq. (1.3) can be written in the form:

$$u(t) = u_0(t) + u_f(t),$$

where  $u_0(t)$  is the solution of the complementary equation (the index 0 refers to the 0 right hand side of the homogeneous equation), while  $u_f(t)$  is a particular solution of the original, nonhomogeneous equation (the index  $f$  refers to the forcing).

If initial conditions are given (e.g. the displacement and the velocity at a given time), then they must be fulfilled for the sum of  $u_0(t)$  and  $u_f(t)$  with the free parameters occurring in  $u_0(t)$ .

### 1.1.2 General solution of the homogeneous ODE

Eq. (1.4) describes the free vibration of the mechanical system. Since it is a linear, homogeneous ODE with constant coefficients, the solution can be obtained with an ansatz function  $u(t) = e^{\lambda t}$ , which is substituted back in Eq. (1.4) alongside with its derivatives. The result is the quadratic polynomial equation

$$m\lambda^2 + c\lambda + k = 0. \quad (1.5)$$

The roots of the above equation are:

$$\lambda_{1,2} = \frac{-c \pm \sqrt{c^2 - 4mk}}{2m}. \quad (1.6)$$

These roots might be either real or complex valued, depending on the ratio of the system parameters.

- If  $c \geq 2\sqrt{km}$ , the discriminant in Eq. (1.6) is non-negative, thus both  $\lambda_{1,2}$  are negative real numbers, and the solution of Eq. (1.4) is the sum of two exponential function asymptotically approaching zero. (Figure 1.3 (a) shows some typical graphs of this vibration.) We call this damping as heavy damping, the system is an overdamped system. The limit value  $2\sqrt{km}$  is the critical damping  $c_{cr}$ .
- If  $c < 2\sqrt{km}$  (or  $c < c_{cr}$ ), the discriminant is negative, the solution of Eq. (1.5) is a conjugate pair of complex numbers. Using *Euler's* formula ( $e^{ix} = \cos x + i \sin x$ ) the solution of Eq. (1.4) can be rewritten in the form:

$$u_0(t) = e^{-\xi\omega_0 t} (A \cos(\omega_0^* t) + B \sin(\omega_0^* t)), \quad (1.7)$$

where

$$\xi = \frac{c}{2\sqrt{km}} = \frac{c}{c_{cr}}$$

is the *relative damping* coefficient

$$\omega_0^* = \omega_0 \sqrt{1 - \xi^2}$$

is the *natural circular frequency* of the (under)damped system,

$$\omega_0 = \sqrt{k/m}$$

is the *natural circular frequency* of the undamped system with the same mass and stiffness. The parameters  $A$  and  $B$  are two free parameters depending on the initial conditions. (Figure 1.3 (b) shows some typical graphs of this vibration.) We call this case as underdamped system.

The solution Eq. (1.7) is a harmonic term ( $A \cos(\omega_0^*t) + B \sin(\omega_0^*t)$ ) multiplied by an exponential term ( $e^{-\xi\omega_0 t}$ ). The latter one indicates an exponential decay in the oscillatory motion of the body, which can be seen as an exponential envelope of the oscillating harmonic function in Figure 1.3 (b). A higher level of damping has two effect on the motion. First, the exponential decay will be more significant, second, the damped natural circular frequency will be lower.

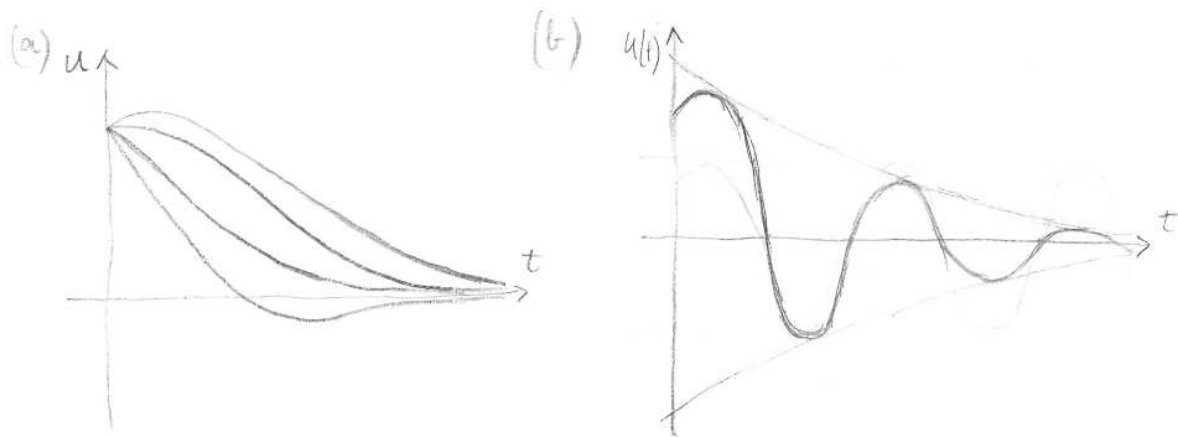


**Figure 1.3:** Typical time-displacement diagrams of free vibration of a damped, elastic supported SDOF system. (a) Overdamped system, no vibration. (b) Underdamped system: harmonic oscillation with the amplitude decaying exponentially.

There are further quantities in use, to describe the vibration of a SDOF system. *Natural cyclic frequency*  $f$  is the number of total oscillations done by the body in a unit time:  $f = \omega_0/(2\pi)$ . The *natural period*  $T_0$  is the time required to make a full cycle of vibration, i.e.  $T_0 = 1/f = 2\pi/\omega_0$ . Both of the above values can be written for the damped system as well, called the damped natural cyclic frequency  $f_D$  and the damped natural period  $T_D$ . They are interrelated to each other with:  $f_D = \omega_0^*/(2\pi)$  and  $T_D = 1/f_D = 2\pi/\omega_0^*$ .

### Logarithmic decrement

Let us analyse the displacements of a mass during its damped free vibration. We have seen, that at a given time instant  $t$  the displacement is (Eq. (1.7)):

$$u_0(t) = e^{-\xi\omega_0 t} (A \cos(\omega_0^*t) + B \sin(\omega_0^*t)).$$

Using the previously introduced damped natural period  $T_D$ , we can write the displacement after a whole period of motion as well:

$$u_0(t + T_D) = e^{-\xi\omega_0(t+T_D)} (A \cos(\omega_0^*(t + T_D)) + B \sin(\omega_0^*(t + T_D))).$$

The ratio of the displacements can be written as:

$$\frac{u_0(t)}{u_0(t + T_D)} = \frac{e^{-\xi\omega_0 t} (A \cos(\omega_0^* t) + B \sin(\omega_0^* t))}{e^{-\xi\omega_0(t+T_D)} (A \cos(\omega_0^*(t + T_D)) + B \sin(\omega_0^*(t + T_D)))}.$$

Since  $T_D$  is the damped period of the motion, the harmonic terms in both time instants have the same value, so we can simplify the above formula as

$$\frac{u_0(t)}{u_0(t + T_D)} = e^{\xi\omega_0 T_D} = e^{(2\xi\pi/\sqrt{1-\xi^2})}. \quad (1.8)$$

This ratio is constant, and depends only on the damping  $\xi$ . Since we did not have any constraint on  $t$ , Eq. (1.8) holds for any two displacements measured in a time distance  $T_D$ . In practice, the natural logarithm of Eq. (1.8) is used for the measurement of damping

$$\vartheta = \ln \frac{u_0(t)}{u_0(t + T_D)} = 2\xi\pi/\sqrt{1-\xi^2}.$$

Here  $\vartheta$  is called the *logarithmic decrement* which is a system property. In typical engineering structures  $\xi \ll 1$ , so the  $\sqrt{1-\xi^2} \approx 1$  approximation can be used:

$$\vartheta = \ln \frac{u_0(t)}{u_0(t + T_D)} \approx 2\xi\pi. \quad (1.9)$$

### Free vibration of undamped systems

The vibration of undamped systems can be derived in a similar way as we did it for the damped system, or we can analyse our damped results in the limit  $c \rightarrow 0$ . According to Eq. (1.3) the differential equation of motion can be written as:

$$m\ddot{u}(t) + ku(t) = F(t).$$

The complementary equation describes the undamped free vibration:

$$m\ddot{u}(t) + ku(t) = 0.$$

The solution of the free vibration is directly obtained from Eq. (1.7) at  $c = 0$  (and  $\xi = 0$ ):

$$u_0(t) = A \cos(\omega_0 t) + B \sin(\omega_0 t).$$

Here  $\omega_0 = \sqrt{k/m}$  is the *natural circular frequency* of the undamped system. The parameters  $A$  and  $B$  can be calculated from the initial conditions. The purely harmonic motion can be rewritten into the form:

$$u_0(t) = C \sin(\omega_0 t + \varphi),$$

with the amplitude of the motion  $C = \sqrt{A^2 + B^2}$  and the phase angle  $\varphi = \arctan \frac{A}{B}$ .

### 1.1.3 Particular solution of the non-homogeneous ODE with harmonic forcing

A simple example for a harmonic excitation force is a rigid body (e.g. a machine) rotating with a constant angular velocity  $\omega$  around an axis which is not going through its center of gravity (COG). The distance between the axis and the center of gravity is called the eccentricity and denoted by  $r_C$ .) The COG of the body undergoes a planar motion on a circular path with an angular velocity  $\omega$ . From kinematics of rigid bodies the acceleration of the COG equals  $a_n = m\omega^2 r_C$ , its direction varies with the motion, its component parallel with an arbitrary chosen, but fixed direction can be written as a harmonic function of time, and the same applies for the net force acting on the rigid body. The opposite of this force acts on the axis of rotation, resulting in a harmonic excitation force on the load bearing structure. (The orthogonal component of the force should be taken into account as well, but the vibration can be prevented by structural constraints, or by applying two well-tuned body rotating in the opposite direction.)

Without loss of generality (for harmonic functions one can translate the time scale to have any other harmonic function with the same frequency and amplitude), we will write the harmonic excitation force in the form:

$$F(t) = F_0 \sin(\omega t).$$

Here  $F_0$  is the amplitude of the force, and  $\omega$  is the circular frequency of the forcing. Substituting this forcing in the right hand side of (1.3) yields:

$$m\ddot{u}(t) + c\dot{u}(t) + ku(t) = F_0 \sin(\omega t). \quad (1.10)$$

To solve Eq. (1.10) we assume that the particular solution is of the form:

$$u_f(t) = u_{f0} \sin(\omega t - \varphi),$$

i.e. it is a harmonic function with the same frequency as the forcing, but with a phase shift of  $\varphi$ . We substitute our ansatz into Eq. (1.10):

$$-m\omega^2 u_{f0} \sin(\omega t - \varphi) + c\omega u_{f0} \cos(\omega t - \varphi) + ku_{f0} \sin(\omega t - \varphi) = F_0 \sin(\omega t).$$

We apply trigonometrical identities for the sums in the sine and cosine functions:

$$\begin{aligned} & -m\omega^2 u_{f0} \sin(\omega t) \cos(-\varphi) - m\omega^2 u_{f0} \cos(\omega t) \sin(-\varphi) + c\omega u_{f0} \cos(\omega t) \cos(-\varphi) \\ & - c\omega u_{f0} \sin(\omega t) \sin(-\varphi) + ku_{f0} \sin(\omega t) \cos(-\varphi) + ku_{f0} \cos(\omega t) \sin(-\varphi) = F_0 \sin(\omega t). \end{aligned}$$

Now we separate the sinusoidal and cosinusoidal parts:

$$\begin{aligned} & u_{f0} \cos(\omega t) (m\omega^2 \sin \varphi + c\omega \cos \varphi - k \sin \varphi) \\ & + u_{f0} \sin(\omega t) (-m\omega^2 \cos \varphi + c\omega \sin \varphi + k \cos \varphi) = F_0 \sin(\omega t). \end{aligned}$$

This equation must hold for any time  $t$ .



- When  $\sin(\omega t) = 0$ , then  $\cos(\omega t) \neq 0$ , so

$$m\omega^2 \sin \varphi + c\omega \cos \varphi - k \sin \varphi = 0$$

must hold, which is true, when

$$\cot \varphi = \frac{k - m\omega^2}{c\omega} = \frac{m\omega_0^2 - \omega^2}{c\omega}, \quad (1.11)$$

with  $0 \leq \varphi \leq \pi$ . (See Figure 1.4 (a) for the dependence of phase angle on the ratio of the forcing and natural frequency.)

- When  $\cos(\omega t) = 0$ , then  $\sin(\omega t) \neq 0$ , so

$$u_{f0} (-m\omega^2 \cos \varphi + c\omega \sin \varphi + k \cos \varphi) = F_0$$

must hold.

We use the identities  $\cos \varphi = \cot \varphi / \sqrt{1 + \cot^2 \varphi}$  and  $\sin \varphi = 1 / \sqrt{1 + \cot^2 \varphi}$  to get

$$u_{f0} \frac{-m\omega^2 \cot \varphi + c\omega + k \cot \varphi}{\sqrt{1 + \cot^2 \varphi}} = F_0$$

and solve the above equation for  $u_{f0}$  using Eq. (1.11):

$$u_{f0} = F_0 \frac{\sqrt{1 + \frac{(k - m\omega^2)^2}{c^2\omega^2}}}{(k - m\omega^2) \frac{k - m\omega^2}{c\omega} + c\omega}.$$

Multiplying both the nominator and the denominator with  $c\omega$  leads to

$$u_{f0} = F_0 \frac{1}{\sqrt{(k - m\omega^2)^2 + c^2\omega^2}} = \frac{F_0}{k} \frac{1}{\sqrt{\left(1 - \frac{m}{k}\omega^2\right)^2 + \frac{c^2}{k^2}\omega^2}}$$

Using the natural circular frequency and the fraction of critical damping coefficient ( $\omega_0 = \sqrt{k/m}$ ,  $\xi = c/(2\sqrt{km})$ ) the solution for  $u_{f0}$  is

$$u_{f0} = \frac{F_0}{k} \frac{1}{\sqrt{\left(1 - \frac{\omega^2}{\omega_0^2}\right)^2 + 4\xi^2 \frac{\omega^2}{\omega_0^2}}}. \quad (1.12)$$

From the above results the particular solution of the differential equation (1.10) of the harmonically forced vibration is:

$$u_f(t) = \frac{F_0}{k} \frac{1}{\sqrt{\left(1 - \frac{\omega^2}{\omega_0^2}\right)^2 + 4\xi^2 \frac{\omega^2}{\omega_0^2}}} \sin \left( \omega t - \operatorname{arccot} \frac{1 - \frac{\omega^2}{\omega_0^2}}{2\xi \frac{\omega}{\omega_0}} \right). \quad (1.13)$$



The complete solution of Eq. (1.10) is the sum of Eq. (1.13) and (1.7):

$$u(t) = \frac{F_0}{k} \frac{1}{\sqrt{\left(1 - \frac{\omega^2}{\omega_0^2}\right)^2 + 4\xi^2 \frac{\omega^2}{\omega_0^2}}} \sin\left(\omega t - \operatorname{arccot} \frac{1 - \frac{\omega^2}{\omega_0^2}}{2\xi \frac{\omega}{\omega_0}}\right) + e^{-\xi\omega_0 t} (A \cos(\omega_0^* t) + B \sin(\omega_0^* t)). \quad (1.14)$$

The second part of Eq. (1.14) becomes very small after a sufficiently long time for any small damping. That part is called the *transient vibration*. The first part, which is equivalent to the particular solution Eq. (1.13), is called the *steady-state* solution of the problem. Since the transient vibration decays exponentially with time, on a long time scale the steady-state vibration determines the dynamics. Usually we are not interested in the phase of the motion, but in the amplitude of the vibration  $u_{f0}$ , given by Eq. (1.12). In that formula the quotient  $F_0/k$  can be regarded as the *static displacement* under a static force  $F_0$  (which is the amplitude of the harmonic forcing). We will refer to it as the static displacement  $u_{st}$ . The static displacement  $u_{st} = F_0/k$  is multiplied by a coefficient in Eq. (1.12), which depends on the damping and on the ratio of the circular frequency of the forcing to the natural circular frequency of the system. We call this quantity as the *response factor*, and denote it by  $\mu$ . Figure 1.4 (b) shows the dependence of the response factor on the ratio of frequencies.

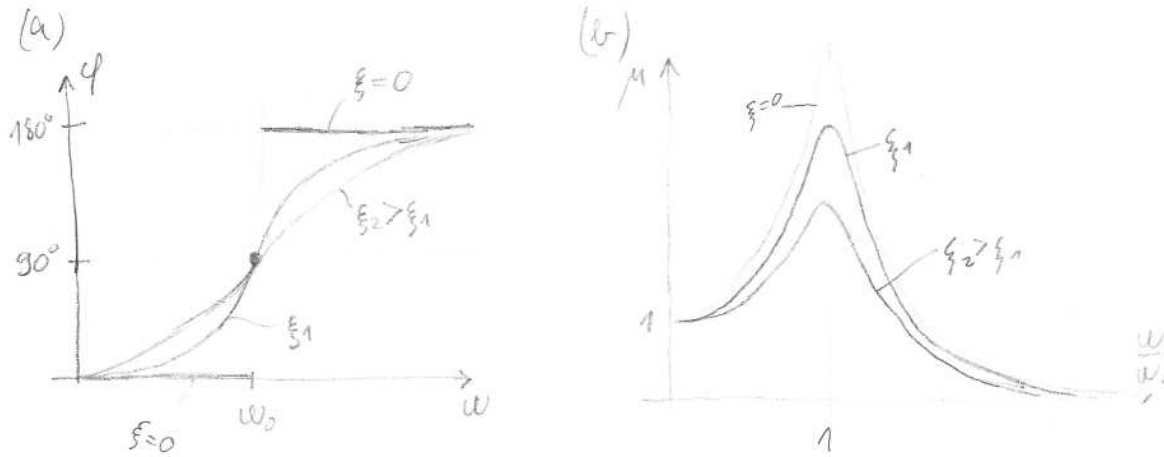


**Figure 1.4:** Responses of a damped SDOF system to a harmonic excitation: (a) phase angle  $\varphi$  as a function of the forcing frequency  $\omega$ , (b) response factor  $\mu$  as a function of the ratio of the forcing and natural frequencies  $\omega/\omega_0$ .

In short, the amplitude of the steady-state vibration can be written as:

$$u_{f0} = u_{st}\mu,$$

where

$$u_{st} = \frac{F_0}{k} \quad (1.15)$$

and

$$\mu = \frac{1}{\sqrt{\left(1 - \frac{\omega^2}{\omega_0^2}\right)^2 + 4\xi^2 \frac{\omega^2}{\omega_0^2}}}. \quad (1.16)$$

Now we further analyse the response factor function  $\mu$ . For small  $\omega/\omega_0$  it is small, but bigger than 1. As  $\omega/\omega_0$  approaches 1 it reaches a maximum. One can derive, that the maximum occurs at  $\omega/\omega_0 = \sqrt{1 - 2\xi^2}$ , but in the practical range of damping  $\xi$  of engineering structures, the difference can be neglected, so in general we can say, that the maximal amplitude is approximately at  $\omega = \omega_0$  with the magnitude  $\mu_{\max} \cong 1/(2\xi)$ . The state when  $\mu$  is maximal is called the *resonance*. For the case, when  $\omega > \omega_0$ , the response factor decreases asymptotically to zero.

The spring force from the steady-state part of the motion can be calculated from the elongation of the spring:

$$F_{S0} = k u_{st} \mu = F_0 \mu,$$

i.e. the amplitude of the excitation force multiplied by the response factor, thus for fast excitation with large  $\omega$  or flexible structure with low  $\omega_0$  the spring force will be small due to the decaying response factor  $\mu$ . But if we are looking for the force transmitted to the base, we also have to take into account the force  $f_D$  in the damping element, which may result higher base forces.

### Effect of zero damping on the phase angle and response factor

The vibration of undamped systems can be derived in a similar way as for the damped system, or we can analyse our damped results in the limit  $c \rightarrow 0$ . In the latter case we can conclude, that the particular solution of the non-homogeneous differential equation (1.10) is a harmonic vibration. The amplitude of the vibration can be calculated from Eq. (1.12) with  $\xi \rightarrow 0$ :

$$u_{f0} = \frac{F_0}{k} \frac{1}{\sqrt{\left(1 - \frac{\omega^2}{\omega_0^2}\right)^2}} = \frac{F_0}{k} \frac{1}{\left|1 - \frac{\omega^2}{\omega_0^2}\right|}.$$

It is the product of the static displacement and the (undamped) response factor (see Fig. 1.4 (b)). In contrast to the damped case, this response factor has an infinite maximum in the state of resonance ( $\omega = \omega_0$ ).

For the phase angle  $\varphi$  we can conclude from Eq. (1.11) that it is zero when  $\omega < \omega_0$ , and it is  $\pi$  when  $\omega > \omega_0$  (see Fig. 1.4 (a)). In the first case the mass moves *in-the-phase* with the excitation force, in the second case the mass moves *out-of-the-phase* with the excitation force. At the resonance state  $\omega = \omega_0$  the phase angle is  $\varphi = \pi/2$ .

### Ideal damping

Analysis of the damped response factor Eq. (1.16) and its derivative with respect to  $\frac{\omega}{\omega_0}$  results that an increasing damping coefficient  $\xi$  decreases the location and the value of the maximum of  $\mu$  (see Fig. 1.4 (b)). If  $\xi$  reaches  $1/\sqrt{2}$ , then the location of the maximum reaches  $\omega = 0$ , and the value of the maximum reaches 1. Further increase of the damping decreases the response factor, but the maximum will be always 1 at  $\omega = 0$ . This damping value  $\xi_{id} = 1/\sqrt{2}$  (or  $c_{id} = \sqrt{2km}$ ) is called the *ideal damping*.

### 1.1.4 Support vibration of SDOF systems

In many cases the support of the structure is not in rest. During an earthquake or because of the noise of traffic the base (which was assumed until now to be in rest) might move, making the structure to vibrate.

In this subsection we will show how to handle the support motion for undamped systems. The steps of the solution would be the same for a damped system as well.

In the case of support vibration we have to modify our mechanical model shown in Fig. 1.2 (a) such that we set the damping to zero ( $c = 0$ ) and apply a support motion  $u_g(t)$  (where the index  $g$  refers to the ground motion). Figure 1.5 (a) shows this model.

If we draw the free body diagram, there is only one force acting on the body from the spring, so we can write Newton's second law of motion based on Figure 1.5 (b) as

$$-f_S(t) = ma(t),$$

or by substituting the spring force  $f_S(t) = ku(t)$  and the acceleration  $a(t) = \ddot{x}(t)$  as

$$-ku(t) = m\ddot{x}(t). \quad (1.17)$$

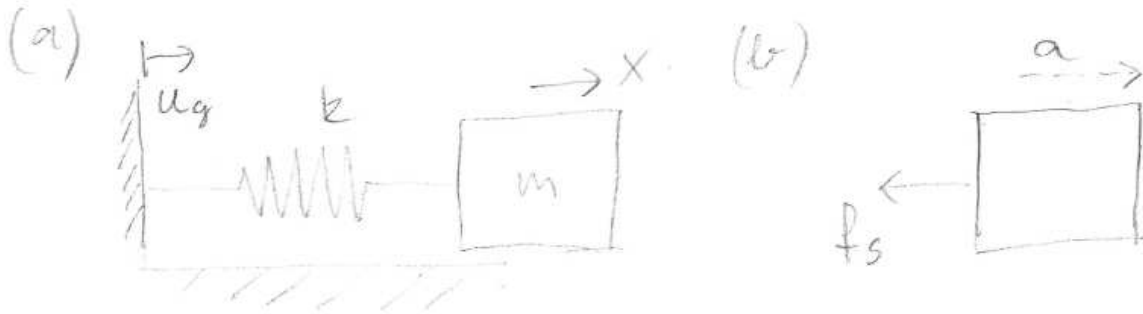


**Figure 1.5:** Support vibration of an undamped system (a) mechanical model, (b) free body diagram

The elongation of the spring is now

$$u(t) = x(t) - u_g(t), \quad (1.18)$$

and the second derivative of the Eq. (1.18) results:

$$\ddot{u}(t) = \ddot{x}(t) - \ddot{u}_g(t). \quad (1.19)$$

One can follow two different approaches.

- Substitution of  $u(t)$  from Eq. (1.18) in Eq. (1.17) leads to

$$-kx(t) + ku_g(t) = m\ddot{x}(t),$$

which is a differential equation for the displacement  $x(t)$  of the body. If we write it in a canonical form

$$m\ddot{x}(t) + kx(t) = ku_g(t) \quad (1.20)$$

one can see, that it is a simple forced vibration.

- Substitution of  $\ddot{x}(t)$  from Eq. (1.19) in Eq. (1.17) implies

$$-ku(t) = m\ddot{u}(t) + m\ddot{u}_g(t),$$

which is a differential equation for the elongation  $u(t)$  of the spring. If we write it in a canonical form

$$m\ddot{u}(t) + ku(t) = -m\ddot{u}_g(t), \quad (1.21)$$

we obtain a simple forced vibration again.

In the next subsections we will show the solutions of the derived differential equations for a harmonic support vibration, i.e.  $u_g(t) = u_{g0} \sin(\omega t)$ .

### Steady-state solution of the elongation of the spring due to a harmonic support motion

To find the solution of Eq. (1.21) we have to substitute the second derivative of  $u_g(t)$

$$\ddot{u}_g(t) = -\omega^2 u_{g0} \sin(\omega t)$$

into Eq. (1.21):

$$m\ddot{u}(t) + ku(t) = m\omega^2 u_{g0} \sin(\omega t).$$

This is the same equation as Eq. (1.10) with  $c = 0$  and  $F_0 = m\omega^2 u_{g0}$ . Therefore, the amplitude of the steady-state solution will be (see Eq. (1.12)):

$$u_{f0} = \frac{m\omega^2 u_{g0}}{k} \frac{1}{\sqrt{\left(1 - \frac{\omega^2}{\omega_0^2}\right)^2}} = \boxed{u_{g0} \frac{\omega^2}{\omega_0^2} \frac{1}{\left|1 - \frac{\omega^2}{\omega_0^2}\right|}}.$$

The amplitude of the elongation  $u(t)$  will be the amplitude of the support vibration multiplied by a response factor and by the square of the ratio of the forcing and natural frequencies. The spring force  $f_S(t)$  is related to the elongation  $u(t)$  of the spring so its amplitude will be:

$$f_S^{max} = ku_{g0} \frac{\omega^2}{\omega_0^2} \frac{1}{\left|1 - \frac{\omega^2}{\omega_0^2}\right|} = f_S^{st} \frac{\omega^2}{\omega_0^2} \frac{1}{\left|1 - \frac{\omega^2}{\omega_0^2}\right|}.$$

Here  $f_S^{st}$  is the static force, which would cause an elongation  $u_{g0}$  in the spring.

Figure 1.6 shows the product of two multipliers ( $\omega^2/\omega_0^2$  and  $1/|1 - \omega^2/\omega_0^2|$ ) as the function of the ratio of the forcing and natural frequencies.

### Steady-state solution of the displacement $x(t)$ for harmonic support vibration

To find the solution of Eq. (1.20) we have to substitute  $u_g(t)$  into Eq. (1.20):

$$m\ddot{x}(t) + kx(t) = ku_{g0} \sin(\omega t).$$

This is the same equation as Eq. (1.10) with  $c = 0$  and  $F_0 = ku_{g0}$ . Thus, the amplitude of the steady-state solution is (see Eq. (1.12)):

$$x_{f0} = \frac{ku_{g0}}{k} \frac{1}{\sqrt{\left(1 - \frac{\omega^2}{\omega_0^2}\right)^2}} = \boxed{u_{g0} \frac{1}{\left|1 - \frac{\omega^2}{\omega_0^2}\right|}}.$$

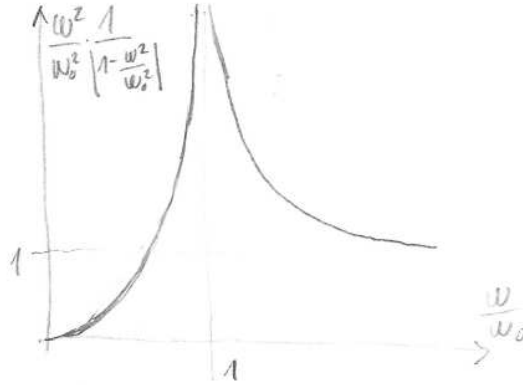


**Figure 1.6:** Response factor of the elongation of the spring as a function of the ratio of the forcing and natural frequencies due to a harmonic support vibration

## 1.2 General forcing of SDOF systems

### 1.2.1 Duhamel's integral

Static (or quasi-static) loads and harmonic forcing represent only a small segment of the possible loads acting on a structure. Although many of the time-dependent loads can be treated as a quasi-static, or a sum of harmonic loads, there are important excitation forms (impact, support vibration due to earthquakes, etc.) where the transient behavior of the structure must be analyzed. For this type of problem the equation of motion Eq. (1.3)

$$m\ddot{u}(t) + c\dot{u}(t) + ku(t) = q(t) \quad (1.22)$$

contains an arbitrary function  $q(t)$  on the right hand side (see Figure 1.7 (a)). We are looking for the particular solution  $u_f(t)$  of Eq. (1.22) for the  $t > 0$  interval, with the assumption that we know the initial displacement and velocity in the time instant  $t = 0$ . We denote these two initial conditions with  $u_f(0) = u^0$  and  $\dot{u}_f(0) = v^0$ . We remind the reader that the solution of a non-homogeneous differential equation always consists of the solution of the complementary equation (the free vibrational part) with free parameters, and a particular solution of the non-homogeneous equation. The free vibration follows the classical scheme we presented in Subsection 1.1.2.

We assumed linear response of the elastic and damping elements ( $k$  and  $c$  are constants), so the differential equation is linear, and the rule of superposition holds. If the excitation force can be written in the form  $q(t) = \sum_{i=1}^N q_i(t)$ , then the particular solution can be expressed as  $u_f(t) = \sum_{i=1}^N u_{fi}(t)$ , where each  $u_{fi}$  is a particular solution of the differential equation

$$m\ddot{u}(t) + c\dot{u}(t) + ku(t) = q_i(t).$$

Let us choose a sufficiently small time interval  $\Delta\tau$  at the time instant  $t = \tau$ , as shown in Figure 1.7 (a), and let us examine the effect of the force  $q(\tau)$  during the interval  $\Delta\tau$  on the displacement  $u_f(t)$ . This specific part of the forcing is shown in Figure 1.7 (b). We denote

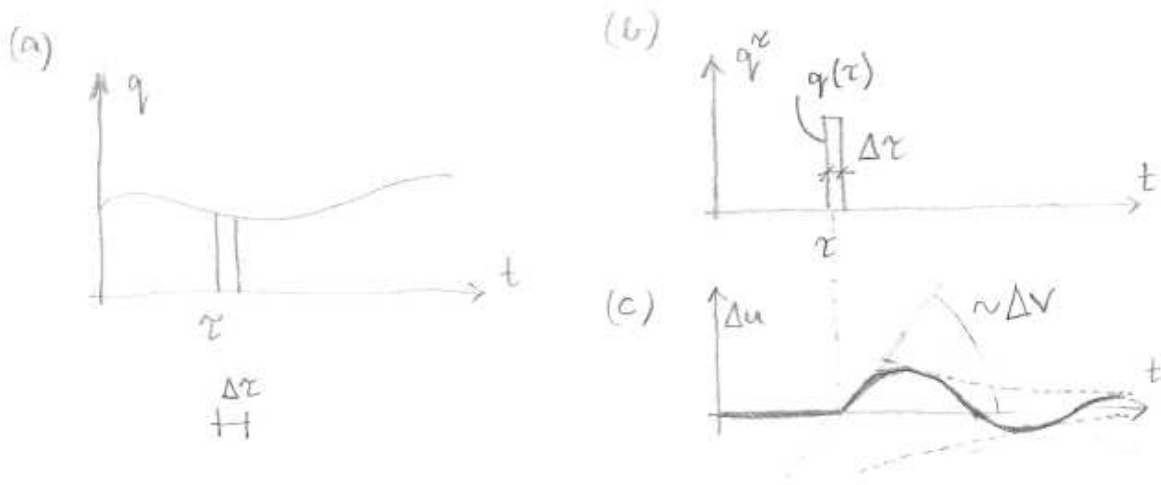


**Figure 1.7:** (a) General time-dependent forcing. (b) Small impulse  $q(\tau)\Delta\tau$  of the forcing. (c) Increment of displacement function from the impulse  $q(\tau)\Delta\tau$ .

the effect of  $q(\tau)$  on  $u_f(t)$  by  $\Delta u(t, \tau)$ . Since  $\Delta\tau$  is small, the change of the force during the interval can be neglected, so the impulse transmitted from the force to the mass is  $q(\tau)\Delta\tau$ . From the theorem of change of linear momentum the impulse results a sudden  $\Delta v(\tau)$  change in the velocity:

$$m\Delta v(\tau) = q(\tau)\Delta\tau \rightarrow \Delta v(\tau) = \frac{q(\tau)}{m}\Delta\tau. \quad (1.23)$$

After this sudden change the force  $q(\tau)$  will be zero, so the mass-damper-spring system starts a free vibration with initial velocity  $\Delta v(\tau)$ . It is reasonable to assume that the force  $q(\tau)$  does not have any effects on the displacements backwards in time, so we can say that the displacement of the mass before the force is applied is zero:

$$\Delta u(t, \tau) = 0, \quad t \leq \tau. \quad (1.24)$$

The time evolution of the increment of displacement  $\Delta u(t, \tau)$  is obtained from the previously derived solution (1.7) of the free vibration of a mass-damper-spring system. For this specific case the initial conditions of Eq. (1.22) come from Eqs. (1.23) and (1.24):

$$\Delta u(\tau, \tau) = 0, \quad \dot{\Delta u}(\tau, \tau) = \frac{q(\tau)}{m}\Delta\tau. \quad (1.25)$$

The exponentially decaying increment of the displacement  $\Delta u(t, \tau)$  comes from Eq. (1.7) with initial conditions (1.25) fulfilling the differential equation (1.22) and the initial conditions (1.25) will be:

$$\Delta u(t, \tau) = e^{-\xi\omega_0(t-\tau)} \left( \frac{q(\tau)}{m\omega_0^*} \Delta\tau \sin(\omega_0^*(t-\tau)) \right).$$

(Note that  $\xi = c/(2\sqrt{km})$  and  $\omega_0^* = \sqrt{k/m}\sqrt{1-\xi^2}$ .) This result is shown in Figure 1.7 (c).

If  $\Delta\tau$  tends to 0, then  $\Delta u(t, \tau)$  becomes an elementary increment  $du(t, \tau)$ . For any time  $t$  we have to integrate these elementary changes for all the past forces, i.e. for  $\tau < t$ :

$$u(t) = \int_0^t \frac{q(\tau)}{m\omega_0^*} e^{-\xi\omega_0(t-\tau)} \sin(\omega_0^*(t-\tau)) d\tau. \quad (1.26)$$

The above formula is the *Duhamel's* integral.

## 1.2.2 Numerical solution of the differential equation

For many types of excitation forces *Duhamel's* integral (1.26) can be computed only numerically. Instead of numerical integration of the formula (1.26) the step-by-step calculation of the displacements and velocities directly from the differential equation (1.22) is possible.

In the numerical calculations it is a quite usual step to reformulate the second order differential equation into two, first order equations. For that, first we introduce a new variable function, the velocity:

$$v(t) = \frac{du(t)}{dt},$$

and put it and its derivative with respect to time in the original, second order differential equation (1.22). The resulting system of first order differential equations is:

$$\begin{aligned} \frac{du(t)}{dt} &= v(t), \\ \frac{dv(t)}{dt} &= -\frac{c}{m}v(t) - \frac{k}{m}u(t) + \frac{q(t)}{m}, \end{aligned} \quad (1.27)$$

with initial conditions  $u(t_0) = u_0$  and  $v(t_0) = v_0$ .

### Cauchy-Euler method

Let us assume, that we know the displacement and the velocity at a given time instant  $t_i$ , and we want to calculate them at the time instant  $t_{i+1}$ . (Let the difference between  $t_{i+1}$  and  $t_i$  be a chosen constant  $\Delta t = t_{i+1} - t_i$ .) We denote the displacement and the velocity at  $t_i$  by  $u_i$  and  $v_i$ . From Eq. (1.27) we can calculate the differences  $\Delta u_i/\Delta t$  and  $\Delta v_i/\Delta t$ :

$$\begin{aligned} \frac{\Delta u_i}{\Delta t} &= \frac{u_{i+1} - u_i}{\Delta t} = v_i, \\ \frac{\Delta v_i}{\Delta t} &= \frac{v_{i+1} - v_i}{\Delta t} = \left( -\frac{c}{m}v_i - \frac{k}{m}u_i + \frac{q(t_i)}{m} \right). \end{aligned}$$

The estimated values of both variables  $u_{i+1}$  and  $v_{i+1}$ , are

$$\begin{aligned} u_{i+1} &= u_i + v_i \Delta t, \\ v_{i+1} &= v_i + \left( -\frac{c}{m}v_i - \frac{k}{m}u_i + \frac{q(t_i)}{m} \right) \Delta t. \end{aligned}$$

We can iterate the above map starting with  $i = 0$ , i.e. with the given initial values  $u_0, v_0$ .

Figure 1.8 (a) shows the concept of the algorithm, and one can see the main problem of this method as well. Using the Cauchy-Euler method involves a small error in every step, accumulating during the calculation. The error depends on the step-size ( $\Delta t$ ). Smaller step-size causes smaller error, but it requires more steps to reach the same time. The most important question of numerical methods is the convergence and the stability, but the discussion of these properties are beyond the scope of this lecture notes. In order to avoid false solutions and crash of the procedure, one has to set the time step  $\Delta t$  sufficiently small.



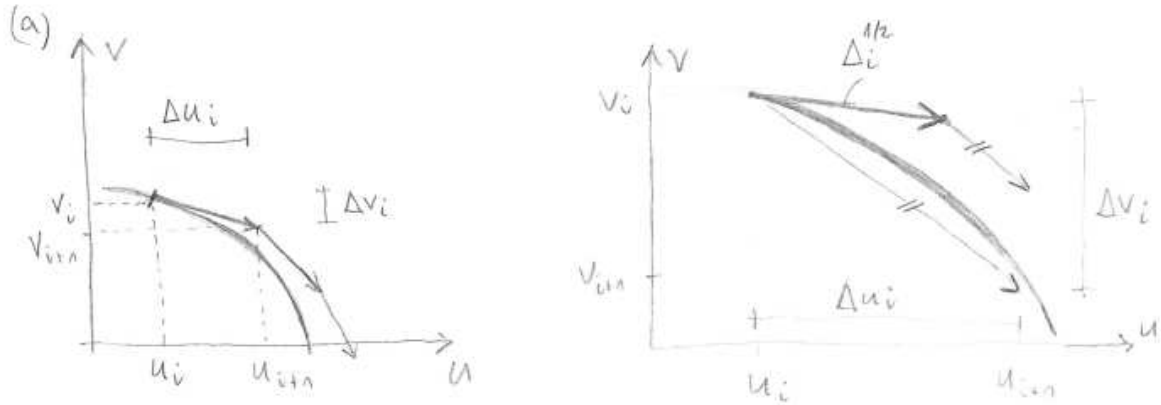


**Figure 1.8:** Explanation of (a) the Cauchy-Euler method and (b) the second order Runge-Kutta method. The continuous is the exact solution, the arrows represent tangents and increments.

### Higher order methods

The key idea behind the higher order methods is to use a better approximation for the increments  $\Delta u_i$ ,  $\Delta v_i$ , than we had from the tangents calculated at the end-point of step  $i$ . It seems to be reasonable, that we rather calculate the tangent somewhere along the current segment (based on one, or more points). These methods are called the *Runge-Kutta* methods. In the second order Runge-Kutta method we calculate the tangent at the middle of the current segment. So, we go forward with a half step-size, calculate the tangents there, and use those values to make the actual step-size. It means, that we have to calculate the derivatives twice as much, but we get a higher precision. The algorithm is of the following steps. First we compute the differences just as before:

$$\begin{aligned}\frac{\Delta u_i^0}{\Delta t} &= \frac{u_{i+1} - u_i}{\Delta t} = v_i, \\ \frac{\Delta v_i^0}{\Delta t} &= \frac{v_{i+1} - v_i}{\Delta t} = \left( -\frac{c}{m}v_i - \frac{k}{m}u_i + \frac{q(t_i)}{m} \right).\end{aligned}$$

Next we step forward with a half step-size:

$$\begin{aligned}u_i^{1/2} &= u_i + \Delta u_i^0/2, \\ v_i^{1/2} &= v_i + \Delta v_i^0/2.\end{aligned}$$

Then we compute the differences at the mid-point (this will be the direction of the actual step):

$$\begin{aligned}\frac{u_{i+1} - u_i}{\Delta t} &= v_i^{1/2}, \\ \frac{v_{i+1} - v_i}{\Delta t} &= \left( -\frac{c}{m}v_i^{1/2} - \frac{k}{m}u_i^{1/2} + \frac{q(t_i + \Delta t/2)}{m} \right).\end{aligned}$$

Finally, the map of the iteration is

$$\begin{aligned}u_{i+1} &= u_i + \Delta u_i = u_i + v_i^{1/2} \Delta t, \\ v_{i+1} &= v_i + \Delta v_i = v_i + \left( -\frac{c}{m}v_i^{1/2} - \frac{k}{m}u_i^{1/2} + \frac{q(t_i + \Delta t/2)}{m} \right) \Delta t.\end{aligned}$$



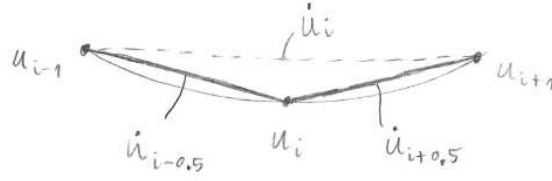


**Figure 1.9:** Explanation of the finite difference approximation of velocity and acceleration using secant lines

### Central difference method

Let us assume, that we know the displacement and the velocity at the given time instances  $t_{i-1}$  and  $t_i$ , and we want to calculate them at the time instant  $t_{i+1}$ . (Let the difference between two time instants be constant:  $\Delta t = t_{i+1} - t_i = t_i - t_{i-1}$ .) We denote the displacement and the velocity at  $t_i$  by  $u_i$  and  $v_i$ , at  $t_{i-1}$  by  $u_{i-1}$  and  $v_{i-1}$ , respectively.

We can write the approximation for the velocity (see Figure 1.9):

$$v_i = \dot{u}_i \cong \frac{u_{i+1} - u_{i-1}}{2\Delta t}, \quad (1.28)$$

while the approximation of the acceleration is:

$$a_i = \ddot{u}_i \cong \frac{\dot{u}_{i+0.5} - \dot{u}_{i-0.5}}{\Delta t} \cong \frac{(u_{i+1} - u_i) - (u_i - u_{i-1})}{\Delta t^2} = \frac{u_{i+1} - 2u_i + u_{i-1}}{\Delta t^2}. \quad (1.29)$$

The equation of motion is (1.22):

$$m\ddot{u}_i + c\dot{u}_i + ku_i = q(t_i) = q_i.$$

Let us substitute the velocity (Eq. (1.28)) and the acceleration (Eq. (1.29)) into the above equation:

$$m \frac{u_{i+1} - 2u_i + u_{i-1}}{\Delta t^2} + c \frac{u_{i+1} - u_{i-1}}{2\Delta t} + ku_i = q_i. \quad (1.30)$$

One can solve Eq. (1.30) for  $u_{i+1}$ :

$$u_{i+1} = \frac{q_i + u_i \left( \frac{2m}{\Delta t^2} - k \right) + u_{i-1} \left( \frac{c}{2\Delta t} - \frac{m}{\Delta t^2} \right)}{\frac{m}{\Delta t^2} + \frac{c}{2\Delta t}}. \quad (1.31)$$

Eq. (1.31) is the map of the iteration containing only the displacements of the previous two steps (but no velocities). Therefore, not only the displacement  $u_0$  in the initial time instant, but also the displacement  $u_{-1}$  is needed to start the iteration. This latter condition can be computed from  $u_0$  and  $v_0$  as

$$u_{-1} = u_0 - v_0 \Delta t.$$

### 1.3 Vibration of multi-degree-of-freedom systems

Behaviour of real life engineering structures usually cannot be described by the displacement of only one point of the structure. In fact, the exact description of the motion requires an approach considering the structure as a continuum. In many cases however, the motion of the continua can be reduced to the motion of a finite-degree-of-freedom system. In a multi-storey building with rigid slabs the displacements of the ends of the columns depend only on the displacements of the floors. In a spatial structure this would be three degree-of-freedom on each level (two translations in the horizontal plane and a rotation around a vertical axis, see Figure 1.10 (a) for a floor plate of one level). If the building is reduced to a planar problem, the translation of each level can be regarded as a degree of freedom. (see Figure 1.10 (b)). Even numerical methods applied in Finite Element programs do the same: they approximate the displacements by interpolating from the displacements of the degrees of freedom. Figure 1.10 (c) shows a simple mechanical model for a two-degree-of-freedom system: two bodies are connected to each other by a spring, one of the bodies is supported by another spring, the other body has an excitation force  $F(t)$ .

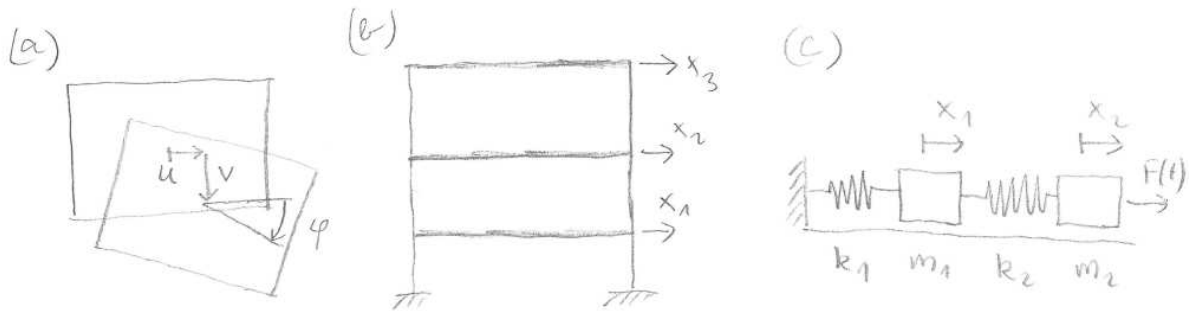


**Figure 1.10:** Examples of multi-degree-of-freedom structures (a) three degrees of freedom of one level of a spatial multi-storey building ( $u$  and  $v$  are the translations,  $\varphi$  is the rotation), (b) mechanical model of a three-storey frame structure (planar frame with three degrees of freedom) (c) mechanical model of an undamped two-degrees-of-freedom system excited at its second degree of freedom

#### 1.3.1 Equation of motion of MDOF systems

There are several ways to derive the equations of motion for a MDOF system. Here we show one for the system on Figure 1.10 (c). The FBD of the system is shown in Figure 1.11. The only displacement which is not constrained is the horizontal translation of the masses  $m_1$  and  $m_2$ . Variables  $x_1(t)$  and  $x_2(t)$  denote the translations of these masses, respectively. The number of degrees of freedom is therefore *two*. *Newton's* second law of motion is written for the two masses:

$$\begin{aligned} -f_{S1}(t) + f_{S2} &= m_1 a_1(t), \\ -f_{S2}(t) + F(t) &= m_2 a_2(t). \end{aligned} \quad (1.32)$$

The forces in the linear springs depend on the elongation of each spring:  $f_{S1}(t) = k_1 \Delta \ell_1(t)$ ,  $f_{S2}(t) = k_2 \Delta \ell_2(t)$ . For the first spring  $\Delta \ell_1(t) = x_1(t)$  (assuming a fixed support) and for the

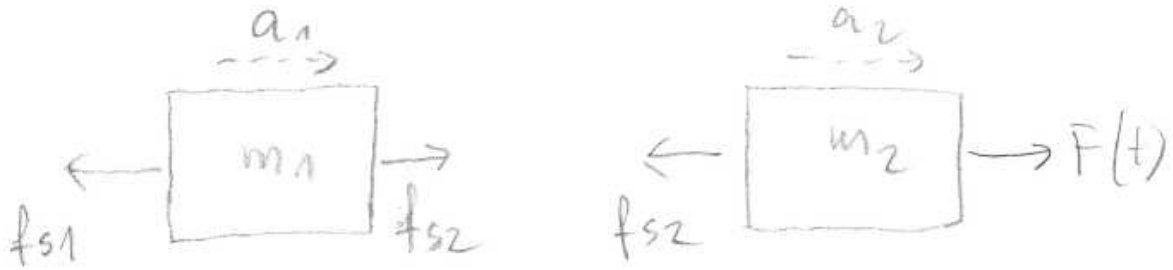


**Figure 1.11:** Free body diagrams of the model shown in Figure 1.10 (c)

second spring  $\Delta\ell_2(t) = x_2(t) - x_1(t)$ . So the spring forces are:  $f_{S1}(t) = k_1x_1(t)$ ,  $f_{S2}(t) = k_2(x_2(t) - x_1(t))$ . The acceleration of each body is the second derivative of its translation with respect to time, i.e.:  $a_1(t) = \ddot{x}_1(t)$ ,  $a_2(t) = \ddot{x}_2(t)$ . Substituting these results into Eq. (1.32) we get

$$\begin{aligned} -k_1x_1(t) + k_2x_2(t) - k_2x_1(t) &= m_1\ddot{x}_1(t), \\ -k_2x_2(t) + k_2x_1(t) + F(t) &= m_2\ddot{x}_2(t), \end{aligned} \quad (1.33)$$

which can be written in the following form:

$$\begin{aligned} m_1\ddot{x}_1(t) + k_1x_1(t) + k_2x_1(t) - k_2x_2(t) &= 0, \\ m_2\ddot{x}_2(t) - k_2x_1(t) + k_2x_2(t) &= F(t). \end{aligned} \quad (1.34)$$

What we obtained is a coupled system of second order ordinary differential equations. Is it worth noting that each equation corresponds to one body (the  $i$ th) with the external force acting on that body (or zero when there is none) on the right hand side of the current equation. On the left hand sides there is always the corresponding  $m_i\ddot{x}_i(t)$  term (inertial term), and the spring force. The springs appearing in each equation such that the spring stiffness multiplied by the displacement of the degree of freedom is added to the equation of the corresponding DOF ( $k_1x_1(t)$  for the first spring in the first equation,  $k_2x_1(t)$  and  $k_2x_2(t)$  for the second spring in the first and second equation respectively). If a spring connects two degrees of freedom, then it couples the equations of the connected DOFs ( $-k_2x_2$  term in the first and  $-k_2x_1$  term in the second equation). The sign of the coupling terms depends on the sense of the coupled DOFs, but is always the same in both equations. If two DOFs are not connected directly, their equations are not coupled directly.

Equation (1.34) can be written in a short form:

$$\mathbf{M}\ddot{\mathbf{u}}(t) + \mathbf{K}\mathbf{u}(t) = \mathbf{q}(t) \quad (1.35)$$

as a matrix differential equation. Here vector  $\mathbf{u}(t)$  contains the displacement variables, the quadratic matrices  $\mathbf{M}$  and  $\mathbf{K}$  are the mass and stiffness matrices, respectively, while vector  $\mathbf{q}(t)$  contains the external forces acting on each degree of freedom. (For an  $N$ -degree-of-freedom system the vectors have  $N$  entries, while the size of the matrices is  $N$  by  $N$ ). Properties explained after Eq. (1.34) yields that the matrices are symmetric matrices.

For the example shown in Figure 1.10 (c) the elements are:

$$\mathbf{M} = \begin{bmatrix} m_1 & 0 \\ 0 & m_2 \end{bmatrix}, \mathbf{K} = \begin{bmatrix} k_1 + k_2 & -k_2 \\ -k_2 & k_2 \end{bmatrix}, \mathbf{u}(t) = \begin{bmatrix} x_1(t) \\ x_2(t) \end{bmatrix}, \ddot{\mathbf{u}}(t) = \begin{bmatrix} \ddot{x}_1(t) \\ \ddot{x}_2(t) \end{bmatrix}, \mathbf{q}(t) = \begin{bmatrix} 0 \\ F(t) \end{bmatrix}.$$

Similarly to the single-degree-of-freedom vibrations, we divide the problems described by Eq. (1.35) in two groups:

- if  $\mathbf{q}(t) = \mathbf{0}$ , then the system of differential equations is homogeneous, and the resulting motion is the free vibration.
- if  $\mathbf{q}(t) \neq \mathbf{0}$ , then the system of differential equations is non-homogeneous, and it is called a forced vibration.

### Equations of motion of a two-storey frame

Let us analyse the equations of motion for a two-storey frame structure with a machine exerting a force on the upper level. The floors are rigid, so we only have two degrees of freedom. Figure 1.12 (a) shows the structure and one possible displacement system. Figure 1.12 (b) shows the free body diagrams for the same structure. The internal forces  $f_{S1}$  (from the columns 1 and 1') and  $f_{S2}$  (from the columns 2 and 2') depend on the inter-storey drifts  $x_1$  and  $x_2 - x_1$ , respectively. Assuming linear elastic columns one can calculate the equivalent stiffness coefficients  $k_1$  and  $k_2$  for the columns on each level. Writing the equations of motion and the elements of the mass and stiffness matrices are left for the reader as an exercise.

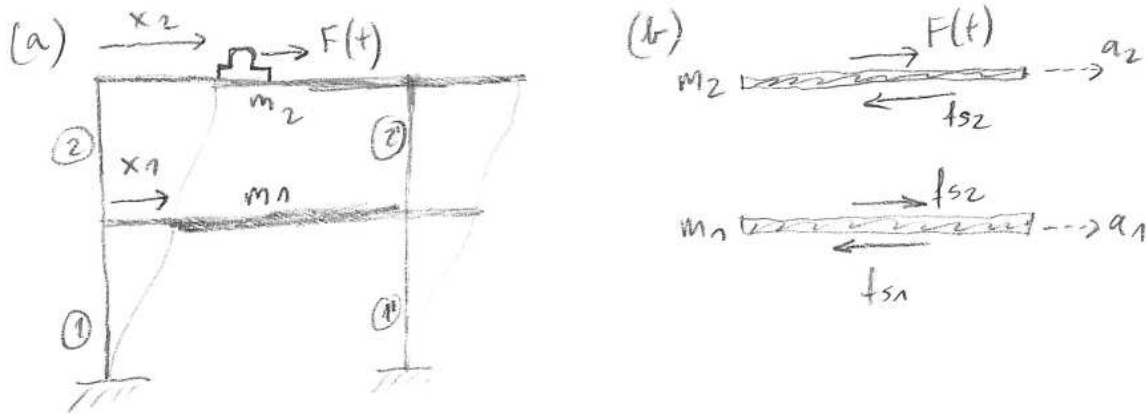


Figure 1.12: Two-storey frame structure with rigid floors. (a) Mechanical model, (b) free body diagram.

### Equations of motion with different variables

The deformed state of the structure in Figure 1.12 can be described not only with the global coordinates of each level, but with the inter-storey drifts as well. (In accordance with the earlier

notation we will denote them by  $\Delta\ell_1$  and  $\Delta\ell_2$ .) Then we have to substitute  $x_1(t) = \Delta\ell_1(t)$ ,  $x_2(t) = \Delta\ell_1(t) + \Delta\ell_2(t)$  and their derivatives into Eq. (1.32), and we get

$$\begin{aligned} -\Delta\ell_1(t) + k_2\Delta\ell_2(t) &= m_1\ddot{\Delta\ell}_1(t), \\ -k_2\Delta\ell_2(t) + F(t) &= m_2\ddot{\Delta\ell}_1(t) + m_2\ddot{\Delta\ell}_2(t) \end{aligned}$$

instead of Eq. (1.33). One can see, that using this description of the problem results non-symmetric mass- and stiffness matrices. This is due to the fact, that the equations still belong to the global  $x_1$  and  $x_2$  translations, while our variables are the relative displacements  $\Delta\ell_1$  and  $\Delta\ell_2$ . Symmetry of the system matrices is often used during the calculations, so we can conclude, that this hybrid approach should be avoided if possible.

### 1.3.2 Free vibration of MDOF systems

During the analysis of a multi-degree-of-freedom system the solution of Eq. (1.35) follows the same steps as for SDOF systems. The free vibration of the system is analysed using the complementary equation of Eq. (1.35). That is the homogeneous matrix differential equation

$$\mathbf{M}\ddot{\mathbf{u}}(t) + \mathbf{K}\mathbf{u}(t) = \mathbf{0}. \quad (1.36)$$

We search for the solution of Eq. (1.36) in the form:

$$\mathbf{u}(t) = \mathbf{u}(a \cos(\omega_0 t) + b \sin(\omega_0 t)), \quad (1.37)$$

i.e. the displacement function  $\mathbf{u}(t)$  is assumed to be a product of a constant vector  $\mathbf{u}_0$  describing the ratio of the degrees of freedom to each other and a harmonic function depending on time, natural frequency  $\omega_0$  and two parameters  $a$  and  $b$ . The cases when  $\mathbf{u} = \mathbf{0}$  or  $a = b = 0$  would lead to the trivial solution of the Eq. (1.36). We are looking for the nontrivial solutions.

The second derivative of the displacement vector  $\mathbf{u}(t)$  is

$$\ddot{\mathbf{u}}(t) = \mathbf{u}(-\omega_0^2)(a \cos(\omega_0 t) + b \sin(\omega_0 t)).$$

We substitute  $\mathbf{u}(t)$  and  $\ddot{\mathbf{u}}(t)$  into the homogeneous differential equation (1.36):

$$\mathbf{M}\mathbf{u}(-\omega_0^2)(a \cos(\omega_0 t) + b \sin(\omega_0 t)) + \mathbf{K}\mathbf{u}(a \cos(\omega_0 t) + b \sin(\omega_0 t)) = \mathbf{0}. \quad (1.38)$$

This equation must hold for any time  $t$ , thus either  $(a \cos(\omega_0 t) + b \sin(\omega_0 t)) = 0$ , or  $\mathbf{M}\mathbf{u}(-\omega_0^2) + \mathbf{K}\mathbf{u} = \mathbf{0}$ . The equation  $(a \cos(\omega_0 t) + b \sin(\omega_0 t)) = 0$  holds for all  $t$  only with the trivial solution  $a = b = 0$ , therefore the time-independent matrix equation  $\mathbf{M}\mathbf{u}(-\omega_0^2) + \mathbf{K}\mathbf{u} = \mathbf{0}$  must be fulfilled, so it is rewritten in the more classical form

$$(\mathbf{K} - \omega_0^2\mathbf{M})\mathbf{u} = \mathbf{0}. \quad (1.39)$$

The above equation is a system of a homogeneous, linear equations, which is called a generalized eigenvalue problem in mathematics. It has nontrivial solutions if and only if the matrix of coefficients is singular, or equivalently if and only if its determinant is zero. The equation:

$$\det(\mathbf{K} - \omega_0^2\mathbf{M}) = 0$$

leads to a polynomial of degree  $N$  for  $\omega_0^2$  (where  $N$  is the degree of freedom of the system). Typically it has  $N$  real, distinct solutions, denoted by  $\omega_{01}^2 < \omega_{02}^2 < \dots < \omega_{0N}^2$  (i.e. the first one is the smallest), and their positive square roots

$$\omega_{01} < \omega_{02} < \dots < \omega_{0N}$$

are the natural circular frequencies of the system. We can define  $N$  natural period of the system as:

$$T_{01} = \frac{2\pi}{\omega_{01}} > T_{02} = \frac{2\pi}{\omega_{02}} > \dots > T_{0N} = \frac{2\pi}{\omega_{0N}}.$$

In the next step we have to find the elements of vector  $\mathbf{u}_0$  of Eq. (1.37). Since we have  $N$  natural circular frequencies, we will have  $N$  different vectors. We will denote the vector corresponding to  $\omega_{0j}$  by  $\mathbf{u}_j$ . The vector  $\mathbf{u}_j$  must fulfill Eq. (1.39):

$$(\mathbf{K} - \omega_{0j}^2 \mathbf{M}) \mathbf{u}_j = \mathbf{0}. \quad (1.40)$$

Because of the matrix  $(\mathbf{K} - \omega_{0j}^2 \mathbf{M})$  is singular,  $\mathbf{u}_j$  has only  $N - 1$  independent rows, i.e. it has not a unique  $\mathbf{u}_j$  solution. If  $\mathbf{u}_j$  is a solution, then the vector  $\alpha \mathbf{u}_j$  will be a solution for any real-valued  $\alpha$ . These vectors are the (generalized) eigenvectors of the system. The meaning of the  $j$ th eigenvector  $\mathbf{u}_j$  is that if we displace the degrees-of-freedom in the same proportion as the elements of the eigenvector, then it will move such a way that the ratios of the displacements will be the same during the motion with frequency  $\omega_{0j}$ . In this case the structure vibrates in its  $j$ th mode. The shape of the vibration (the modal shape) is described by the eigenvector (or mode vector).

### Normalized eigenvectors

For further calculations we have to make the eigenvector unique. It can be done in different ways:

- making the first element of the vector be equal to 1,
- making the largest (in absolute value) element of the vector be equal to 1,
- making the length of the vector be equal to 1 (i.e.  $\mathbf{u}_j^T \mathbf{u}_j = 1$ ),
- making the vector be normalized to the mass matrix (i.e.  $\mathbf{u}_j^T \mathbf{M} \mathbf{u}_j = 1$ ).

The first method is useful when the calculations are done by hand. The second method has an important role in numerical solution of the eigenvalue problem. The third method would result in possible small numbers in the case of a large system. The last method has positive consequences on further results so we assume that the eigenvectors are normalized to the mass matrix. (If we have a non-normalized eigenvector  $\bar{\mathbf{u}}_j$ , we can still calculate the product  $\bar{\mathbf{u}}_j^T \mathbf{M} \bar{\mathbf{u}}_j = \alpha_j$ . It follows from the rules of matrix operations that the vector  $(1/\sqrt{\alpha_j}) \bar{\mathbf{u}}_j$  will be normalized to the mass matrix.)

If we substitute the  $j$ th normalized eigenvector into Eq. (1.39), and multiply it with the transpose of the same vector from the left we get:

$$\mathbf{u}_j^T \mathbf{K} \mathbf{u}_j - \omega_{0j}^2 \mathbf{u}_j^T \mathbf{M} \mathbf{u}_j = 0.$$

Because of the eigenvector is normalized, the vector-matrix-vector product on the left hand side equals 1, resulting in:

$$\boxed{\mathbf{u}_j^T \mathbf{K} \mathbf{u}_j = \omega_{0j}^2}. \quad (1.41)$$

### Orthogonality of eigenvectors

Let us take two different natural circular frequencies  $\omega_{0i} \neq \omega_{0j}$ , and the corresponding eigenvectors  $\mathbf{u}_i$  and  $\mathbf{u}_j$ . Then it holds from Eq. (1.40) that

$$\mathbf{K} \mathbf{u}_i = \omega_{0i}^2 \mathbf{M} \mathbf{u}_i, \quad (1.42)$$

$$\mathbf{K} \mathbf{u}_j = \omega_{0j}^2 \mathbf{M} \mathbf{u}_j. \quad (1.43)$$

Multiplying Eq. (1.42) by  $\mathbf{u}_j^T$  and Eq. (1.43) by  $\mathbf{u}_i^T$  from the left and subtracting the resultant equations lead to:

$$\mathbf{u}_j^T \mathbf{K} \mathbf{u}_i - \mathbf{u}_i^T \mathbf{K} \mathbf{u}_j = \omega_{0i}^2 \mathbf{u}_j^T \mathbf{M} \mathbf{u}_i - \omega_{0j}^2 \mathbf{u}_i^T \mathbf{M} \mathbf{u}_j.$$

Due to the symmetry of matrices  $\mathbf{K}$  and  $\mathbf{M}$

$$\mathbf{u}_j^T \mathbf{K} \mathbf{u}_i = \mathbf{u}_i^T \mathbf{K} \mathbf{u}_j, \quad \mathbf{u}_j^T \mathbf{M} \mathbf{u}_i = \mathbf{u}_i^T \mathbf{M} \mathbf{u}_j, \quad (1.44)$$

so we have:

$$0 = (\omega_{0i}^2 - \omega_{0j}^2) \mathbf{u}_j^T \mathbf{M} \mathbf{u}_i.$$

The above equality only holds for different  $\omega_{0i}$  and  $\omega_{0j}$  if:

$$\boxed{\mathbf{u}_j^T \mathbf{M} \mathbf{u}_i = 0}. \quad (1.45)$$

Dividing both side of Eq. (1.42) by  $\omega_{0i}^2$ , then multiplying the result by  $\mathbf{u}_j^T$  from the left, dividing both side of Eq. (1.43) by  $\omega_{0j}^2$ , then multiplying the result by  $\mathbf{u}_i^T$  from the left, finally subtracting the resultant equations lead to:

$$\frac{1}{\omega_{0i}^2} \mathbf{u}_j^T \mathbf{K} \mathbf{u}_i - \frac{1}{\omega_{0j}^2} \mathbf{u}_i^T \mathbf{K} \mathbf{u}_j = \mathbf{u}_j^T \mathbf{M} \mathbf{u}_i - \mathbf{u}_i^T \mathbf{M} \mathbf{u}_j.$$

Due to Eq. (1.44)

$$\left( \frac{1}{\omega_{0i}^2} - \frac{1}{\omega_{0j}^2} \right) \mathbf{u}_j^T \mathbf{K} \mathbf{u}_i = 0,$$

which holds for different nonzero  $\omega_{0i}$  and  $\omega_{0j}$  only when:

$$\boxed{\mathbf{u}_j^T \mathbf{K} \mathbf{u}_i = 0}. \quad (1.46)$$

We refer to this latter properties as the orthogonality of the eigenvectors  $\mathbf{u}_i$  and  $\mathbf{u}_j$  to the mass matrix (Eq. (1.45)) and to the stiffness matrix (Eq. (1.46)).



### General solution of the homogeneous differential equation

The general solution of the homogeneous differential equation Eq. (1.36) is constructed from the sum of the solutions corresponding to the eigenmodes:

$$\mathbf{u}(t) = \sum_{j=1}^N \mathbf{u}_j (a_j \cos(\omega_{0j}t) + b_j \sin(\omega_{0j}t)). \quad (1.47)$$

To find the parameters  $a_j$  and  $b_j$  we need the vector of velocities:

$$\dot{\mathbf{u}}(t) = \sum_{j=1}^N \mathbf{u}_j \omega_{0j} (-a_j \sin(\omega_{0j}t) + b_j \cos(\omega_{0j}t)). \quad (1.48)$$

Initial conditions of a multi-degree-of-freedom system are displacements and velocities of the degrees of freedom at a given time instant  $t_0$ :

$$\mathbf{u}(t_0) = \mathbf{u}_0, \quad \dot{\mathbf{u}}(t_0) = \mathbf{v}_0.$$

By substituting Eq. (1.47) and (1.48) into the above formula  $2N$  constraints are obtained which can be used to find the parameters  $a_j$  and  $b_j$  in the general solution Eq. (1.47). Using the orthogonal properties of the eigenvectors one can avoid the solution of a system of  $2N$  linear equations. If we multiply these  $2N$  equations from the left by  $\mathbf{u}_j^T \mathbf{M}$ , then we get

$$\begin{aligned} a_j \cos(\omega_{0j}t_0) + b_j \sin(\omega_{0j}t_0) &= \mathbf{u}_j^T \mathbf{M} \mathbf{u}_0, \\ \omega_{0j} (-a_j \sin(\omega_{0j}t_0) + b_j \cos(\omega_{0j}t_0)) &= \mathbf{u}_j^T \mathbf{M} \mathbf{v}_0, \end{aligned}$$

so, varying  $j$  from 1 to  $N$  we have to solve  $N$  system of 2 linear equations instead of a system of  $2N$  equations for the coefficients  $a_j$  and  $b_j$ .

The resultant motion will be the sum of harmonic vibrations, which is not necessarily a periodic motion!

### 1.3.3 Harmonic forcing of MDOF systems

The solution of forced vibration problems of multi-degree-of-freedom systems follows a similar schema as we saw with SDOF systems. The complete solution is the sum of the general solution of the complementary differential equation and a particular solution of the nonhomogeneous differential equation. So the solution of Eq. (1.35) is Eq. (1.47) plus a particular solution  $\mathbf{u}_f(t)$ , which is the answer of the system to the forcing.

In this subsection we will give a solution for the problem, in the case of the excitation force is harmonic. Then  $\mathbf{q}(t)$  can be written in the form:

$$\mathbf{q}(t) = \mathbf{q}_0 \sin(\omega t). \quad (1.49)$$

Here  $\omega$  is the circular frequency of the forcing, and the vector  $\mathbf{q}_0$  stores the amplitudes of the forcing. Thus each DOF is excited with the same frequency  $\omega$ . Is it worth mentioning that a



zero external force acting on a degree-of-freedom can be treated as a harmonic force with zero amplitude and arbitrary circular frequency.

While solving the inhomogeneous equation we are only looking for the steady-state part of the vibration. We show two possible solution methods:

- the direct solution,
- solution with the modal shape vectors and natural circular frequencies.

### Direct solution

In the case of the direct solution we assume the particular solution of the form:

$$\mathbf{u}_f(t) = \mathbf{u}_{f0} \sin(\omega t), \quad (1.50)$$

i.e. it is a harmonic response with the same harmonic term as the forcing, with constant amplitudes given in the vector  $\mathbf{u}_{f0}$ . The second derivative of Eq. (1.50) with respect to time is:

$$\ddot{\mathbf{u}}_f(t) = -\omega^2 \mathbf{u}_{f0} \sin(\omega t). \quad (1.51)$$

Substituting the load, the ansatz and its derivative (Eqs. (1.49), (1.50), and (1.51)) into Eq. (1.35) we get:

$$-\omega^2 \mathbf{M} \mathbf{u}_{f0} \sin(\omega t) + \mathbf{K} \mathbf{u}_{f0} \sin(\omega t) = \mathbf{q}_0 \sin(\omega t). \quad (1.52)$$

The above equation fulfills either if  $\sin(\omega t) = 0$ , or if  $\mathbf{K} \mathbf{u}_{f0} - \omega^2 \mathbf{M} \mathbf{u}_{f0} = \mathbf{q}_0$ . Because the loading is a real, time dependent harmonic force, the term  $\sin(\omega t)$  cannot be zero for every time instant. So, we can write the latter condition as:

$$(\mathbf{K} - \omega^2 \mathbf{M}) \mathbf{u}_{f0} = \mathbf{q}_0. \quad (1.53)$$

The solution of this non-homogeneous matrix differential equation for the amplitude  $\mathbf{u}_{f0}$  is needed. The coefficient matrix in Eq. (1.53) is quadratic, so it has a solution if and only if there exists its inverse matrix, i.e. the matrix is non-singular, or with other words, its determinant is nonzero. In that case we get the solution by multiplying both sides of Eq. (1.53) by the inverse  $(\mathbf{K} - \omega^2 \mathbf{M})^{-1}$ :

$$\mathbf{u}_{f0} = (\mathbf{K} - \omega^2 \mathbf{M})^{-1} \mathbf{q}_0. \quad (1.54)$$

The particular solution then can be written as:

$$\mathbf{u}_f(t) = (\mathbf{K} - \omega^2 \mathbf{M})^{-1} \mathbf{q}_0 \sin(\omega t). \quad (1.55)$$

This is the steady-state part of the vibration. We can see that each degree of freedom vibrates with the same frequency. Without computing the inverse matrix, we cannot read out directly whether a degree of freedom is in an in-phase or in an out-of-phase vibration.

We note that the inverse of the matrix  $(\mathbf{K} - \omega^2 \mathbf{M})$  does not exist if its determinant equals zero. But if  $\det(\mathbf{K} - \omega^2 \mathbf{M}) = 0$ , then the circular frequency of the forcing equals one of the natural circular frequencies of the system, hence the system is in the state of resonance.

It means that if the forcing frequency coincides with one of the natural frequencies of the structure, then the direct method gives an infinite amplitude of the vibration. However, in real structures it does not occur, because there is always some damping in the system.

Direct solution requires the calculation of the inverse of an  $N$ -by- $N$  matrix. In general, the required computational capacity increases proportional to the second- or third power of  $N$  (the order of the computational time is  $\mathcal{O}(N^2 \sim N^3)$ ). Thus for large systems this method has a very high computational costs.

### Modal analysis

Instead of the direct solution one can make use of the solutions of the unforced system, i.e. of the generalized eigenvalue problem Eq. (1.36). These solutions are of the natural circular frequencies ( $\omega_{01}, \omega_{02}, \dots, \omega_{0N}$ ) and the corresponding modal shape vectors normalized to the mass matrix ( $\mathbf{u}_1, \mathbf{u}_2, \dots, \mathbf{u}_N$ ). These eigenvectors are linearly independent and span an  $N$  dimensional linear space. Let the displacements be written as a linear combination of the normalized mode shape vectors:

$$\mathbf{u}_f(t) = \sum_{j=1}^N \mathbf{u}_j y_j(t), \quad (1.56)$$

where functions  $y_i(t)$  are the modal displacements. The modal shape vectors are invariant in time, so the second derivative of the displacement is:

$$\ddot{\mathbf{u}}_f(t) = \sum_{j=1}^N \mathbf{u}_j \ddot{y}_j(t). \quad (1.57)$$

Substituting the load, the ansatz and its derivative (Eqs. (1.49), (1.56), and (1.57)) into Eq. (1.35) we get:

$$\mathbf{M} \sum_{j=1}^N \mathbf{u}_j \ddot{y}_j(t) + \mathbf{K} \sum_{j=1}^N \mathbf{u}_j y_j(t) = \mathbf{q}_0 \sin(\omega t). \quad (1.58)$$

Let us multiply both sides of Eq. (1.58) from the left by  $\mathbf{u}_i^T$ . Using the orthogonality of the eigenvectors (Eq. (1.45), and (1.46)) we only have nonzero values for  $j = i$ :

$$\mathbf{u}_i^T \mathbf{M} \mathbf{u}_i \ddot{y}_i(t) + \mathbf{u}_i^T \mathbf{K} \mathbf{u}_i y_i(t) = \mathbf{u}_i^T \mathbf{q}_0 \sin(\omega t).$$

Moreover, the eigenvectors are normalized to the mass matrix, so:

$$\mathbf{u}_i^T \mathbf{M} \mathbf{u}_i = 1, \quad \mathbf{u}_i^T \mathbf{K} \mathbf{u}_i = \omega_{0i}^2,$$

which leads to the modal differential equations of vibration:

$$\ddot{y}_i(t) + \omega_{0i}^2 y_i(t) = f_i \sin(\omega t), \quad i = 1, 2, \dots, N. \quad (1.59)$$

Here  $f_i = \mathbf{u}_i^T \mathbf{q}_0$  is the modal amplitude of the harmonic excitation force.

For the particular solution  $y_{if}(t)$  of the non-homogeneous differential equation (1.59) we assume the solution in the harmonic form:

$$y_{if} = y_{if0} \sin(\omega t).$$

Its second derivative is

$$\ddot{y}_{if} = -\omega^2 y_{if0} \sin(\omega t).$$

Substitute these equalities into Eq. (1.59), and solve for arbitrary nonzero  $\sin(\omega t)$ :

$$-\omega^2 y_{if0} + \omega_{0i}^2 y_{if0} = f_i.$$

If  $\omega = \omega_{0i}$  and  $f_i \neq 0$ , then the frequency  $\omega$  of the load and the  $i$ th natural frequency  $\omega_{0i}$  coincide, thus the system is in the state of resonance. It results in an infinitely large  $i$ th modal displacement. Otherwise, the unique, finite solution is:

$$y_{if0} = f_i \frac{1}{\omega_{0i}^2 - \omega^2} = f_i \frac{1}{\omega_{0i}^2} \frac{1}{1 - \frac{\omega^2}{\omega_{0i}^2}}.$$

The last term in the above product is a *response factor* of an undamped oscillatory system of natural circular frequency  $\omega_{0i}$ , excited by a harmonic force of circular frequency  $\omega$ . The absolute value of this coefficient is denoted by  $\mu_i$ .

Let us summarize the above results. In the absence of resonance the steady-state part of the motion (the particular solution) can be written in the form:

$$\mathbf{u}_f(t) = \sum_{i=1}^N \frac{1}{\omega_{0i}^2} \frac{1}{1 - \frac{\omega^2}{\omega_{0i}^2}} \mathbf{u}_i \mathbf{u}_i^T \mathbf{q}_0 \sin(\omega t). \quad (1.60)$$

Checking the terms of the above equation from right to left we can conclude that the response is harmonic ( $\sin(\omega t)$ ). For each mode the amplitude of the modal load ( $\mathbf{u}_i^T \mathbf{q}_0$ ) is calculated. It is then multiplied by the response factor  $\mu_i$  (but without evaluating the absolute value) which depends on the ratio of the circular frequency of the forcing and the natural circular frequency of the corresponding mode. Finally, the amplitude of each mode is divided by the square of the natural circular frequency  $\omega_{0i}^2$  of the same mode. Due to this last term the effect of higher modes is usually much smaller, except for the case when the excitation occurs close to one of the natural frequencies of the system.

Apparently, the solution of the problem with modal analysis seems to need even more computational effort, than that of the direct solution, because we first have to solve a generalized eigenvalue problem corresponding to the free vibration. For large systems, with many degrees of freedom, the solution of the eigenvalue problem has high computational needs. However, higher modes typically play a less significant role in the solution. There are numerical algorithms which do not compute all the eigenvalues and eigenvectors of the generalized eigenvalue problem, but only the first few of them. Later in the semester we will show that a reduced set of mode shape vectors calculated with these methods can be sufficient to approximate well the motion of the MDOF system.

**Problem 1.3.1** (Example on harmonic forcing of a three-storey frame structure). Figure 1.13 shows the dynamical model of a three-storey building with rigid girders. On each level the stiffness of the columns is the same and the levels have the same mass. On the top level a machine exerts a harmonic force on the structure. We are looking for the amplitudes of each degree-of-freedom in the steady-state motion.

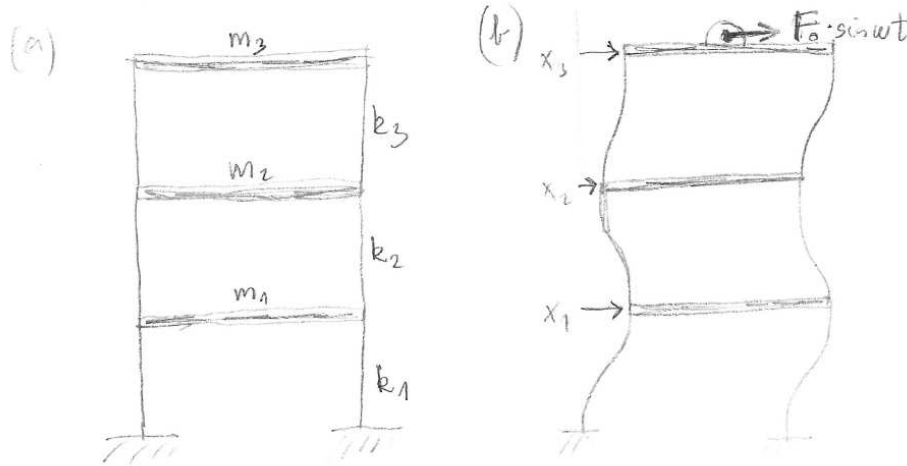


**Figure 1.13:** Vibration of a three-storey frame structure with rigid interstorey girders and elastic columns. (a) Dynamical model with system properties  $k_1 = k_2 = k_3 = 25 \text{ MN/m}$ , and  $m_1 = m_2 = m_3 = 150 \text{ t}$ . (b) Degrees of freedom in a displaced position and the excitation force  $F_0 = 150 \text{ kN}$ ,  $\omega = 9 \text{ rad/s}$ .

**Solution.** The matrix differential equation of the motion is:

$$\mathbf{M}\ddot{\mathbf{u}}(t) + \mathbf{K}\mathbf{u}(t) = \mathbf{q}_0 \sin(\omega t),$$

where

$$\mathbf{u}(t) = [x_1(t), x_2(t), x_3(t)]^T,$$

$$\mathbf{q}_0 = [F_0, 0, 0]^T = [150, 0, 0]^T \text{ kN},$$

$$\mathbf{M} = \begin{bmatrix} m_1 & 0 & 0 \\ 0 & m_2 & 0 \\ 0 & 0 & m_3 \end{bmatrix} = \begin{bmatrix} 150 & 0 & 0 \\ 0 & 150 & 0 \\ 0 & 0 & 150 \end{bmatrix} \text{ t}$$

$$\mathbf{K} = \begin{bmatrix} k_1 + k_2 & -k_2 & 0 \\ -k_2 & k_2 + k_3 & -k_3 \\ 0 & -k_3 & k_3 \end{bmatrix} = \begin{bmatrix} 50000 & -25000 & 0 \\ -25000 & 50000 & -25000 \\ 0 & -25000 & 25000 \end{bmatrix} \text{ kN/m}.$$

- *Direct solution*

The system of linear equations of the problem (Eq. (1.53)) with substitution of  $\mathbf{K}$ ,  $\mathbf{M}$  and  $\mathbf{q}_0$  is:

$$\begin{bmatrix} 37850 & -25000 & 0 \\ -25000 & 37850 & -25000 \\ 0 & -25000 & 12850 \end{bmatrix} \mathbf{u}_{f0} = \begin{bmatrix} 0 \\ 0 \\ 150 \end{bmatrix} \quad (1.61)$$

The solution of the above equation requires the inverse of the matrix of coefficients:

$$\begin{bmatrix} 37850 & -25000 & 0 \\ -25000 & 37850 & -25000 \\ 0 & -25000 & 12850 \end{bmatrix}^{-1} = \begin{bmatrix} 0.01044 & -0.02419 & -0.04707 \\ -0.02419 & -0.03663 & -0.07126 \\ -0.04707 & -0.07126 & -0.06082 \end{bmatrix} \cdot 10^{-3}$$

We have to multiply both sides of Eq. (1.61) from the left, resulting:

$$\mathbf{u}_{f0} = \begin{bmatrix} 0.01044 & -0.02419 & -0.04707 \\ -0.02419 & -0.03663 & -0.07126 \\ -0.04707 & -0.07126 & -0.06082 \end{bmatrix} \cdot 10^{-3} \cdot \begin{bmatrix} 0 \\ 0 \\ 150 \end{bmatrix}$$

$$\mathbf{u}_{f0} = \begin{bmatrix} -0.0070604 \\ -0.010689 \\ 0.0091234 \end{bmatrix} \text{ m.} \quad (1.62)$$

- *Modal analysis*

This solution requires the solution of the generalized eigenvalue problem:

$$(\mathbf{K} - \omega_0^2 \mathbf{M}) \mathbf{u}_0 = \mathbf{0}. \quad (1.63)$$

First we compute the eigenvalues of the problem. The condition we use is that the determinant of the matrix  $(\mathbf{K} - \omega_0^2 \mathbf{M})$  must be zero:

$$0 = \begin{vmatrix} 50000 - 150\omega_0^2 & -25000 & 0 \\ -25000 & 50000 - 150\omega_0^2 & -25000 \\ 0 & -25000 & 25000 - 150\omega_0^2 \end{vmatrix} =$$

$$(50000 - 150\omega_0^2) ((50000 - 150\omega_0^2) (25000 - 150\omega_0^2) - (-25000)(-25000)) -$$

$$(-25000) ((-25000) (25000 - 150\omega_0^2) - 0) + 0,$$

which results the following cubic equation for  $\omega_0^2$ :

$$-3375 \cdot 10^3 \omega_0^6 + 2812.5 \cdot 10^6 \omega_0^4 - 562.5 \cdot 10^9 \omega_0^2 + 15.625 \cdot 10^{12} = 0.$$

There are three real valued solution of the above polynomial equation:

$$\omega_{01}^2 = 33.010, \quad \omega_{02}^2 = 259.16, \quad \omega_{03}^2 = 541.16,$$

resulting the natural circular frequencies in:

$$\omega_{01} = 5.7455 \text{ rad/s}, \quad \omega_{02} = 16.098 \text{ rad/s}, \quad \omega_{03} = 23.263 \text{ rad/s}.$$

(The corresponding natural periods are:  $T_{01} = 1.0936$  s,  $T_{02} = 0.39030$  s, and  $T_{03} = 0.27009$  s.)

We show only the calculation of the first eigenvector ( $\mathbf{u}_1$ ). It must fulfill the equation:

$$(\mathbf{K} - \omega_{01}^2 \mathbf{M}) \mathbf{u}_1 = \mathbf{0},$$

which has the form after substitution of previous results:

$$\begin{bmatrix} 50000 - 150 \cdot 33.01 & -25000 & 0 \\ -25000 & 50000 - 150 \cdot 33.01 & -25000 \\ 0 & -25000 & 25000 - 150 \cdot 33.01 \end{bmatrix} \begin{bmatrix} u_{11} \\ u_{12} \\ u_{13} \end{bmatrix} = \mathbf{0}.$$

Here we assume a trial vector in the form  $\hat{\mathbf{u}}_1 = [c_1, 1, c_3]^T$ . So, with the first and the last equation we avoid multi-variable equations. (It is not always possible, in that case we should solve a system of linear equations.) From the mentioned rows we have:

$$45048c_1 - 25000 \cdot 1 = 0 \quad \rightarrow \quad c_1 = 0.55496$$

$$-25000 \cdot 1 + 20048c_3 = 0 \quad \rightarrow \quad c_3 = 1.2470$$

(The second equation is linearly dependent, but it can be used to check our results both for the natural circular frequency and the vector elements.)

Now the trial eigenvector  $\hat{\mathbf{u}}_1$  is normalized to the mass matrix  $\mathbf{M}$ . To do this, first we calculate:

$$\alpha_1 = \hat{\mathbf{u}}_1^T \mathbf{M} \hat{\mathbf{u}}_1 = \begin{bmatrix} 0.55496 & 1 & 1.2470 \end{bmatrix} \begin{bmatrix} 150 & 0 & 0 \\ 0 & 150 & 0 \\ 0 & 0 & 150 \end{bmatrix} \begin{bmatrix} 0.55496 \\ 1 \\ 1.2470 \end{bmatrix}$$

$$\begin{bmatrix} = 83.244 & 150 & 187.05 \end{bmatrix} \begin{bmatrix} 0.55496 \\ 1 \\ 1.2470 \end{bmatrix} = 429.44,$$

then the normalized shape vector corresponding to the first natural mode will be:

$$\mathbf{u}_1 = \frac{1}{\sqrt{\alpha_1}} \hat{\mathbf{u}}_1 = \begin{bmatrix} 0.02678 & 0.04826 & 0.06017 \end{bmatrix}^T. \quad (1.64)$$

The steps between Eq. (1.13) and (1.64) must be repeated for  $\omega_{02}$  and for  $\omega_{03}$  as well, to calculate the corresponding normalized eigenvectors. The final results of that calculations are:

$$\mathbf{u}_2 = \begin{bmatrix} 0.06017 & 0.02678 & -0.04826 \end{bmatrix}^T$$

and

$$\mathbf{u}_3 = \begin{bmatrix} -0.04826 & 0.06017 & -0.02678 \end{bmatrix}^T.$$

Figure 1.14 shows the deformed shape of the structure corresponding to the three modal vector. Now we can calculate the amplitude vector of the steady-state vibration using the formula of Eq. (1.60). The terms are summarized in Table 1.1.

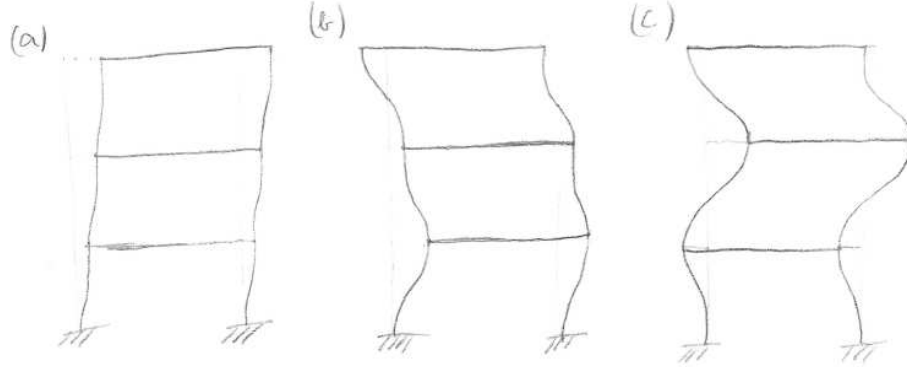


**Figure 1.14:** Mode shapes of the three-storey structure of Figure 1.13 corresponding to the natural circular frequencies (a)  $\omega_{01} = 5.7455$  rad/s, (b)  $\omega_{02} = 16.098$  rad/s, and (c)  $\omega_{03} = 23.263$  rad/s.

i	1	2	3
$\mathbf{u}_i^T \mathbf{q}$	9.026	-7.238	-4.017
$\mu_i$	-0.6879	1.4556	1.176
$\frac{1}{\omega_{0i}^2} \mu_i$	-0.02084	0.005613	0.002173
$\frac{1}{\omega_{0i}^2} \mu_i \mathbf{u}_i^T \mathbf{q}$	-0.1881	-0.04053	-0.00873

**Table 1.1:** Harmonic forcing of a three-storey structure. Modal loads, coefficients of resonance, this coefficient divided by the square of the  $i$ th natural circular frequency, participation of the mode in the steady-state vibration.

From Table 1.1 we can see, that this specific loading has a projection in the same order of magnitude in each mode, and the coefficient of resonance does not change this proportion much. Contrary to this, the whole participation of the first mode is 4.5 times higher than the participation of the second mode, and 20 times higher, than that of the third mode, due to the division by  $\omega_{0i}^2$ .

The amplitude vector of the steady-state vibration will be:

$$\mathbf{u}_{f0} = -0.1881\mathbf{u}_1 - 0.04053\mathbf{u}_2 - 0.00873\mathbf{u}_3 = \begin{bmatrix} -0.0070604 \\ -0.010689 \\ 0.0091234 \end{bmatrix} \text{ m.} \quad (1.65)$$

For both solution methods we can conclude, that in the steady-state vibration each level oscillates in a cm range, the lower two levels are out-of-phase, the upper level is in-phase with the forcing.

### 1.3.4 Approximate solution of the generalized eigenvalue problem (Ritz-Rayleigh's method)

We have seen already, that a higher natural frequency of a multi-degrees-of-freedom system plays an important role only if the forcing has a frequency close to that natural frequency. In practical problems, the first few natural modes are sufficient to describe the vibration of the structure. On the mode shape level, a mode vector of a higher natural frequency results more changes in the sense of displacements of DOFs. So, the *simpler* mode shapes correspond to lower natural frequencies, and an eigenvector (normalized to the mass matrix) can be used as a base for the calculation of the eigenvalue (see Eq. (1.41)).

#### The Rayleigh quotient

Approximate solutions can be obtained by guessing the mode shape vector of the structure, and finding the corresponding natural frequency. This is the opposite of the classical solution of the generalized eigenvalue problem, where we started with finding the eigenvalues from the polynomial equation defined by the determinant of the matrix of coefficients  $\mathbf{K} - \omega_0^2\mathbf{M}$  of the homogeneous equation, and then the eigenvectors were calculated.

Let us assume, that  $\mathbf{v}$  is a vector of  $N$  element. We define the Rayleigh quotient as:

$$R = \frac{\mathbf{v}^T \mathbf{K} \mathbf{v}}{\mathbf{v}^T \mathbf{M} \mathbf{v}}. \quad (1.66)$$

Although we do not know the eigenvectors,  $\mathbf{v}$  can be written as a linear combination of them with coefficients  $\alpha_j$ :

$$\mathbf{v} = \sum_{j=1}^N \alpha_j \mathbf{u}_j.$$

Let us expand the denominator and the numerator of Eq. (1.66). The denominator can be written as:

$$\mathbf{v}^T \mathbf{M} \mathbf{v} = \left( \sum_{j=1}^N \alpha_j \mathbf{u}_j \right)^T \mathbf{M} \left( \sum_{i=1}^N \alpha_i \mathbf{u}_i \right) = \sum_{j=1}^N \sum_{i=1}^N \alpha_j \alpha_i \mathbf{u}_j^T \mathbf{M} \mathbf{u}_i.$$

Orthogonality of the normalized eigenvectors (Eq. (1.45)) implies that the quadratic product  $\mathbf{u}_j^T \mathbf{M} \mathbf{u}_i = 1$  if  $j = i$  and zero otherwise, thus

$$\mathbf{v}^T \mathbf{M} \mathbf{v} = \sum_{j=1}^N \alpha_j^2.$$

The numerator of Eq. (1.66) can be written as:

$$\mathbf{v}^T \mathbf{K} \mathbf{v} = \left( \sum_{j=1}^N \alpha_j \mathbf{u}_j \right)^T \mathbf{K} \left( \sum_{i=1}^N \alpha_i \mathbf{u}_i \right) = \sum_{j=1}^N \sum_{i=1}^N \alpha_j \alpha_i \mathbf{u}_j^T \mathbf{K} \mathbf{u}_i.$$

Orthogonality of the normalized eigenvectors (Eq. (1.46)) implies that the quadratic product  $\mathbf{u}_j^T \mathbf{K} \mathbf{u}_i = \omega_{0j}^2$  if  $j = i$  and zero otherwise. Therefore

$$\mathbf{v}^T \mathbf{K} \mathbf{v} = \sum_{j=1}^N \alpha_j^2 \omega_{0j}^2.$$

The above formula can be expanded to:

$$\mathbf{v}^T \mathbf{K} \mathbf{v} = \sum_{j=1}^N \left( \alpha_j^2 (\omega_{0j}^2 - \omega_{01}^2) + \alpha_j^2 \omega_{01}^2 \right) = \sum_{j=1}^N \alpha_j^2 (\omega_{0j}^2 - \omega_{01}^2) + \sum_{j=1}^N \alpha_j^2 \omega_{01}^2.$$

The first summation term is zero if  $j = 1$ , so we got finally:

$$\mathbf{v}^T \mathbf{K} \mathbf{v} = \sum_{j=1}^N \alpha_j^2 \omega_{01}^2 + \sum_{j=2}^N \alpha_j^2 (\omega_{0j}^2 - \omega_{01}^2).$$

If we write the result into the definition of the Rayleigh quotient (1.66) we get:

$$R = \frac{\sum_{j=1}^N \alpha_j^2 \omega_{01}^2 + \sum_{j=2}^N \alpha_j^2 (\omega_{0j}^2 - \omega_{01}^2)}{\sum_{j=1}^N \alpha_j^2 \omega_{01}^2} = \omega_{01}^2 + \frac{\sum_{j=2}^N \alpha_j^2 (\omega_{0j}^2 - \omega_{01}^2)}{\sum_{j=1}^N \alpha_j^2 \omega_{01}^2}. \quad (1.67)$$

The sum on the right hand side of Eq. (1.67) contains only positive numbers (here we remind, that  $\omega_{01}$  is the smallest natural frequency), or zeros (if a specific  $\alpha_j$  is zero). So we can conclude, that the Rayleigh quotient is always higher than, or equal to the square of the first natural circular frequency. The accuracy of the result depends naturally on the initial guess on the mode shape vector ( $\mathbf{v}$ ): the closer the guessed shape vector  $\mathbf{v}$  is to the exact one  $\mathbf{u}_1$ , the more precise  $\omega_{01}$  is.

Seeding the  $\omega_{0N}^2$  element instead of  $\omega_{01}^2$  results in a proof for the Rayleigh quotient to be smaller than, or equal to the square of the highest natural circular frequency.



**Problem 1.3.2** (Example on finding an approximate solution for a two-storey frame). Find an approximate solution of the first natural circular frequency of the two-storey structure shown in Figure 1.12. The masses of the storeys are  $m_1 = m_2 = 2 \text{ t}$ , and the stiffness of the columns is given by spring stiffnesses  $k_1 = k_2 = 50 \text{ kN/m}$ . The first mode shape should be assumed as:  $\mathbf{v} = [1 \ 2]^T$

**Solution.** The system has the following mass and stiffness matrices:

$$\mathbf{M} = \begin{bmatrix} 2 & 0 \\ 0 & 2 \end{bmatrix}, \mathbf{K} = \begin{bmatrix} 100 & -50 \\ -50 & 50 \end{bmatrix}.$$

The numerator and the denominator of the Rayleigh quotient are:

$$\mathbf{v}^T \mathbf{M} \mathbf{v} = [1 \ 2] \begin{bmatrix} 2 & 0 \\ 0 & 2 \end{bmatrix} \begin{bmatrix} 1 \\ 2 \end{bmatrix} = [2 \ 4] \begin{bmatrix} 1 \\ 2 \end{bmatrix} = 10,$$

$$\mathbf{v}^T \mathbf{K} \mathbf{v} = [1 \ 2] \begin{bmatrix} 100 & -50 \\ -50 & 50 \end{bmatrix} \begin{bmatrix} 1 \\ 2 \end{bmatrix} = [0 \ 50] \begin{bmatrix} 1 \\ 2 \end{bmatrix} = 100.$$

So, the Rayleigh quotient is:

$$R = \frac{\mathbf{v}^T \mathbf{K} \mathbf{v}}{\mathbf{v}^T \mathbf{M} \mathbf{v}} = \frac{100}{10} = 10,$$

resulting in the approximation:

$$\omega_{01}^2 \leq 10, \quad \omega_{01} \leq 3.162 \text{ rad/s}.$$

**Exercise 1.3.1.** Find first natural circular frequency  $\omega_{01}$  of the above problem with the exact first mode shape vector:

$$\mathbf{u}_1 = [1 \ 1.618]^T.$$

**Problem 1.3.3** (Example on finding an approximate solution for a multi-storey frame). Let us find the first natural circular frequency of a 10-storey frame. (See Figure 1.15 (a).) The inter-storey stiffnesses and the level masses are the same on each level,  $m = 150 \text{ t}$  and  $k = 25000 \text{ kN/m}$  respectively.

**Solution.** The mass matrix of the structure is a  $10 \times 10$  diagonal matrix, where each element equals  $m$ . The stiffness matrix is

$$\mathbf{K} = \begin{bmatrix} k+k & -k & 0 & \dots & 0 \\ -k & k+k & -k & \ddots & \vdots \\ 0 & -k & k+k & \ddots & 0 \\ \vdots & \ddots & \ddots & \ddots & -k \\ 0 & \dots & 0 & -k & k \end{bmatrix}.$$

It is a crucial step of the method to find a good assumption of the trial vector. During the drift of the storeys, the rigid girders are staying horizontal, and so the structure follows a pattern of displacements similar to a rod with finite shear stiffness. The frame can be treated as a discrete model of the sheared (continuous) column (Figure 1.15 (b)). A sheared rod has a modal shape of a sinusoidal function with a zero value at the bottom and a zero tangent at the free end. Similar displacement vector can be used with:

$$v_j = \sin \frac{j\pi}{2N+1}, \quad j = 1, \dots, N.$$

Displacements are shown in Fig. 1.15 (c). The numerator and the denominator of the Rayleigh quotient are:

$$\mathbf{v}^T \mathbf{M} \mathbf{v} = \sum_{j=1}^N v_j m v_j = m \sum_{j=1}^N \sin^2 \frac{j\pi}{2N+1} = m \frac{2N+1}{4} = 787.5,$$

$$\mathbf{v}^T \mathbf{K} \mathbf{v} = v_1 k v_1 + \sum_{j=2}^N (v_{j-1} k v_{j-1} - 2v_{j-1} k v_j + v_j k v_j) = v_1 k v_1 + \sum_{j=2}^N (v_j - v_{j-1})^2 k = 2931.9.$$

The Rayleigh quotient is:

$$R = \frac{\mathbf{v}^T \mathbf{K} \mathbf{v}}{\mathbf{v}^T \mathbf{M} \mathbf{v}} = \frac{2931.9}{787.5} = 3.723.$$

This will be an upper bound for the square of the first natural circular frequency:

$$\omega_{01}^2 \leq 3.723, \rightarrow \omega_{01} \leq 1.930 \text{ rad/s.}$$

Note: in this specific case the supposed shape vector was the actual first mode vector, so in this problem the accurate solution was obtained.

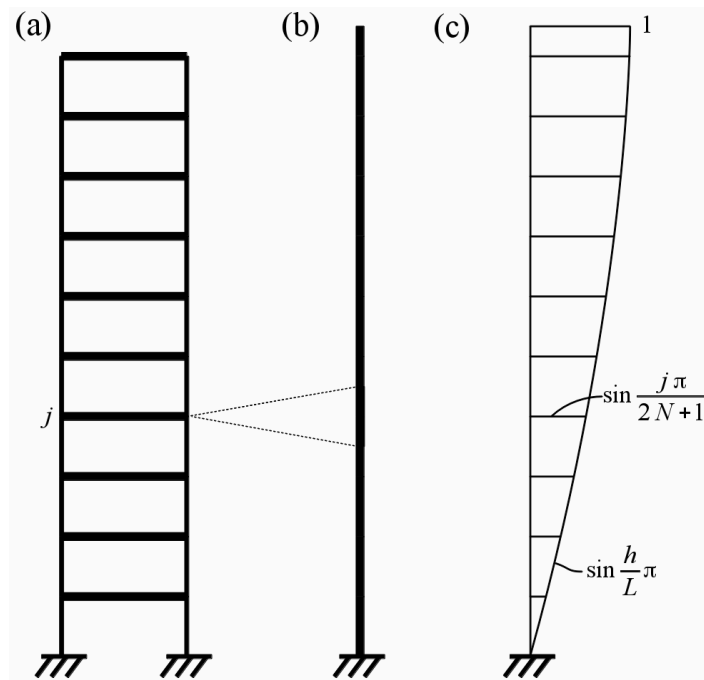


**Figure 1.15:** A 10-storey frame structure with rigid interstorey girders and elastic columns. (a) Dynamical model of the structure. (b) Equivalent continuous rod with finite shear stiffness. (c) First modal shape of the continuous rod.

### The Ritz-Rayleigh method

We have seen in the previous problems what effect the assumed shape on the accuracy of the result has. If, instead of guessing one vector, we make our trial vector as a linear combination of fixed base vectors, then the Rayleigh quotient will be a function of the coefficients of the base vectors. The first natural frequency will be equal to, or smaller than any Rayleigh quotients, so the minimum of the available values in the space of the base vectors will give an upper bound for the first natural frequency. This is the theory behind the Ritz-Rayleigh method.

We have to choose some linearly independent base vectors  $\Phi_i (i = 0, \dots, n)$  in the  $N$ -dimensional space (where  $N$  is the number of degree-of-freedom of the system), and make the trial vector as a linear combination of these vectors. (Here we call the attention, that the

inequality  $n + 1 \leq N$ , must hold, otherwise the vector  $\Phi_i$  can not make a base of the  $N$ -space.) We want to make our  $\mathbf{v}$  unique among all vectors parallel with it. We have seen, that normalizing the eigenvector to the mass matrix is a very practical way, but now it gives a nonlinear constraint to the system, and that makes difficult to use. Instead of that, we set the coefficient of one base vector ( $\Phi_i$ ) equal to one, and write the trial vector as:

$$\mathbf{v}(c_1, \dots, c_n) = \Phi_0 + \sum_{i=1}^n c_i \Phi_i.$$

Using this trial vector the Rayleigh quotient will depend on the variables  $c_1, \dots, c_n$ :

$$R(c_1, \dots, c_n) = \frac{\mathbf{v}^T(c_1, \dots, c_n) \mathbf{K} \mathbf{v}(c_1, \dots, c_n)}{\mathbf{v}^T(c_1, \dots, c_n) \mathbf{M} \mathbf{v}(c_1, \dots, c_n)}.$$

We are looking for the possible smallest  $R$  in the space of the vectors  $\Phi_1, \dots, \Phi_n$ :

$$R(c_1, \dots, c_n) = \min!$$

- *If  $n = 1$ :*

The quotient depends on one single variable. At the minimum the first derivative vanishes:

$$\frac{dR(c_1)}{dc_1} = 0. \quad (1.68)$$

The solution of the (nonlinear) equation (1.68) results in a possible best result for the trial vector coefficient  $c_1$  in the space of the base vectors.

- *If  $n > 1$ :*

The quotient depends on multiple variables. At the minimum the gradient of the quotient is zero:

$$\frac{\partial R(c_1, \dots, c_n)}{\partial c_i} = 0. \quad i = 1, \dots, n, \quad (1.69)$$

which is a nonlinear system of equations for  $n$  variables. This type of equations does not necessarily have a unique solution, thus solution method must be chosen according to this.

We mention here, that the Ritz-Rayleigh method is capable of finding the exact solution if  $n + 1 = N$ , i.e., if the base vectors  $\Phi_i (i = 0, \dots, n)$  span the whole  $N$  space. Otherwise, for the trial vector the method minimizes the error to the the exact solution, i.e. it finds the projection of the exact solution on the space spanned by the base vectors  $\Phi_i (i = 0, \dots, n)$ , and gives the corresponding Rayleigh quotient.

**Problem 1.3.4** (Exact solution of a two-storey frame). Find the exact solution for the first natural circular frequency of the two-storey structure of Problem 1.3.2.

**Solution.** Let us assume the trial vector as  $\mathbf{v}(c_1) = [1 \quad c_1]^T$ , i.e. we chose the base vectors:

$$\Phi_0 = \begin{bmatrix} 1 \\ 0 \end{bmatrix}, \quad \Phi_1 = \begin{bmatrix} 0 \\ 1 \end{bmatrix}$$

Here  $n = 1$  and  $N = 2$ , so  $1 + 1 = 2$ , i.e. we will get the exact solutions.

The numerator and the denominator of the Rayleigh quotient are:

$$\mathbf{v}^T(c_1)\mathbf{M}\mathbf{v}(c_1) = [1 \quad c_1] \begin{bmatrix} 2 & 0 \\ 0 & 2 \end{bmatrix} \begin{bmatrix} 1 \\ c_1 \end{bmatrix} = [2 \quad 2c_1] \begin{bmatrix} 1 \\ c_1 \end{bmatrix} = 2 + 2c_1^2.$$

$$\begin{aligned} \mathbf{v}^T(c_1)\mathbf{K}\mathbf{v}(c_1) &= [1 \quad c_1] \begin{bmatrix} 100 & -50 \\ -50 & 50 \end{bmatrix} \begin{bmatrix} 1 \\ c_1 \end{bmatrix} = [1 \quad c_1] \begin{bmatrix} 100 - 50c_1 \\ -50 + 50c_1 \end{bmatrix} \\ &= 100 - 100c_1 + 50c_1^2. \end{aligned}$$

The resulting Rayleigh quotient is:

$$R(c_1) = \frac{\mathbf{v}^T(c_1)\mathbf{K}\mathbf{v}(c_1)}{\mathbf{v}^T(c_1)\mathbf{M}\mathbf{v}(c_1)} = \frac{100 - 100c_1 + 50c_1^2}{2 + 2c_1^2}.$$

The first derivative is:

$$\begin{aligned} \frac{dR(c_1)}{dc_1} &= \frac{(-100 + 100c_1)(2 + 2c_1^2) - (100 - 100c_1 + 50c_1^2)(4c_1)}{(2 + 2c_1^2)^2} \\ &= \frac{200(c_1^2 - c_1 - 1)}{4(c_1^4 + 2c_1^2 + 1)} = 0 \end{aligned}$$

It is sufficient, if the nominator equals zero, so the coefficient  $c_1$  we are looking for is the solution of the quadratic equation:

$$c_1^2 - c_1 - 1 = 0.$$

There are two solutions:  $(1 + \sqrt{5})/2$  and  $(1 - \sqrt{5})/2$ . If we substitute them back to the Rayleigh quotient, the first one results the smaller number, so this will be the first mode

$$R(1.618) = 9.549 \rightarrow \omega_{01} = 3.090 \text{ rad/s,}$$

while for the second solution we get

$$R(-0.618) = 65.45 \rightarrow \omega_{01} = 8.090 \text{ rad/s.}$$

The resultant modal shape vectors are:

$$\mathbf{v}_1 = \begin{bmatrix} 1 \\ 1.618 \end{bmatrix}, \quad \mathbf{v}_2 = \begin{bmatrix} 0 \\ -0.618 \end{bmatrix}.$$

**Problem 1.3.5** (Exact solution for a three-storey structure). Find the exact solution for the first natural circular frequency of the three-storey structure of Problem 1.3.1.

**Solution.** First we repeat the matrices of the system from Problem 1.3.1:

$$\mathbf{M} = \begin{bmatrix} 150 & 0 & 0 \\ 0 & 150 & 0 \\ 0 & 0 & 150 \end{bmatrix},$$

$$\mathbf{K} = \begin{bmatrix} 50000 & -25000 & 0 \\ -25000 & 50000 & -25000 \\ 0 & -25000 & 25000 \end{bmatrix}.$$

Let us assume the trial vector as  $\mathbf{v}(c_1, c_2) = [1 \ c_1 \ c_2]^T$ , i.e. we chose the base vectors:

$$\Phi_0 = \begin{bmatrix} 1 \\ 0 \\ 0 \end{bmatrix}, \quad \Phi_1 = \begin{bmatrix} 0 \\ 1 \\ 0 \end{bmatrix}, \quad \Phi_2 = \begin{bmatrix} 0 \\ 0 \\ 1 \end{bmatrix}$$

Here  $n = 2$  and  $N = 3$ , so  $2 + 1 = 3$ , i.e. the Ritz-Rayleigh method leads to the exact solutions of the problem.

The numerator and the denominator of the Rayleigh quotient are:

$$\begin{aligned} \mathbf{v}^T(c_1, c_2)\mathbf{M}\mathbf{v}(c_1, c_2) &= [1 \ c_1 \ c_2] \begin{bmatrix} 150 & 0 & 0 \\ 0 & 150 & 0 \\ 0 & 0 & 150 \end{bmatrix} \begin{bmatrix} 1 \\ c_1 \\ c_2 \end{bmatrix} \\ &= [1 \ c_1 \ c_2] \begin{bmatrix} 150 \\ 150c_1 \\ 150c_2 \end{bmatrix} = \boxed{150(1 + c_1^2 + c_2^2)}, \end{aligned}$$

$$\begin{aligned} \mathbf{v}^T(c_1, c_2)\mathbf{K}\mathbf{v}(c_1, c_2) &= [1 \ c_1 \ c_2] \begin{bmatrix} 50000 & -25000 & 0 \\ -25000 & 50000 & -25000 \\ 0 & -25000 & 25000 \end{bmatrix} \begin{bmatrix} 1 \\ c_1 \\ c_2 \end{bmatrix} \\ &= [1 \ c_1 \ c_2] \begin{bmatrix} 50000 - 25000c_1 \\ -25000 + 50000c_1 - 25000c_2 \\ -25000c_1 + 25000c_2 \end{bmatrix} \\ &= \boxed{25000(2 - 2c_1 + 2c_1^2 - 2c_1c_2 + c_2^2)}. \end{aligned}$$

The resulting Rayleigh quotient is

$$R(c_1, c_2) = \frac{25000(2 - 2c_1 + 2c_1^2 - 2c_1c_2 + c_2^2)}{150(1 + c_1^2 + c_2^2)} \quad (1.70)$$

The first partial derivatives are:

$$\frac{\partial R(c_1, c_2)}{\partial c_1} = 0, \quad \frac{\partial R(c_1, c_2)}{\partial c_2} = 0.$$

The partial derivatives result a cumbersome system of two equations. However, the solution can be calculated numerically, resulting in the following solution pairs:

- $c_1 = 1.802, c_2 = 2.247,$
- $c_1 = 0.445, c_2 = -0.802,$
- $c_1 = -1.247, c_2 = 0.555.$

These points are on the surface defined by the Rayleigh quotient over the  $(c_1, c_2)$ -plane (see Eq. (1.70)). The shape of the surface is shown in Figure 1.16.

To decide, which one of the above three solution pairs leads to the first natural frequency, we have two options:

- We decide which one of the solution pairs correspond to the minimum point of the surface given by the function  $R(c_1, c_2)$ .
- We calculate the Rayleigh quotient with the solution points and pick the smallest one.

Either way, the smallest possible Rayleigh quotient of this problem, and so the square of the first natural circular frequency is

$$R = 33.01, \rightarrow \boxed{\omega_{01} = 5.745 \text{ rad/s}},$$

which is the same as the analytical result.

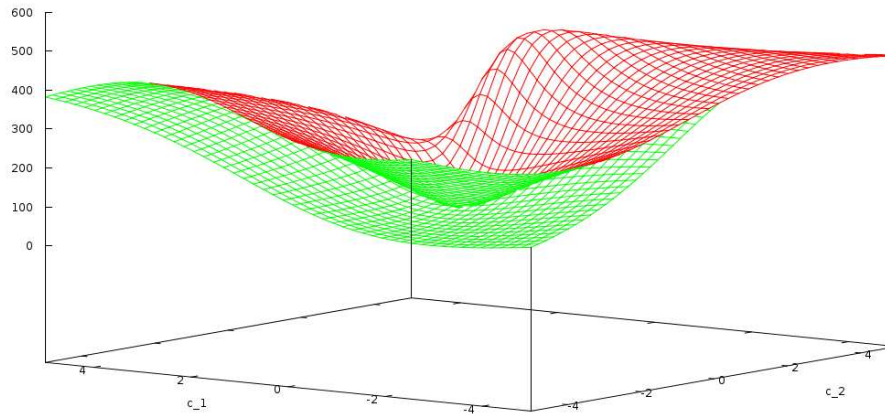


**Figure 1.16:** Rayleigh quotient of Problem 1.3.1

**Exercise 1.3.2.** Find an approximate solution of the above problem for the first natural circular frequency  $\omega_{01}$  using the base vectors:

$$\Phi_0 = \begin{bmatrix} 1 \\ 1.5 \\ 0 \end{bmatrix}, \quad \Phi_1 = \begin{bmatrix} 0 \\ 0 \\ 1 \end{bmatrix}.$$

## 1.4 Summation theorems

Let us study the undamped free vibration of a MDOF, linear mechanical system described by the matrix differential equation

$$\mathbf{M}\ddot{\mathbf{u}}(t) + \mathbf{K}\mathbf{u}(t) = \mathbf{0}.$$

It leads to the generalised eigenvalue problem

$$(\mathbf{K} - \omega_0^2 \mathbf{M}) \mathbf{u}_0 = \mathbf{0}, \quad (1.71)$$

the smallest eigenvalue of which is  $\omega_{01}^2$ , the square of the lowest natural circular frequency of the system. Here both  $\mathbf{M}$  and  $\mathbf{K}$  are constant, symmetric, real valued,  $N$ -by- $N$  matrices, called *linear, symmetric operators* in mathematics. We deal with simple models of engineering structures which are not statically overdeterminate. Then the mass matrix  $\mathbf{M}$  and the stiffness matrix  $\mathbf{K}$  are *positive definite*.<sup>1</sup> Physically it means that the kinetic and elastic energies of the structure must be positive due to any displacements.

These properties of the system allow us to make use of a few summation theorems. These theorems are used to get approximate estimates of the lowest natural circular frequency  $\omega_{01}$  of a structure by combining natural frequencies of different subproblems. Here we do not provide the reader with the proofs of the theorems, they can be found in the literature (for instance in [9]), but we show some simple examples for their applications.

### 1.4.1 Dunkerley theorem

Let us decompose the *mass matrix* as

$$\mathbf{M} = \sum_{j=1}^n \mathbf{M}_j,$$

where  $\mathbf{M}_j$  ( $j = 1, 2, \dots, n$ ). We write the generalised eigenvalue problem

$$(\mathbf{K} - \omega^2 \mathbf{M}_j) \mathbf{u} = \mathbf{0}$$

and denote its smallest eigenvalue by  $\omega_j^2$  for  $j = 1, 2, \dots, n$ .

Using these values the *Dunkerley* formula

$$\frac{1}{\omega_{01}^2} \leq \sum_{j=1}^n \frac{1}{\omega_j^2} \quad (1.72)$$

allows us to approximate the lowest natural circular frequency  $\omega_{01}$  of the original problem. From this the first natural period of vibration is

$$T_{01}^2 \leq \sum_{j=1}^n T_j^2.$$

<sup>1</sup>Matrix  $\mathbf{A}$  is positive definite if  $\mathbf{v}^T \mathbf{A} \mathbf{v} \geq \alpha \mathbf{v}^T \mathbf{v}$  for some  $\alpha > 0$ , which implies that all the eigenvalues of  $\mathbf{A}$  are positive.

This theorem states that the reciprocal of the square of the smallest natural circular frequency of the structure is not greater than the sum of reciprocals of the squares of the smallest natural circular frequencies of the same structure subjected to subsystems of the mass.

This approximation underestimates the natural circular frequency and overestimates the natural period of vibration, thus it shows the structure *softer* than in reality. The usage of this summation theorem is preferable if the structure is such that its mass can be split into parts and the natural circular frequencies of the resulting substructures are easy to compute. The application of this theorem is referred to as the “*method of split the masses*”. The closer the eigenshapes of the substructures are, the more precise this approximation is.

**Problem 1.4.1** (Estimation of the natural circular frequency using *Dunkerley* theorem). There is a clamped rod of length  $3h$  and bending stiffness  $EI$ . The total mass of the rod is concentrated at three points of the rod: mass  $m_1$  is at the free end, mass  $m_2$  is at  $h$  from the free end, and mass  $m_3$  is at  $2h$  from the free end, as it is shown in Figure 1.17 (a). Estimate the first natural circular frequency of the structure!

**Solution.** We make use of the method of split the masses. First we take  $m_2$  and  $m_3$  to be equal to zero and compute the natural circular frequency  $\omega_1$  of a clamped, massless rod with one lumped mass  $m_1$  at its top (see Figure 1.17 (b)). The compliance  $f_1$  of this structure equals to the horizontal translation of the top due to a unit force acting horizontally at the top. We compute the displacement using the theorem of virtual forces (*Castigliano's* method).

The spring stiffness  $k_1$  is the inverse of the compliance, and the square of the natural frequency is  $\omega_1^2 = k_1/m_1$ . Then, we set  $m_1$  and  $m_3$  to zero and compute the natural circular frequency  $\omega_2$  of the clamped rod with only one mass  $m_2$  at  $h$  from the top (see Figure 1.17 (c)) in a similar way. Finally,  $m_1$  and  $m_2$  are set to zero and  $\omega_3$  is computed. A brief summary of the computation is as follows:

$$\begin{aligned} f_1 &= \frac{1}{2EI} \{3h\}^2 \frac{2}{3} 3h = 9 \frac{h^3}{EI} \quad \rightarrow \quad k_1 = \frac{1}{9} \frac{EI}{h^3} \quad \rightarrow \quad \omega_1^2 = \frac{1}{9} \frac{EI}{h^3 m_1}, \\ f_2 &= \frac{1}{2EI} \{2h\}^2 \frac{2}{3} 2h = \frac{8}{3} \frac{h^3}{EI} \quad \rightarrow \quad k_2 = \frac{3}{8} \frac{EI}{h^3} \quad \rightarrow \quad \omega_2^2 = \frac{3}{8} \frac{EI}{h^3 m_2}, \\ f_3 &= \frac{1}{2EI} \{h\}^2 \frac{2}{3} h = \frac{1}{3} \frac{h^3}{EI} \quad \rightarrow \quad k_3 = 3 \frac{EI}{h^3} \quad \rightarrow \quad \omega_3^2 = 3 \frac{EI}{h^3 m_3}. \end{aligned}$$

The estimation of the first natural circular frequency of the original structure is based on (1.72):

$$\begin{aligned} \frac{1}{\omega_{01}^2} &\leq \frac{h^3}{EI} \left\{ 9m_1 + \frac{8}{3}m_2 + \frac{1}{3}m_3 \right\}, \quad \text{thus} \\ \omega_{01} &\geq \sqrt{\frac{3EI}{h^3 \{27m_1 + 8m_2 + m_3\}}}, \quad \text{and} \\ T_{01} &\leq 2\pi \sqrt{\frac{h^3 \{27m_1 + 8m_2 + m_3\}}{3EI}}. \end{aligned}$$



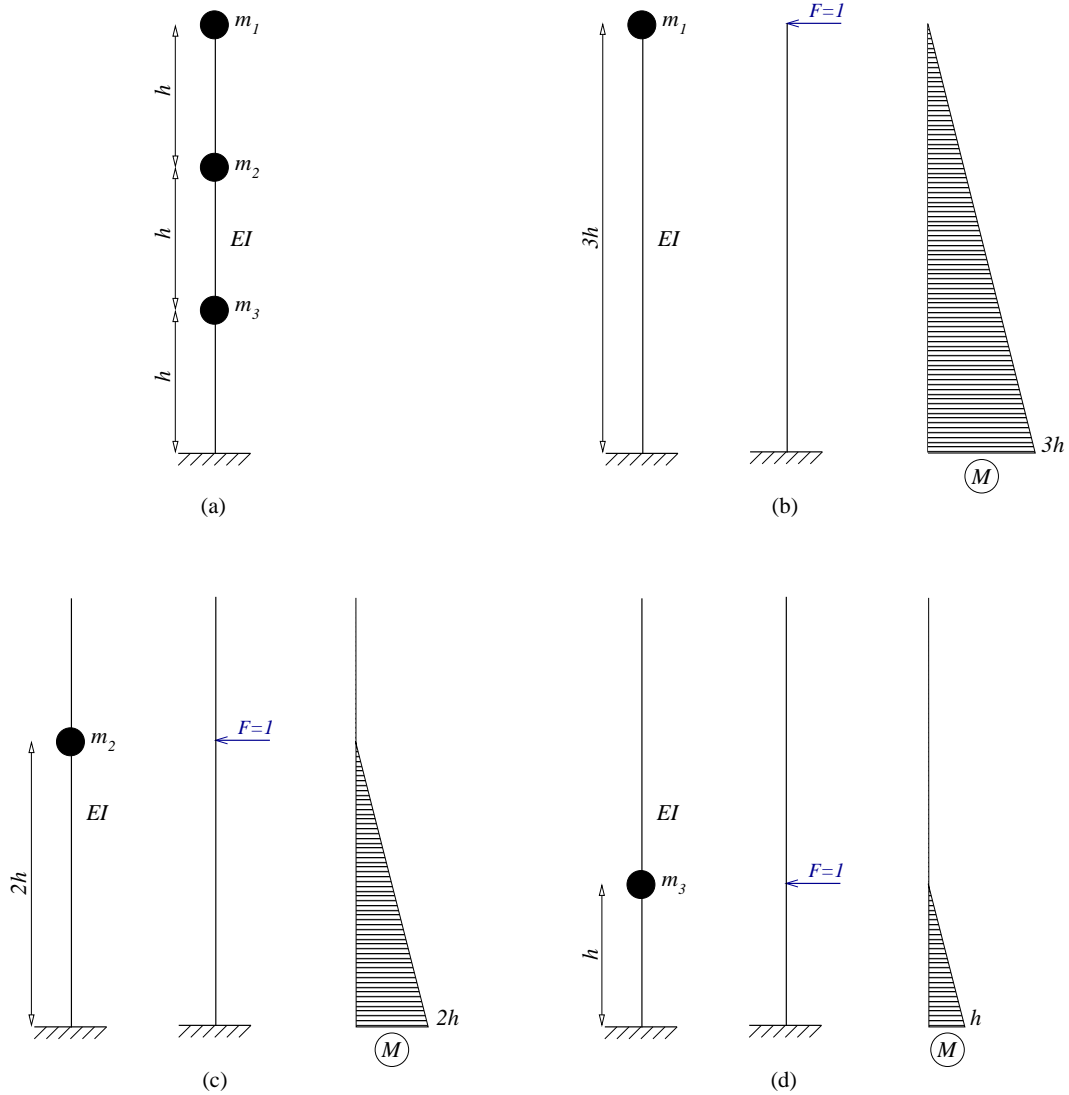


**Figure 1.17:** (a) A clamped rod of length  $3h$  and bending stiffness  $EI$  with its mass concentrated at three points of equal distances  $h$ . (b) The case when masses  $m_2$  and  $m_3$  are zero with the corresponding substructure and the bending moment diagram due to a horizontal unit force  $F = 1$  at the top. (c) The case when masses  $m_1$  and  $m_3$  are zero with the corresponding model and the bending moment diagram due to a horizontal unit force  $F = 1$  acting at  $h$  from the top. (d) The case when masses  $m_1$  and  $m_2$  are zero and the substructure with the bending moment diagram due to a unit force  $F = 1$  acting at  $2h$  from the top.

### 1.4.2 Southwell theorem

Let us write the *stiffness matrix* in the form

$$\mathbf{K} = \sum_{j=1}^n \mathbf{K}_j.$$

It is assumed that  $\mathbf{K}_j$  ( $j = 1, 2, \dots, n$ ) possesses the same properties as  $\mathbf{K}$  (i.e. symmetric and positive definite). The generalised eigenvalue problem

$$(\mathbf{K}_j - \omega^2 \mathbf{M}) \mathbf{u} = \mathbf{0}, \quad j = 1, 2, \dots, n \quad (1.73)$$

has  $N$  eigenvalues for each  $j$ . The smallest of them is denoted by  $\omega_j^2$ .

The lowest natural circular frequency  $\omega_{01}$  of the original problem can be approximated using the *Southwell* formula

$$\omega_{01}^2 \geq \sum_{j=1}^n \omega_j^2. \quad (1.74)$$

The first natural period of vibration is estimated as

$$T_{01}^2 \leq \left( \sum_{j=1}^n \frac{1}{T_j^2} \right)^{-1}.$$

Thus this formula states that if the stiffness of the structure is composed of parts, then the square of the smallest natural circular frequency of the structure is not less than the sum of the squares of the smallest natural circular frequencies corresponding to the partial stiffnesses.

The formula underestimates the natural circular frequency of the structure, i.e. the result shows the structure *softer* than in reality. We refer to this theorem as the “*effect of stiffening*”. Let a structure have  $S$  stiffness parameters. We can group these parameters into  $n$  sets. If the structure *does not become statically overdeterminate* when all but one of the stiffness parameter sets equal *zero*, then the *Southwell* theorem can be applied. Practically, we *decrease* all but the  $j$ th sets of stiffness parameters to *zero* and then compute the corresponding smallest natural circular frequency  $\omega_j$  for  $j = 1, 2, \dots, n$ . Finally, we apply the *Southwell* formula (1.74).

**Problem 1.4.2** (Estimation of the natural circular frequency using *Southwell* theorem). There is a rigid roof of mass  $m$  supported by two clamped rods of length  $h$  and bending stiffnesses  $EI_1, EI_2$ . The rods are connected to the roof through hinges and the mass of the rods is neglected. In addition, there is a linear spring of stiffness  $k$  attached to the roof. The model is shown in Figure 1.18 (a). Estimate the first natural circular frequency of the structure!

**Solution.** We apply *Southwell* theorem, since the structure is such that if we set any 2 stiffness parameters out of  $EI_1, EI_2$ , or  $k$ , to zero, then the structure remains stable. First we take  $EI_2$  and  $k$  to be equal to zero and compute the natural circular frequency  $\omega_1$  of a clamped, massless rod of length  $h$  and bending stiffness  $EI_1$  with one lumped mass  $m$  at its top (see Figure 1.18 (b) and (e)). Then, we take  $EI_1$  and  $k$  to be equal to zero and compute the natural circular frequency  $\omega_2$  of a clamped rod of length  $h$  and stiffness  $EI_2$  with the mass  $m$  at its the top (see Figure 1.18 (c) and (e)) in a very similar way. Finally,  $EI_1$  and  $EI_2$  are taken to be zero

and  $\omega_3$  is computed simply: in this case the mass  $m$  is supported by a spring of stiffness  $k$ , so  $\omega_3^2 = k/m$ . The computation of  $\omega_1^2$  and  $\omega_2^2$  briefly is

$$f_1 = \frac{1}{2EI_1} \frac{2}{3} h^3 = \frac{h^3}{3EI_1} \rightarrow k_1 = \frac{3EI_1}{h^3} \rightarrow \omega_1^2 = \frac{3EI_1}{h^3 m},$$

$$f_2 = \frac{1}{2EI_2} \frac{2}{3} h^3 = \frac{h^3}{3EI_2} \rightarrow k_2 = \frac{3EI_2}{h^3} \rightarrow \omega_2^2 = \frac{3EI_2}{h^3 m},$$

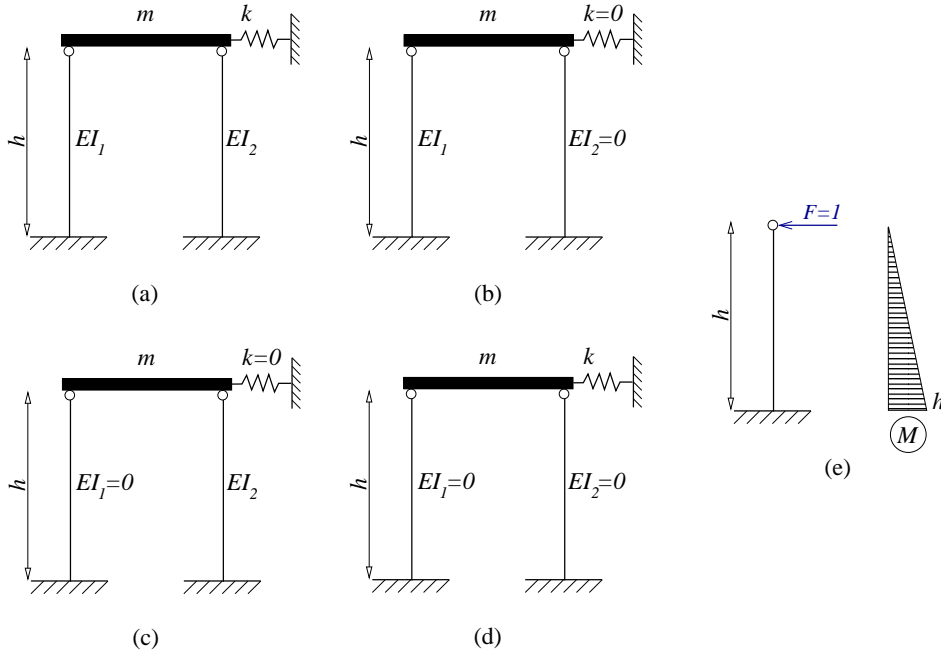


**Figure 1.18:** (a) Model of a rigid roof of mass  $m$  supported by a linear spring of stiffness  $k$  and by two clamped, massless rods of equal length  $h$  and bending stiffnesses  $EI_1$  and  $EI_2$ . (b) The case when the stiffness parameters  $EI_2$  and  $k$  are set to zero. (c) The case when  $EI_1$  and  $k$  are set to zero. (d) The case when  $EI_1$  and  $EI_2$  are taken to be zero. (e) A clamped rod of length  $h$  and its bending moment diagram due to a horizontal unit force at the top.

The estimation of the first natural circular frequency of the original structure following (1.74) is

$$\omega_{01}^2 \geq \frac{3EI_1}{h^3 m} + \frac{3EI_2}{h^3 m} + \frac{k}{m}, \quad \text{thus}$$

$$\omega_{01} \geq \sqrt{\frac{1}{m} \left\{ \frac{3}{h^3} \{EI_1 + EI_2\} + k \right\}}, \quad \text{and}$$

$$T_{01} \leq \frac{2\pi\sqrt{m}}{\frac{3}{h^3} \{EI_1 + EI_2\} + k}.$$

### 1.4.3 Föppl–Papkovich theorem

Let the eigenvector  $\mathbf{u}_0$  of (1.71) be a sum of pairwise  $K$ -orthogonal vectors  $\mathbf{u}_j$ ,  $j = 1, 2, \dots, n$ . (Vectors  $\mathbf{u}_j$  and  $\mathbf{u}_i$  are  $K$ -orthogonal if  $\mathbf{u}_j^T \mathbf{K} \mathbf{u}_i = 0$ .) Practically it means that the deformation modes of the structure are independent, i.e. the strain energy of the structure does not contain mixed terms of the deformation modes.

The smallest eigenvalues  $\omega_j^2$  of the generalised eigenvalue problems

$$(\mathbf{K} - \omega^2 \mathbf{M}) \mathbf{u}_j = \mathbf{0}, \quad j = 1, 2, \dots, n \quad (1.75)$$

are the basis of the approximation of  $\omega_{01}$ . The formula we can use is

$$\frac{1}{\omega_{01}^2} \leq \sum_{j=1}^n \frac{1}{\omega_j^2}. \quad (1.76)$$

From this the first natural period of vibration is

$$T_{01}^2 \leq \sum_{j=1}^n T_j^2.$$

This approach again shows the structure *softer* than it is.

We refer to this theorem as the “*method of split rigidities*”, or partial rigidizing. If a structure has  $S$  stiffness parameters, then we can group them into  $n$  sets. If the structure *becomes statically overdeterminate* when all but one of the stiffness parameter sets equal zero, then the Föppl–Papkovich theorem can be applied. In practice, we *increase* all but the  $j$ th sets of stiffness parameters to *infinity* and compute the corresponding smallest natural circular frequency  $\omega_j$  for  $j = 1, 2, \dots, n$ . Then we can utilise formula (1.76).

**Problem 1.4.3** (Estimation of the natural circular frequency using Föppl–Papkovich theorem). There is a massless rod of length  $h$  and bending stiffness  $EI$ . The top end of the bar is free and a mass  $m$  is attached to it, while the bottom end is connected to a fixed hinge and equipped with a linear rotational spring of stiffness  $s$ . See the model in Figure 1.19 (a). Estimate the first natural circular frequency of the structure!

**Solution.** The structure becomes statically overdeterminate if either one of its stiffness parameters ( $EI$  or  $s$ ) is set to zero. Therefore, we apply the Föppl–Papkovich theorem. First we stiffen the rotational spring, i.e. we take  $s \rightarrow \infty$ , which implies that the bar is rigidly clamped at the bottom. Now we compute the compliance  $f_1$  (the translation of the top of the bar caused by a horizontal unit force), then the stiffness is  $k_1 = 1/f_1$ , and the natural circular frequency equals to  $\omega_1^2 = k_1/m$ . See Figure 1.19 (b). Next we stiffen the bar against bending deformation, i.e.  $EI \rightarrow \infty$ . Now the rod is a rigid body capable to rotate about the hinge at the bottom end, which generates a moment in the rotational spring. The compliance  $f_2$  is the horizontal translation of the top end caused by a horizontal unit force. The moment of equilibria of the structure is  $\phi s - Fh = 0$  (assuming small displacements), as it is indicated in Figure 1.19 (c). From this, if we take  $F = 1$ , the rotation of the rigid body is  $\phi = h/s$ , and the horizontal translation of its top is  $f_2 = \phi h = h^2/s$ . (Again, we consider small displacements.) The stiffness  $k_2$  is the inverse of  $f_2$ , and  $\omega_2^2 = k_2/m$ . This computation is summarised below.

$$f_1 = \frac{1}{2EI} \frac{2}{3} h^3 = \frac{h^3}{3EI} \rightarrow k_1 = \frac{3EI}{h^3} \rightarrow \omega_1^2 = \frac{3EI}{h^3 m},$$

$$f_2 = \frac{h^2}{s} \rightarrow k_2 = \frac{s}{h^2} \rightarrow \omega_2^2 = \frac{s}{h^2 m}.$$

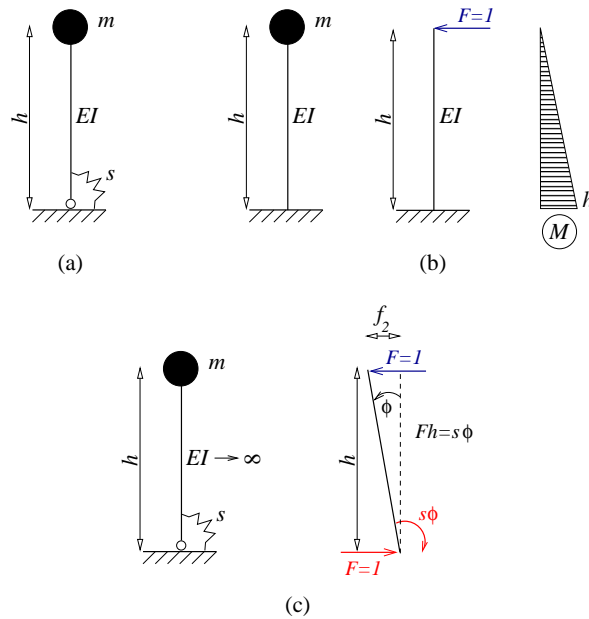


**Figure 1.19:** (a) A straight, massless rod of length  $h$  and bending stiffness  $EI$  carrying a lumped mass  $m$  at the top, connected to a fixed hinge and a rotational spring of stiffness  $s$  at the bottom. (b) The case when  $s \rightarrow \infty$  (rigidly clamped elastic rod) and the bending moment diagram due to a horizontal unit force acting at the top. (c) The case when  $EI \rightarrow \infty$  (elastically clamped rigid bar) and the free body diagram due to a horizontal unit force.

The estimation of the first natural circular frequency of the original structure using Eq. (1.76) is

$$\frac{1}{\omega_{01}^2} \leq \frac{h^3 m}{3EI} + \frac{h^2 m}{s}, \quad \text{thus}$$

$$\omega_{01} \geq \frac{1}{\sqrt{\frac{h^3 m}{3EI} + \frac{h^2 m}{s}}}, \quad \text{and}$$

$$T_{01} \leq 2\pi \sqrt{\frac{h^3 m}{3EI} + \frac{h^2 m}{s}}.$$

## Chapter 2

# Dynamics of slender continua

Main load bearing members of engineering structures often have one significant dimension: the extent of the member along this direction is larger with at least one order of magnitude than in other (orthogonal) directions. The behaviour of these *slender* members can be characterized by fewer variables, than needed for a complete three-dimensional description. In this chapter we derive the equation of motion of some specific *slender continuum rods*, give the solution for the free vibrations and, in some cases, forced vibrations are also studied.

First we collect the assumptions used hereafter for the studied rods. Since in engineering practice the most commonly used structural element is the *prismatic rod*, which is a slender, straight rod of uniform cross-sections, we restrict our investigations on this type of rods. It is assumed to be homogeneous, isotropic, and linearly elastic. We neglect the effect of damping. The axis of the rod in the stress-free state is the straight line connecting the centroids of the cross-sections. In the stress-free state, the axis of the rod coincides with axis  $x$  of a left handed *Cartesian* coordinate system (see Figure 2.1 (a)). The rod obeys the principle of planar cross-sections: during the deformation every cross-section remains plane and undistorted. The cross-section of the rod is assumed to be reflection symmetric to axis  $y$ . The displacements are considered to be small. The *length* of the studied rod is denoted by  $\ell$ , its *cross-sectional area* is  $A$ , the *second moment of the cross-section* with respect to  $z$  is  $I$ , and the *polar inertia of the cross-section* with respect to axis  $x$  is  $I_0$ . The material of the rod is characterised by: the *mass density*  $\rho$ , the *Young's modulus*  $E$ , the *shear modulus*  $G$ , and the *Poisson's ratio*  $\nu$ .<sup>1</sup> The *mass per unit length* of the rod is  $\mu = \rho A$ .

We analyse the following simple vibration modes:

- *Longitudinal vibration of prismatic bars.* The rod deforms along its axis  $x$ , while all the cross-sections remain parallel, thus their motion can be characterised by the translation  $u(x, t)$  of the rod axis. The only non-zero internal force in this case is the normal force  $N$ . A simple model is shown in Figure 2.1 (a), and free vibrations are solved using both standing and travelling waves in Section 2.1.
- *Torsional vibration of prismatic shafts.* The cross-sections of the rod rotate about axis  $x$  and this rotation is denoted by  $\varphi_x(x, t)$ . The cross-sections remain parallel. The only

<sup>1</sup>Although  $E$ ,  $G$ , and  $\nu$  are not independent:  $E = 2(1 + \nu)G$ .

non-zero internal force is the torque  $T$ . The free vibration of this structure is discussed in Section 2.2.

- *Shear vibration of prismatic beams.* The rod deforms along axis  $y$ . The non-zero internal forces in this case are the shear  $V$  and the bending moment  $M$ , but the rod is assumed to be *unbendable*. Thus all the cross-sections remain parallel, their motion can be described by the translation  $v(x, t)$  of the rod axis. A simple model is shown in Figure 2.2 (a), and the solution of the free vibration is given in Section 2.3.
- *Transverse vibration of prismatic beams.* The rod axis translates along  $y$  and the cross-sections rotate about axis  $z$ . The translation and the rotation are denoted by  $v(x, t)$  and  $\varphi(x, t)$ , respectively. The non-zero internal forces in this case are the shear  $V$  and the bending moment  $M$ , but rod is assumed to be *unshearable*, therefore  $v(x, t)$  and  $\varphi(x, t)$  are not independent. A simple model is shown in Figure 2.4 (a), and a thorough vibration analysis is given in Section 2.4.

## 2.1 Longitudinal vibration of prismatic bars

In this section we analyse the longitudinal vibrations of the prismatic bar, and introduce the general steps of any continuous modeling.

In the stress-free state, the axis of the bar coincides with axis  $x$  of a left handed *Cartesian* coordinate system. There is a longitudinal distributed load  $q_n(x, t)$  acting in the axis of the bar (see Figure 2.1 (a)). If we restrict buckling, then these conditions imply that the bar undergoes a rectilinear vibration: the motion of each cross-section of the bar occurs parallel to axis  $x$ .

The only displacement is characterized by the translation  $u(x, t)$  of the centroid of the cross-sections. The deformation of the bar is the normal strain  $\varepsilon_x(x, t)$ : the relative displacement of two "neighbouring" cross-sections. Assuming small displacements, its value is:

$$\varepsilon_x(x, t) = \frac{\partial u(x, t)}{\partial x}.$$

Since the prismatic bar has planar and homogeneous cross-sections, the relationship between the internal stress (normal stress,  $\sigma_x(x, t)$ ) and internal force (normal force,  $N(x, t)$ ) is:

$$N(x, t) = \sigma_x(x, t)A,$$

where  $A$  is the cross-sectional area. The linear elastic material response provides the material equation (*Hooke's law*):

$$\sigma_x(x, t) = E\varepsilon_x(x, t),$$

where  $E$  is the elastic (*Young's*) modulus of the material. Summarizing the above kinematical, equilibrium and material equations yield:

$$N(x, t) = EA \frac{\partial u(x, t)}{\partial x}. \quad (2.1)$$

### 2.1.1 Differential equation of motion

We derive the equation of motion for an elementary segment of the bar. Figure 2.1 (b) shows this small segment of length  $\Delta x$  between the coordinates  $x$  and  $x + \Delta x$ . We assume  $\Delta x$  to be sufficiently small, hence the change of  $q_n(x)$  and the acceleration  $\partial^2 u(x, t)/\partial t^2$  along  $\Delta x$  can be neglected.

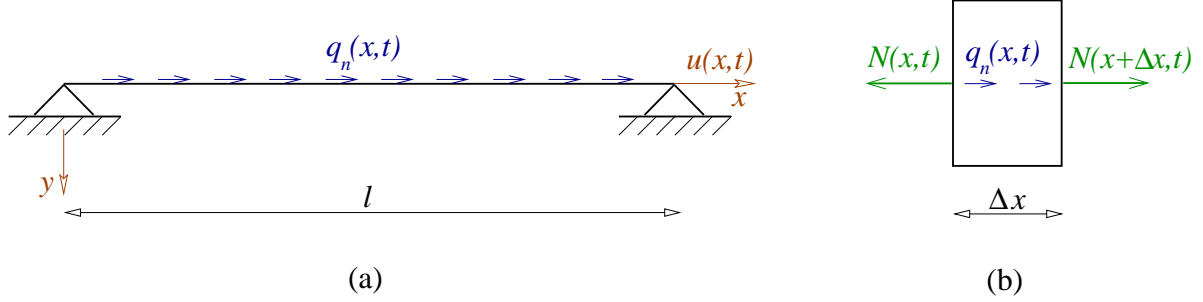


**Figure 2.1:** Sketch of (a) a prismatic bar subjected to a longitudinal distributed load  $q_n(x, t)$  and (b) a bar element of length  $\Delta x$  subjected to the internal forces and the distributed load. (The deformation of the bar element is neglected due to the small displacements.)

We write *Newton's* second law of motion for this segment:

$$\mu \Delta x \frac{\partial^2 u(x, t)}{\partial t^2} = q_n(x, t) \Delta x - N(x, t) + N(x + \Delta x, t). \quad (2.2)$$

We write a *Taylor* expansion of  $N(x, t)$  around  $x$

$$N(x + \Delta x, t) = N(x, t) + \frac{\partial N(x, t)}{\partial x} \Delta x + \mathcal{O}(\Delta x^2)$$

and substitute it into Eq. (2.2):

$$\mu \Delta x \frac{\partial^2 u(x, t)}{\partial t^2} = q_n(x, t) \Delta x - N(x, t) + N(x, t) + \frac{\partial N(x, t)}{\partial x} \Delta x + \mathcal{O}(\Delta x^2).$$

The symbol  $\mathcal{O}(\Delta x^2)$  means, that those parts are in the order of magnitude of  $\Delta x^2$ . We simplify the above equation as

$$\mu \Delta x \frac{\partial^2 u(x, t)}{\partial t^2} = q_n(x, t) \Delta x + \frac{\partial N(x, t)}{\partial x} \Delta x + \mathcal{O}(\Delta x^2),$$

and divide both sides by  $\Delta x$ . If we take the limit  $\Delta x \rightarrow 0$  of both sides, then the term  $\mathcal{O}(\Delta x^2)/\Delta x$  vanishes, resulting in:

$$\mu \frac{\partial^2 u(x, t)}{\partial t^2} = q_n(x, t) + \frac{\partial N(x, t)}{\partial x}.$$

We substitute Eq. (2.1) into the above equation

$$\mu \frac{\partial^2 u(x, t)}{\partial t^2} = q_n(x, t) + EA \frac{\partial^2 u(x, t)}{\partial x^2}, \quad (2.3)$$



rearrange it, and introduce the new quantity  $c_n^2 = EA/\mu$ :

$$\boxed{\frac{\partial^2 u(x, t)}{\partial t^2} - c_n^2 \frac{\partial^2 u(x, t)}{\partial x^2} = \frac{q_n(x, t)}{\mu}}. \quad (2.4)$$

Equation (2.4) is the differential equation of the longitudinal vibration of the prismatic bar. The quantity

$$c_n = \sqrt{\frac{E}{\rho}} \quad (2.5)$$

is the *velocity of the travelling longitudinal waves*.

### 2.1.2 Free longitudinal vibration

The solution of the differential equation of motion of a continuous system consists of two parts. The complementary equation of (2.4) has the same left hand side, but the right hand side is zero: it is a *homogeneous* differential equation. The solution of this equation gives the free longitudinal vibration. Then a particular solution of the *non-homogeneous* equation (2.4) can also be obtained. The sum of these solutions (i.e. the homogeneous and the non-homogeneous) is the *complete solution*, which must fulfill the initial conditions through the free parameters of the homogeneous solution.

For longitudinal vibrations, we show only the solution of the homogeneous differential equation

$$\boxed{\frac{\partial^2 u(x, t)}{\partial t^2} - c_n^2 \frac{\partial^2 u(x, t)}{\partial x^2} = 0}, \quad (2.6)$$

thus we deal only with the free vibration of the bar. There exists two methods for finding the nontrivial solution (i.e.  $u(x, t) \neq 0$ ) of Eq. (2.6):

- solution with standing waves,
- solution with travelling waves.

We will show the solution for a bar of length  $\ell$  with fixed-fixed ends (i.e. with boundary conditions  $u(0, t) = u(\ell, t) = 0$ ) using the standing-wave method first. In this case we separate the variables and seek the solution of the form:

$$u(x, t) = \hat{u}(x) (a \cos(\omega_0 t) + b \sin(\omega_0 t)). \quad (2.7)$$

We substitute the above *Ansatz* into Eq. (2.6):

$$\left\{ -\omega_0^2 \hat{u}(x) - c_n^2 \frac{d^2 \hat{u}(x)}{dx^2} \right\} (a \cos(\omega_0 t) + b \sin(\omega_0 t)) = 0.$$

The harmonic part  $(a \cos(\omega_0 t) + b \sin(\omega_0 t))$  is not zero for all time instant  $t$  (unless  $a = b = 0$ , which is the trivial solution  $u(x, t) = 0$ ), so we have to solve the equation:

$$\omega_0^2 \hat{u}(x) + c_n^2 \frac{d^2 \hat{u}(x)}{dx^2} = 0. \quad (2.8)$$

Now we assume the solution of Eq. (2.8) has the harmonic form:

$$\hat{u}(x) = A \sin\left(\frac{\psi_0}{\ell}x\right) + B \cos\left(\frac{\psi_0}{\ell}x\right).$$

If we substitute the above formula and its second derivate with respect to  $x$  back into Eq. (2.8), then we get

$$\omega_0^2 \hat{u}(x) - c_n^2 \left(\frac{\psi_0}{\ell}\right)^2 \hat{u}(x) = 0,$$

which results in the relationship:

$$\omega_0 = c_n \frac{\psi_0}{\ell}.$$

The value of  $\omega_0$ ,  $\psi_0$ , and the ratio of  $A$  to  $B$  depends on the boundary conditions.

In our example the bar is fixed at its both ends, thus  $u(0, t) = 0 \rightarrow \hat{u}(0) = 0$  and  $u(\ell, t) = 0 \rightarrow \hat{u}(\ell) = 0$ , according to (2.7). Therefore  $\hat{u}(0) = 0$  implies

$$\hat{u}(0) = A \sin\left(\frac{\psi_0}{\ell}0\right) + B \cos\left(\frac{\psi_0}{\ell}0\right) = 0 \rightarrow B = 0,$$

and using this result on the other end-condition  $\hat{u}(\ell) = 0$  yields

$$\hat{u}(\ell) = A \sin\left(\frac{\psi_0}{\ell}\ell\right) = 0 \rightarrow \sin(\psi_0) = 0.$$

This second constraint holds in the trivial case ( $\psi_0 = 0$ ) and in the case  $\psi_{0j} = j\pi$  for any positive integer  $j$ . So the shape of the bar during the free vibration will be the sum of sinusoidal wave-functions. Different shapes exhibit different natural circular frequencies:

$$\omega_{0j} = \frac{j\pi c_n}{\ell}.$$

The solution of the free vibration is:

$$u(x, t) = \sum_{j=1}^{\infty} \sin\frac{j\pi x}{\ell} \left( a_j \cos\frac{j\pi c_n t}{\ell} + b_j \sin\frac{j\pi c_n t}{\ell} \right), \quad (2.9)$$

with infinitely many parameters  $a_j$  and  $b_j$ , which must be determined from the initial conditions.

We note that using the trigonometric identities

$$\begin{aligned} \sin \alpha \sin \beta &= \frac{\cos(\alpha - \beta) - \cos(\alpha + \beta)}{2}, & \cos \alpha \cos \beta &= \frac{\cos(\alpha - \beta) + \cos(\alpha + \beta)}{2} \\ \sin \alpha \cos \beta &= \frac{\sin(\alpha - \beta) + \sin(\alpha + \beta)}{2} \end{aligned} \quad (2.10)$$

we can reformulate (2.9) as

$$\begin{aligned}
 u(x, t) &= \sum_{j=1}^{\infty} \frac{a_j}{2} \left[ \sin \left\{ \frac{j\pi}{\ell} (x - c_n t) \right\} + \sin \left\{ \frac{j\pi}{\ell} (x + c_n t) \right\} \right] \\
 &\quad + \frac{b_j}{2} \left[ \cos \left\{ \frac{j\pi}{\ell} (x - c_n t) \right\} - \cos \left\{ \frac{j\pi}{\ell} (x + c_n t) \right\} \right] \\
 &= \sum_{j=1}^{\infty} \frac{a_j}{2} \sin \left\{ \frac{j\pi}{\ell} (x + c_n t) \right\} - \frac{b_j}{2} \cos \left\{ \frac{j\pi}{\ell} (x + c_n t) \right\} \\
 &\quad + \frac{a_j}{2} \sin \left\{ \frac{j\pi}{\ell} (x - c_n t) \right\} + \frac{b_j}{2} \cos \left\{ \frac{j\pi}{\ell} (x - c_n t) \right\},
 \end{aligned}$$

or, using (A.11), as

$$\begin{aligned}
 u(x, t) &= \sum_{j=1}^{\infty} \frac{\sqrt{a_j^2 + b_j^2}}{2} \left[ \sin \left\{ \frac{j\pi}{\ell} (x + c_n t) - \operatorname{arccot} \frac{a_j}{b_j} \right\} \right. \\
 &\quad \left. + \cos \left\{ \frac{j\pi}{\ell} (x - c_n t) - \operatorname{arccot} \frac{b_j}{a_j} \right\} \right].
 \end{aligned}$$

The above forms coincide with the outcome of the *travelling-wave method*, discussed in details in Appendix A.1.

### 2.1.3 Forced longitudinal vibration: kinematic loading

Let us study a bar fixed at the far end and vibrated at the starting end harmonically in time following  $f(\omega t)$ . There is not any force load on the bar, thus  $q_n(x, t) = 0$  and we have to solve (2.6) with boundary conditions

$$u(0, t) = f(\omega t), \quad u(\ell, t) = 0. \quad (2.11)$$

Assuming that the response of the bar is also harmonic in time we can separate the spatial and temporal variables as

$$u(x, t) = \hat{u}(x)f(\omega t).$$

**The harmonic function is**  $f(\omega t) = \cos(\omega t)$

In the case of  $f(\omega t) = \cos(\omega t)$  Eq. (2.6) becomes

$$\left\{ -\omega^2 \hat{u}(x) - c_n^2 \frac{d^2 \hat{u}(x)}{dx^2} \right\} \cos(\omega t) = 0,$$

yielding the solution

$$\hat{u}(x) = A \cos \left( \frac{\omega}{c_n} x \right) + B \sin \left( \frac{\omega}{c_n} x \right).$$

The constants  $A$  and  $B$  are computed from the boundary conditions (2.11):

$$\begin{aligned}\hat{u}(0) &= A = 1, \\ \hat{u}(\ell) &= \cos\left(\frac{\omega}{c_n}\ell\right) + B \sin\left(\frac{\omega}{c_n}\ell\right) = 0 \quad \rightarrow \quad B = -\cot\left(\frac{\omega}{c_n}\ell\right).\end{aligned}$$

Therefore, the solution of the forced vibration is:

$$u(x, t) = \left\{ \cos\left(\frac{\omega}{c_n}x\right) - \cot\left(\frac{\omega}{c_n}\ell\right) \sin\left(\frac{\omega}{c_n}x\right) \right\} \cos(\omega t). \quad (2.12)$$

This is the solution in a standing-wave form. However, we can again use trigonometric identities (2.10) to write a travelling-wave form:

$$\begin{aligned}u(x, t) &= \hat{u}(x) \cos(\omega t) = \left\{ A \cos\left(\frac{\omega}{c_n}x\right) + B \sin\left(\frac{\omega}{c_n}x\right) \right\} \cos(\omega t) \\ &= \frac{A}{2} \left[ \cos\left\{\frac{\omega}{c_n}(x - c_n t)\right\} + \cos\left\{\frac{\omega}{c_n}(x + c_n t)\right\} \right] \\ &\quad + \frac{B}{2} \left[ \sin\left\{\frac{\omega}{c_n}(x - c_n t)\right\} + \sin\left\{\frac{\omega}{c_n}(x + c_n t)\right\} \right] \\ &= \frac{1}{2} \left[ A \cos\left\{\frac{\omega}{c_n}(x + c_n t)\right\} + B \sin\left\{\frac{\omega}{c_n}(x + c_n t)\right\} \right] \\ &\quad + \frac{1}{2} \left[ A \cos\left\{\frac{\omega}{c_n}(x - c_n t)\right\} + B \sin\left\{\frac{\omega}{c_n}(x - c_n t)\right\} \right],\end{aligned}$$

which, using the calculated constants  $A$  and  $B$  yields

$$\begin{aligned}u(x, t) &= \frac{1}{2} \left[ \cos\left\{\frac{\omega}{c_n}(x + c_n t)\right\} - \cot\left(\frac{\omega}{c_n}\ell\right) \sin\left\{\frac{\omega}{c_n}(x + c_n t)\right\} \right] \\ &\quad + \frac{1}{2} \left[ \cos\left\{\frac{\omega}{c_n}(x - c_n t)\right\} - \cot\left(\frac{\omega}{c_n}\ell\right) \sin\left\{\frac{\omega}{c_n}(x - c_n t)\right\} \right].\end{aligned}$$

The above form can be compacted using the trigonometric identity (A.11):

$$u(x, t) = \frac{\sqrt{1 + \cot^2\left(\frac{\omega}{c_n}\ell\right)}}{2} \left[ -\sin\left\{\frac{\omega}{c_n}(x - \ell + c_n t)\right\} - \sin\left\{\frac{\omega}{c_n}(x - \ell - c_n t)\right\} \right]. \quad (2.13)$$

**The harmonic function is**  $f(\omega t) = \sin(\omega t)$

Now Eq. (2.6) is

$$\left\{ -\omega^2 \hat{u}(x) - c_n^2 \frac{d^2 \hat{u}(x)}{dx^2} \right\} \sin(\omega t) = 0,$$

yielding again

$$\hat{u}(x) = A \cos\left(\frac{\omega}{c_n}x\right) + B \sin\left(\frac{\omega}{c_n}x\right).$$

The constants  $A$  and  $B$  are computed from the boundary conditions (2.11):

$$\begin{aligned}\hat{u}(0) &= A = 1, \\ \hat{u}(\ell) &= \cos\left(\frac{\omega}{c_n}\ell\right) + B \sin\left(\frac{\omega}{c_n}\ell\right) = 0 \quad \rightarrow \quad B = -\cot\left(\frac{\omega}{c_n}\ell\right).\end{aligned}$$

Therefore, the solution of the forced vibration is:

$$u(x, t) = \left\{ \cos\left(\frac{\omega}{c_n}x\right) - \cot\left(\frac{\omega}{c_n}\ell\right) \sin\left(\frac{\omega}{c_n}x\right) \right\} \sin(\omega t). \quad (2.14)$$

This is the solution in a standing-wave form. We can again use trigonometric identities (2.10) to rewrite a (general) travelling-wave form:

$$\begin{aligned}u(x, t) &= \hat{u}(x) \sin(\omega t) = \left\{ A \cos\left(\frac{\omega}{c_n}x\right) + B \sin\left(\frac{\omega}{c_n}x\right) \right\} \sin(\omega t) \\ &= \frac{A}{2} \left[ -\sin\left\{\frac{\omega}{c_n}(x - c_n t)\right\} + \sin\left\{\frac{\omega}{c_n}(x + c_n t)\right\} \right] \\ &\quad + \frac{B}{2} \left[ \cos\left\{\frac{\omega}{c_n}(x - c_n t)\right\} - \cos\left\{\frac{\omega}{c_n}(x + c_n t)\right\} \right] \\ &= \frac{1}{2} \left[ -B \cos\left\{\frac{\omega}{c_n}(x + c_n t)\right\} + A \sin\left\{\frac{\omega}{c_n}(x + c_n t)\right\} \right] \\ &\quad + \frac{1}{2} \left[ B \cos\left\{\frac{\omega}{c_n}(x - c_n t)\right\} - A \sin\left\{\frac{\omega}{c_n}(x - c_n t)\right\} \right],\end{aligned}$$

which, using the appropriate  $A$  and  $B$  yields

$$\begin{aligned}u(x, t) &= \frac{1}{2} \left[ \cot\left(\frac{\omega}{c_n}\ell\right) \cos\left\{\frac{\omega}{c_n}(x + c_n t)\right\} + \sin\left\{\frac{\omega}{c_n}(x + c_n t)\right\} \right] \\ &\quad - \frac{1}{2} \left[ \cot\left(\frac{\omega}{c_n}\ell\right) \cos\left\{\frac{\omega}{c_n}(x - c_n t)\right\} + \sin\left\{\frac{\omega}{c_n}(x - c_n t)\right\} \right].\end{aligned}$$

The above form can be compacted using the trigonometric identity (A.10):

$$u(x, t) = \frac{\sqrt{1 + \cot^2\left(\frac{\omega}{c_n}\ell\right)}}{2} \left[ \cos\left\{\frac{\omega}{c_n}(x - \ell + c_n t)\right\} - \cos\left\{\frac{\omega}{c_n}(x - \ell - c_n t)\right\} \right]. \quad (2.15)$$

## 2.2 Free torsional vibration of prismatic shafts

In this section we discuss the torsional vibration of a straight shaft with rigid circular cross-sections of radius  $R$ . The length of the shaft is  $\ell$ , its mass per unit length is  $\mu = \rho R^2 \pi$ . The only displacement the cross-sections undergo is the rotation  $\varphi_x(x, t)$  about the shaft axis  $x$ . The twist  $\kappa_x(x, t)$  is the first derivative of the rotation with respect to  $x$ :

$$\kappa_x(x, t) = \frac{\partial \varphi_x(x, t)}{\partial x}. \quad (2.16)$$

This twist induces shear strain in the shaft. We assume a linear elastic material, so the torque  $T(x, t)$  can be written as:

$$T(x, t) = GI_0\kappa_x(x, t). \quad (2.17)$$

Here  $G$  is the shear modulus of the material and  $I_0 = R^4\pi/2$  is the polar inertia of the cross-section with respect to the axis of rotation  $x$ .

We take a short segment  $\Delta x$  of the shaft at coordinate  $x$ , with the torque at both ends  $T(x, t)$  and  $T(x + \Delta x, t)$ , respectively. The theorem of angular momentum can be written for this segment as:

$$T(x + \Delta x, t) - T(x, t) = \hat{I}_0 \frac{\partial^2 \varphi_x(x, t)}{\partial t^2}. \quad (2.18)$$

Here  $\hat{I}_0 = (\mu\Delta x) R^2/2$  is the kinetic inertia of the segment, and  $\partial^2 \varphi_x(x, t)/\partial t^2$  is its angular acceleration.

$T(x + \Delta x, t)$  can be approximated by its Taylor series with respect to  $x$ :

$$T(x + \Delta x, t) = T(x, t) + \frac{\partial T(x, t)}{\partial x} \Delta x + \mathcal{O}(\Delta x^2).$$

Substituting this approximation into the equation of motion (2.18) we get:

$$\frac{\partial T(x, t)}{\partial x} \Delta x + \mathcal{O}(\Delta x^2) = \frac{(\rho R^2 \pi \Delta x) R^2}{2} \frac{\partial^2 \varphi_x(x, t)}{\partial t^2}.$$

Now we substitute the material equation (2.17) and the kinematical equation (2.16) into the above equation, and divide both sides by  $\Delta x$ , then calculate the limit as  $\Delta x \rightarrow 0$ . A few simplification results in:

$$G \frac{\partial^2 \varphi_x(x, t)}{\partial x^2} = \rho \frac{\partial^2 \varphi_x(x, t)}{\partial t^2}.$$

Introducing the *velocity of shear waves*

$$c_s = \sqrt{\frac{G}{\rho}} \quad (2.19)$$

we can write the differential equation of the free torsional vibration of prismatic shafts:

$$\boxed{\frac{\partial^2 \varphi_x(x, t)}{\partial t^2} - c_s^2 \frac{\partial^2 \varphi_x(x, t)}{\partial x^2} = 0}. \quad (2.20)$$

This is a PDE with similar structure as the PDE (2.6) of the free longitudinal vibration, so the solution methods are the same.

## 2.3 Shear vibration of prismatic beams

In this section we analyse the planar vibration of a beam which is inextensional, unbendable, but *shearable*. Considering small displacements the only deformation of the cross-sections of the beam is the translation  $v(x, t)$  parallel to axis  $y$  (see Figure 2.2 (a)).

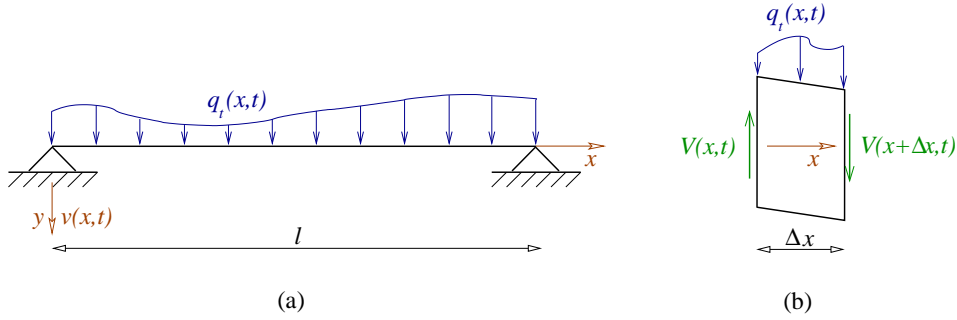


**Figure 2.2:** (a) Sketch of an inextensional, unbendable prismatic beam subjected to a transverse distributed load  $q_t(x, t)$ . (b) A beam element of length  $\Delta x$  subjected to the internal forces and the distributed load. (Internal bending moment is not indicated.)

The material is linearly elastic and homogeneous. Hence, according to *Hooke's* law, the connection between the shear strain  $\gamma_{xy}$  and the shear stress  $\tau_{xy}$  is:

$$\tau_{xy} = G\gamma_{xy}.$$

Here  $G$  is the *shear modulus* of the material which can be computed from the *Young's* modulus  $E$  and *Poisson's* ratio  $\nu$  as

$$G = \frac{E}{2(1 + \nu)}.$$

Since the *Poisson's* ratio  $\nu$  must be between 0 and 0.5, the shear modulus is between one-third and one-half of the *Young's* modulus:  $G = E/3 \sim E/2$ .

According to earlier studies, the distribution of shear stress  $\tau_{xy}$  is constant along the width, but quadratic along the height of the cross-section [2]. Therefore, the shear strain  $\gamma_{xy}$  is also quadratic in  $y$ . That would violate the principle of planar cross-sections, so based on *Timoshenko's* method [10], we introduce the effective shear area  $A_{\text{eff}}$  of the cross-section. The ratio  $k_s$  of the effective shear area  $A_{\text{eff}}$  to the area  $A$

$$k_s = \frac{A_{\text{eff}}}{A}$$

is called the *shear correction factor*. For instance,  $k_s = 5/6$  for a rectangular cross-section, while  $k_s = 0.9$  for a circular shaft. In this manner, the elastic energy accumulating in a beam element computed with the quadratic stress and strain distributions equals to the elastic energy computed with constant strain  $\bar{\gamma}_{xy}$  and stress

$$\bar{\tau}_{xy} = G\bar{\gamma}_{xy}$$

distributions. For small displacements the shear strain  $\bar{\gamma}_{xy}$  of a beam element is:

$$\bar{\gamma}_{xy}(x, t) = \frac{\partial v(x, t)}{\partial x}.$$

On any cross-section of the beam the resultant of the shear stress  $\bar{\tau}_{xy}$  must be equal to the (internal) shear force  $V(x, t)$ , thus

$$V(x, t) = \bar{\tau}_{xy}(x, t)k_s A.$$

If we combine the above relationships, then the following equality is obtained:

$$\boxed{V(x, t) = k_s GA \frac{\partial v(x, t)}{\partial x}}. \quad (2.21)$$

Here  $k_s GA$  is the *shear stiffness* of the beam.

### 2.3.1 Differential equation of motion

We write *Newton's* second law of motion along direction  $y$  on a small beam element of length  $\Delta x$  (see Figure 2.2 (b)):

$$q_t(x, t)\Delta x - V(x, t) + V(x + \Delta x, t) = \mu\Delta x \frac{\partial^2 v(x, t)}{\partial t^2}. \quad (2.22)$$

The *Taylor* expansion of the shear force  $V(x, t)$  around  $x$  is

$$V(x + \Delta x, t) = V(x, t) + \frac{\partial V(x, t)}{\partial x} \Delta x + \mathcal{O}(\Delta x^2). \quad (2.23)$$

After substituting this expansion into Eq. (2.22) and doing some simplification we can write

$$q_t(x, t)\Delta x + \frac{\partial V(x, t)}{\partial x} \Delta x + \mathcal{O}(\Delta x^2) = \mu\Delta x \frac{\partial^2 v(x, t)}{\partial t^2}.$$

Dividing both sides by  $\Delta x$  and taking  $\Delta x \rightarrow 0$  leads to

$$q_t(x, t) + \frac{\partial V(x, t)}{\partial x} = \mu \frac{\partial^2 v(x, t)}{\partial t^2}. \quad (2.24)$$

Finally we substitute Eq. (2.21) in the above equality to obtain

$$q_t(x, t) + k_s GA \frac{\partial^2 v(x, t)}{\partial x^2} = \mu \frac{\partial^2 v(x, t)}{\partial t^2},$$

which is the second order partial differential equation of shear vibration of the unbendable beam. If we introduce the velocity of shear waves

$$\boxed{c_s = \sqrt{\frac{GA}{\mu}} = \sqrt{\frac{G}{\rho}}}, \quad (2.25)$$

then PDE (2.24) divided by  $\mu$  yields the simple form

$$\boxed{\frac{\partial^2 v(x, t)}{\partial t^2} - k_s c_s^2 \frac{\partial^2 v(x, t)}{\partial x^2} = \frac{q_t(x, t)}{\mu}}. \quad (2.26)$$

Formally it is the same PDE as (2.4), except for the coefficient here is  $k_s c_s^2$  instead of  $c_n^2$ , and that the unknown function is the vertical translation  $v(x, t)$  instead of the longitudinal translation  $u(x, t)$  of the axis. Therefore, the solution of (2.26) follows identical derivation as of the solution of (2.4). When pure shear vibration is needed in structural design is the case of the vibration of fixed-free shearable beams. It is often used to approximate the dynamical behaviour of high buildings with rigid slabs and elastic columns. Hence we shortly study the free shear vibration of a fixed-free beam.



### 2.3.2 Free vibration of a fixed-free beam

The complementary part of (2.26) is the homogeneous second order PDE

$$\frac{\partial^2 v(x, t)}{\partial t^2} - k_s c_s^2 \frac{\partial^2 v(x, t)}{\partial x^2} = 0, \quad (2.27)$$

which governs the free shear vibration of the beam. Using the concept of standing waves, we assume that the solution of (2.27) is of the separated form

$$v(x, t) = \hat{v}(x) \cdot \{a \cos(\omega_0 t) + b \sin(\omega_0 t)\}. \quad (2.28)$$

Substituting the above expression into (2.27) yields

$$\left\{ -\omega_0^2 \hat{v}(x) - k_s c_s^2 \frac{d^2 \hat{v}(x)}{dx^2} \right\} \cdot \{a \cos(\omega_0 t) + b \sin(\omega_0 t)\},$$

which is fulfilled for any time instant  $t$  if the *second order ODE*

$$k_s c_s^2 \frac{d^2 \hat{v}(x)}{dx^2} + \omega_0^2 \hat{v}(x) = 0 \quad (2.29)$$

holds. From previous mathematical studies [1], the above ODE has the solution of

$$\hat{v}(x) = A \cos\left(\frac{\omega_0}{\sqrt{k_s c_s}} x\right) + B \sin\left(\frac{\omega_0}{\sqrt{k_s c_s}} x\right). \quad (2.30)$$

Here the coefficients  $A$  and  $B$  can be computed from two *boundary conditions* of the beam. For the studied fixed-free beam we can write the following boundary conditions:

$$v(0, t) = 0, \quad V(\ell, t) = k_s G A \frac{\partial v(x, t)}{\partial x} \Big|_{x=\ell} = 0, \quad (2.31)$$

i.e. the translation of the fixed end of the beam is restricted and the shear force at the free end of the beam is zero. It can be easily seen from Eq. (2.27) that

$$\begin{aligned} \hat{v}(0) = 0 & \text{ implies } v(0, t) = 0 \text{ and} \\ \frac{d\hat{v}(x)}{dx} \Big|_{x=\ell} = 0 & \text{ implies } \frac{\partial v(x, t)}{\partial x} \Big|_{x=\ell} = 0. \end{aligned}$$

It follows from the above statements, Eq. (2.30), and Eq. (2.31) that

$$\begin{aligned} \hat{v}(0) &= A \cos(0) + B \sin(0) = 0 \\ &\rightarrow A = 0, \\ \frac{d\hat{v}(x)}{dx} \Big|_{x=\ell} &= \frac{\omega_0}{\sqrt{k_s c_s}} \left\{ -A \sin\left(\frac{\omega_0}{\sqrt{k_s c_s}} \ell\right) + B \cos\left(\frac{\omega_0}{\sqrt{k_s c_s}} \ell\right) \right\} = 0 \\ &\rightarrow B \cos\left(\frac{\omega_0}{\sqrt{k_s c_s}} \ell\right) = 0. \end{aligned}$$

The last equality fulfills either if  $B = 0$  (which corresponds to a straight beam, no vibration) or if the natural circular frequency equals any of the following values:

$$\omega_{0r} = \frac{\sqrt{k_s c_s}}{\ell} \left\{ r\pi - \frac{\pi}{2} \right\} \quad r = 1, 2, \dots, \infty. \quad (2.32)$$

Thus there are infinitely many natural circular frequencies,  $\omega_{0r}$ , of the shear vibration of unbendable beams. These frequencies form an arithmetic sequence with common difference  $\pi\sqrt{k_s c_s}/\ell$ . There is a corresponding shape functions for each natural frequency:

$$\hat{v}_r(x) = B_r \sin \left( \frac{\{r - 1/2\}\pi}{\ell} x \right). \quad (2.33)$$

Finally, the shear vibration of a prismatic beam is the following combination of the natural modes:

$$v(x, t) = \sum_{r=1}^{\infty} B_r \sin \left( \frac{\{r - 1/2\}\pi}{\ell} x \right) \cdot \left\{ a_r \cos \left( \sqrt{k_s c_s} \frac{\{r - 1/2\}\pi}{\ell} t \right) + b_r \sin \left( \sqrt{k_s c_s} \frac{\{r - 1/2\}\pi}{\ell} t \right) \right\}. \quad (2.34)$$

**Problem 2.3.1** (Elastically clamped, shearable column). Estimate the first natural circular frequency of a in-extensional, unbendable column of rectangular cross-section! The length of the column is  $\ell$ , its mass per unit length is  $\mu$ . The area of the cross-section is  $A$ , the shear modulus of the material is  $G$ . The structure is elastically clamped at the bottom with a rotational spring of stiffness  $s$ , and it is free at the top end, as shown in Figure 2.3 (a).

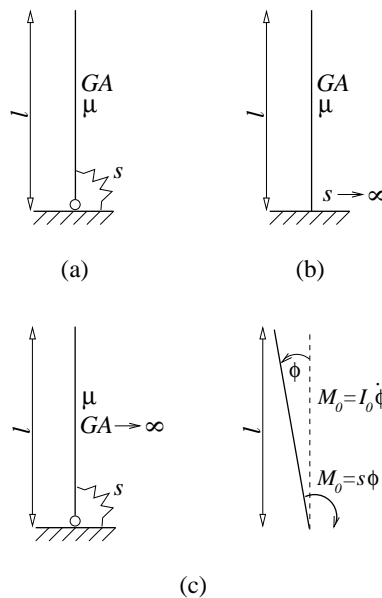


**Figure 2.3:** (a) Model of an inextensional and unbendable beam which is elastically clamped at one end and free at the other end. (b) The case when the rotational spring is rigid. (c) The case when the beam is totally rigid.

**Solution.** We have not derived the natural frequencies of a beam with the boundary conditions given in this problem. Therefore we make use of one of the summation theorems introduced in Section 1.4 in order to approximate the first frequency. Since the structure becomes statically overdeterminate if either the spring stiffness  $s$  or the shear stiffness  $GA$  is set to zero, we need to apply the Föppl-Papkovics' theorem (see Subsec. 1.4.3). First we stiffen the rotational spring  $s \rightarrow \infty$  as shown in Figure 2.3 (b), and compute the natural frequency  $\omega_1$  from Eq. (2.32) evaluated at  $r = 1$ :

$$\omega_1 = \frac{\sqrt{k_s c_s} \pi}{\ell} \frac{\pi}{2} = \sqrt{k_s \frac{GA}{\mu}} \frac{\pi}{2\ell}.$$

Here the shear correction factor  $k_s = 5/6$ , since the cross-section of the beam is rectangular.

Next we stiffen the beam, i.e.  $GA \rightarrow \infty$ , and compute the natural frequency  $\omega_2$  of a rigid beam of length  $\ell$  and mass  $m = \mu\ell$ , supported by a rotational spring at one end. That is shown in Figure 2.3 (c). We write the theorem of angular momentum for the rigid beam:

$$\frac{\mu\ell^3}{3} \ddot{\phi}(t) = -\rho\phi(t).$$

This second order linear ODE has a solution

$$\phi(t) = A \cos\left(\sqrt{\frac{3\rho}{\mu\ell^3}} t\right) + B \sin\left(\sqrt{\frac{3\rho}{\mu\ell^3}} t\right).$$

from which the natural frequency can be read out:

$$\omega_2 = \sqrt{\frac{3\rho}{\mu\ell^3}}.$$

According to Eq. (1.76), the first natural circular frequency of the original structure is

$$\begin{aligned} \frac{1}{\omega_{01}^2} &\leq \frac{1}{\omega_1^2} + \frac{1}{\omega_2^2} \quad \rightarrow \quad \frac{1}{\omega_{01}^2} \leq \mu \frac{4\ell^2}{k_s GA \pi^2} + \mu \frac{\ell^3}{3s}, \\ \omega_{01} &\geq \frac{1}{\sqrt{\mu \left\{ \frac{4\ell^2}{k_s GA \pi^2} + \frac{\ell^3}{3s} \right\}}}. \end{aligned}$$

## 2.4 Transverse vibration of prismatic beams

The cross-sections of the studied beam are reflection symmetric to axis  $y$ . There is a transverse distributed load  $q_t(x, t)$  acting in the plane of symmetry  $x - y$  of the beam, as shown in Figure 2.4 (a). If we restrict flexural-torsional buckling, then these conditions imply that the beam undergoes planar deformation: the motion of the beam axis occurs in the plane  $x - y$ .

The beam is assumed to be *inextensible and unshearable*. The curve  $v(x, t)$  describes the deflection of the beam axis along  $y$  at some position  $x$  and time  $t$ . Since the beam is unshearable, the rotation  $\alpha(x, t)$  of the cross-sections about axis  $z$  equals the slope of the axis:  $\alpha(x, t) = \partial v(x, t)/\partial x$ . The only deformation which is not constrained is the curvature  $\kappa(x, t)$

of the axis of the beam:

$$\kappa(x, t) = \frac{\frac{\partial^2 v(x, t)}{\partial x^2}}{\left(1 + \left(\frac{\partial v(x, t)}{\partial x}\right)^2\right)^{3/2}}.$$

The *Bernoulli-Euler* constitutive equation says that the (internal) bending moment  $M(x, t)$  is linear in the change in  $\kappa(x, t)$ , i.e.

$$M(x, t) = EI\kappa(x, t).$$

Here  $E$  is the *Young's* modulus of the isotropic material,  $I$  is the second moment of the cross-section with respect to  $z$ , and their product  $EI$  is called the bending stiffness of the beam, which is constant along  $x$ . If the deflection  $v(x, t)$  is small, and so is the slope  $\partial v(x, t)/\partial x$ , then we can make the following approximation:

$$M(x, t) \approx -EI \frac{\partial^2 v(x, t)}{\partial x^2}. \quad (2.35)$$

Besides, in the case of small displacements, the transverse load causes only transverse translation  $v(x, t)$  of the axis, so no translation occurs along axis  $x$ .

### 2.4.1 The equation of transverse vibration

Let us cut the beam at two nearby cross-sections  $x = x_0$  and  $x = x_0 + \Delta x$ , so that we obtain a *beam element* of length  $\Delta x$ . We substitute the mechanical effect of the material by an (internal) normal force  $N$ , a shear force  $V$ , and a bending moment  $M$  at  $x_0$ , and by an (internal) normal force  $N + \Delta N$ , a shear force  $V + \Delta V$ , and a bending moment  $M + \Delta M$  at  $x_0 + \Delta x$ . This beam element is shown in Figure 2.4 (b). The acceleration of the center of mass of the beam element is approximated by  $\partial^2 v(x, t)/\partial t^2$  (evaluated at  $x = x_0$ ). The resultant of the distributed load  $q_t(x, t)$  is approximately  $q_t(x_0, t)\Delta x$ . The smaller  $\Delta x$  is, the more precise these approximations are.

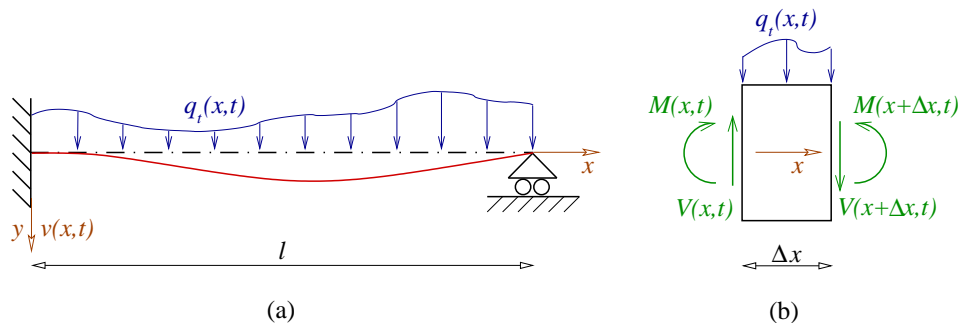


**Figure 2.4:** Sketch of (a) a prismatic beam subjected to a transverse, distributed load  $q_t(x, t)$  and (b) a beam element of length  $\Delta x$  subjected to the internal forces and the distributed load. (The normal forces are not indicated, and the deformation of the beam element is neglected due to small displacements.)

Now we write *Newton's second law of motion* in the vertical direction:

$$V(x + \Delta x, t) - V(x, t) + q_t(x, t)\Delta x = \mu\Delta x \frac{\partial^2 v(x, t)}{\partial t^2}, \quad (2.36)$$

which is evaluated at  $x = x_0$ . The *Taylor expansion* of  $V(x, t)$  with respect to  $x$  around  $x_0$  is:

$$\begin{aligned} V(x + \Delta x, t) &= V(x, t) + \frac{\partial V(x, t)}{\partial x} \Delta x + \frac{\partial^2 V(x, t)}{\partial x^2} \Delta x^2 + \dots \\ &= V(x, t) + \frac{\partial V(x, t)}{\partial x} \Delta x + \mathcal{O}(\Delta x^2) \end{aligned} \quad (2.37)$$

If we substitute (2.37) into (2.36), divide it by  $\Delta x$  and apply  $\Delta x \rightarrow 0$ , then the following formula is obtained:

$$\frac{\partial V(x, t)}{\partial x} + q_t(x, t) = \mu \frac{\partial^2 v(x, t)}{\partial t^2}. \quad (2.38)$$

Now we write the *theorem of angular momentum*. We approximate the moment of inertia of the beam element with

$$\int_{(V)} y^2 dm = \int_{(A)} y^2 \rho dA \Delta x = I \rho \Delta x = \frac{I}{A} \mu \Delta x = i_0^2 \mu \Delta x,$$

and its rotation with  $\partial v(x, t)/\partial x$ . The quantity  $i_0 = \sqrt{I/A}$  is called the radius of gyration. The smaller  $\Delta x$  is, the more precise these approximations are, again. The theorem of angular momentum states that the angular momentum of the beam element equals the moment exerted by the (internal and external) forces and couples about the centre of mass, thus

$$-M(x + \Delta x, t) + M(x, t) + V(x, t) \frac{\Delta x}{2} + V(x + \Delta x, t) \frac{\Delta x}{2} = i_0^2 \mu \Delta x \frac{\partial^3 v(x, t)}{\partial x \partial t^2}. \quad (2.39)$$

Now we substitute (2.37) and the *Taylor expansion* of  $M(x + \Delta x, t)$  in (2.39), divide the result by  $\Delta x$  and tend  $\Delta x$  to zero. The result is

$$-\frac{\partial M(x, t)}{\partial x} + V(x, t) = i_0^2 \mu \frac{\partial^3 v(x, t)}{\partial x \partial t^2}. \quad (2.40)$$

Differentiating the above equation partially with respect to  $x$  and combining it with Eqs. (2.35), (2.38) yields the fourth order, linear, inhomogeneous partial differential equation (PDE):

$$\mu \left( \frac{\partial^2 v(x, t)}{\partial t^2} - i_0^2 \frac{\partial^4 v(x, t)}{\partial x^2 \partial t^2} \right) + EI \frac{\partial^4 v(x, t)}{\partial x^4} = q_t(x, t). \quad (2.41)$$

The above PDE describes the vibration of the beam axis caused by an arbitrary forcing  $q_t(x, t)$ .

It is often reasonable to neglect the effect of rotary inertia (for example when  $i_0$  is small). Then (2.41) simplifies to

$$\mu \frac{\partial^2 v(x, t)}{\partial t^2} + EI \frac{\partial^4 v(x, t)}{\partial x^4} = q_t(x, t). \quad (2.42)$$

We restrict our studies to (2.42). In order to solve it, we need to define boundary and initial conditions. Let us start with the boundary conditions. We discuss only some well known type of external constraints.

If the beam of length  $\ell$  is supported by a fixed hinge and a roller at its ends (called *pinned-pinned* hereafter, shown in Figure 2.5 (a)), then the deflection  $v(x, t)$  and the bending moment  $M(x, t) = -EI \partial^2 v(x, t)/\partial x^2$  are zero at both ends for any time  $t$ . Since  $EI$  is not zero, these conditions can be written as

$$v(x, t)|_{x=0} = 0, \quad \frac{\partial^2 v(x, t)}{\partial x^2} \Big|_{x=0} = 0, \quad v(x, t)|_{x=\ell} = 0, \quad \frac{\partial^2 v(x, t)}{\partial x^2} \Big|_{x=\ell} = 0. \quad (2.43)$$

If the beam is clamped at one end and free at the other one, then it is called *fixed-free*, as shown in Figure 2.5 (b). In this case the deflection  $v(x, t)$  and the slope  $\alpha = \partial v(x, t)/\partial x$  are zero at the clamped end, while the bending moment  $M(x, t)$  and the shear force  $V(x, t) = -EI \partial^3 v(x, t)/\partial x^3$  (which comes from (2.35), (2.40), neglecting the rotary inertia) are zero at the free end. These conditions are essentially:

$$v(x, t)|_{x=0} = 0, \quad \frac{\partial v(x, t)}{\partial x} \Big|_{x=0} = 0, \quad \frac{\partial^2 v(x, t)}{\partial x^2} \Big|_{x=\ell} = 0, \quad \frac{\partial^3 v(x, t)}{\partial x^3} \Big|_{x=\ell} = 0. \quad (2.44)$$

The beam can be clamped at one end and supported by a roller at the other one, which is called *fixed-pinned*, as visualised in Figure 2.5 (c). In this case the deflection  $v(x, t)$  are zero at both ends, the slope  $\alpha = \partial v(x, t)/\partial x$  is zero at the clamped end, and the bending moment  $M(x, t)$  is zero at the pinned end. These conditions yield

$$v(x, t)|_{x=0} = 0, \quad \frac{\partial v(x, t)}{\partial x} \Big|_{x=0} = 0, \quad v(x, t)|_{x=\ell} = 0, \quad \frac{\partial^2 v(x, t)}{\partial x^2} \Big|_{x=\ell} = 0. \quad (2.45)$$

The beam can be clamped at both ends, called *fixed-fixed*, shown in Figure 2.5 (d). In this case the deflection  $v(x, t)$  and the slope  $\alpha = \partial v(x, t)/\partial x$  are zero at both ends, thus

$$v(x, t)|_{x=0} = 0, \quad \frac{\partial v(x, t)}{\partial x} \Big|_{x=0} = 0, \quad v(x, t)|_{x=\ell} = 0, \quad \frac{\partial v(x, t)}{\partial x} \Big|_{x=\ell} = 0. \quad (2.46)$$

## 2.4.2 Free vibration of prismatic beams

The simplest form of Eq. (2.42) is when  $q_t(x, t) = 0$ , which is also the complementary equation of (2.42) for any  $q_t(x, t) \neq 0$  exciting force. It is physically the unforced case, the *free vibration* of the beam. Thus the homogeneous, linear partial differential equation of the free vibration is

$$\boxed{EI \frac{\partial^4 v(x, t)}{\partial x^4} + \mu \frac{\partial^2 v(x, t)}{\partial t^2} = 0}. \quad (2.47)$$

We could divide the above equation by  $\mu$  and write

$$i_0^2 c_n^2 \frac{\partial^4 v(x, t)}{\partial x^4} + \frac{\partial^2 v(x, t)}{\partial t^2} = 0,$$

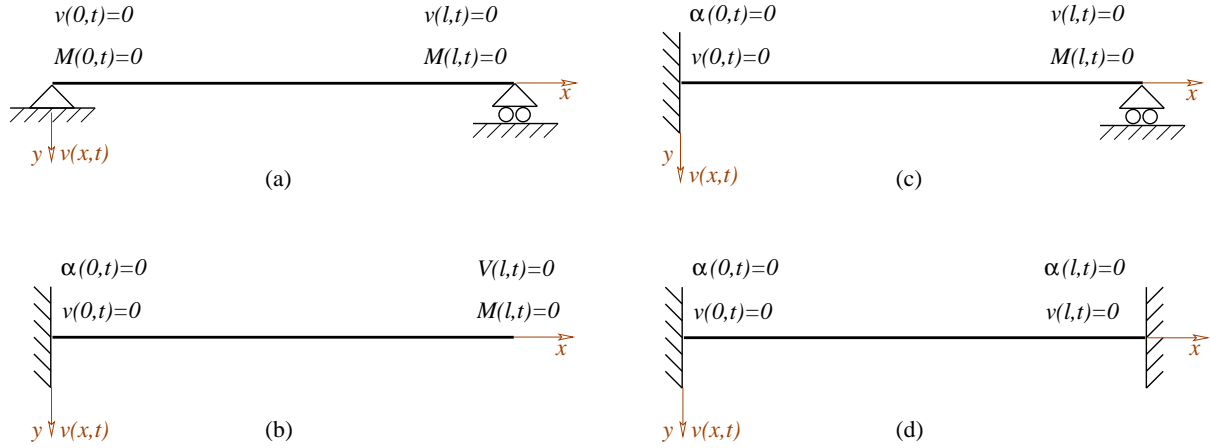


**Figure 2.5:** Common types of supporting modes: (a) pinned-pinned, (b) fixed-free, (c) fixed-pinned, and (d) fixed-fixed beams. The corresponding boundary conditions are indicated at the end points.

where  $i_0 = \sqrt{I/A}$  is the radius of gyration and  $c_n = \sqrt{E/\rho}$  is the velocity of the travelling longitudinal waves, which was introduced already in Subsec. 2.1.1 (see Eq. (2.5)).

We search for the solution of PDE (2.47) using the method of *separation of variables*. That means that we attempt to find a solution of (2.47) as a sum of products of functions in which the dependence of  $v(x, t)$  on  $x$  and  $t$  is separated:

$$v(x, t) = \hat{v}(x) \cdot \{a \cos(\omega_0 t) + b \sin(\omega_0 t)\}. \quad (2.48)$$

It implies that the deflection of all the points of the beam axis varies harmonically with time  $t$ . Here  $\omega_0$  is the *natural circular frequency* of the free vibration, while the coefficients  $a$  and  $b$  come from initial conditions. It is clear that with the above formalism

$$\begin{aligned} \frac{\partial^4 v(x, t)}{\partial x^4} &= \frac{d^4 \hat{v}(x)}{dx^4} \cdot \{a \cos(\omega_0 t) + b \sin(\omega_0 t)\}, \\ \frac{\partial^2 v(x, t)}{\partial t^2} &= \hat{v}(x) \cdot \{-a\omega_0^2 \sin(\omega_0 t) - b\omega_0^2 \cos(\omega_0 t)\}. \end{aligned}$$

Substituting (2.48) into (2.47) yields

$$\left\{ EI \frac{d^4 \hat{v}(x)}{dx^4} - \omega_0^2 \mu \hat{v}(x) \right\} \cdot \{a \cos(\omega_0 t) + b \sin(\omega_0 t)\} = 0.$$

The above equation is fulfilled for any time instant  $t$  if the following *ordinary differential equation* (ODE) holds:

$$EI \frac{d^4 \hat{v}(x)}{dx^4} - \omega_0^2 \mu \hat{v}(x) = 0. \quad (2.49)$$

The solution of the above linear, homogeneous ODE (2.49) is of the form

$$\hat{v}(x) = A \cos\left(\frac{\lambda_0}{\ell} x\right) + B \sin\left(\frac{\lambda_0}{\ell} x\right) + C \cosh\left(\frac{\lambda_0}{\ell} x\right) + D \sinh\left(\frac{\lambda_0}{\ell} x\right), \quad (2.50)$$

where we introduced the dimensionless natural frequency

$$\lambda_0 = \ell \sqrt[4]{\frac{\omega_0^2 \mu}{EI}}.$$

For the computations of  $\lambda_0$ , and of the coefficients  $A, B, C, D$ , we need to take boundary conditions into account. Here we discuss only the case of the pinned-pinned beam.

### The case of the pinned-pinned beam

It is a consequence of (2.48) that

$$\frac{d^n \hat{v}(x)}{dx^n} = 0 \quad \rightarrow \quad \frac{\partial^n v(x, t)}{\partial x^n} = 0, \quad n = 0, 1, 2, \dots$$

The boundary conditions of the pinned-pinned beam are given by (2.43). Thus we need to express the second derivative ( $n = 2$ ) of (2.50) with respect to  $x$ :

$$\frac{d^2 \hat{v}(x)}{dx^2} = \frac{\lambda_0^2}{\ell^2} \left\{ -A \cos\left(\frac{\lambda_0}{\ell} x\right) - B \sin\left(\frac{\lambda_0}{\ell} x\right) + C \cosh\left(\frac{\lambda_0}{\ell} x\right) + D \sinh\left(\frac{\lambda_0}{\ell} x\right) \right\}.$$

We substitute (2.50) and the above expression into (2.43) and write the appropriate boundary conditions in the compact matrix form

$$\mathbf{F}(\lambda_0) \cdot \mathbf{c} = \begin{bmatrix} 1 & 0 & 1 & 0 \\ -\frac{\lambda_0^2}{\ell^2} & 0 & \frac{\lambda_0^2}{\ell^2} & 0 \\ \cos(\lambda_0 r) & \sin(\lambda_0) & \cosh(\lambda_0) & \sinh(\lambda_0) \\ -\frac{\lambda_0^2}{\ell^2} \cos(\lambda_0) & -\frac{\lambda_0^2}{\ell^2} \sin(\lambda_0) & \frac{\lambda_0^2}{\ell^2} \cosh(\lambda_0) & \frac{\lambda_0^2}{\ell^2} \sinh(\lambda_0) \end{bmatrix} \cdot \begin{bmatrix} A \\ B \\ C \\ D \end{bmatrix} = \mathbf{0}. \quad (2.51)$$

Here  $\mathbf{F}(\lambda_0)$  is called the *frequency matrix* and  $\mathbf{c}$  stores the coefficients of (2.50). The equation  $\mathbf{F}(\lambda_0) \cdot \mathbf{c} = \mathbf{0}$  is satisfied for nontrivial  $\mathbf{c} \neq \mathbf{0}$  if the determinant of  $\mathbf{F}(\lambda_0)$

$$\det(\mathbf{F}(\lambda_0)) = -4 \frac{\lambda_0}{\ell} \sin(\lambda_0) \sinh(\lambda_0)$$

is zero, thus either if  $\lambda_0 = 0$ , or if  $\sin(\lambda_0) = 0$ , or if  $\sinh(\lambda_0) = 0$ . The trivial solution,  $\lambda_0 = 0$ , implies  $v(x, t) \equiv 0$ , the steady state solution, when there is no vibration. The nontrivial solutions are  $\lambda_{0r} = r\pi$ ,  $r = 1, 2, \dots, \infty$ . There is a countable infinity of such solutions, from which the  $r$ th natural circular frequency of the free transverse vibration of the pinned-pinned beam can be obtained:

$$\omega_{0r} = \frac{r^2 \pi^2}{\ell^2} \sqrt{\frac{EI}{\mu}} \quad r = 1, 2, \dots, \infty. \quad (2.52)$$



The coefficients  $A_r, B_r, C_r, D_r$  are derived from back substitution of  $\lambda_{0r} = r\pi$  into (2.51):

$$\mathbf{F}(r\pi) \cdot \mathbf{c}_r = \begin{bmatrix} 1 & 0 & 1 & 0 \\ -\frac{r^2\pi^2}{\ell^2} & 0 & \frac{r^2\pi^2}{\ell^2} & 0 \\ \{-1\}^r & 0 & \cosh(r\pi) & \sinh(r\pi) \\ \frac{r^2\pi^2}{\ell^2}\{-1\}^{r+1} & 0 & \frac{r^2\pi^2}{\ell^2}\cosh(r\pi) & \frac{r^2\pi^2}{\ell^2}\sinh(r\pi) \end{bmatrix} \cdot \begin{bmatrix} A_r \\ B_r \\ C_r \\ D_r \end{bmatrix} = \mathbf{0}.$$

From the 1st and the 2nd equations we get

$$A_r + C_r = 0, \quad -A_r + C_r = 0, \quad \rightarrow \quad A_r = C_r = 0.$$

From the 3rd equation  $D_r = 0$ . Since  $\det(\mathbf{F}(r\pi)) = 0$ , the 4th equation is linearly dependent. Therefore the coefficient  $B_r$  can be chosen arbitrary. Finally, the  $r$ th *shape function* of the free transverse vibration is

$$\hat{v}_r(x) = B_r \sin\left(\frac{r\pi}{\ell}x\right). \quad (2.53)$$

The shape functions are *orthogonal*, which means that

$$\begin{aligned} \int_0^\ell \hat{v}_p(x)\hat{v}_r(x) dx &= \int_0^\ell B_p \sin\left(\frac{p\pi}{\ell}x\right) B_r \sin\left(\frac{r\pi}{\ell}x\right) dx \\ &= \begin{cases} B_p B_r \left[ \frac{\sin\left(\frac{\{p-r\}\pi}{\ell}x\right)}{2\frac{\{p-r\}\pi}{\ell}} - \frac{\sin\left(\frac{\{p+r\}\pi}{\ell}x\right)}{2\frac{\{p+r\}\pi}{\ell}} \right]_0^\ell & \text{if } p \neq r \\ B_r^2 \left[ \frac{x - \sin\left(\frac{2r\pi}{\ell}x\right)/\left(\frac{2r\pi}{\ell}\right)}{2} \right]_0^\ell & \text{if } p = r. \end{cases} \end{aligned} \quad (2.54)$$

It is often convenient to normalise the shape functions to the mass of the beam, i.e. to satisfy

$$\mu \int_0^\ell \hat{v}_r(x)\hat{v}_r(x) dx = 1. \quad (2.55)$$

This allows us to determine a specific value for  $B_r$  using Eqs. (2.54), (2.55):

$$\mu \int_0^\ell \hat{v}_r(x)\hat{v}_r(x) dx = \mu B_r^2 \frac{\ell}{2} = 1 \quad \rightarrow \quad B_r = \sqrt{\frac{2}{\mu\ell}}.$$

Thus the  $r$ th *normalised (modal) shape function* of the pinned-pinned beam is

$$\boxed{\hat{v}_r(x) = \sqrt{\frac{2}{\mu\ell}} \sin\left(\frac{r\pi}{\ell}x\right)}. \quad (2.56)$$

The solution of (2.47) is expressed as a combination of the normalised shape functions:

$$\boxed{v(x, t) = \sqrt{\frac{2}{\mu\ell}} \sum_{r=1}^{\infty} \sin\left(\frac{r\pi}{\ell}x\right) \cdot \{a_r \cos(\omega_{0r}t) + b_r \sin(\omega_{0r}t)\}}. \quad (2.57)$$

The coefficients  $a_r$  and  $b_r$  can be determined from *initial conditions*. Let us assume that the deflection of the beam at time  $t = 0$

$$v(x, 0) = \sqrt{\frac{2}{\mu\ell}} \sum_{r=1}^{\infty} \sin\left(\frac{r\pi}{\ell}x\right) \cdot a_r$$

and the velocity of each point at time  $t = 0$

$$\dot{v}(x, 0) = \sqrt{\frac{2}{\mu\ell}} \sum_{r=1}^{\infty} \sin\left(\frac{r\pi}{\ell}x\right) \cdot b_r \omega_{0r}$$

are given functions (fulfilling the boundary conditions). Thus these functions  $v(x, 0)$  and  $\dot{v}(x, 0)$  can be written as purely sine *Fourier* series. Now we multiply the above equations by the  $p$ th normalised shape function  $\hat{v}_p(x)$ , integrate the result from 0 to  $\ell$  with respect to  $x$ , and apply the orthogonality (2.54):

$$\int_0^{\ell} v(x, 0) \hat{v}_p(x) dx = \int_0^{\ell} v(x, 0) \sqrt{\frac{2}{\mu\ell}} \sin\left(\frac{p\pi}{\ell}x\right) dx = \frac{2}{\mu\ell} a_p \int_0^{\ell} \sin^2\left(\frac{p\pi}{\ell}x\right) dx = \frac{a_p}{\mu},$$

$$\int_0^{\ell} \dot{v}(x, 0) \hat{v}_p(x) dx = \int_0^{\ell} \dot{v}(x, 0) \sqrt{\frac{2}{\mu\ell}} \sin\left(\frac{p\pi}{\ell}x\right) dx = \frac{2}{\mu\ell} b_p \omega_{0p} \int_0^{\ell} \sin^2\left(\frac{p\pi}{\ell}x\right) dx = \frac{b_p \omega_{0p}}{\mu}.$$

From the above formula we can extract the coefficients  $a_p$  and  $b_p$  from the *known* initial deflection function  $v(x, 0)$  and initial velocity function  $\dot{v}(x, 0)$  of the beam axis as

$$a_p = \sqrt{\frac{2\mu}{\ell}} \int_0^{\ell} v(x, 0) \sin\left(\frac{p\pi}{\ell}x\right) dx, \quad (2.58)$$

$$b_p = \frac{1}{\omega_{0r}} \sqrt{\frac{2\mu}{\ell}} \int_0^{\ell} \dot{v}(x, 0) \sin\left(\frac{p\pi}{\ell}x\right) dx.$$

It can be shown that the orthogonality of the shape functions are a general property. Thus

$$\mu \int_0^{\ell} \hat{v}_p(x) \hat{v}_r(x) dx = \delta_{pr} \quad (2.59)$$

holds for the normalised shape functions in case of other types of boundary conditions, too. Here the symbol  $\delta_{pr}$  is the *Kronecker* delta, which equals to one if  $p = r$  and zero otherwise. Moreover, the following equality could be derived for arbitrary boundary conditions:

$$EI \int_0^{\ell} \frac{d^4 \hat{v}_p(x)}{dx^4} \hat{v}_r(x) dx = \omega_{0r}^2 \delta_{pr}, \quad (2.60)$$

where, again,  $\hat{v}_r(x)$  is the  $r$ th normalised (modal) shape function. For the pinned-pinned beam it is simple to prove the above formula:

$$\begin{aligned} EI \int_0^\ell \frac{d^4 \hat{v}_p(x)}{dx^4} \hat{v}_r(x) dx &= EI \frac{p^4 \pi^4}{\ell^4} \int_0^\ell \hat{v}_p(x) \hat{v}_r(x) dx = \\ &= \begin{cases} EI \frac{p^4 \pi^4}{\ell^4} \cdot 0 = 0 & \text{if } p \neq r \\ EI \frac{p^4 \pi^4}{\ell^4} \cdot \frac{1}{\mu} = \omega_{0p}^2 & \text{if } p = r. \end{cases} \end{aligned}$$

### The effect of axial compression on the natural frequencies

During the examination of the free vibration of the prismatic beam, we neglected the effect of the normal force. However, if an *axial compression*  $P$  acts at the ends of the beam, and the deflection of the originally straight axis is taken into account, an additional moment  $P\Delta v(x, t)$  is exerted on the beam element, as indicated in Figure 2.6 (a) and (b). Therefore, the left hand side of (2.39) must be appended by  $P\Delta v(x, t)$  to deal with such an effect. Then, instead of (2.47), the following equation can be derived for the free vibration of the axially compressed beam:

$$\boxed{EI \frac{\partial^4 v(x, t)}{\partial x^4} + P \frac{\partial^2 v(x, t)}{\partial x^2} + \mu \frac{\partial^2 v(x, t)}{\partial t^2} = 0.} \quad (2.61)$$

(Here we neglected again the effect of rotary inertia.)

Separating the variables as in (2.48), the equation

$$\sum_r \left\{ EI \frac{d^4 \hat{v}_r(x)}{dx^4} + P \frac{d^2 \hat{v}_r(x)}{dx^2} - \omega_{0r}^2 \mu \frac{d^2 \hat{v}_r(x)}{dt^2} \right\} \cdot \{a_r \cos(\omega_{0r} t) + b_r \sin(\omega_{0r} t)\} = 0$$

must be satisfied at any time  $t$ . Without going into details of the derivation (which follows a very similar procedure as in the previous case), we give the formula of the natural circular frequencies of the pinned-pinned prismatic beam subjected to an axial compression  $P$ :

$$\boxed{\hat{\omega}_{0r} = \omega_{0r} \sqrt{1 - \frac{P}{P_r^{\text{cr}}}} \quad r = 1, 2, \dots, \infty.} \quad (2.62)$$

Here  $\omega_{0r}$  is (2.52) and the  $r$ th (*Euler*) critical load  $P_r^{\text{cr}}$  of the pinned-pinned beam is known from earlier studies:

$$P_r^{\text{cr}} = \frac{EI r^2 \pi^2}{\ell^2}. \quad (2.63)$$

The constant axial compression thus *decreases* the natural circular frequencies. At the limit when  $P = P_1^{\text{cr}}$   $\omega_{01}$  becomes zero, thus the first mode of natural vibration about the original, straight state vanishes, and the beam *buckles*. The effect of an axial *tension* is the opposite, it *increases* the natural circular frequencies. Just think of a guitar string: the more it is stretched, the “faster” it vibrates if twanged slightly.

The shape functions are not infected by the axial tension/compression, hence they are identical to (2.53).

**Problem 2.4.1** (On the natural frequencies). There is a beam of length  $\ell = 12$  m, total mass  $m = 6$  t, and bending moment  $EI = 200000$  kNm<sup>2</sup> given. Determine the first three natural circular frequencies and the corresponding normalised modal shape functions of the beam! How the first frequency is affected by a constant normal force  $P = 2 \cdot 10^7$  N?

**Solution.** First we exchange the given data into SI units and compute the mass per unit length  $\mu$ :  $EI = 2 \cdot 10^9$  Nm<sup>2</sup>,  $\mu = m/\ell = 500$  kg/m. The natural circular frequencies can be computed from (2.52):

$$\begin{aligned}\omega_{01} &= \frac{\pi^2}{\ell^2} \sqrt{\frac{EI}{\mu}} = \frac{\pi^2}{144} \sqrt{\frac{2 \cdot 10^9}{500}} = 137.08 \text{ rad/s}, \\ \omega_{02} &= \frac{4\pi^2}{\ell^2} \sqrt{\frac{EI}{\mu}} = \frac{4\pi^2}{144} \sqrt{\frac{2 \cdot 10^9}{500}} = 2^2 \omega_{01} = 548.31 \text{ rad/s}, \\ \omega_{03} &= \frac{9\pi^2}{\ell^2} \sqrt{\frac{EI}{\mu}} = \frac{9\pi^2}{144} \sqrt{\frac{2 \cdot 10^9}{500}} = 3^2 \omega_{01} = 1233.70 \text{ rad/s}.\end{aligned}$$

The normalised shape functions are from (2.56):

$$\begin{aligned}\hat{v}_1(x) &= \sqrt{\frac{2}{\mu\ell}} \sin\left(\frac{\pi}{\ell}x\right) = \sqrt{\frac{2}{500 \cdot 12}} \sin\left(\frac{\pi}{12}x\right) = 0.01826 \sin(0.2618x), \\ \hat{v}_2(x) &= \sqrt{\frac{2}{\mu\ell}} \sin\left(\frac{2\pi}{\ell}x\right) = \sqrt{\frac{2}{500 \cdot 12}} \sin\left(\frac{3\pi}{12}x\right) = 0.01826 \sin(0.5236x), \\ \hat{v}_3(x) &= \sqrt{\frac{2}{\mu\ell}} \sin\left(\frac{3\pi}{\ell}x\right) = \sqrt{\frac{2}{500 \cdot 12}} \sin\left(\frac{2\pi}{12}x\right) = 0.01826 \sin(0.7854x).\end{aligned}$$

Note, that the argument of function sine is in radian!

For the computation of the effect of the axial compression  $P = 2 \cdot 10^7$  N, on the natural circular frequencies first we need to calculate the critical loads from (2.63):

$$\begin{aligned}P_1^{\text{cr}} &= \frac{EI\pi^2}{\ell^2} = 0.06845EI = 13.71 \cdot 10^7 \text{ N}, \\ P_2^{\text{cr}} &= \frac{EI4\pi^2}{\ell^2} = 0.2742EI = 54.83 \cdot 10^7 \text{ N}, \\ P_3^{\text{cr}} &= \frac{EI9\pi^2}{\ell^2} = 0.6169EI = 123.37 \cdot 10^7 \text{ N}.\end{aligned}$$

Since the given axial compression  $P$  is smaller than the lowest critical load  $P_1^{\text{cr}}$ , there exists a harmonic free vibration around the straight equilibrium position of the beam. The first three natural circular frequencies of this harmonic oscillation are computed using Eq. (2.62):

$$\begin{aligned}\hat{\omega}_{01} &= \omega_{01} \sqrt{1 - \frac{P}{P_1^{\text{cr}}}} = 137.08 \cdot 0.9242 = 126.69 \text{ rad/s}, \\ \hat{\omega}_{02} &= \omega_{02} \sqrt{1 - \frac{P}{P_2^{\text{cr}}}} = 548.31 \cdot 0.9816 = 538.22 \text{ rad/s}, \\ \hat{\omega}_{03} &= \omega_{03} \sqrt{1 - \frac{P}{P_3^{\text{cr}}}} = 1233.70 \cdot 0.9919 = 1223.71 \text{ rad/s}.\end{aligned}$$

Notice, that the axial compression has a smaller effect on the higher natural frequencies. If  $P$  equals to the 1st critical load, then  $\hat{\omega}_{01}$  vanishes, and if  $P$  is further increased, then  $\hat{\omega}_{01}$  becomes a complex number: there is no harmonic vibration about the stress-free straight state of the beam any more, a buckling occurs at  $P_1^{cr}$  and the stability of the beam is lost.

**Exercise 2.4.1.** Estimate the first natural circular frequency of the beam given in Problem 2.4.1 with and additional lumped mass  $m_l = 2t$  at the midspan!

### Effect of elastic support on the natural frequencies

If the beam is *continuously supported* by elastic springs of stiffness  $s$ , then a transverse load proportional to the deflection

$$q_t(x, t) = -sv(x, t)$$

is exerted to the beam, as sketched in Figure 2.6 (c) and (d). The dynamical equation of the elastically supported prismatic beam can be obtained by substituting this load into (2.41):

$$\boxed{EI \frac{\partial^4 v(x, t)}{\partial x^4} + sv(x, t) + \mu \frac{\partial^2 v(x, t)}{\partial t^2} = 0.} \quad (2.64)$$

Without going into details of the derivation, we give the natural circular frequencies of the free vibration of the beam laying on a continuous elastic support:

$$\boxed{\tilde{\omega}_{0r} = \omega_{0r} \sqrt{1 + s \frac{\ell^4}{EI r^4 \pi^4}},} \quad (2.65)$$

where  $\omega_{0r}$  is (2.52). Thus the elastic foundation *increases* the natural frequencies.

The shape functions are not infected by the continuous elastic supports either, so they are the same as (2.53).

### Rayleigh's method for estimating natural frequencies

Since we neglected the damping due to internal friction of the elastic body, the *total mechanical energy*  $T(t) + U(t)$  is *preserved* during the free vibration

$$T(t) + U(t) = \text{constant.} \quad (2.66)$$

The *kinetic energy*  $T(t)$  of the prismatic beam expressed with the modal shape functions is

$$T(t) = \frac{1}{2} \int_0^\ell \mu \left\{ \frac{\partial v(x, t)}{\partial t} \right\}^2 dx = \frac{\mu}{2} \int_0^\ell \left\{ \sum_r \hat{v}_r(x) \cdot \omega_{0r} d_r \cos(\omega_{0r} t - \phi_r) \right\}^2 dx.$$

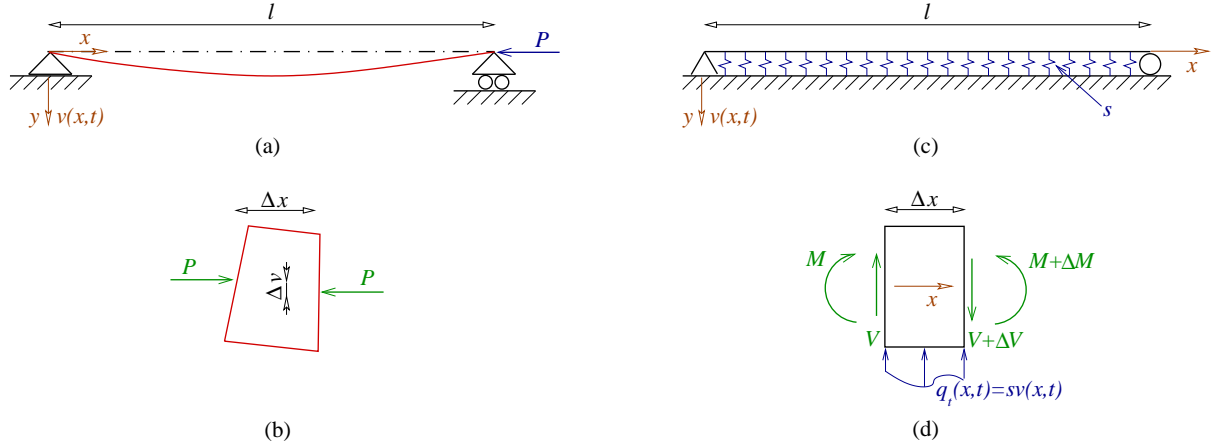


**Figure 2.6:** Sketch of (a) a prismatic beam subjected to an axial compressive force  $P$  and (b) a beam element of length  $\Delta x$ . (The deformed shape of the beam element is shown, but only the internal normal force  $N = -P$  is indicated, the shear force and bending moment are not, they are the same as in (d).) (c) A prismatic beam on an elastic foundation of stiffness  $s$  and (d) a beam element of length  $\Delta x$  of this case. Deformation of the beam element is visualised in (b) but not in (d).

(Here we used (2.48), but rewrote the harmonic term  $a_r \cos(\omega_{0r}t) + b_r \cos(\omega_{0r}t)$  as  $d_r \sin(\omega_{0r}t - \phi_r)$ .) The *potential energy*  $U(t)$  is

$$U(t) = \frac{1}{2} \int_0^\ell EI \left\{ \frac{\partial^2 v(x,t)}{\partial x^2} \right\}^2 dx = \frac{EI}{2} \int_0^\ell \left\{ \sum_r \frac{d^2 \hat{v}_r(x)}{dx^2} \cdot d_r \sin(\omega_{0r}t - \phi_r) \right\}^2 dx.$$

Since the modal shape functions  $\hat{v}_r(x)$  are orthogonal, if we extract the square of the summation in the above equations, then the definite integrals of the mixed terms  $\hat{v}_p(x) \cdot \hat{v}_r(x)$  (and also  $d^2 \hat{v}_p(x)/dx^2 \cdot d^2 \hat{v}_r(x)/dx^2$ ) vanish for  $p \neq r$ , therefore

$$T(t) = \sum_r T_r(t) = \frac{\mu}{2} \sum_r \omega_{0r}^2 d_r^2 \cos^2(\omega_{0r}t - \phi_r) \int_0^\ell \hat{v}_r^2(x) dx$$

and

$$U(t) = \sum_r U_r(t) = \frac{EI}{2} \sum_r d_r^2 \sin^2(\omega_{0r}t - \phi_r) \int_0^\ell \left\{ \frac{d^2 \hat{v}_r(x)}{dx^2} \right\}^2 dx.$$

Therefore, if  $T_r(t) + U_r(t) = \text{constant}$  fulfils for each independent mode  $r$ , then it implies that Eq. (2.66) holds. Let us use the first modal shape function

$$\begin{aligned} T_1(t) + U_1(t) &= \frac{\mu \omega_{01}^2}{2} d_1^2 \cos^2(\omega_{01}t - \phi_1) \int_0^\ell \hat{v}_1^2(x) dx \\ &\quad + \frac{EI}{2} d_1^2 \sin^2(\omega_{01}t - \phi_1) \int_0^\ell \left\{ \frac{d^2 \hat{v}_1(x)}{dx^2} \right\}^2 dx. \end{aligned}$$

Now, when  $\cos(\omega_{01}t - \phi_1) = 1$ , then  $T_1$  is maximal and  $U_1$  is zero, while when  $\sin(\omega_{01}t - \phi_1) = 1$ , then  $T_1$  is zero and  $U_1$  is maximal. (The former case belongs to the straight state of the beam, when its curvature changes, and the velocity is maximal, while the latter case belongs to the state when the beam has the largest deflection and stops: all the points of the axis has zero velocity at that moment.) Therefore, the following equality holds for the first mode for these two limit states:

$$T_1^{\max} + 0 = 0 + U_1^{\max} \quad \rightarrow$$

$$\frac{\mu}{2}\omega_{01}^2 d_1^2 \int_0^\ell \hat{v}_1^2(x) dx = \frac{EI}{2} d_1^2 \int_0^\ell \left\{ \frac{d^2 \hat{v}_1(x)}{dx^2} \right\}^2 dx,$$

which allows us to express the first natural circular frequency as

$$\omega_{01} = \sqrt{\frac{EI}{\mu} \frac{\int_0^\ell \left\{ \frac{d^2 \hat{v}_1(x)}{dx^2} \right\}^2 dx}{\int_0^\ell \hat{v}_1^2(x) dx}}. \quad (2.67)$$

If the first modal shape function  $\hat{v}_1(x)$  is not known, but estimated, then the above formula gives an *upper bound solution* for  $\omega_{01}$ . The assumption for  $\hat{v}_1(x)$  can be based on a polynomial of degree  $n$ , if  $n$  boundary condition can be written for the beam. An example is shown in the following problem.

**Problem 2.4.2** (Applying Rayleigh's method for transverse vibrations). Estimate the first natural circular frequency of a fixed-free beam of length  $\ell = 12$  m, total mass  $m = 6$  t, and bending stiffness  $EI = 200000$  kNm<sup>2</sup>.

**Solution.** Since we can write four boundary conditions for the fixed-pinned beam, as it is given by Eq. (2.44), and also indicated in Figure 2.5 (b), we use the following fourth order polynomial with four unknown coefficients for the estimation of the first shape function:

$$\hat{v}_1(x) \approx p(x) = x^4 + a_3 x^3 + a_2 x^2 + a_1 x^1 + a_0.$$

We need the first, second, and third derivatives of  $p(x)$  with respect to  $x$ :

$$\begin{aligned} \frac{dp(x)}{dx} &= 4x^3 + 3a_3 x^2 + 2a_2 x + a_1, \\ \frac{d^2 p(x)}{dx^2} &= 12x^2 + 6a_3 x + 2a_2, \\ \frac{d^3 p(x)}{dx^3} &= 24x + 6a_3. \end{aligned}$$

Using the boundary conditions given by (2.44) the following equations must be solved for the coefficients  $a_0, a_1, a_2, a_3$ :

$$\begin{aligned} \hat{v}_1(0) &= 0 \quad \rightarrow \quad 0^4 + a_3 \cdot 0^3 + a_2 \cdot 0^2 + a_1 \cdot 0^1 + a_0 = 0 \quad \rightarrow \quad a_0 = 0, \\ \left. \frac{d\hat{v}_1(x)}{dx} \right|_{x=0} &= 0 \quad \rightarrow \quad 4 \cdot 0^3 + 3a_3 \cdot 0^2 + 2a_2 \cdot 0 + a_1 = 0 \quad \rightarrow \quad a_1 = 0, \\ \left. \frac{d^2 \hat{v}_1(x)}{dx^2} \right|_{x=\ell} &= 0 \quad \rightarrow \quad 12\ell^2 + 6a_3 \ell + 2a_2 = 0, \\ \left. \frac{d^3 \hat{v}_1(x)}{dx^3} \right|_{x=\ell} &= 0 \quad \rightarrow \quad 24\ell + 6a_3 = 0. \end{aligned}$$

The last two equations imply that  $a_2 = 6\ell^2$  and  $a_3 = -4\ell$ . Thus the approximated shape function is

$$\hat{v}_{1,\text{ap}}(x) = x^4 - 4\ell x^3 + 6\ell^2 x^2.$$

The approximated first natural circular frequency of the beam is then

$$\begin{aligned} \omega_{01,\text{ap}} &= \sqrt{\frac{EI}{\mu}} \sqrt{\frac{\int_0^\ell \left\{ \frac{d^2 \hat{v}_{1,\text{ap}}(x)}{dx^2} \right\}^2 dx}{\int_0^\ell \hat{v}_{1,\text{ap}}^2(x) dx}} = \sqrt{\frac{EI}{\mu}} \sqrt{\frac{\int_0^\ell \{12x^2 - 24\ell x + 12\ell^2\}^2 dx}{\int_0^\ell \{x^4 - 4\ell x^3 + 6\ell^2 x^2\}^2 dx}} \\ &= \sqrt{\frac{EI}{\mu}} \sqrt{\frac{144\ell^5/5}{104\ell^9/45}} = 3.530 \sqrt{\frac{EI}{\mu\ell^4}} = \underline{49.03 \text{ rad/s.}} \end{aligned}$$

According to [11], the first natural frequency of a fixed-free beam is:

$$\omega_{01} = 3.516 \sqrt{\frac{EI}{\mu\ell^4}} = 48.83 \text{ rad/s.} \quad (2.68)$$

### 2.4.3 Forced vibration of prismatic beams

Now we get back to the partial differential equation (2.42) of forced prismatic beams with the rotary inertia neglected. The homogeneous solution ( $q_t(x, t) = 0$ ) was derived in the previous subsection. The case when  $q_t(x, t) \neq 0$  is called the forced vibration and there is a corresponding *particular solution* of the PDE (2.42). The complete solution of the forced vibration is the sum of the homogeneous and the particular solutions. For the derivation of the particular solution, we make use of the homogeneous one, i.e. the solution of the free vibration of the beam. We assume that the response of the structure to the exciting forces can be expressed as a *time dependent combination of the normalised shape functions*  $\hat{v}_r(x)$  of the free vibration. (Thus we again utilise the method of separation of variables.) This unknown combination of the shape functions is written as

$$v(x, t) = \sum_{r=1}^{\infty} \hat{v}_r(x) \eta_r(t). \quad (2.69)$$

We search for the unknown time dependent functions  $\eta_r(t)$ . Notice that here  $\eta_r(t)$  is not supposed to be a harmonic function of time  $t$ , as it was in the case of the free vibration in Eq. (2.48). With the aid of (2.69) we reformulate (2.42) as

$$EI \sum_{r=1}^{\infty} \frac{d^4 \hat{v}_r(x)}{dx^4} \eta_r(t) + \mu \sum_{r=1}^{\infty} \hat{v}_r(x) \frac{d^2 \eta_r(t)}{dt^2} = q_t(x, t). \quad (2.70)$$

Now we multiply the above equation by  $\hat{v}_p(x)$  and integrate the result from 0 to  $\ell$  with respect to  $x$ :

$$EI \sum_{r=1}^{\infty} \eta_r(t) \int_0^\ell \frac{d^4 \hat{v}_r(x)}{dx^4} \hat{v}_p(x) dx + \mu \sum_{r=1}^{\infty} \frac{d^2 \eta_r(t)}{dt^2} \int_0^\ell \hat{v}_r(x) \hat{v}_p(x) dx = \int_0^\ell q_t(x, t) \hat{v}_p(x) dx.$$



Concerning the orthogonal properties (2.59) and (2.60) of modal shape functions we can write the following system of second order *ordinary differential equations*:

$$\boxed{\frac{d^2\eta_p(t)}{dt^2} + \omega_{0p}^2\eta_p(t) = Q_p(t)}, \quad (2.71)$$

where

$$\boxed{Q_p(t) = \int_0^\ell q_t(x, t)\hat{v}_p(x) dx} \quad (2.72)$$

is the  $p$ th modal force ( $p = 1, 2, \dots, \infty$ ).

Thus, we have managed to transform the solution of the *partial differential equation* (2.42) into solutions of *infinitely many, independent ODEs* (2.71). Each of these ODEs can be regarded as a single-degree-of-freedom, undamped oscillation of a unit mass under an arbitrary forcing  $Q_p(t)$ . According to Eq. (1.7) (with  $c = 0$ ) and Eq. (1.26), the solution of (2.71) is

$$\eta_p(t) = a_p \cos(\omega_{0p}t) + b_p \sin(\omega_{0p}t) + \frac{1}{\omega_{0p}} \int_0^t Q_p(\tau) \sin(\omega_{0p}\{t - \tau\}) d\tau. \quad (2.73)$$

The first two terms of the right hand side form the homogeneous solution of (2.71), which vanishes if there is a slight damping in the system—so slight that we neglected it during our analysis. The third term is *Duhamel's integral* (1.26), the particular solution of (2.71). The coefficients  $a_p$  and  $b_p$  can be determined from the initial conditions. Now we concentrate only on the particular solution of (2.42), which is the following sum of products of separated functions:

$$\boxed{v(x, t) = \sum_{p=1}^{\infty} \frac{\hat{v}_p(x)}{\omega_{0p}} \int_0^t Q_p(\tau) \sin(\omega_{0p}\{t - \tau\}) d\tau.}$$

Some simple examples of forced vibrations and the corresponding particular solutions are given below.

### Prismatic beam under a harmonic force

This example studies a prismatic beam loaded by a transverse harmonic force  $F \sin(\omega t)$  at  $x = a$ . (See Figure 2.7 (a) in the case of a pinned-pinned beam.) The force  $q_t(x, t)$  in (2.42) can be written as

$$q_t(x, t) = F \sin(\omega t)\delta(x - a).$$

Here  $\delta(\xi)$  is the *Dirac delta function* which has the properties

$$\begin{aligned} \delta(\xi) &= \begin{cases} +\infty, & \text{if } \xi = 0 \\ 0, & \text{if } \xi \neq 0 \end{cases}, \\ \int_{-\infty}^{+\infty} \delta(\xi) d\xi &= 1, \text{ and} \\ \int_{-\infty}^{+\infty} f(\xi)\delta(\xi) d\xi &= f(0). \end{aligned} \quad (2.74)$$

With this specific load the modal force due to (2.72) is

$$Q_p(t) = \int_0^\ell F \sin(\omega t) \delta(x - a) \hat{v}_p(x) dx = F \sin(\omega t) \hat{v}_p(a)$$

and  $\eta_p(t)$  from (2.73) is

$$\eta_p(t) = \frac{F \hat{v}_p(a)}{\omega_{0p}} \int_0^t \sin(\omega \tau) \sin(\omega_{0p}\{t - \tau\}) d\tau.$$

Here we can simplify the integral

$$\begin{aligned} &\int_0^t \sin(\omega \tau) \sin(\omega_{0p}\{t - \tau\}) d\tau \\ &= \int_0^t \frac{1}{2} \{ \cos(\{\omega + \omega_{0p}\}\tau - \omega_{0p}t) - \cos(\{\omega - \omega_{0p}\}\tau + \omega_{0p}t) \} d\tau \\ &= \frac{1}{2} \left[ \frac{\sin(\{\omega + \omega_{0p}\}\tau - \omega_{0p}t)}{\omega + \omega_{0p}} - \frac{\sin(\{\omega - \omega_{0p}\}\tau + \omega_{0p}t)}{\omega - \omega_{0p}} \right]_0^t \\ &= \frac{\omega_{0p}}{\omega_{0p}^2 - \omega^2} \sin(\omega t) - \frac{\omega}{\omega_{0p}^2 - \omega^2} \sin(\omega_{0p}t). \end{aligned} \quad (2.75)$$

The first term of the result is the definite integral evaluated at  $\tau = t$ , which is the steady-state vibration of the forced beam. The second term is from the evaluation at  $\tau = 0$ . This and the first two terms of Eq. (2.73) form the transient solution of the vibration. The initial conditions can be chosen such that the transient solution is zero. (Besides, this transient vibration vanishes with time if even a small friction is present.) Therefore, we ignore the second term in Eq. (2.75) and take the particular solution of this forced vibration to be

$$v(x, t) = F \sum_{p=1}^{\infty} \frac{\hat{v}_p(a)}{\omega_{0p}^2 - \omega^2} \hat{v}_p(x) \sin(\omega t) = F \sum_{p=1}^{\infty} \frac{1}{\omega_{0p}^2} \frac{1}{1 - \frac{\omega^2}{\omega_{0p}^2}} \hat{v}_p(a) \hat{v}_p(x) \sin(\omega t). \quad (2.76)$$

We call the attention of the reader to the similarity of this solution and the solution of the harmonically excited MDOF system solved with modal analysis. Compare the above equation with Eq. (1.60)! The influence of higher modes on the response is small, unless the system is around the state of resonance, i.e. if the circular frequency of the exciting force is near to one of the natural circular frequencies of the beam:  $\omega \approx \omega_{0p}$ .

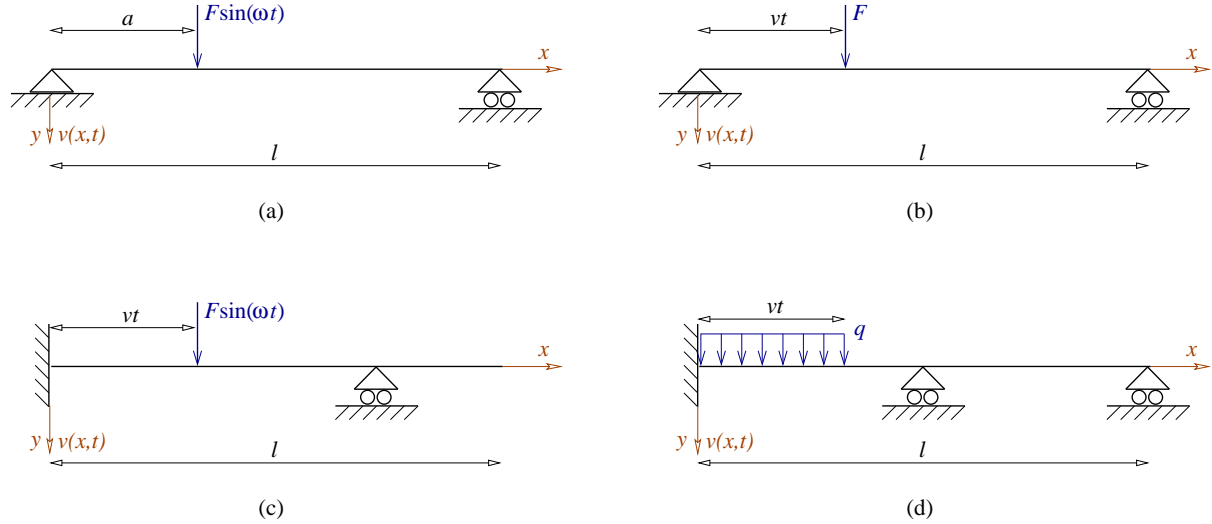


**Figure 2.7:** Prismatic beam subjected to (a) a harmonic exciting force  $F \sin(\omega t)$  acting at a fixed position  $x = a$ , (b) a constant force  $F$  moving with a constant velocity  $v$ , (c) a harmonic force  $F \sin(\omega t)$  moving with a constant velocity  $v$ , and (d) a constant distributed load  $q$  moving with a constant velocity  $v$ .

**Problem 2.4.3** (Machine excited beam). There is a machine installed on the first storey of an industrial building. It is placed at one fourth of the total length 12 m of a pinned-pinned roof beam. The mass of the beam is 500 kg/m and its bending stiffness is  $2 \cdot 10^9 \text{ Nm}^2$ . Due to the eccentric rotating parts of the machine, it exerts a harmonic force of amplitude 1500 N and frequency 80 rad/s on the beam. Determine the maximum deflection of the beam at its mid point! Take only the first three modal shape functions into account!

**Solution.** The normalised (modal) shape functions and the corresponding natural circular frequencies are from (2.56) and (2.52):

$$\hat{v}_p(x) = \sqrt{\frac{2}{\mu \ell}} \sin\left(\frac{p\pi}{\ell} x\right), \quad \omega_{0p} = \frac{p^2 \pi^2}{\ell^2} \sqrt{\frac{EI}{\mu}}.$$

We substitute the above shape functions and frequencies into (2.76) up to  $p = 3$

$$v(x, t) \approx F \sum_{p=1}^3 \frac{\hat{v}_p(a)}{\omega_{0p}^2 - \omega^2} \hat{v}_p(x) \sin(\omega t) = \frac{2F}{\mu \ell} \sum_{p=1}^3 \frac{\sin\left(\frac{p\pi}{\ell} a\right)}{\frac{p^4 \pi^4}{\ell^4} \frac{EI}{\mu} - \omega^2} \sin\left(\frac{p\pi}{\ell} x\right) \sin(\omega t).$$

The bending moment is

$$M(x, t) = -EI \frac{\partial^2 v(x, t)}{\partial x^2} \approx \frac{2F}{\mu \ell} \sum_{p=1}^3 \frac{\sin\left(\frac{p\pi}{\ell} a\right)}{\frac{p^4 \pi^4}{\ell^4} \frac{EI}{\mu} - \omega^2} \frac{p^2 \pi^2}{\ell^2} \sin\left(\frac{p\pi}{\ell} x\right) \sin(\omega t).$$

The given dataset is  $\ell = 12 \text{ m}$ ,  $a = \ell/4$ ,  $F = 1500 \text{ N}$ ,  $\mu = 500 \text{ kg/m}$ ,  $EI = 2 \cdot 10^9 \text{ Nm}^2$ , and  $\omega = 80 \text{ rad/s}$ . The above formula is evaluated at  $x = \ell/2$  and  $t = 2k\pi/\omega$  to get the maximum deflection of the mid point:

$$v_{\max}\left(\frac{\ell}{2}\right) \approx \frac{2F}{\mu \ell} \sum_{p=1}^3 \frac{\sin\left(\frac{p\pi}{\ell} a\right)}{\frac{p^4 \pi^4}{\ell^4} \frac{EI}{\mu} - \omega^2} \sin\left(\frac{p\pi}{2}\right) = 0.02853 \cdot 10^{-3} + 0 - 0.0002333 \cdot 10^{-3} = \underline{0.02830 \cdot 10^{-3} \text{ m}},$$

and to obtain the maximal bending moment at the mid point:

$$M_{\max}\left(\frac{\ell}{2}\right) \approx EI \frac{2F}{\mu\ell} \sum_{p=1}^3 \frac{\sin\left(\frac{p\pi}{\ell}a\right)}{\frac{p^4\pi^4 EI}{\ell^4} - \omega^2} \frac{p^2\pi^2}{\ell^2} \sin\left(\frac{p\pi}{2}\right) = 3911 + 0 - 287.8 = \underline{3624 \text{ Nm}}.$$

Notice that the second mode is intact in this load case because  $\hat{v}_2(\ell/2) = 0$ , and that the third term is smaller than the first term by two order of magnitude in case of the displacement, and by one order of magnitude in case of the bending moment. In general it is true that the higher modes have larger influence on the bending moment than on the displacement.

Finally, we also compute the maximal deflection and bending moment at the point where the machine is placed, i.e. at  $x = \ell/4$  (and at time  $t = 2k\pi/\omega$  again):

$$\begin{aligned} v_{\max}\left(\frac{\ell}{4}\right) &\approx \frac{2F}{\mu\ell} \sum_{p=1}^3 \frac{\sin\left(\frac{p\pi}{\ell}a\right)}{\frac{p^4\pi^4 EI}{\ell^4} - \omega^2} \sin\left(\frac{p\pi}{2}\right) = 0.02018 \cdot 10^{-3} + 0.001699 \cdot 10^{-3} + 0.0001649 \cdot 10^{-3} \\ &= \underline{0.02204 \cdot 10^{-3} \text{ m}}. \end{aligned}$$

$$M_{\max}\left(\frac{\ell}{4}\right) \approx EI \frac{2F}{\mu\ell} \sum_{p=1}^3 \frac{\sin\left(\frac{p\pi}{\ell}a\right)}{\frac{p^4\pi^4 EI}{\ell^4} - \omega^2} \frac{p^2\pi^2}{\ell^2} \sin\left(\frac{p\pi}{2}\right) = 2766 + 931.7 + 203.5 = \underline{3901 \text{ Nm}}.$$

We can see here again that the higher modes have greater influence on the bending moment than on the displacement.

### Prismatic beam under a moving constant force

In a lot of examples in structural design, the forces acting on the load bearing structures are moving: trains, truck, cars, cyclists, or pedestrians moving along bridges, cranes carrying loads along steel beams, etc. These loads can all be modelled by *moving forces*. Here we only deal with the simplest example, when one single constant force  $F$  moves along a prismatic beam with a constant velocity  $v$ , as it is shown in Figure 2.7 (b) for a pinned-pinned beam. The force  $q_t(x, t)$  that the beam is subjected to is

$$q_t(x, t) = F\delta(x - vt).$$

With the above load we can compute the modal force

$$Q_p(t) = \int_0^{\ell} F\delta(x - vt)\hat{v}_p(x) dx = F\hat{v}_p(vt)$$

and  $\eta_p(t)$

$$\eta_p(t) = \frac{F}{\omega_{0p}} \int_0^t \hat{v}_p(v\tau) \sin(\omega_{0p}\{t - \tau\}) d\tau$$

from (2.73) and (2.72), respectively. Finally, the particular solution of this load case is

$$v(x, t) = F \sum_{p=1}^{\infty} \frac{\hat{v}_p(x)}{\omega_{0p}} \int_0^t \hat{v}_p(v\tau) \sin(\omega_{0p}\{t - \tau\}) d\tau. \quad (2.77)$$

**Problem 2.4.4** (Vibration of a bridge under a moving vehicle). There is a vehicle going through the bridge with constant speed  $v = 130$  km/h. This vehicle is modelled with one constant force  $F = 80$  kN. The load bearing structure is a reinforced concrete beam with a single-celled box girder cross section. The length of the beam is  $\ell = 30$  m, its mass is  $\mu = 8$  t/m, and the bending stiffness is  $EI = 4 \cdot 10^7$  kNm<sup>2</sup>. Compute the deflection of the mid point of the beam when the force arrives to the middle of the bridge!

**Solution.** The normalised (modal) shape functions and the corresponding natural circular frequencies of a pinned-pinned beam are:

$$\hat{v}_p(x) = \sqrt{\frac{2}{\mu\ell}} \sin\left(\frac{p\pi}{\ell}x\right), \quad \omega_{0p} = \frac{p^2\pi^2}{\ell^2} \sqrt{\frac{EI}{\mu}}.$$

We substitute these results into (2.77):

$$v(x, t) = F \frac{2}{\mu\ell} \sum_{p=1}^{\infty} \frac{1}{\omega_{0p}} \sin\left(\frac{p\pi}{\ell}x\right) \int_0^t \sin\left(\frac{p\pi}{\ell}v\tau\right) \sin(\omega_{0p}\{t - \tau\}) d\tau.$$

Now, using (2.75), we can simplify the integral in the above equality and obtain

$$\begin{aligned} v(x, t) &= F \frac{2}{\mu\ell} \sum_{p=1}^{\infty} \frac{\sin\left(\frac{p\pi}{\ell}x\right)}{\omega_{0p}} \left\{ \frac{\omega_{0p}}{\omega_{0p}^2 - \frac{p^2\pi^2}{\ell^2}v^2} \sin\left(\frac{p\pi}{\ell}vt\right) - \frac{\frac{p\pi}{\ell}v}{\omega_{0p}^2 - \frac{p^2\pi^2}{\ell^2}v^2} \sin(\omega_{0p}t) \right\} \\ &= F \frac{2}{\mu\ell} \sum_{p=1}^{\infty} \sin\left(\frac{p\pi}{\ell}x\right) \frac{1}{\omega_{0p}^2 - \frac{p^2\pi^2}{\ell^2}v^2} \left\{ \sin\left(\frac{p\pi}{\ell}vt\right) - \frac{\frac{p\pi}{\ell}v}{\omega_{0p}} \sin(\omega_{0p}t) \right\} \\ &= F \frac{2}{\mu\ell} \sum_{p=1}^{\infty} \frac{\ell^2 \sin\left(\frac{p\pi}{\ell}x\right)}{p^2\pi^2 \left\{ \frac{p^2\pi^2}{\ell^2} \frac{EI}{\mu} - v^2 \right\}} \left\{ \sin\left(\frac{p\pi}{\ell}vt\right) - \frac{\ell v}{p\pi} \sqrt{\frac{\mu}{EI}} \sin\left(\frac{p^2\pi^2}{\ell^2} \sqrt{\frac{EI}{\mu}} t\right) \right\}. \end{aligned}$$

It is worth mentioning that the displacement becomes singular if the velocity of the moving force equals to one of the *resonant speeds*

$$v_p^{\text{crit}} = \frac{p\pi}{\ell} \sqrt{\frac{EI}{\mu}} = \omega_{0p} \frac{\ell}{p\pi}.$$

The deflection of the mid point ( $x = \ell/2$ ) of the beam at the time instant when the force arrives to the mid point, i.e.  $vt = \ell/2 \rightarrow t = \ell/2v$ , can be obtained from back substitution in the above formula. Without going into details, the result concerning the first three or the first five modes ( $p = 1, \dots, 3$  and  $p = 1, \dots, 5$ , respectively) is

$$\begin{aligned} v\left(\frac{\ell}{2}, \frac{\ell}{2v}\right)_{p=1, \dots, 3} &= \underline{1.087 \cdot 10^{-3} \text{ m}}, \\ v\left(\frac{\ell}{2}, \frac{\ell}{2v}\right)_{p=1, \dots, 5} &= \underline{1.088 \cdot 10^{-3} \text{ m}}. \end{aligned}$$

The bending moment is  $M = -EI d^2v(x, t)/dx^2$  which gives

$$\begin{aligned} M\left(\frac{\ell}{2}, \frac{\ell}{2v}\right)_{p=1, \dots, 3} &= \underline{5.253 \cdot 10^5 \text{ Nm}}, \\ M\left(\frac{\ell}{2}, \frac{\ell}{2v}\right)_{p=1, \dots, 5} &= \underline{5.446 \cdot 10^5 \text{ Nm}}. \end{aligned}$$

Notice that higher modes have significant effects on the bending moment, but not on the displacement.

According to earlier studies, the static deflection of the mid point of a simply supported beam if force  $F$  acts at the midspan is

$$v_{x=\ell/2}^{\text{static}} = \frac{F\ell^3}{48EI} = \underline{1.125 \text{ mm}}.$$

Finally, the ratio of the static and dynamic deflections is

$$v_{x=\ell/2}^{\text{def}} = \frac{1.088}{1.025} = \underline{1.0615} \rightarrow 6.15\%.$$

This can be much higher if the velocity of the force is close to one of the resonant speed of the structure.

### Prismatic beam under a moving harmonic force

In this load case a force  $F$  moves along the beam with a constant velocity  $v$ , while the amplitude of the force pulsates harmonically in time with frequency  $\omega$  (see Figure 2.7 (c)). Thus the force  $q_t(x, t)$  is given as

$$q_t(x, t) = F \sin(\omega t) \delta(x - vt).$$

The modal force is

$$Q_p(t) = \int_0^\ell F \sin(\omega t) \delta(x - vt) \hat{v}_p(x) dx = F \sin(\omega t) \hat{v}_p(vt)$$

and  $\eta_p(t)$  is

$$\eta_p(t) = \frac{F}{\omega_{0p}} \int_0^t \sin(\omega \tau) \hat{v}_p(v\tau) \sin(\omega_{0p}\{t - \tau\}) d\tau$$

due to (2.72) and (2.73). The particular solution of this forced vibration is

$$v(x, t) = F \sum_{p=1}^{\infty} \frac{\hat{v}_p(x)}{\omega_{0p}} \int_0^t \sin(\omega \tau) \hat{v}_p(v\tau) \sin(\omega_{0p}\{t - \tau\}) d\tau.$$

### Prismatic beam under a moving constant distributed load

Another, fairly simple way to model moving loads on structures is to assume that the loading is equally distributed and moves with a constant speed  $v$ , as shown in Figure 2.7 (d). It is applicable, for example, to approximate the dynamics of a simple bridge under a magnetic train, which exerts a fairly constant distributed load to the guideway. The force  $q_t(x, t)$  is now a constant distributed load  $q$  moving with a constant speed  $v$ :

$$q_t(x, t) = qH(x)\{1 - H(x - vt)\}. \quad (2.78)$$

Here  $H(\xi)$  is the *Heaviside function* which obeys

$$H(\xi) = \begin{cases} 0, & \text{if } \xi < 0 \\ 1/2, & \text{if } \xi = 0 \\ 1, & \text{if } \xi > 0 \end{cases},$$

$$\int_{-\infty}^{+\infty} f(\xi)H(\xi) d\xi = \int_0^{+\infty} f(\xi) d\xi.$$

The consequence of the latter property is that

$$\int_{-\infty}^{+\infty} f(\xi)\{1 - H(\xi)\} d\xi = \int_{-\infty}^0 f(\xi) d\xi, \quad \text{and therefore}$$

$$\int_{-\infty}^{+\infty} f(\xi)H(\xi)\{1 - H(\xi - a)\} d\xi = \int_0^a f(\xi) d\xi.$$

The modal force is computed from (2.72):

$$Q_p(t) = \int_0^\ell qH(x)\{1 - H(x - vt)\}\hat{v}_p(x) dx = q \int_0^{vt} \hat{v}_p(x) dx.$$

It means that the distributed load  $q$  acts on the beam in between  $x = 0$  and  $x = vt$ , which is the load case when the train arrives on the bridge. The time dependent  $\eta_p(t)$  comes from (2.73):

$$\eta_p(t) = \frac{q}{\omega_{0p}} \int_0^t \left\{ \int_0^{v\tau} \hat{v}_p(x) dx \right\} \sin(\omega_{0p}\{t - \tau\}) d\tau.$$

Finally, the forced vibration finally is determined by the integral

$$v(x, t) = q \sum_{p=1}^{\infty} \frac{\hat{v}_p(x)}{\omega_{0p}} \int_0^t \left\{ \int_0^{v\tau} \hat{v}_p(x) dx \right\} \sin(\omega_{0p}\{t - \tau\}) d\tau.$$

Further interesting problems concerning the dynamics of forced slender continua, vibrations of beams with various boundary conditions, non-uniform beams, coupled beam-vehicle systems, etc. can be found in the literature [5, 6, 11].

## Chapter 3

# Dynamics of planar frame structures

In this chapter we study the dynamics of planar frame structures. Planar frames are widely used in engineering practice. They can be modeled by slender beam members connected by hinges, rigid or elastic connections.

The beam members are prismatic. The axes of the beams are in a common plane, the cross-sections of the beams and the loads are symmetric to that common plane. We neglect stability questions, thus the frame remains planar during the deformations. The beams are assumed to be unsharable, but extensible and bendable. The material of the beams is linearly elastic with *Young's* modulus  $E$ . The cross-sectional area of a beam is denoted by  $A$ , while the second moment of area with respect to the axis perpendicular to the plane of the frame is  $I$ . The beam is of length  $\ell$ , and its mass per unit length is denoted by  $\mu$ . In this chapter we neglect the effect of damping, and we also neglect the effect of rotary inertia of the cross-sections.

First we overview the basics about static equilibria of planar frames. The calculation of the static stiffness matrix of one beam member and of the whole structure are shown. We introduce two possible models to handle different support conditions.

Then we go on with dynamical effects and demonstrate how to calculate the dynamic stiffness matrix of the structure. We also show approximate methods to generate the dynamic stiffness matrix. Based on the accurate or on the approximate stiffness matrices, a system of differential equations of motion can be compiled. These equations can be solved for external dynamical loadings either directly or by using modal analysis. A special loading very important in structural design is the support vibration, which is also discussed in details. Finally, we present the reduced modal analysis technique and study its accuracy.

Although planar frames are not the most general structures one can meet in structural design, the concepts shown in this chapter can be generalized to other types of load bearing structures. The reader can adopt the notations used here for the applications of these methods to FE modeling readily.



### 3.1 Static matrix displacement method

We have already seen in our earlier studies, and also in Section 1.3, that the continuous structures constructed of slender *rods* can be approximated by multi-degree-of-freedom systems. In the simplest model, we divided the structure into individual (beam) members, and the displacements of the end points of these members became the degrees of freedom. In the dynamical analysis, we concentrated the masses of each beam into its end points, which resulted in a *diagonal* mass matrix. The rotational inertia of the beams was neglected, but sufficiently short members implied sufficiently accurate results in terms of the vibration of the structure. The accuracy was comparable to the results of the continuous system. The matrix differential equation of motion is

$$\mathbf{M}\ddot{\mathbf{u}}(t) + \mathbf{K}\mathbf{u}(t) = \mathbf{q}(t).$$

We have also seen, that there are two simple method for the construction of the stiffness matrix  $\mathbf{K}$ .

- Calculation of the stiffness matrix based on its physical meaning.  
The product  $\mathbf{K}\mathbf{u}$  (stiffness matrix times the displacements of the DOFs) results in the forces  $\mathbf{f}_S$  needed to be applied on the DOF in order to induce the displacements  $\mathbf{u}$ . If we multiply the stiffness matrix by the  $i$ th unit vector  $\mathbf{e}_i$ , then the  $i$ th column of the stiffness matrix is obtained. The entries of this column are the forces that act on each degree-of-freedom in such a way, that the displacements of all degrees-of-freedom are zero, except for the  $i$ th, which is one. These  $N$  constrains make the calculation of the entries of the  $i$ th column of the stiffness matrix possible.
- Calculation of the stiffness matrix based on the flexibility matrix.  
In contrast to the stiffness matrix, the *flexibility matrix*  $\mathbf{F}$  multiplied by the forces  $\mathbf{f}_S$  results in the displacements caused by the forces. If we substitute the  $i$ th unit vector  $\mathbf{e}_i$  into the vector of forces acting on the nodes, the product  $\mathbf{F} \cdot \mathbf{e}_i$ , i.e. the  $i$ th column of the flexibility matrix. This column contains the displacements of each degree-of-freedom caused by a unit force acting on the  $i$ th degree-of-freedom, while the others are unloaded. These displacements can be calculated with various methods of Strength of Materials, or Structural Analysis. Finally, the stiffness matrix is the inverse of the flexibility matrix:  $\mathbf{K} = \mathbf{F}^{-1}$ .

For practical purposes the above methods are not recommended, because the degrees-of-freedom are connected to each other, so calculations of the inverse of full matrices are needed.

A better approximation can be achieved by the matrix displacement method of frame structures, thoroughly discussed in the field of Structural Analysis Theory [8]. Here we are going through its main steps only.

#### 3.1.1 Nodal decomposition of planar frames

A planar frame is composed of beam members connected together by hinges, rigid or elastic connections, and the whole frame is attached to the ground in a statically determinate (or indeterminate) way. If we are to analyse the structure by means of the matrix displacement

method, the first step we need to make is to decompose the frame into *nodes* and *frame members*. The nodes are at the connections of the beams and at the supporting points. The total number of nodes of the frame is denoted by  $M$ . The frame members are the beam members connecting these nodes. Thus each beam is connected to two nodes at its ends. A general beam member between nodes  $i$  and  $j$  is called beam  $ij$ . (We consistently take  $i < j$  everywhere in this chapter.) As we will see, the deformation of beam  $ij$  (and so its internal forces) can be fully described by the displacements of its end nodes  $i$  and  $j$ . Since we study the planar deformation of the plane, one node has three degrees of freedom: two translations and one rotation. Therefore the total DOF of the frame is  $N = 3M$ . We can reduce both the external loadings and the elastic forces of the beams to the nodes of the frame. Then we can compile a system of equilibrium equations where the unknowns are the displacements of the nodes. In this manner, the statical analysis of a continuum frame structure can be reduced to the analysis of a model with finite number of degrees-of-freedom.

The easiest way to deal with the elastic forces that act from the end of the beams to the nodes is the following. First, we release only one DOF of the frame and apply a unit displacement there, while the other degrees-of-freedom are kept zero. Second, we collect the elastic forces acting from the ends of the beams onto the nodes. There are used to compose one column of the total stiffness matrix. Then we repeat these steps for all the other DOF independently. As a result, we can compile the total static stiffness matrix  $\mathbf{K}$  of the frame. This compilation requires that the displacements of a node induce forces on a different node only if these nodes are connected by a beam member. That is the reason why we have to constrain the rotation of the nodes too, and not just their translations, as it is demonstrated in Figure 3.1.

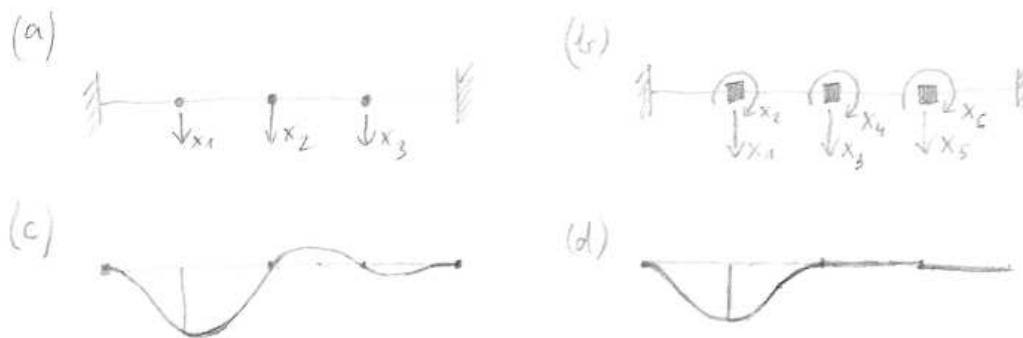


**Figure 3.1:** Comparing various discretization of a fixed-fixed beam. (a) Discrete model with three translational degrees-of-freedom. (b) Discrete model with three translational and three rotational degrees-of-freedom. (c) Deformed shape of the 3DOF model due to a displacement of the first DOF. (d) Deformed shape of the 6DOF model caused by a displacement of the first DOF.

### 3.1.2 Global and local reference systems, transformations

We use two distinct *Cartesian* reference systems. One is called the *global reference system*, which is a left-handed coordinate system  $XYZ$  fixed in the space. The frame structure is in the plane  $XY$ , and the axis  $Z$  points outward from the plane. The other coordinate system,

the *local* one is the left-handed  $xyz$  system. Figure 3.2 shows a planar vector  $\mathbf{w}$  in both coordinate systems. From the figure one can conclude, that the transformation between the local coordinates  $w_x, w_y$  and the global coordinates  $w_X, w_Y$  can be done as

$$\begin{aligned} w_X &= w_x \cos \alpha - w_y \sin \alpha, & w_Y &= w_x \sin \alpha + w_y \cos \alpha & \text{and} \\ w_x &= w_X \cos \alpha + w_Y \sin \alpha, & w_y &= -w_X \sin \alpha + w_Y \cos \alpha. \end{aligned} \quad (3.1)$$

We define a local coordinate system for each beam member. The local reference system of beam  $ij$  is oriented in such a way that axis  $x$  points from node  $i$  to the node  $j$ . (Note, that  $i < j$  holds.) The local axis  $z$  is parallel with the global axis  $Z$ , and axis  $y$  is oriented accordingly to  $x$  and  $z$ .

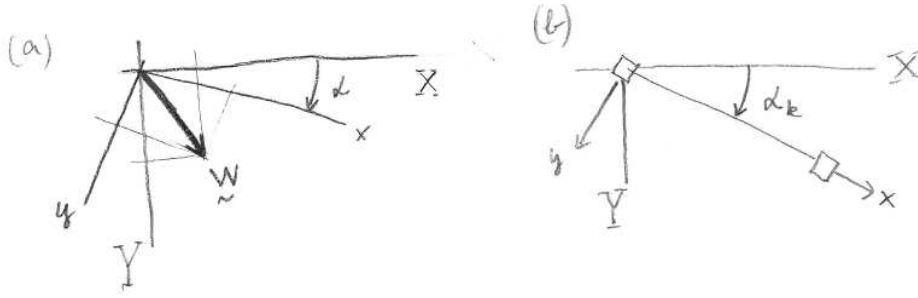


**Figure 3.2:** (a) Transformation of the components of a planar vector  $\mathbf{w}$  between the local and the global reference systems. (b) The local reference system  $xy$  of the  $ij$ th beam member and the global reference system  $XY$ .

The displacements (two components of the translation and one rotation) of node  $i$  is collected into the vector  $\mathbf{u}_i$ . In the global reference system these components are

$$\mathbf{u}_i^{\text{glob}} = \begin{bmatrix} u_{iX}^{\text{glob}} \\ u_{iY}^{\text{glob}} \\ \varphi_{iZ}^{\text{glob}} \end{bmatrix}, \quad (3.2)$$

while in the local reference system of the beam  $ij$ th they are

$$\mathbf{u}_i^{\text{loc}} = \begin{bmatrix} u_{ix}^{\text{loc}} \\ u_{iy}^{\text{loc}} \\ \varphi_{iz}^{\text{loc}} \end{bmatrix}. \quad (3.3)$$

Since axes  $z$  and  $Z$  coincide, the rotations are the same in both reference systems, i.e.  $\varphi_{iz}^{\text{loc}} = \varphi_{iZ}^{\text{glob}}$ . Therefore we leave the superscripts “loc” and “glob” in the case of the rotations. We write the relation between the components of the displacement vector in the global and local systems (Eq. (3.2), (3.3)) as:

$$\mathbf{u}_i^{\text{glob}} = \mathbf{T}_{ij} \mathbf{u}_i^{\text{loc}}, \quad \mathbf{u}_i^{\text{loc}} = \mathbf{T}_{ij}^T \mathbf{u}_i^{\text{glob}}. \quad (3.4)$$

In the above equations matrix  $\mathbf{T}_{ij}$  is called the *transformation matrix* of the local reference system of beam  $ij$ . Assuming, that the beam  $ij$  is rotated by  $\alpha_{ij}$  with respect to the global

system (see in Figure 3.2 (b)), and using the transformation for the rotation (3.1), the entries of the transformation matrix are:

$$\mathbf{T}_{ij} = \begin{bmatrix} \cos \alpha_{ij} & -\sin \alpha_{ij} & 0 \\ \sin \alpha_{ij} & \cos \alpha_{ij} & 0 \\ 0 & 0 & 1 \end{bmatrix}.$$

The transformation matrix  $\mathbf{T}_{ij}$  is a *proper orthogonal rotation*, so its inverse is its transpose:

$$\mathbf{T}_{ij}^{-1} = \mathbf{T}_{ij}^T = \begin{bmatrix} \cos \alpha_{ij} & \sin \alpha_{ij} & 0 \\ -\sin \alpha_{ij} & \cos \alpha_{ij} & 0 \\ 0 & 0 & 1 \end{bmatrix}.$$

The displacements of the nodes of beam  $ij$  given in the local reference system are

$$\mathbf{u}_{ij}^{\text{loc}} = \begin{bmatrix} \mathbf{u}_i^{\text{loc}} \\ \mathbf{u}_j^{\text{loc}} \end{bmatrix} = \begin{bmatrix} u_{ix}^{\text{loc}} \\ u_{iy}^{\text{loc}} \\ \varphi_{iz} \\ u_{jx}^{\text{loc}} \\ u_{jy}^{\text{loc}} \\ \varphi_{jz} \end{bmatrix}. \quad (3.5)$$

An example on the above modeling steps are presented in Figure 3.3. The structure in Figure 3.3 (a) is divided into five members and five nodes. This decomposition is shown in Figure 3.3 (b) alongside with the global and the local reference systems. The supports are replaced by (support) nodes 1 and 5. They are treated equivalently with the internal nodes during the compilation of the total stiffness matrix. The support conditions (whether they are fixed, hinged, or elastic) are counted for in the total stiffness matrix.

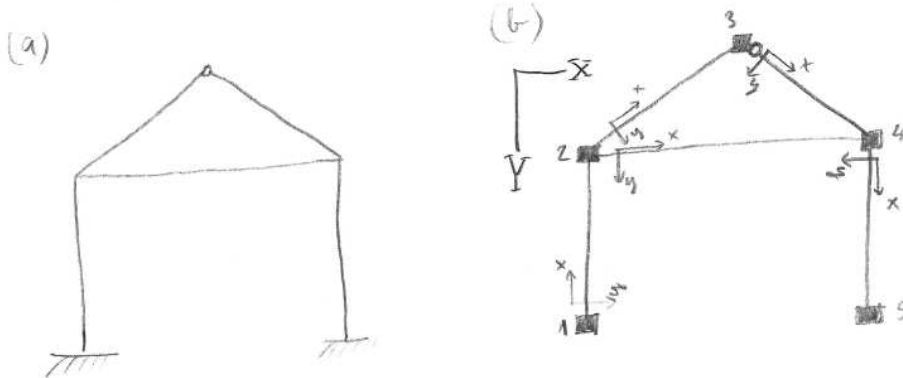


**Figure 3.3:** (a) Mechanical model of a planar frame structure. (b) Nodes and members of the structure (a) with the global and local reference systems.

Finally, we define two further rules that we follow during the model building process.

- We set three degrees-of-freedom to every node, and there is at least one member rigidly connected to every node (see node 3 of the frame in Fig. 3.3(b)).
- Elastic supports are modeled by introducing additional *supporting nodes*.

### 3.1.3 Elementary static stiffness matrix in the local reference system

The elementary (static) stiffness matrix  $\mathbf{K}_{ij}^{\text{loc}}$  transforms the nodal displacements Eq. (3.5) into nodal forces  $(f_{ix}^{\text{loc}}, f_{iy}^{\text{loc}}, f_{jx}^{\text{loc}}, f_{jy}^{\text{loc}})$  and moments  $(w_{iz}, w_{jz})$  acting on the end of the beam:

$$\mathbf{f}_{ij}^{\text{loc}} = \begin{bmatrix} f_{ix}^{\text{loc}} \\ f_{iy}^{\text{loc}} \\ w_{iz} \\ f_{jx}^{\text{loc}} \\ f_{jy}^{\text{loc}} \\ w_{jz} \end{bmatrix} = \mathbf{K}_{ij}^{\text{loc}} \mathbf{u}_{ij}^{\text{loc}}. \quad (3.6)$$

These are called the *end-of-beam internal forces*. The opposite of these forces act on the nodes.

The elementary (static) stiffness matrix  $\mathbf{K}_{ij}^{\text{loc}}$  of beam  $ij$  can be derived in several ways. In matrix  $\mathbf{K}_{ij}^{\text{loc}}$ , entry  $p,r$  (i.e., the  $p$ th element of the  $r$ th column of the matrix) denotes the end-of-beam internal force in the  $p$ th DOF due to a unit displacement applied at the  $r$ th DOF. The first DOF of beam  $ij$  is the translation of the starting end  $i$  along the beam axis  $x$ . Due to a unit displacement of this DOF, the deformed shape of the beam axis is denoted by  $u_{ix}(x)$ . The corresponding end-of-beam internal forces are assigned by  $N_{iix}, V_{iix}, M_{iix}$  at end  $i$  and  $N_{jix}, V_{jix}, M_{jix}$  at end  $j$ . Thus the notation of these internal forces are such that the first subscript refers to the “place”, while the rest are for the “cause”. These end-of-beam internal forces define the first column of the elementary stiffness matrix of beam  $ij$  in the local reference system. The second DOF of the beam is the translation of end  $i$  along axis  $y$ . The second column of the elementary stiffness matrix thus contains the end-of-beam internal forces due to a unit translation of its starting end  $i$  along  $y$ . This is visualised in Figure 3.4 (a): the unit translation of end  $i$  induces deformation and internal forces in the beam. The positive definition of the internal forces are well known from Statics. The end-of-beam internal forces and a sketch of the bending moment diagram are shown in Figure 3.4 (b). The positive definition of the entries of the columns of the stiffness matrix corresponds to the right handed coordinate system  $xyz$ , as indicated in Figure 3.4 (c). The internal forces at the ends of the beam due to the unit translation of end  $i$  along  $y$  are denoted by  $N_{iiy}, V_{iiy}, M_{iiy}, N_{jiy}, V_{jiy}, M_{jiy}$ , while the corresponding deformed shape of the axis of the beam is assigned by  $v_{iy}(x)$ . The third DOF of beam  $ij$  is the rotation of end  $i$ . A unit rotation of end  $i$  induces the deformation  $v_{i\varphi}(x)$  of the beam axis, and the corresponding end-of-beam internal forces are:  $N_{ii\varphi}, V_{ii\varphi}, M_{ii\varphi}, N_{ji\varphi}, V_{ji\varphi}, M_{ji\varphi}$ . The same notation is used for the other 3DOF of the beam. The fourth, and the fifth DOF of beam  $ij$  are the translations of end  $j$  along  $x$  and  $y$ , respectively. Unit translations corresponded to these DOF are used to construct the fourth and fifth column of the elementary stiffness matrix. At last, the sixth DOF is the rotation of end  $j$ . The deformed beam axis due to a unit rotation of end  $j$  is denoted by  $v_{j\varphi}(x)$ , and the corresponding end-of-beam internal forces are  $N_{ij\varphi}, V_{ij\varphi}, M_{ij\varphi}$  at end  $i$  and  $N_{jj\varphi}, V_{jj\varphi}, M_{jj\varphi}$  at end  $j$ . These are the entries of the sixth column of the elementary stiffness matrix given in the local reference system of beam  $ij$ .

We show two methods for the calculation of the entries of  $\mathbf{K}_{ij}^{\text{loc}}$ .

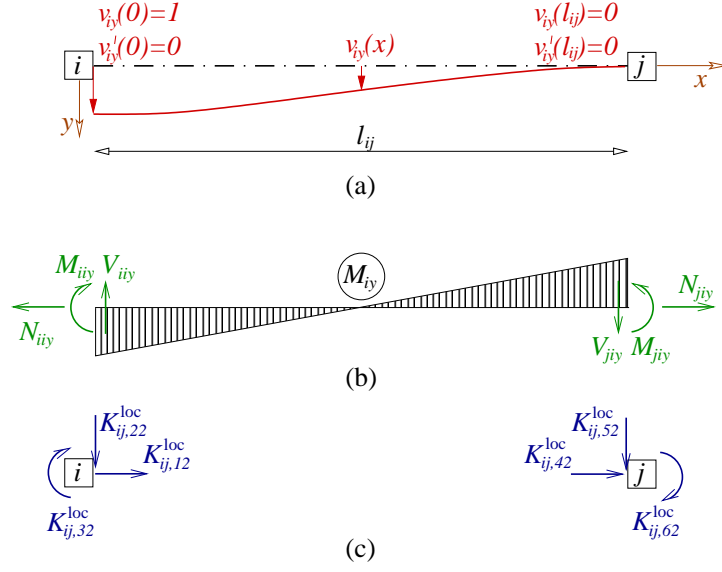


**Figure 3.4:** (a) Sketch of the deformed shape of a fixed-fixed beam  $ij$  due to a unit translation of end  $i$  along axis  $y$ . (b) The bending moment diagram and the positive definition of the internal forces at the ends of the beam. (c) Physical meaning and positive definition of the entries of the second column of the elementary stiffness matrix.

### Solving the differential equations of rods

The entries of the first and the fourth columns of  $\mathbf{K}_{ij}^{loc}$  are computed from the differential equation of the stretched bar (Eq. (2.3) at  $\mu = 0$  and  $q(x, t) = 0$ )

$$EAu''(x) = 0, \quad (3.7)$$

which is fulfilled by the first order polynomial

$$u(x) = B_1x + B_0. \quad (3.8)$$

Here the unknown coefficients  $B_0, B_1$  can be computed from two prescribed boundary conditions. These are

$$u_{ix}(0) = 1, \quad u_{ix}(\ell) = 0 \quad (3.9)$$

for the first column and

$$u_{jx}(0) = 0, \quad u_{jx}(\ell) = 1 \quad (3.10)$$

for the fourth column. The solution  $u_{ix}(x)$  is the deformed shape of the beam caused by a unit translation of end  $i$  along  $x$ . The corresponding end-of-beam internal forces are

$$\begin{aligned} N_{iix} &= EAu'_{ix}(0), & V_{iix} &= 0, & M_{iix} &= 0, \\ N_{jix} &= EAu'_{ix}(\ell), & V_{jix} &= 0, & M_{jix} &= 0. \end{aligned} \quad (3.11)$$

The entries of the first column of the stiffness matrix are

$$\mathbf{k}_{ij,1}^{loc} = [-N_{iix}, 0, 0, N_{jix}, 0, 0]^T. \quad (3.12)$$

The positive definition of the entries of matrix  $\mathbf{K}_{ij}^{\text{loc}}$  is given by the local coordinate system  $xyz$ , while a positive normal force denotes tension. That is the reason why the first entry is the opposite of the normal force here. See the positive definition of the internal forces and of the entries of  $\mathbf{K}_{ij}^{\text{loc}}$  in Figure 3.4 (b) and (c).

**Problem 3.1.1** (Entries of the first column of the elementary stiffness matrix). The fixed-fixed beam  $ij$  is of length  $\ell$ , normal stiffness  $EA$ , bending stiffness  $EI$ , and mass per unit length  $\mu$ . Determine the entries of the first column of the elementary stiffness matrix of the beam!

**Solution.** Entries of the first column of the elementary stiffness matrix are the end-of-beam internal forces caused by a unit translation of end  $i$  along the axis  $x$  of the member. First we compute the deformation  $u_{ix}(x)$  of the bar due to the unit translation of end  $i$ , i.e. the solution of (3.7) with boundary conditions (3.9). The solution of (3.7) is (3.8), where the unknown coefficients  $B_0, B_1$  are from boundary conditions (3.9). We write these boundary conditions using (3.8):

$$\begin{aligned} u_{ix}(0) &= B_1 \cdot 0 + B_0 = 1 & \rightarrow & B_0 = 1, \\ u_{ix}(\ell) &= B_1 \cdot \ell + 1 = 0 & \rightarrow & B_1 = -1/\ell \end{aligned}$$

Thus the deformed shape is given by

$$u_{ix}(x) = B_0 + B_1 x = 1 - \frac{1}{\ell} x. \quad (3.13)$$

The first derivative of this function is

$$u'_{ix}(x) = -\frac{1}{\ell}.$$

Now, according to (3.11) and (3.12), the entries of the first column of  $\mathbf{K}_{ij}^{\text{loc}}$  are

$$\begin{aligned} K_{ij,11}^{\text{loc}} &= -EAu'_{ix}(0) = \frac{EA}{\ell}, \\ K_{ij,21}^{\text{loc}} &= 0, \\ K_{ij,31}^{\text{loc}} &= 0, \\ K_{ij,41}^{\text{loc}} &= EAu'_{ix}(\ell) = -\frac{EA}{\ell}, \\ K_{ij,51}^{\text{loc}} &= 0, \\ K_{ij,61}^{\text{loc}} &= 0. \end{aligned}$$

We can compute an entry of the second, third, fifth, or sixth columns of the elementary stiffness matrix by solving the differential equation of the bent beam (Eq. (2.47) with  $\mu = 0$ )

$$EIv''''(x) = 0. \quad (3.14)$$

Eq. (3.14) is fulfilled by a third order polynomial

$$v(x) = A_3 x^3 + A_2 x^2 + A_1 x + A_0. \quad (3.15)$$

The unknown coefficients  $A_0, A_1, A_2, A_3$  can be computed from four prescribed boundary conditions. For the second column, these conditions are

$$v_{iy}(0) = 1, \quad v'_{iy}(0) = 0, \quad v_{iy}(\ell) = 0, \quad v'_{iy}(\ell) = 0, \quad (3.16)$$



i.e. there are a unit translation of end  $i$  along  $y$ , zero rotations of the ends, zero translation at end  $j$ . See the corresponding shape in Figure 3.4 (a). In case of the third column, the boundary conditions are

$$v_{i\varphi}(0) = 0, \quad v'_{i\varphi}(0) = 1, \quad v_{i\varphi}(\ell) = 0, \quad v'_{i\varphi}(\ell) = 0 \quad (3.17)$$

(no translations at the ends, unit rotation at end  $i$ , zero rotation at the other end  $j$ ). For the fifth and the sixth columns, we have to use

$$\begin{aligned} v_{jy}(0) = 0, \quad v'_{jy}(0) = 0, \quad v_{jy}(\ell) = 1, \quad v'_{jy}(\ell) = 0 \quad \text{and} \quad (3.18) \\ v_{j\varphi}(0) = 0, \quad v'_{j\varphi}(0) = 0, \quad v_{j\varphi}(\ell) = 0, \quad v'_{j\varphi}(\ell) = 1, \end{aligned}$$

respectively. The end-of-beam internal forces due to, for instance, a unit translation of end  $i$  are:

$$\begin{aligned} N_{iyy} = 0, \quad V_{iyy} = -EIv'''_{iy}(0), \quad M_{iyy} = -EIv''_{iy}(0), \\ N_{jyy} = 0, \quad V_{jyy} = -EIv'''_{iy}(\ell), \quad M_{jyy} = -EIv''_{iy}(\ell). \end{aligned} \quad (3.19)$$

The entries of the second column of the elementary stiffness matrix are then

$$\mathbf{k}_{ij,2}^{\text{loc}} = [0, -V_{iyy}, M_{iyy}, 0, V_{jyy}, -M_{jyy}]^T.$$

The positive definition of the internal forces and the entries of the stiffness matrix is visualized in Figure 3.4 (b) and (c).

The whole stiffness matrix has the following structure:

$$\mathbf{K}_{ij}^{\text{loc}} = \left[ \begin{array}{ccc|ccc} -N_{iix} & 0 & 0 & -N_{ijx} & 0 & 0 \\ 0 & -V_{iyy} & -V_{i\varphi} & 0 & -V_{jyy} & -V_{j\varphi} \\ 0 & M_{iyy} & M_{i\varphi} & 0 & M_{jyy} & M_{j\varphi} \\ \hline N_{jix} & 0 & 0 & N_{jxx} & 0 & 0 \\ 0 & V_{jyy} & V_{j\varphi} & 0 & V_{jyy} & V_{j\varphi} \\ 0 & -M_{jyy} & -M_{j\varphi} & 0 & -M_{jyy} & -M_{j\varphi} \end{array} \right]. \quad (3.20)$$

**Problem 3.1.2** (Entries of the third column of the elementary stiffness matrix). Beam  $ij$  is of length  $\ell$ , normal stiffness  $EA$ , bending stiffness  $EI$ , and mass per unit length  $\mu$ . Determine the entries of the third column of its elementary stiffness matrix!

**Solution.** Entries of the third column of the elementary stiffness matrix are the end-of-beam internal forces caused by a unit rotation of end  $i$ . Figure 3.5 shows (a) the model, (b) the internal forces at the ends, and (c) the positive definition of the corresponding entries of the stiffness matrix.

First we need to compute the shape function  $v_{i\varphi}(x)$ , which is the deformation of the beam due to a unit rotation of end  $i$ , i.e. the solution of (3.14) with boundary conditions (3.17). The solution of (3.14) is (3.15). Here the unknown coefficients  $A_0, A_1, A_2, A_3$  are from boundary conditions (3.17). We write these boundary conditions using (3.15):

$$\begin{aligned} v_{i\varphi}(0) = A_3 \cdot 0^3 + A_2 \cdot 0^2 + A_1 \cdot 0 + A_0 = 0 & \rightarrow A_0 = 0, \\ v'_{i\varphi}(0) = 3A_3 \cdot 0^2 + 2A_2 \cdot 0 + A_1 = 1 & \rightarrow A_1 = 1, \\ v_{i\varphi}(\ell) = A_3 \cdot \ell^3 + A_2 \cdot \ell^2 + \ell = 0 & \rightarrow A_2 = -1/\ell - A_3\ell, \\ v'_{i\varphi}(\ell) = 3A_3 \cdot \ell^2 + 2(-1/\ell - A_3\ell)\ell + 1 = 0 & \rightarrow A_3 = 1/\ell^2. \end{aligned}$$



Thus the shape function is

$$v_{i\varphi}(x) = \frac{1}{\ell^2}x^3 - \frac{2}{\ell}x^2 + x = \ell \left( \left\{ \frac{x}{\ell} \right\}^3 - 2 \left\{ \frac{x}{\ell} \right\}^2 + \frac{x}{\ell} \right). \quad (3.21)$$

The second and the third derivatives of this function are

$$v''_{i\varphi}(x) = \frac{6}{\ell^2}x - \frac{4}{\ell},$$

$$v'''_{i\varphi}(x) = \frac{6}{\ell^2}.$$

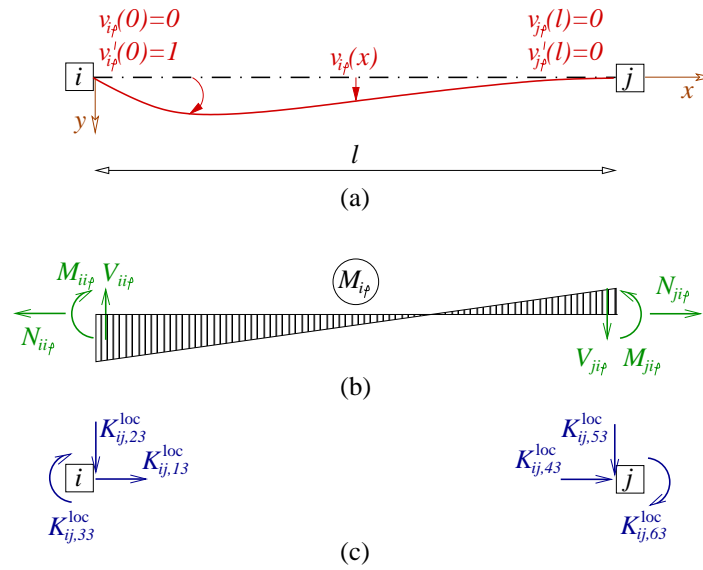


**Figure 3.5:** (a) Sketch of the deformed shape of a fixed-fixed beam  $ij$  due to a unit rotation of end  $i$ . (b) The bending moment diagram and the positive definition of the internal forces at the ends of the beam. (c) Physical meaning and positive definition of the entries of the third column of the elementary stiffness matrix.

Finally, according to (3.19) and (3.20), the entries of the third column of the stiffness matrix of the fixed-fixed beam  $ij$  are

$$K_{ij,13}^{loc} = 0,$$

$$K_{ij,23}^{loc} = EIv'''_{i\varphi}(0) = \frac{6EI}{\ell^2},$$

$$K_{ij,33}^{loc} = -EIv''_{i\varphi}(0) = \frac{4EI}{\ell},$$

$$K_{ij,43}^{loc} = 0,$$

$$K_{ij,53}^{loc} = -EIv'''_{i\varphi}(\ell) = -\frac{6EI}{\ell^2},$$

$$K_{ij,63}^{loc} = EIv''_{i\varphi}(\ell) = \frac{2EI}{\ell}.$$

### Applying the principle of virtual displacements

Alternatively, we can apply the principle of virtual displacements to determine the entries of the stiffness matrix. This principle is within the scope of Strength of Materials. The principle states that “*The work of a statically admissible force system on any arbitrary virtual displacement system must be zero*” [7].

We show how to use this principle to compute, for example, entry 3,2 of matrix  $\mathbf{K}_{ij}^{\text{loc}}$ . This entry is the bending moment at end  $i$  due to a unit translation of end  $i$  along  $y$ . Therefore, we have to compute  $M_{iyy}$ , which is the bending moment at end  $i$  from the shape function  $v_{iy}(x)$  fulfilling (3.16). See Figure 3.4 for further explanations. First we take the force system shown in Figure 3.4 (b) as statically admissible. Then we consider the displacement system caused by a unit rotation of end  $i$  as virtual, and apply the principle to these force and displacement systems. The displacement system  $v_{i\varphi}(x)$  caused by a unit rotation of end  $i$  is sketched in Figure 3.5 (a). The corresponding end-of-beam internal forces are shown in Figure 3.5 (b).

The virtual work done by the force system on the virtual displacement system is:

$$\delta W_{\text{ss}} = M_{iyy} \cdot 1 - \int_0^\ell M_{iy}(x) \kappa_{i\varphi}(x) dx = M_{iyy} - EI \int_0^\ell v_{iy}''(x) v_{i\varphi}''(x) dx = 0.$$

Thus

$$K_{ij,32}^{\text{loc}} = M_{iyy} = EI \int_0^\ell v_{iy}''(x) v_{i\varphi}''(x) dx.$$

We can also take the force system corresponds to a unit rotation of end  $i$  as statically admissible, and consider the displacement system shown in Figure 3.4 (b) as virtual and apply the principle of virtual displacements. We get

$$\delta W_{\text{ss}} = -V_{ii\varphi} \cdot 1 - \int_0^\ell M_{i\varphi}(x) \kappa_{iy}(x) dx = -V_{ii\varphi} - EI \int_0^\ell v_{i\varphi}''(x) v_{iy}''(x) dx = 0,$$

thus

$$K_{ij,23}^{\text{loc}} = -V_{ii\varphi} = EI \int_0^\ell v_{i\varphi}''(x) v_{iy}''(x) dx = K_{ij,32}^{\text{loc}}. \quad (3.22)$$

The stiffness matrix is symmetric.

In order to write the formula of  $\mathbf{K}_{ij}^{\text{loc}}$  in a compact form, first we construct the matrix of shape functions

$$\mathbf{N} = \begin{bmatrix} u_{ix}(x) & 0 & 0 & u_{jx}(x) & 0 & 0 \\ 0 & v_{iy}(x) & v_{i\varphi}(x) & 0 & v_{jy}(x) & v_{j\varphi}(x) \end{bmatrix}. \quad (3.23)$$

Here  $u_{ix}(x)$  is the shape function of the beam due to a unit translation of end  $i$  along  $x$ . This is the solution of (3.7) with boundary conditions (3.9). Function  $v_{iy}(x)$  is the shape function

due to a unit translation of end  $i$  along  $y$ , i.e. the solution of (3.14) with boundary conditions (3.16). The shape function  $v_{i\varphi}(x)$  is corresponded to a unit rotation of end  $i$ . It is the solution of (3.14) with boundary conditions (3.17). The same holds for subscript  $j$  with the appropriate boundary conditions. <sup>1</sup> Second, we introduce the matrix  $\mathbf{L}$  of differential operators

$$\mathbf{L} = \begin{bmatrix} \frac{d}{dx} & 0 \\ 0 & -\frac{d^2}{dx^2} \end{bmatrix} \quad (3.24)$$

and denote the product of  $\mathbf{L}$  and  $\mathbf{N}$  by  $\mathbf{B}$ : <sup>2</sup>

$$\mathbf{B} = \mathbf{L}\mathbf{N}. \quad (3.25)$$

Now, we collect the normal and the bending stiffnesses of the member in matrix  $\mathbf{D}$ :

$$\mathbf{D} = \begin{bmatrix} EA & 0 \\ 0 & EI \end{bmatrix}. \quad (3.26)$$

Finally, with the aid of these matrices, the elementary stiffness matrix  $\mathbf{K}_{ij}^{\text{loc}}$  of the beam can be written as

$$\mathbf{K}_{ij}^{\text{loc}} = \int_0^\ell \mathbf{B}^T \mathbf{D} \mathbf{B} \, dx. \quad (3.27)$$

From this formulation it can be easily seen, that the stiffness matrix is *symmetric*.

**Problem 3.1.3** (Entry 3,5 of the elementary stiffness matrix). There is a fixed-fixed beam  $ij$  of length  $\ell$ , normal stiffness  $EA$ , bending stiffness  $EI$ , and mass per unit length  $\mu$ . Determine the entry 3,5 of its elementary stiffness matrix!

**Solution.** Entry 3,5 is the bending moment at end  $i$  due to a unit translation of end  $j$ . From Eq. (3.27) we need only the 3rd row and the 5th column.

$$K_{ij,35}^{\text{loc}} = \int_0^\ell \mathbf{b}_3^T \mathbf{D} \mathbf{b}_5 \, dx = \int_0^\ell \begin{bmatrix} 0 & -v_{i\varphi}''(x) \end{bmatrix} \begin{bmatrix} EA & 0 \\ 0 & EI \end{bmatrix} \begin{bmatrix} 0 \\ -v_{jy}''(x) \end{bmatrix} dx = EI \int_0^\ell v_{i\varphi}''(x) v_{jy}''(x) \, dx.$$

Here  $v_{i\varphi}(x)$  is the deformation of beam due to a unit rotation of end  $i$ , i.e. it is the solution of (3.14) with boundary conditions (3.17). The deformation of the beam due to a unit translation of end  $j$  is denoted by  $v_{jy}(x)$ , which is the solution of (3.14) with boundary conditions (3.18). The former shape function  $v_{i\varphi}(x)$  was already determined (see Eq. (3.21) in Problem 3.1.2):

$$v_{i\varphi}(x) = \frac{1}{\ell^2} x^3 - \frac{2}{\ell} x^2 + x.$$

Its second derivative is

$$v_{i\varphi}''(x) = \frac{6}{\ell^2} x - \frac{4}{\ell}.$$

<sup>1</sup>If we used FE approximations, these function would be the shape functions of the corresponding member.

<sup>2</sup>This is called the strain matrix in FE modelling.

The shape function  $v_{jy}(x)$  is the solution of (3.14), i.e. it is (3.15). The unknown coefficients  $A_0, A_1, A_2, A_3$  are from the boundary conditions (3.18). We write these boundary conditions using (3.15):

$$\begin{aligned} v_{jy}(0) &= A_3 \cdot 0^3 + A_2 \cdot 0^2 + A_1 \cdot 0 + A_0 = 0 & \rightarrow & A_0 = 0, \\ v'_{jy}(0) &= 3A_3 \cdot 0^2 + 2A_2 \cdot 0 + A_1 = 0 & \rightarrow & A_1 = 0, \\ v_{jy}(\ell) &= A_3 \cdot \ell^3 + A_2 \cdot \ell^2 = 1 & \rightarrow & A_2 = 1/\ell^2 - A_3\ell, \\ v'_{jy}(\ell) &= 3A_3 \cdot \ell^2 + 2(1/\ell^2 - A_3\ell)\ell = 0 & \rightarrow & A_3 = -2/\ell^3. \end{aligned}$$

Thus the shape function is

$$v_{jy}(x) = -\frac{2}{\ell^3}x^3 + \frac{3}{\ell^2}x^2.$$

The second derivative of this function is

$$v''_{jy}(x) = -\frac{12}{\ell^3}x + \frac{6}{\ell^2}.$$

Finally, the entry 3,5 is

$$\begin{aligned} K_{35}^{\text{loc}} &= EI \int_0^\ell v''_{i\varphi}(x)v''_{jy}(x) dx = EI \int_0^\ell \left\{ \frac{6}{\ell^2}x - \frac{4}{\ell} \right\} \left\{ -\frac{12}{\ell^3}x + \frac{6}{\ell^2} \right\} dx \\ &= EI \int_0^\ell \left( -\frac{72x^2}{\ell^5} + \frac{84x}{\ell^4} - \frac{24}{\ell^3} \right) dx = EI \left[ -\frac{24x^3}{\ell^5} + \frac{42x^2}{\ell^4} - \frac{24x}{\ell^3} \right]_0^\ell = -\frac{6EI}{\ell^2} \end{aligned}$$

Whether we apply one method or the other, it makes no difference in the final result. The entries of the elementary static stiffness matrix of a fixed-fixed beam of length  $\ell$ , mass per unit length  $\mu$ , normal stiffness  $EA$ , and bending stiffness  $EI$  are

$$\mathbf{K}_{ij}^{\text{loc}} = \begin{bmatrix} \frac{EA}{\ell} & 0 & 0 & -\frac{EA}{\ell} & 0 & 0 \\ 0 & \frac{12EI}{\ell^3} & \frac{6EI}{\ell^2} & 0 & -\frac{12EI}{\ell^3} & \frac{6EI}{\ell^2} \\ 0 & \frac{6EI}{\ell^2} & \frac{4EI}{\ell} & 0 & -\frac{6EI}{\ell^2} & \frac{2EI}{\ell} \\ -\frac{EA}{\ell} & 0 & 0 & \frac{EA}{\ell} & 0 & 0 \\ 0 & -\frac{12EI}{\ell^3} & -\frac{6EI}{\ell^2} & 0 & \frac{12EI}{\ell^3} & -\frac{6EI}{\ell^2} \\ 0 & \frac{6EI}{\ell^2} & \frac{2EI}{\ell} & 0 & -\frac{6EI}{\ell^2} & \frac{4EI}{\ell} \end{bmatrix}. \quad (3.28)$$

### 3.1.4 Equivalent nodal forces

We have computed already the end-of-beam forces due to the elastic deformations of beams. Now we discuss the effects of static loading. There are two possible cases: either forces and

moments act directly on the nodes of the structures, or the load is exerted on the beams. In the latter case we have to reduce the loads on the nodes, obtaining equivalent nodal forces.

Let us study the beam shown in Figure 3.6, which is loaded by a transverse distributed load  $q_t(x)$ . The transverse deflection of the beam due to the load is denoted by  $v_q(x)$ , while the end-of-beam forces are  $N_{iq}$ ,  $V_{iq}$ ,  $M_{iq}$ ,  $N_{jq}$ ,  $V_{jq}$  and  $M_{jq}$ .

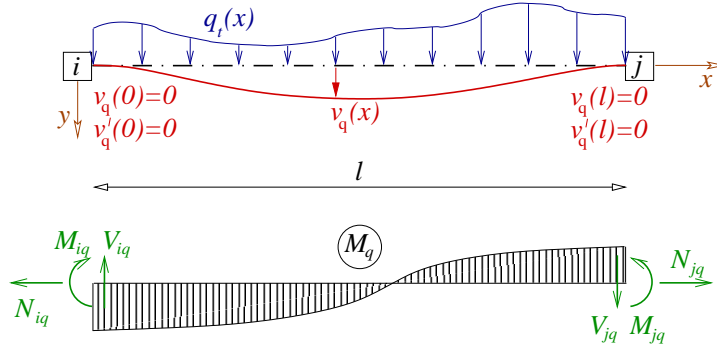


**Figure 3.6:** Beam  $ij$  under a transverse, static, distributed load  $q_t(x)$

First we determine the equivalent nodal moment at end  $i$ , namely  $M_{iq}$ . For this we write the virtual work done by the force system on the virtual displacement system due to a unit rotation of end  $i$  (see Figure 3.5):

$$\begin{aligned} \delta W_{qs} &= M_{iq} \cdot 1 + \int_0^\ell q_t(x) v_{i\varphi}(x) dx - \int_0^\ell M_q(x) \kappa_{i\varphi}(x) dx \\ &= M_{iq} + \int_0^\ell q_t(x) v_{i\varphi}(x) dx - EI \int_0^\ell v_q''(x) v_{i\varphi}''(x) dx = 0. \end{aligned}$$

Now the virtual work done by the force system due to a unit rotation of end  $i$  on the virtual displacement system caused by loading  $q_t(x)$  is formulated:

$$\delta W_{sq} = - \int_0^\ell M_{i\varphi}(x) \kappa_q(x) dx = -EI \int_0^\ell v_{i\varphi}''(x) v_q''(x) dx = 0.$$

The above equations yield

$$M_{iq} = - \int_0^\ell q_t(x) v_{i\varphi}(x) dx.$$

This is the end-of-beam moment at end  $i$  originated from the transverse load  $q_t(x)$ . The opposite of this moment acts on the node, thus the third entry of the equivalent nodal force is:

$$q_3 = \int_0^\ell q_t(x) v_{i\varphi}(x) dx.$$

If the distributed load has both longitudinal and transverse components, denoted by  $q_n(x)$  and  $q_t(x)$ , respectively, then they can be collected in the vector  $\mathbf{f}(x) = [q_n(x), q_t(x)]^T$  and all the entries of the nodal forces are computed shortly as

$$\mathbf{q}_{\text{eq},ij}^{\text{loc}} = \int_0^\ell \mathbf{N}^T \mathbf{f} \, dx. \quad (3.29)$$

If there is also a distributed moment  $m(x)$  on the beam, then matrix  $\mathbf{N}$  needs to be appended by an extra row carrying the tangent of those shape functions that correspond to the transverse translation. This extended matrix is

$$\mathbf{N}_{\text{ext}} = \begin{bmatrix} u_{ix}(x) & 0 & 0 & u_{jx}(x) & 0 & 0 \\ 0 & v_{iy}(x) & v_{i\varphi}(x) & 0 & v_{jy}(x) & v_{j\varphi}(x) \\ 0 & v'_{iy}(x) & v'_{i\varphi}(x) & 0 & v'_{jy}(x) & v'_{j\varphi}(x) \end{bmatrix}, \quad (3.30)$$

while the distributed loads are collected in the vector  $\mathbf{f}_{\text{ext}}(x) = [q_n(x), q_t(x), m(x)]^T$ . With the above notations the formula for computing the equivalent nodal forces is

$$\mathbf{q}_{\text{eq},ij}^{\text{loc}} = \int_0^\ell \mathbf{N}_{\text{ext}}^T \mathbf{f}_{\text{ext}} \, dx. \quad (3.31)$$

If a concentrated force, denoted by two components  $\mathbf{F} = [F_x, F_y]^T$ , acts on the beam at  $x = a$ , then the equivalent nodal force is

$$\mathbf{q}_{\text{eq},ij}^{\text{loc}} = \mathbf{N}^T|_{x=a} \mathbf{F}. \quad (3.32)$$

If there is also a moment  $M$ , i.e.  $\mathbf{F}_{\text{ext}} = [F_x, F_y, M]^T$ , then

$$\mathbf{q}_{\text{eq},ij}^{\text{loc}} = \mathbf{N}_{\text{ext}}^T|_{x=a} \mathbf{F}_{\text{ext}}. \quad (3.33)$$

**Problem 3.1.4** (Static nodal forces of a fixed-fixed beam under a constant transverse distributed load). There is fixed-fixed a beam of length  $\ell$ , loaded by a constant transverse distributed load  $q_t(x) = q_0$ . Determine the static nodal force vector  $\mathbf{q}$ !

**Solution.** We apply formula (3.29) with load vector  $\mathbf{Q} = [0, q_0]^T$ . The entries of  $\mathbf{N}$  are given in Appendix A.2.

$$\begin{aligned} \mathbf{q} &= \int_0^\ell \mathbf{N}^T \mathbf{Q} \, dx = q_0 \int_0^\ell \begin{bmatrix} 0 & 0 & 0 & 0 & 0 & 0 \\ 0 & v_{iy}(x) & v_{i\varphi}(x) & 0 & v_{jy}(x) & v_{j\varphi}(x) \end{bmatrix}^T dx \\ &= q_0 \int_0^\ell \begin{bmatrix} 0 & 0 & 0 & 0 & 0 & 0 \\ 0 & 2\frac{x^3}{\ell^3} - 3\frac{x^2}{\ell^2} + 1 & \frac{x^3}{\ell^2} - 2\frac{x^2}{\ell} + x & 0 & -2\frac{x^3}{\ell^3} + 3\frac{x^2}{\ell^2} & \frac{x^3}{\ell^2} - \frac{x^2}{\ell} \end{bmatrix}^T dx \\ &= q_0 \left[ \begin{bmatrix} 0 & 0 & 0 & 0 & 0 & 0 \\ 0 & \frac{1}{2}\frac{x^4}{\ell^3} - \frac{x^3}{\ell^2} + x & \frac{1}{4}\frac{x^4}{\ell^2} - \frac{2}{3}\frac{x^3}{\ell} + \frac{1}{2}x^2 & 0 & -\frac{1}{2}\frac{x^4}{\ell^3} + \frac{x^3}{\ell^2} & \frac{1}{4}\frac{x^4}{\ell^2} - \frac{1}{3}\frac{x^3}{\ell} \end{bmatrix}^T \right]_0^\ell = q_0 \begin{bmatrix} 0 \\ \ell/2 \\ \ell^2/12 \\ 0 \\ \ell/2 \\ -\ell^2/12 \end{bmatrix}. \end{aligned}$$

### 3.1.5 Different end conditions of beam members

We have shown so far the elementary static stiffness matrix of the fixed-fixed beam. Although we could derive this matrix for other end conditions from the corresponding shape functions, there is another option, which is based on the *dyadic decomposition* of a matrix.

Let us consider the beam shown in Fig. 3.7: its ends 0 and  $\ell$  are elastically connected to the coinciding nodes  $i$  and  $j$  through linearly elastic springs. The compliances of the springs are collected in a diagonal matrix

$$\mathbf{R} = \left[ \begin{array}{ccc|ccc} r_1 & 0 & 0 & 0 & 0 & 0 \\ 0 & r_2 & 0 & 0 & 0 & 0 \\ 0 & 0 & r_3 & 0 & 0 & 0 \\ \hline 0 & 0 & 0 & r_4 & 0 & 0 \\ 0 & 0 & 0 & 0 & r_5 & 0 \\ 0 & 0 & 0 & 0 & 0 & r_6 \end{array} \right]$$

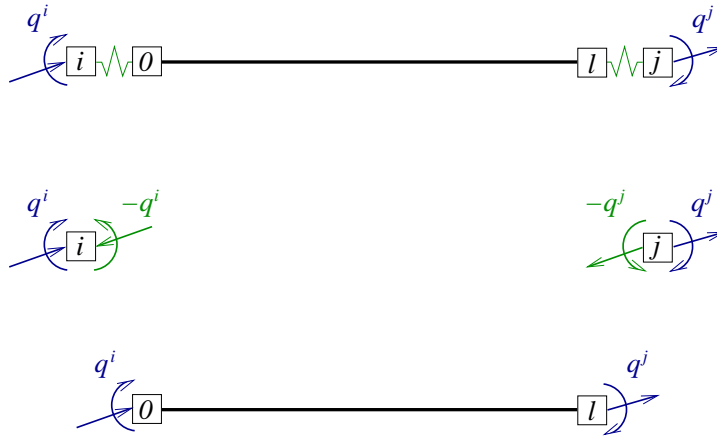


**Figure 3.7:** A beam with its ends 0 and  $\ell$  are elastically connected to the coinciding nodes  $i$  and  $j$  through linearly elastic springs

First we use fictitious nodes 0 and  $\ell$  at the ends of the beam, connected rigidly to the beam. The equilibrium equation of these nodes are:

$$\mathbf{K}_0 \mathbf{u}_0 = \mathbf{q}_0 + \mathbf{q}_i. \quad (3.34)$$

Here  $\mathbf{K}_0$  is the static stiffness matrix of the fixed-fixed beam,  $\mathbf{u}_0$  contains the displacements of ends 0 and  $\ell$ ,  $\mathbf{q}_0$  collect the force components reduced to nodes 0 and  $\ell$  from the load of the beam, and  $\mathbf{q}_i$  contains the spring forces acting on nodes 0 and  $\ell$ . The spring forces should satisfy

$$\mathbf{u}_i - \mathbf{u}_0 = \mathbf{R} \mathbf{q}_i, \quad (3.35)$$

where  $\mathbf{u}_i$  contains the displacements of nodes  $i$  and  $j$ . Let us express  $\mathbf{u}_0$  from (3.35) and substitute it in (3.34):

$$\mathbf{K}_0 \mathbf{u}_i = \mathbf{q}_0 + (\mathbf{I} + \mathbf{K}_0 \mathbf{R}) \mathbf{q}_i.$$

(Here  $\mathbf{I}$  is the 6-by-6 identity matrix.) Now the above equation is multiplied by  $(\mathbf{I} + \mathbf{K}_0\mathbf{R})^{-1}$  from the left:

$$(\mathbf{I} + \mathbf{K}_0\mathbf{R})^{-1}\mathbf{K}_0\mathbf{u}_i = (\mathbf{I} + \mathbf{K}_0\mathbf{R})^{-1}\mathbf{q}_0 + \mathbf{q}_i.$$

On the right hand side the load  $\mathbf{q}^i$  indicates that the above equation corresponds to nodes  $i$  and  $j$ . Therefore

$$\mathbf{K} = (\mathbf{I} + \mathbf{K}_0\mathbf{R})^{-1}\mathbf{K}_0 \quad (3.36)$$

is the stiffness matrix of the elastically connected beam and

$$\mathbf{q} = (\mathbf{I} + \mathbf{K}_0\mathbf{R})^{-1}\mathbf{q}_0 \quad (3.37)$$

is the nodal force, the beam loads reduced to nodes  $i$  and  $j$ . In this way we have managed to eliminate the fictitious nodes 0 and  $\ell$ .

Let us study now the case when only one degree of freedom of the ends of the beam is connected elastically, the others are rigidly connected. This degree of freedom is denoted by  $p$  ( $1 \leq p \leq 6$ ). Matrix  $\mathbf{R}$  has only one non-zero in its diagonal, the  $p$ th one. The matrix can be therefore easily formulated as

$$\mathbf{R} = r_p \mathbf{e}_p \mathbf{e}_p^T. \quad (3.38)$$

Here the entries of vector  $\mathbf{e}_p$  are all zero except for its  $p$ th entry, it is 1. The product  $\mathbf{e}_p \mathbf{e}_p^T$  gives a 6-by-6 matrix, called a dyad, which in this special case has only one non-zero entry: its entry  $p,p$  is one. Using (3.38)  $\mathbf{K}_0\mathbf{R}$  yields

$$\mathbf{K}_0\mathbf{R} = r_p \mathbf{k}_p \mathbf{e}_p^T,$$

where  $\mathbf{k}_p$  is the  $p$ th column of matrix  $\mathbf{K}_0$ .

If a dyad  $\mathbf{vw}^T$  is added to a matrix  $\mathbf{A}$ , then the inverse of the resulting matrix can be computed as

$$(\mathbf{A} + \mathbf{vw}^T)^{-1} = \mathbf{A}^{-1} - \frac{\mathbf{A}^{-1}\mathbf{vw}^T\mathbf{A}^{-1}}{1 + \mathbf{w}^T\mathbf{A}^{-1}\mathbf{v}}.$$

Applying this rule to the matrix inverse in (3.36), using (3.1.5), with the substitution  $\mathbf{A} \rightarrow \mathbf{I}$ ,  $\mathbf{vw}^T \rightarrow r_p \mathbf{k}_p \mathbf{e}_p^T$ , yields

$$(\mathbf{I} - r_p \mathbf{k}_p \mathbf{e}_p^T)^{-1} = \mathbf{I} - r_p \frac{\mathbf{k}_p \mathbf{e}_p^T}{1 + r_p \mathbf{e}_p^T \mathbf{k}_p} = \mathbf{I} - \frac{r_p}{1 + r_p k_{pp}} \mathbf{k}_p \mathbf{e}_p^T = \mathbf{I} - \frac{1}{k_{pp} + \frac{1}{r_p}} \mathbf{k}_p \mathbf{e}_p^T. \quad (3.39)$$

With the above formula we can simplify the stiffness matrix (3.36) for a beam which has its  $p$ th degree of freedom elastically connected to the adjacent node as:

$$\mathbf{K} = \mathbf{K}_0 - \frac{1}{k_{pp} + \frac{1}{r_p}} \mathbf{k}_p \mathbf{k}_p^T. \quad (3.40)$$

Similarly, the nodal force is

$$\mathbf{q} = \mathbf{q}_0 - \frac{q_p}{k_{pp} + \frac{1}{r_p}} \mathbf{k}_p. \quad (3.41)$$



**Problem 3.1.5** (Elementary static stiffness matrix of a fixed-pinned beam). There is a beam of length  $\ell$ , normal stiffness  $EA$ , bending stiffness  $EI$ , and mass per unit length  $\mu$ . The beam is fixed at end  $i$  and pinned at end  $j$ . (It is fixed-pinned.) Determine its elementary static stiffness matrix  $\mathbf{K}_{ij}^{\text{loc,fp}}$ !

**Solution.** We start with the stiffness matrix  $\mathbf{K}_{ij}^{\text{loc}}$  of the fixed-fixed beam member detailed by (3.28). Because of the rotation of end  $j$  (the sixth degree-of-freedom of the member) is relaxed,  $p = 6$  and  $r_p \rightarrow \infty$ . Thus the entry 6,6 and the 6th column of  $\mathbf{K}_{ij}^{\text{loc}}$  are needed. We apply formula (3.40) with these input data:

$$\mathbf{K}_{ij}^{\text{loc,fp}} = \mathbf{K}_{ij}^{\text{loc}} - \frac{1}{k_{66}} \mathbf{k}_6 \mathbf{k}_6^T$$

$$= \begin{bmatrix} \frac{EA}{\ell} & 0 & 0 & -\frac{EA}{\ell} & 0 & 0 \\ 0 & \frac{12EI}{\ell^3} & \frac{6EI}{\ell^2} & 0 & -\frac{12EI}{\ell^3} & \frac{6EI}{\ell^2} \\ 0 & \frac{6EI}{\ell^2} & \frac{4EI}{\ell} & 0 & -\frac{6EI}{\ell^2} & \frac{2EI}{\ell} \\ -\frac{EA}{\ell} & 0 & 0 & \frac{EA}{\ell} & 0 & 0 \\ 0 & -\frac{12EI}{\ell^3} & -\frac{6EI}{\ell^2} & 0 & \frac{12EI}{\ell^3} & -\frac{6EI}{\ell^2} \\ 0 & \frac{6EI}{\ell^2} & \frac{2EI}{\ell} & 0 & -\frac{6EI}{\ell^2} & \frac{4EI}{\ell} \end{bmatrix} - \frac{1}{\frac{4EI}{\ell}} \begin{bmatrix} 0 \\ \frac{6EI}{\ell^2} \\ \frac{2EI}{\ell} \\ 0 \\ -\frac{6EI}{\ell^2} \\ \frac{4EI}{\ell} \end{bmatrix} \left[ 0 \quad \frac{6EI}{\ell^2} \quad \frac{2EI}{\ell} \mid 0 \quad -\frac{6EI}{\ell^2} \quad \frac{4EI}{\ell} \right]$$

$$\mathbf{K}_{ij}^{\text{loc,fp}} = \begin{bmatrix} \frac{EA}{\ell} & 0 & 0 & -\frac{EA}{\ell} & 0 & 0 \\ 0 & \frac{3EI}{\ell^3} & \frac{3EI}{\ell^2} & 0 & -\frac{3EI}{\ell^3} & 0 \\ 0 & \frac{3EI}{\ell^2} & \frac{3EI}{\ell} & 0 & -\frac{3EI}{\ell^2} & 0 \\ -\frac{EA}{\ell} & 0 & 0 & \frac{EA}{\ell} & 0 & 0 \\ 0 & -\frac{3EI}{\ell^3} & -\frac{3EI}{\ell^2} & 0 & \frac{3EI}{\ell^3} & 0 \\ 0 & 0 & 0 & 0 & 0 & 0 \end{bmatrix}.$$

**Problem 3.1.6** (Elementary static stiffness matrix of a pinned-pinned beam). There is a beam of length  $\ell$ , normal stiffness  $EA$ , bending stiffness  $EI$ , and mass per unit length  $\mu$ . The beam is pinned at both ends  $i$  and  $j$ . (It is pinned-pinned.) Determine the elementary static stiffness matrix  $\mathbf{K}_{ij}^{\text{loc,pp}}$ !

**Solution.** We start with the stiffness matrix  $\mathbf{K}_{ij}^{\text{loc,fp}}$  of the *fixed-pinned* beam detailed by Problem 3.1.5. Because of the rotation of end  $i$  (the third degree-of-freedom of the member) is relaxed,  $p = 3$  and  $r_p \rightarrow \infty$ .

Therefore  $\mathbf{K}_{ij}^{\text{loc,fp}}$ , its entry 3,3, and its 3rd column are needed in formula (3.40):

$$\begin{aligned}
 \mathbf{K}_{ij}^{\text{loc,pp}} &= \mathbf{K}_{ij}^{\text{loc,fp}} - \frac{1}{k_{33}} \mathbf{k}_3 \mathbf{k}_3^T \\
 &= \begin{bmatrix} \frac{EA}{\ell} & 0 & 0 & -\frac{EA}{\ell} & 0 & 0 \\ 0 & \frac{3EI}{\ell^3} & \frac{3EI}{\ell^2} & 0 & -\frac{3EI}{\ell^3} & 0 \\ 0 & \frac{3EI}{\ell^2} & \frac{3EI}{\ell} & 0 & -\frac{3EI}{\ell^2} & 0 \\ \hline -\frac{EA}{\ell} & 0 & 0 & \frac{EA}{\ell} & 0 & 0 \\ 0 & -\frac{3EI}{\ell^3} & -\frac{3EI}{\ell^2} & 0 & \frac{3EI}{\ell^3} & 0 \\ 0 & 0 & 0 & 0 & 0 & 0 \\ \hline \frac{EA}{\ell} & 0 & 0 & -\frac{EA}{\ell} & 0 & 0 \\ 0 & \frac{3EI}{\ell^3} & 0 & 0 & -\frac{3EI}{\ell^3} & \frac{3EI}{\ell^2} \\ 0 & 0 & 0 & 0 & 0 & 0 \\ \hline -\frac{EA}{\ell} & 0 & 0 & \frac{EA}{\ell} & 0 & 0 \\ 0 & -\frac{3EI}{\ell^3} & 0 & 0 & \frac{3EI}{\ell^3} & -\frac{3EI}{\ell^2} \\ 0 & \frac{3EI}{\ell^2} & 0 & 0 & -\frac{3EI}{\ell^2} & \frac{3EI}{\ell} \end{bmatrix} - \frac{1}{\frac{3EI}{\ell}} \begin{bmatrix} 0 \\ \frac{3EI}{\ell^2} \\ \frac{3EI}{\ell} \\ 0 \\ -\frac{3EI}{\ell^2} \\ 0 \end{bmatrix} \begin{bmatrix} 0 & \frac{3EI}{\ell^2} & \frac{3EI}{\ell} & 0 & -\frac{3EI}{\ell^2} & 0 \end{bmatrix} \\
 &= \begin{bmatrix} \frac{EA}{\ell} & 0 & 0 & -\frac{EA}{\ell} & 0 & 0 \\ 0 & \frac{3EI}{\ell^3} & 0 & 0 & -\frac{3EI}{\ell^3} & \frac{3EI}{\ell^2} \\ 0 & 0 & 0 & 0 & 0 & 0 \\ \hline -\frac{EA}{\ell} & 0 & 0 & \frac{EA}{\ell} & 0 & 0 \\ 0 & -\frac{3EI}{\ell^3} & 0 & 0 & \frac{3EI}{\ell^3} & -\frac{3EI}{\ell^2} \\ 0 & \frac{3EI}{\ell^2} & 0 & 0 & -\frac{3EI}{\ell^2} & \frac{3EI}{\ell} \end{bmatrix} .
 \end{aligned}$$

**Problem 3.1.7** (Nodal forces from a fixed-pinned beam under constant distributed load  $q_t$ ). There is a beam of length  $\ell$ , normal stiffness  $EA$ , bending stiffness  $EI$ , and mass per unit length  $\mu$ . The beam is fixed at end  $i$ , pinned at end  $j$ , and loaded by a constant transverse load  $q_t(x) = q_0$ . Determine the nodal force vector  $\mathbf{q}^{\text{loc,fp}}$ !

**Solution.** We start with the nodal force vector  $\mathbf{q}^{\text{loc,ff}} = q_0[0, \ell/2, \ell^2/12, 0, \ell/2, -\ell^2/12]^T$  of the *fixed-fixed* beam. (See Problem 3.1.4.) Because of the rotation of end  $i$  (the third degree-of-freedom of the member) is relaxed,  $p = 3$  and  $r_p \rightarrow \infty$ . Therefore the vector  $\mathbf{q}^{\text{loc,ff}}$  and its third entry are needed in formula (3.41) alongside with the entry 3,3 and the 3rd column of  $\mathbf{K}_{ij}^{\text{loc,ff}}$ :

$$\mathbf{q}^{\text{loc,fp}} = \mathbf{q}^{\text{loc,ff}} - \frac{q_3^{\text{loc,ff}}}{k_{33}^{\text{loc,ff}}} \mathbf{k}_3^{\text{loc,ff}} = \begin{bmatrix} 0 \\ \frac{q_0 \ell}{2} \\ \frac{q_0 \ell^2}{12} \\ 0 \\ \frac{q_0 \ell}{2} \\ -\frac{q_0 \ell^2}{12} \end{bmatrix} - \frac{\frac{q_0 \ell^2}{12}}{\frac{4EI}{\ell}} \begin{bmatrix} 0 \\ \frac{6EI}{\ell^2} \\ \frac{2EI}{\ell} \\ 0 \\ -\frac{6EI}{\ell^2} \\ \frac{4EI}{\ell} \end{bmatrix} = \begin{bmatrix} 0 \\ \frac{5q_0 \ell}{8} \\ \frac{q_0 \ell^2}{8} \\ 0 \\ \frac{3q_0 \ell}{8} \\ 0 \end{bmatrix}$$

### 3.1.6 Transformation of the elementary stiffness matrix

The elementary stiffness matrix can be written in the block form:

$$\mathbf{K}_{ij}^{\text{loc}} = \left[ \begin{array}{c|c} \mathbf{K}_{ij}^{\text{loc,ii}} & \mathbf{K}_{ij}^{\text{loc,ij}} \\ \hline \mathbf{K}_{ij}^{\text{loc,ji}} & \mathbf{K}_{ij}^{\text{loc,jj}} \end{array} \right].$$

The nodal forces  $\mathbf{f}_{ij}^{\text{loc}}$  can be calculated from the nodal displacements  $\mathbf{u}_{ij}^{\text{loc}}$  with Eq. (3.6). If the nodal displacements are given in the global reference system  $XYZ$ , first we have to transform them into the local reference system:

$$\mathbf{u}_{ij}^{\text{loc}} = \bar{\mathbf{T}}_{ij}^T \mathbf{u}_{ij}^{\text{glob}},$$

with the hypermatrix:

$$\bar{\mathbf{T}}_{ij}^T = \left[ \begin{array}{c|c} \mathbf{T}_{ij}^T & \mathbf{0} \\ \hline \mathbf{0} & \mathbf{T}_{ij}^T \end{array} \right].$$

We transform the resulting nodal forces

$$\mathbf{f}_{ij}^{\text{loc}} = \mathbf{K}_{ij}^{\text{loc}} \mathbf{u}_{ij}^{\text{loc}} = \mathbf{K}_{ij}^{\text{loc}} \bar{\mathbf{T}}_{ij}^T \mathbf{u}_{ij}^{\text{glob}} \quad (3.42)$$

into the global reference system with the hyper matrix

$$\bar{\mathbf{T}}_{ij} = \left[ \begin{array}{c|c} \mathbf{T}_{ij} & \mathbf{0} \\ \hline \mathbf{0} & \mathbf{T}_{ij} \end{array} \right].$$

We multiply both sides of Eq. (3.42) from the left by  $\bar{\mathbf{T}}_{ij}$ :

$$\bar{\mathbf{T}}_{ij} \mathbf{f}_{ij}^{\text{loc}} = \mathbf{f}_{ij}^{\text{glob}} = \bar{\mathbf{T}}_{ij} \mathbf{K}_{ij}^{\text{loc}} \bar{\mathbf{T}}_{ij}^T \mathbf{u}_{ij}^{\text{glob}}.$$

In the above formula the matrix product  $\bar{\mathbf{T}}_{ij} \mathbf{K}_{ij}^{\text{loc}} \bar{\mathbf{T}}_{ij}^T$  transforms the nodal displacements  $\mathbf{u}_{ij}^{\text{glob}}$  into the nodal forces  $\mathbf{f}_{ij}^{\text{glob}}$ . Therefore, the elementary stiffness matrix in the global reference system (the global stiffness matrix, for short) is

$$\mathbf{K}_{ij}^{\text{glob}} = \bar{\mathbf{T}}_{ij} \mathbf{K}_{ij}^{\text{loc}} \bar{\mathbf{T}}_{ij}^T, \quad (3.43)$$

and the nodal forces can be calculated as

$$\mathbf{f}_{ij}^{\text{glob}} = \mathbf{K}_{ij}^{\text{glob}} \mathbf{u}_{ij}^{\text{glob}}.$$

The matrix product (3.43) can be written in a simpler form using the hypermatrix structure:

$$\mathbf{K}_{ij}^{\text{glob}} = \left[ \begin{array}{c|c} \mathbf{T}_{ij} \mathbf{K}_{ij}^{\text{loc,ii}} \mathbf{T}_{ij}^T & \mathbf{T}_{ij} \mathbf{K}_{ij}^{\text{loc,ij}} \mathbf{T}_{ij}^T \\ \hline \mathbf{T}_{ij} \mathbf{K}_{ij}^{\text{loc,ji}} \mathbf{T}_{ij}^T & \mathbf{T}_{ij} \mathbf{K}_{ij}^{\text{loc,jj}} \mathbf{T}_{ij}^T \end{array} \right] = \left[ \begin{array}{c|c} \mathbf{K}_{ij}^{\text{glob,ii}} & \mathbf{K}_{ij}^{\text{glob,ij}} \\ \hline \mathbf{K}_{ij}^{\text{glob,ji}} & \mathbf{K}_{ij}^{\text{glob,jj}} \end{array} \right].$$

We cannot stress enough the physical meaning of the stiffness matrix. Entry  $p, r$  of matrix  $\mathbf{K}_{ij}^{\text{glob}}$  (i.e. the entry of  $\mathbf{K}_{ij}^{\text{glob}}$  in the intersection of the  $p$ th row and  $r$ th column) is multiplied by the displacement (rotation, if  $r = 3$  or  $6$ , and translation otherwise) of the  $r$ th degree-of-freedom the beam  $ij$ . The result is the force or the moment (moment, if  $p = 3$  or  $6$ , and force component otherwise) acting on the  $p$ th degree of freedom of beam  $ij$  arising from the elastic deformation of the beam member  $ij$ .

### 3.1.7 Compilation of the total stiffness matrix

In various displacement methods the equation of motion is written for every degree-of-freedom of the system, so the forces acting on each degree-of-freedom must be calculated. In the stiffness matrix we collect the (stiffness) coefficients of the displacements needed to calculate the forces arising from the elastic deformation of the structure. We use a linear theory, so the forces acting on the same degree-of-freedom from different members must be summed. This summation of the elastic forces (more accurately the coefficients of displacements) is called the *compilation* of the total stiffness matrix of the structure.

The first step of the compilation is to find out which local node of beam  $ij$  corresponds to which global node. We used the global indexes  $i$  and  $j$  for the local nodes as well, so they are the same. The effect of the member  $ij$  on the whole structure is particular, only the displacements of nodes  $i$  and  $j$  affect the forces and moments on the  $i$ th and  $j$ th nodes. The global stiffness matrix of member  $ij$  can be expanded on the structure level into a matrix  $\mathbf{K}_{ij}$ . The matrix  $\mathbf{K}_{ij}$  is of size  $3M$  by  $3M$  corresponding to the DOF of the structure. It has one block row and one block column for each node (each block is of size 3 by 3):

$$\mathbf{K}_{ij} = \begin{array}{c} \begin{array}{cc|cc|cc} & & i & & j & & \\ \hline \dots & & \vdots & & \vdots & & \\ \dots & \mathbf{K}_{ij}^{\text{glob,ii}} & & & \mathbf{K}_{ij}^{\text{glob,ij}} & & \\ \hline & & \vdots & \dots & \vdots & & \\ \dots & \mathbf{K}_{ij}^{\text{glob,ji}} & & & \mathbf{K}_{ij}^{\text{glob,jj}} & & \\ \hline & & \vdots & & \vdots & \dots & \end{array} & \begin{array}{c} i \\ j \end{array} \end{array} \quad (3.44)$$

The matrix  $\mathbf{K}_{ij}$  represents the effect of beam  $ij$  to all nodes. The total stiffness matrix of the structure can be constructed as the sum of the expanded stiffness matrices of all the beams of the structure:

$$\mathbf{K} = \sum \mathbf{K}_{ij}.$$

Technically, it is more practical to carry out the compilation by adding the blocks of the elementary stiffness matrix  $\mathbf{K}_{ij}^{\text{glob}}$  to the corresponding blocks of the total stiffness matrix  $\mathbf{K}$  with the scheme shown in Eq. (3.44).

### 3.1.8 Boundary conditions

Boundary conditions of frame structures are defined by the support conditions. The displacement of some degrees of freedom is constrained to a prescribed value (*rigid* support) or it is proportional to the reaction (*elastic* support). These constraints must be incorporated into the equilibrium equation:

$$\mathbf{K}\mathbf{u} = \mathbf{q},$$

where  $\mathbf{q}$  is the external load vector of the system. There are two ways to handle the boundary conditions.

- The *fixed support model* is based on the solution of the equilibrium equations of the prescribed degrees of freedom, and the application of its results.

- The *spring model* uses springs in the directions of the prescribed, elastically supported degrees-of-freedom. The rigid supports are approximated by springs of very high stiffness (bigger than any other entry of the stiffness matrix by some orders of magnitude).

It is more accurate to handle the support displacements with the fixed support model. Later on, in dynamical analysis of structures, an important load case is the support motion.

### Rigid supports in the fixed support model

We analyse the case when the  $q$ th degree-of-freedom of a structure is rigidly supported, so its displacement is prescribed by  $\hat{u}_q$ . (The prescribed displacement can be a translation or a rotation depending on  $q$ , and the prescribed value can be zero as well.) Then, in the equilibrium equation the  $q$ th row differs from the other rows, because the displacement  $\hat{u}_q$  is known, but the reaction force  $r_q$  represents an additional unknown in the  $q$ th entry of the force vector.

Let us exchange the order of the displacements such a way that the prescribed displacement becomes the last. This implies an exchange of columns of  $\mathbf{K}$ . In order to resolve the symmetry of  $\mathbf{K}$ , we need to change the order of the equations as well. That implies an exchange in the entries of the load vector. If we denote the blocks of the stiffness matrix  $\mathbf{K}$  before the  $q$ th degree-of-freedom by the superscript  $P$ , and the blocks of the stiffness matrix  $\mathbf{K}$  after the  $q$ th degree-of-freedom by the superscript  $R$ , then above procedure leads to the following structure of the stiffness matrix, the displacement and the load vectors:

$$\begin{aligned} & \left[ \begin{array}{c|c|c} \mathbf{K}^{PP} & \mathbf{K}^{Pq} & \mathbf{K}^{PR} \\ \mathbf{K}^{qP} & k^{qq} & \mathbf{K}^{qR} \\ \mathbf{K}^{RP} & \mathbf{K}^{Rq} & \mathbf{K}^{RR} \end{array} \right] \begin{bmatrix} \mathbf{u}^P \\ \hat{u}_q \\ \mathbf{u}^R \end{bmatrix} = \begin{bmatrix} \mathbf{q}^P \\ q_q + r_q \\ \mathbf{q}^R \end{bmatrix} \\ \rightarrow & \left[ \begin{array}{c|c|c} \mathbf{K}^{PP} & \mathbf{K}^{PR} & \mathbf{K}^{Pq} \\ \mathbf{K}^{RP} & \mathbf{K}^{RR} & \mathbf{K}^{Rq} \\ \mathbf{K}^{qP} & \mathbf{K}^{qR} & k^{qq} \end{array} \right] \begin{bmatrix} \mathbf{u}^P \\ \mathbf{u}^R \\ \hat{u}_q \end{bmatrix} = \begin{bmatrix} \mathbf{q}^P \\ \mathbf{q}^R \\ q_q + r_q \end{bmatrix}. \end{aligned} \quad (3.45)$$

Once we find the unknown displacements  $\mathbf{u}^P$  and  $\mathbf{u}^R$ , the last row of the matrix equation can be used to calculate the unknown reaction force  $r_q$ . The first  $P + R$  equations can be partitioned into a known and an unknown part:

$$\left[ \begin{array}{c|c} \mathbf{K}^{PP} & \mathbf{K}^{PR} \\ \mathbf{K}^{RP} & \mathbf{K}^{RR} \end{array} \right] \begin{bmatrix} \mathbf{u}^P \\ \mathbf{u}^R \end{bmatrix} = \begin{bmatrix} \mathbf{q}^P \\ \mathbf{q}^R \end{bmatrix} - \left[ \frac{\mathbf{K}^{Pq}}{\mathbf{K}^{Rq}} \right] \hat{u}_q. \quad (3.46)$$

The matrix on the left hand side of Eq. (3.46) can be regarded as the stiffness matrix of the reduced system, the vector on the left hand side is the vector of the unknown displacements, while the vector sum on the right hand side is the reduced load vector, which also contains the kinematical load caused by the support displacement  $\hat{u}_q$ . The resulting equations can be written in the classic form  $\mathbf{K}\mathbf{u} = \mathbf{q}$ , but  $\mathbf{K}$  and  $\mathbf{u}$  are of reduced size, and  $\mathbf{q}$  contains the kinematical loads as well.

Further supports can be treated in a similar way, only the above steps need to be repeated on the already reduced equation  $\mathbf{K}\mathbf{u} = \mathbf{q}$ .

**Elastic supports in the fixed support model**

Now imagine, that node  $i$  is supported elastically against the horizontal and vertical translations and the rotation. The equivalent spring stiffnesses of the horizontal and vertical elastic support are  $\rho_X$  and  $\rho_Y$ , respectively, and the rotational spring is of stiffness  $\rho_\varphi$  (see Figure 3.8 (a)).

In the *fixed support model* we introduce an additional *supporting node*  $g$  in the same geometric location as node  $i$ . Then the degrees-of-freedom of nodes  $i$  and  $g$  are connected to each other by the massless springs  $\rho_X$ ,  $\rho_Y$  and  $\rho_\varphi$  (see Figure 3.8 (b)). The global stiffness matrix of the member connecting nodes  $i$  and  $g$  is

$$\mathbf{K}_{ig}^{\text{glob}} = \left[ \begin{array}{ccc|ccc} \rho_X & 0 & 0 & -\rho_X & 0 & 0 \\ 0 & \rho_Y & 0 & 0 & -\rho_Y & 0 \\ 0 & 0 & \rho_\varphi & 0 & 0 & -\rho_\varphi \\ \hline -\rho_X & 0 & 0 & \rho_X & 0 & 0 \\ 0 & -\rho_Y & 0 & 0 & \rho_Y & 0 \\ 0 & 0 & -\rho_\varphi & 0 & 0 & \rho_\varphi \end{array} \right].$$

The displacements of the supporting node  $g$  are prescribed (here zero), so we can use the method described in the previous subsection to eliminate it from the system of equations.

We note, that in the *spring model* we need to add the spring stiffnesses directly to the corresponding main diagonal entries of the total stiffness matrix. (In the case of rigid supports, springs of numerically large stiffnesses need to be used.) Support displacements are taken into account by external forces applied on the node, resulting in exactly the prescribed displacement.

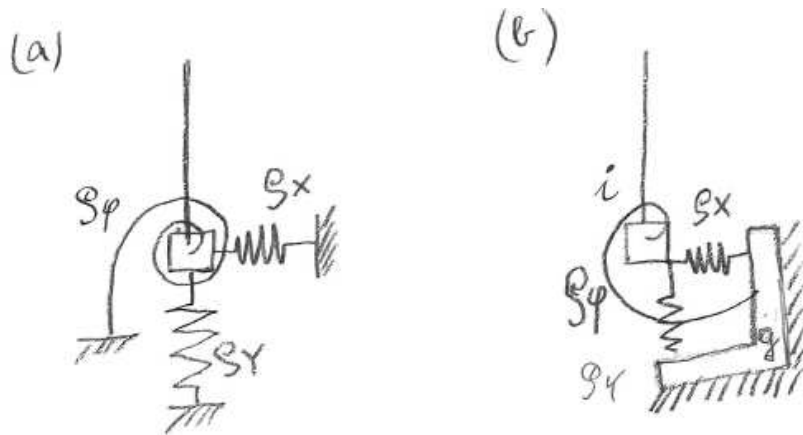


**Figure 3.8:** (a) *Spring model*: the  $i$ th supported node of a frame structure constrained against translations and rotation by the equivalent springs  $\rho_X$ ,  $\rho_Y$ , and  $\rho_\varphi$ . (b) *Fixed support model* with an elastically supported node  $i$ . Kinematical loads arising from the support displacements are applied on the supporting node  $g$ . (The supporting node  $g$  is drawn in a distance from the supported node  $i$  in order to make the connecting springs visible.)

## 3.2 Dynamic stiffness matrix of frame structures

Let us have an undamped MDOF dynamical system governed by the system of ordinary differential equations

$$\mathbf{M}\ddot{\mathbf{u}}(t) + \mathbf{K}\mathbf{u}(t) = \mathbf{q}(t). \quad (3.47)$$

Here dot denotes differentiation with respect to time. The mass matrix  $\mathbf{M}$  and the (static) stiffness matrix  $\mathbf{K}$  are of size  $N$  by  $N$ , where  $N$  is the total degrees-of-freedom of the system. Vector  $\mathbf{u}(t)$  is of size  $N$  and it contains the unknown displacements of the nodes. Force vector  $\mathbf{q}(t)$  is a given vector of size  $N$ : it contains the forces reduced to the nodes. The  $p$ th entry of force  $\mathbf{q}(t)$  is work-compatible with the  $p$ th entry of  $\mathbf{u}(t)$ .

If the force is harmonic, for instance  $\mathbf{q}(t) = \mathbf{q}_0 \sin(\omega t)$ , then the steady-state response of the undamped system is also harmonic. We have seen that in this case the particular solution of the forced vibration is  $\mathbf{u}_f(t) = \mathbf{u}_{f0} \sin(\omega t)$  and the equation to solve for  $\mathbf{u}_{f0}$  is:

$$(\mathbf{K} - \omega^2 \mathbf{M}) \mathbf{u}_{f0} = \mathbf{q}_0.$$

We can alternatively introduce the dynamic stiffness matrix  $\hat{\mathbf{K}} = \mathbf{K} - \omega^2 \mathbf{M}$  and write the above equation as

$$\hat{\mathbf{K}} \mathbf{u}_{f0} = \mathbf{q}_0. \quad (3.48)$$

The question here is that how we can formulate the mass matrix  $\mathbf{M}$ , or, equivalently, how we can compose the dynamic stiffness matrix  $\hat{\mathbf{K}}$ ? We can follow three different approaches. The first, easier way is to apportion the mass of the members of the frame into the nodes, which results in a total *diagonally lumped mass matrix*. This is a rough approximation. The second way is to derive the elementary dynamic stiffness matrix of a beam with continuous mass distribution, and then to compile the total dynamic stiffness matrix of the frame in the same manner as for the static analysis. This approach leads to the exact *frequency-dependent mass matrix* of the frame. The main difficulty of this method is that it requires the dynamic shape functions of the beam. In practice, dynamic shape functions are often substituted by the static shape functions. In that case, the shape function system used for the computation of the static stiffness matrix is consistent with the shape functions applied to approximate the mass matrix. This third approach leads to the construction of a simpler *consistent mass matrix*, which is an estimation of the accurate dynamic mass matrix.

We review these methods in the following subsections. We always deal with an unshearable beam of length  $\ell$ , mass per unit length  $\mu$ , bending stiffness  $EI$ . The ends of the studied beam member are denoted by  $i$  and  $j$ , and the member itself is referred to as beam  $ij$ .

### 3.2.1 Diagonally lumped mass matrix

In this case first we divide the beam into two equal parts: half  $i$  is the part which is closer to the end  $i$ , and half  $j$  is the other part. Then the mass of half  $i$  is concentrated to node  $i$ , and the mass of half  $j$  is reduced to node  $j$ .

Several members can be attached to one node of the frame. In order to compile the total, diagonally lumped mass matrix  $\mathbf{M}$  of the structure, we need to make the following steps. If the  $p$ th degree-of-freedom of the frame is a translation, then the  $p$ th diagonal entry of mass

matrix  $\mathbf{M}$  is the total mass of the halves of the beams attached to the corresponding node. If the  $r$ th degree-of-freedom is a rotation, then the  $r$ th diagonal entry of matrix  $\mathbf{M}$  is the moment of inertia of the (closer) halves of the rods attached to the corresponding node. If the center of mass of the halves of the beams connected to one node coincides with the node itself, then the mass matrix  $\mathbf{M}$  is *diagonal*. Otherwise, the translation of the node induces both a linear momentum and an angular momentum with respect to the node, and the rotation of the node induces not only an angular momentum, but also a linear momentum. Thus the mass matrix is not diagonal in this general case. Although, the off-diagonal terms are usually neglected in practice.

### 3.2.2 Dynamic stiffness matrix

Apportioning the masses to the nodes in the manner shown in the previous subsection is the easiest way to approximate the mass matrix of the frame structure. However, the precise approach is to directly derive the *dynamic elementary stiffness matrix* of a beam, and then compile the total (dynamic) stiffness matrix of the whole structure in the same way as for the static case.

Let us examine a beam that is excited such that one DOF of one of its ends vibrates harmonically with frequency  $\omega$ . According to our earlier studies, the steady state vibration has the same frequency  $\omega$ . Thus we assume that the translations  $u(x, t)$ ,  $v(x, t)$  of the beam axis along  $x$  and  $y$ , respectively, the rotation of the cross-sections  $v'(x, t)$ , and also the internal forces  $N(x, t)$ ,  $V(x, t)$ ,  $M(x, t)$  are harmonic functions of time with frequency  $\omega$ . We write these functions in the separated forms

$$\begin{aligned} v(x, t) &= \hat{v}(x) \sin(\omega t), & u(x, t) &= \hat{u}(x) \sin(\omega t), & v'(x, t) &= \hat{v}'(x) \sin(\omega t), \\ N(x, t) &= \hat{N}(x) \sin(\omega t), & V(x, t) &= \hat{V}(x) \sin(\omega t), & M(x, t) &= \hat{M}(x) \sin(\omega t). \end{aligned} \quad (3.49)$$

We show two methods suitable to calculate the end-of-beam internal forces, which are used to construct the dynamic stiffness matrix of the beam.

#### Solving the differential equations of motion

The entries of the first and the fourth columns of the elementary dynamic stiffness matrix  $\hat{\mathbf{K}}_{ij}^{\text{loc}}$  are computed from the differential equation of the stretched bar (see Eq. (2.6))

$$\mu \ddot{u}(x, t) - EAu''(x, t) = 0 \quad (3.50)$$

subjected to boundary conditions

$$u(0, t) = 1 \cdot \sin(\omega t), \quad u(\ell, t) = 0, \quad \text{or} \quad (3.51)$$

$$u(0, t) = 0, \quad u(\ell, t) = 1 \cdot \sin(\omega t). \quad (3.52)$$

Boundary conditions (3.51) express that end  $i$  of the bar vibrates harmonically along  $x$  with a unit amplitude, while end  $j$  is fixed. The other two boundary conditions (3.52) mean that end  $j$  vibrates while end  $i$  is kept fixed.



We split the variables  $t$  and  $x$  of the unknown function

$$u(x, t) = \hat{u}(x) \sin(\omega t),$$

substitute it into Eq. (3.50), and divide both side by  $\sin(\omega t) \neq 0$ :

$$\omega^2 \mu \hat{u}(x) + EA \hat{u}''(x) = 0. \quad (3.53)$$

The solution of the above differential equation is

$$\hat{u}(x) = D_1 \cos\left(\frac{\psi}{\ell} x\right) + D_2 \sin\left(\frac{\psi}{\ell} x\right), \quad (3.54)$$

where

$$\psi = \ell \sqrt{\frac{\omega^2 \mu}{EA}}.$$

The unknown coefficients  $D_1, D_2$  can be computed from two prescribed boundary conditions. According to (3.51) and (3.52) these are

$$\hat{u}_{ix}(0) = 1, \quad \hat{u}_{ix}(\ell) = 0, \quad \text{and} \quad (3.55)$$

$$\hat{u}_{jx}(0) = 0, \quad \hat{u}_{jx}(\ell) = 1 \quad (3.56)$$

for the first and the fourth columns, respectively. The amplitudes of the internal forces at the ends of the bar are

$$\hat{N}_{iix} = EA \hat{u}'_{ix}(0), \quad \hat{V}_{iix} = 0, \quad \hat{M}_{iix} = 0,$$

$$\hat{N}_{jix} = EA \hat{u}'_{ix}(\ell), \quad \hat{V}_{jix} = 0, \quad \hat{M}_{jix} = 0.$$

The entries of the first column of the dynamic stiffness matrix are

$$\hat{\mathbf{k}}_{ij,1}^{\text{loc}} = [-\hat{N}_{iix}, 0, 0, \hat{N}_{jix}, 0, 0]^T,$$

while the fourth column is composed of

$$\hat{\mathbf{k}}_{ij,4}^{\text{loc}} = [-\hat{N}_{ijx}, 0, 0, \hat{N}_{jjx}, 0, 0]^T.$$

**Problem 3.2.1** (The fourth column of the elementary dynamic stiffness matrix). There is a fixed-fixed beam  $ij$ , which is of length  $\ell$ , normal stiffness  $EA$ , bending stiffness  $EI$ , and mass per unit length  $\mu$ . Determine the entries of the fourth column of its elementary dynamic stiffness matrix!

**Solution.** Entries of column 4 are the end-of-beam internal forces due to a harmonic translation of unit amplitude of end  $j$  along the axis of the beam. Since the translation along the beam axis induces only normal forces, the entries 2,4 (shear at end  $i$ ), 3,4 (bending moment at end  $i$ ), 5,4 (shear at end  $j$ ), and 6,4 (moment at end  $j$ ) are all zero:

$$\hat{K}_{ij,24}^{\text{loc}} = 0, \quad \hat{K}_{ij,34}^{\text{loc}} = 0, \quad \hat{K}_{ij,54}^{\text{loc}} = 0, \quad \hat{K}_{ij,64}^{\text{loc}} = 0.$$

Entry 1,4 is the normal force at end  $i$

$$\hat{K}_{ij,14}^{\text{loc}} = -\hat{N}_{ijx} = -EA \hat{u}'_{jx}(0),$$

while entry 4,4 is the normal force at end  $j$

$$\hat{K}_{ij,44}^{\text{loc}} = \hat{N}_{jjx} = EA\hat{u}'_{jx}(\ell).$$

Here  $\hat{u}_{jx}(x)$  is the solution of (3.53) with boundary conditions (3.56), i.e. it is the dynamic shape function of the bar due to a harmonic translation of unit amplitude of end  $j$ . The solution of (3.53) is (3.54). Here the unknown coefficients  $D_1$  and  $D_2$  are from the boundary conditions (3.56). We write these boundary conditions using (3.54):

$$\begin{aligned}\hat{u}_{jx}(0) &= D_1 \cos(0) + D_2 \sin(0) = 0, \quad \rightarrow \quad D_1 = 0, \\ \hat{u}_{jx}(x) &= D_1 \cos\left(\frac{\psi}{\ell}x\right) + D_2 \sin\left(\frac{\psi}{\ell}x\right) = 1, \quad \rightarrow \quad D_2 = 1/\sin(\psi).\end{aligned}$$

(Here we suppose that  $\sin(\psi) \neq 0$ , i.e. the system is not in the state of resonance.) The dynamic displacement function is:

$$\hat{u}_{jx}(x) = \frac{1}{\sin(\psi)} \sin\left(\frac{\psi}{\ell}x\right). \quad (3.57)$$

It is differentiated with respect to  $x$ , multiplied by  $EA$ , and evaluated at end  $i$  ( $x = 0$ ) and  $j$  ( $x = \ell$ ). Positive value of the result is a tension. However, a compression at end  $i$ , and a tension at end  $j$  coincide with the positive direction of  $x$ . Thus

$$\begin{aligned}\hat{K}_{ij,14}^{\text{loc}} &= -EA\hat{u}'_{jx}(0) = -EA\frac{\psi}{\ell} \frac{1}{\sin(\psi)} \cos\left(\frac{\psi}{\ell}0\right) = -\frac{EA}{\ell} \frac{\psi}{\sin(\psi)}, \\ \hat{K}_{ij,44}^{\text{loc}} &= EA\hat{u}'_{jx}(\ell) = EA\frac{\psi}{\ell} \frac{1}{\sin(\psi)} \cos\left(\frac{\psi}{\ell}\ell\right) = \frac{EA}{\ell} \psi \cot(\psi).\end{aligned}$$

**Exercise 3.2.1.** Draw  $\hat{K}_{ij,14}^{\text{loc}}$  and  $\hat{K}_{ij,44}^{\text{loc}}$  as a function of the forcing frequency  $\omega$  in the domain  $\omega = 0 \dots 10\omega_{01}$ !

An entry of the second, third, fifth, or sixth columns of the elementary dynamic stiffness matrix  $\hat{\mathbf{K}}_{ij}^{\text{loc}}$  can be obtained from the differential equation of the transverse vibration of the beam (2.47), which is repeated here:

$$\mu\ddot{v}(x, t) + EIv''''(x, t) = 0. \quad (3.58)$$

Here dot and prime denote partial differentiation with respect to  $t$  and  $x$ , respectively. There are again harmonic boundary conditions defined for (3.58):

$$\begin{aligned}v_{iy}(0, t) &= \sin(\omega t), & v'_{iy}(0, t) &= 0, & v_{iy}(\ell, t) &= 0, & v'_{iy}(\ell, t) &= 0, \text{ or} \\ v_{i\varphi}(0, t) &= 0, & v'_{i\varphi}(0, t) &= \sin(\omega t), & v_{i\varphi}(\ell, t) &= 0, & v'_{i\varphi}(\ell, t) &= 0, \text{ or} \\ v_{jy}(0, t) &= 0, & v'_{jy}(0, t) &= 0, & v_{jy}(\ell, t) &= \sin(\omega t), & v'_{jy}(\ell, t) &= 0, \text{ or} \\ v_{j\varphi}(0, t) &= 0, & v'_{j\varphi}(0, t) &= 0, & v_{j\varphi}(\ell, t) &= 0, & v'_{j\varphi}(\ell, t) &= \sin(\omega t).\end{aligned} \quad (3.59)$$

The first four conditions express that there is a harmonic transverse translation of unit amplitude at end  $i$ , while the rotations of the ends, and the translation of end  $j$  are zero. The next four conditions are for a harmonic rotation of unit amplitude of end  $i$ , then the next four correspond to the harmonic transverse translation of unit amplitude of end  $j$ , while the last four are devoted for the harmonic rotation of unit amplitude of end  $j$ .

We split the variables  $t$  and  $x$  as

$$v(x, t) = \hat{v}(x) \sin(\omega t).$$

Substituting the above formula into Eq. (3.58) the ODE

$$\omega^2 \mu \hat{v}(x) - EI \hat{v}''''(x) = 0 \quad (3.60)$$

is obtained. The solution of the above differential equation is

$$\hat{v}(x) = C_1 \cos\left(\frac{\lambda}{\ell}x\right) + C_2 \sin\left(\frac{\lambda}{\ell}x\right) + C_3 \cosh\left(\frac{\lambda}{\ell}x\right) + C_4 \sinh\left(\frac{\lambda}{\ell}x\right), \quad (3.61)$$

where

$$\lambda = \ell \sqrt[4]{\frac{\omega^2 \mu}{EI}},$$

similarly to Eq. (2.50). The unknown coefficients  $C_1, C_2, C_3, C_4$  can be computed from four prescribed boundary conditions. According to (3.59), these conditions for the computation of the second column of  $\mathbf{K}_{ij}^{\text{loc}}$  are

$$\hat{v}_{iy}(0) = 1, \quad \hat{v}'_{iy}(0) = 0, \quad \hat{v}_{iy}(\ell) = 0, \quad \hat{v}'_{iy}(\ell) = 0. \quad (3.62)$$

Similarly, the boundary conditions are

$$\hat{v}_{i\varphi}(0) = 0, \quad \hat{v}'_{i\varphi}(0) = 1, \quad \hat{v}_{i\varphi}(\ell) = 0, \quad \hat{v}'_{i\varphi}(\ell) = 0, \quad (3.63)$$

$$\hat{v}_{jy}(0) = 0, \quad \hat{v}'_{jy}(0) = 0, \quad \hat{v}_{jy}(\ell) = 1, \quad \hat{v}'_{jy}(\ell) = 0, \quad \text{and} \quad (3.64)$$

$$\hat{v}_{j\varphi}(0) = 0, \quad \hat{v}'_{j\varphi}(0) = 0, \quad \hat{v}_{j\varphi}(\ell) = 0, \quad \hat{v}'_{j\varphi}(\ell) = 1 \quad (3.65)$$

for the third, fifth and sixth columns, respectively. Then the amplitudes of the internal forces at the ends are evaluated as

$$\hat{N}_{iiy} = 0, \quad \hat{V}_{iiy} = -EI \hat{v}'''_{iy}(0), \quad \hat{M}_{iiy} = -EI \hat{v}''_{iy}(0),$$

$$\hat{N}_{jiy} = 0, \quad \hat{V}_{jiy} = -EI \hat{v}'''_{iy}(\ell), \quad \hat{M}_{jiy} = -EI \hat{v}''_{iy}(\ell).$$

in the case of boundary conditions (3.62), i.e. for the second column of the dynamic stiffness matrix. The entries of the second column of the stiffness matrix are

$$\hat{\mathbf{k}}_{ij,2}^{\text{loc}} = [0, -\hat{V}_{iiy}, \hat{M}_{iiy}, 0, \hat{V}_{jiy}, -\hat{M}_{jiy}]^T.$$

The positive definition of the end-of-beam internal forces and the entries of the dynamic stiffness matrix are the same as in the case of the static stiffness matrix, which is shown in Figure 3.4 (c). Therefore, the dynamic stiffness matrix has the same structure as the static one (3.20):

$$\hat{\mathbf{K}}_{ij}^{\text{loc}} = \left[ \begin{array}{ccc|ccc} -\hat{N}_{iix} & 0 & 0 & -\hat{N}_{ijx} & 0 & 0 \\ 0 & -\hat{V}_{iiy} & -\hat{V}_{ii\varphi} & 0 & -\hat{V}_{ijy} & -\hat{V}_{ij\varphi} \\ 0 & \hat{M}_{iiy} & \hat{M}_{ii\varphi} & 0 & \hat{M}_{ijy} & \hat{M}_{ij\varphi} \\ \hline \hat{N}_{jix} & 0 & 0 & \hat{N}_{jxx} & 0 & 0 \\ 0 & \hat{V}_{jiy} & \hat{V}_{ji\varphi} & 0 & \hat{V}_{jyy} & \hat{V}_{jy\varphi} \\ 0 & -\hat{M}_{jiy} & -\hat{M}_{ji\varphi} & 0 & -\hat{M}_{jyy} & -\hat{M}_{jy\varphi} \end{array} \right]. \quad (3.66)$$

### Application of the principle of virtual displacements

Let a beam be vibrating such that the translation of its end  $i$  is  $v_{iy}(0, t) = 1 \cdot \sin(\omega t)$ , while all other displacements of its ends are zero (see Figure 3.9 top). The end-of-beam internal forces are the harmonic functions

$$\begin{aligned} N_{iy}(0, t) &= \hat{N}_{iyy} \sin(\omega t), & V_{iy}(0, t) &= \hat{V}_{iyy} \sin(\omega t), & M_{iy}(0, t) &= \hat{M}_{iyy} \sin(\omega t), \\ N_{iy}(\ell, t) &= \hat{N}_{jyy} \sin(\omega t), & V_{iy}(\ell, t) &= \hat{V}_{jyy} \sin(\omega t), & M_{iy}(\ell, t) &= \hat{M}_{jyy} \sin(\omega t). \end{aligned} \quad (3.67)$$

These internal forces and the bending moment diagram at a certain time instant are sketched at the bottom of Figure 3.9.

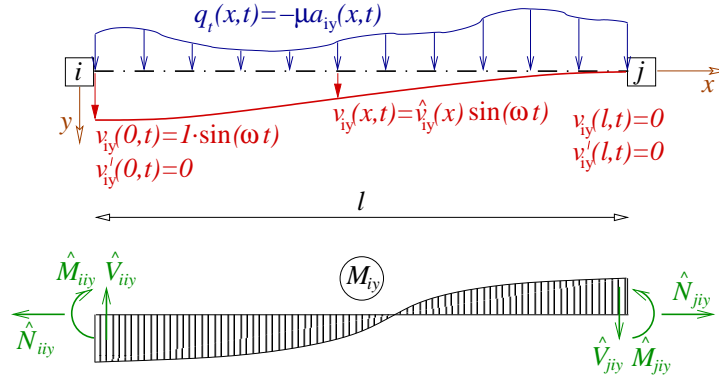


**Figure 3.9:** (top) Sketch of the deformed shape of beam  $ij$  due to a harmonic translation of unit amplitude of end  $i$  along axis  $y$ . (bottom) The corresponding bending moment diagram and the positive definition of the internal forces at the ends of the beam.

Our aim is to determine the amplitudes of the end-of-beam internal forces  $\hat{N}_{iyy}$ ,  $\hat{V}_{iyy}$ ,  $\hat{M}_{iyy}$ ,  $\hat{N}_{jyy}$ ,  $\hat{V}_{jyy}$ ,  $\hat{M}_{jyy}$  due to a harmonic translation of unit amplitude of end  $i$ . From these values the entries of the second column of the 6-by-6 elementary dynamic stiffness matrix  $\hat{\mathbf{K}}_{ij}^{\text{loc}}$  can be obtained following (3.66).

The computation of the end-of-beam internal forces of the beam is based on the principle of virtual displacements. At any time instant  $t$ , we apply the fictitious inertial force  $q_t(x, t) = -\mu a_{iy}(x, t)$  as shown in Figure 3.9. Thus we have a statically admissible force system: the internal forces and the fictitious inertial force are in equilibrium. We take the (static) displacement system  $v_{i\varphi}(x)$ , which is caused by a unit translation of end  $i$  (shown in Figure 3.5) as the virtual displacement system. We compute the virtual work that the force system shown in Figure 3.9 does on this virtual displacement system at time instant  $t$ :

$$\delta W_{\text{ds}} = M_{iy}(0, t) \cdot 1 + \int_0^\ell \{-\mu a_{iy}(x, t)\} v_{i\varphi}(x) dx - \int_0^\ell M_{iy}(x, t) \frac{M_{i\varphi}(x)}{EI} dx = 0.$$

Here the first term is the work done by the moment  $M_{iy}(0, t)$  on the unit rotation of end  $i$ . The last term is the internal work done by the bending moment  $M_{iy}(x, t)$  on the curvature  $\kappa_{i\varphi}(x) = M_{i\varphi}(x)/EI$ . The second term is the work done by the (distributed) inertia force

$$-\mu a_{iy}(x, t) = -\mu \ddot{v}_{iy}(x, t) = \mu \omega^2 \hat{v}_{iy}(x) \sin(\omega t)$$

on the translation  $v_{i\varphi}(x)$  along the whole length of the beam. This, Eq. (3.49), and Eq (3.67) implies that the above work is

$$\delta W_{\text{ds}} = \left\{ \hat{M}_{iyy} + \mu\omega^2 \int_0^\ell \hat{v}_{iy}(x)v_{i\varphi}(x) dx - \int_0^\ell \hat{M}_{iy}(x) \frac{M_{i\varphi}(x)}{EI} dx \right\} \sin(\omega t) = 0. \quad (3.68)$$

Next, we express the virtual work that the static force system (shown in Figure 3.5) does on the dynamic displacement system (sketched in Figure 3.9) at certain time instant  $t$ :

$$\delta W_{\text{sd}} = V_{ii\varphi} \cdot \{-1 \cdot \sin(\omega t)\} - \int_0^\ell M_{i\varphi}(x) \frac{M_{iy}(x, t)}{EI} dx = 0.$$

Using Eqs. (3.49) and (3.67) the above work is reformulated as

$$\delta W_{\text{sd}} = \left\{ -V_{ii\varphi} - \int_0^\ell M_{i\varphi}(x) \frac{\hat{M}_{iy}(x)}{EI} dx \right\} \sin(\omega t) = 0. \quad (3.69)$$

Both Eqs. (3.68) and (3.69) have zero on the right hand side. Therefore their left hand sides are equal, which implies that the terms in the curl brackets are equal, yielding

$$\hat{M}_{iyy} + \mu\omega^2 \int_0^\ell \hat{v}_{iy}(x)v_{iy}(x) dx = -V_{ii\varphi}.$$

In the above expression  $-V_{ii\varphi}$  equals the entry 2, 3 of the static stiffness matrix of the beam by definition. In addition, and due to the symmetry (3.22) of the static stiffness matrix,  $-V_{ii\varphi} = K_{ij,23}^{\text{loc}} = K_{ij,32}^{\text{loc}}$ .

Finally, we can express the amplitude of the dynamic bending moment at end  $i$  caused by a harmonic translation of the same end, i.e. the entry 3,2 of the dynamic stiffness matrix  $\hat{K}_{ij}^{\text{loc}}$ :

$$\hat{K}_{ij,32}^{\text{loc}} = \hat{M}_{iyy} = K_{ij,32}^{\text{loc}} - \mu\omega^2 \int_0^\ell \hat{v}_{iy}(x)v_{i\varphi}(x) dx.$$

We can derive all the end-of-beam internal forces due to longitudinal and transverse (harmonic) translations and (harmonic) rotations of unit amplitudes of the ends in a similar way. We can construct a matrix similar to (3.23):

$$\hat{\mathbf{N}} = \begin{bmatrix} \hat{u}_{ix}(x) & 0 & 0 & \hat{u}_{jx}(x) & 0 & 0 \\ 0 & \hat{v}_{iy}(x) & \hat{v}_{i\varphi}(x) & 0 & \hat{v}_{jy}(x) & \hat{v}_{j\varphi}(x) \end{bmatrix}. \quad (3.70)$$

Here  $\hat{u}_{ix}(x)$  is the dynamic shape function of the beam due to a harmonic translation of unit amplitude of end  $i$  along  $x$ . This is the solution of (3.53) with boundary conditions (3.55). The shape function  $\hat{v}_{iy}(x)$  is due to a harmonic translation of unit amplitude of end  $i$  along  $y$ , i.e.

the solution of (3.60) with boundary conditions (3.62). The shape function  $\hat{v}_{i\varphi}(x)$  describes the deformed shape of the beam caused by a harmonic rotation of unit amplitude of end  $i$ . It is the solution of (3.60) with boundary conditions (3.63). The same holds for superscript  $j$  with the appropriate boundary conditions. It is important to note that these shape functions are functions of  $x$ , but they depend on the parameters  $\mu$ ,  $EI$ ,  $EA$ ,  $\ell$  (which are given for the studied beam), and also on  $\omega$  (which is the frequency of the vibration). Therefore,  $\hat{\mathbf{N}}$  is *frequency dependent*.

Now we can write the elementary dynamic stiffness matrix of beam  $ij$  in the short form

$$\hat{\mathbf{K}}_{ij}^{\text{loc}}(\omega) = \mathbf{K}_{ij}^{\text{loc}} - \omega^2 \hat{\mathbf{M}}_{ij}^{\text{loc}}(\omega). \quad (3.71)$$

Here  $\mathbf{K}_{ij}^{\text{loc}}$  is its elementary static stiffness matrix of beam  $ij$ , and  $\hat{\mathbf{M}}_{ij}^{\text{loc}}(\omega)$  is the elementary mass matrix:

$$\hat{\mathbf{M}}_{ij}^{\text{loc}}(\omega) = \mu \int_0^\ell \hat{\mathbf{N}}^T \mathbf{N} \, dx, \quad (3.72)$$

which depends on the circular frequency  $\omega$  of the external forcing. As a conclusion, we can say that the elementary dynamic stiffness matrix equals to the elementary static stiffness matrix minus the mass matrix (3.72) times the square of the forcing frequency. This dynamic stiffness matrix is *frequency dependent*. From Eq. (3.72) it can be verified that the mass matrix  $\hat{\mathbf{M}}_{ij}^{\text{loc}}(\omega)$  is *symmetric*, and so is the dynamic stiffness matrix  $\hat{\mathbf{K}}_{ij}^{\text{loc}}(\omega)$ , which is evident from Eq. (3.71).

**Problem 3.2.2** (Entry 1,4 of the elementary dynamic stiffness matrix). The fixed-fixed beam  $ij$  is of length  $\ell$ , normal stiffness  $EA$ , bending stiffness  $EI$ , and mass per unit length  $\mu$ . Determine the entry 1,4 of its elementary dynamic stiffness matrix!

**Solution.** Entry 1,4 is the normal force at end  $i$  due to a harmonic translation of unit amplitude of end  $j$  along the axis of the beam:

$$\hat{K}_{ij,14}^{\text{loc}} = K_{ij,14}^{\text{loc}} - \omega^2 \mu \int_0^\ell \hat{u}_{jx}(x) u_{ix}(x) \, dx.$$

Here  $\hat{u}_{jx}(x)$  is the dynamic shape function due to the harmonic (axial) vibration of end  $j$ , while  $u_{ix}(x)$  is the (static) deformation of the bar caused by an axial unit translation of end  $i$ . The former function  $\hat{u}_{jx}(x)$  was already determined in Problem 3.2.1, its is given by Eq. (3.57), which is repeated here:

$$\hat{u}_{jx}(x) = \frac{1}{\sin(\psi)} \sin\left(\frac{\psi}{\ell} x\right).$$

The function  $u_{ix}(x)$  was derived in Problem 3.1.1, its is given by Eq. (3.13) as:

$$u_{ix}(x) = B_0 + B_1 x = 1 - \frac{1}{\ell} x.$$

Entry 4,1 of the static stiffness matrix was also computed in Problem 3.1.1. Due to the symmetry of the stiffness matrix, entries 4,1 and 1,4 are equal:

$$K_{ij,14}^{\text{loc}} = K_{ij,41}^{\text{loc}} = -\frac{EA}{\ell}.$$

Now, we can compute the entry of the dynamic stiffness matrix according to (3.71):

$$\begin{aligned}
 \hat{K}_{ij,14}^{\text{loc}} &= K_{ij,14}^{\text{loc}} - \omega^2 \mu \int_0^\ell \hat{u}_{jx}(x) u_{ix}(x) dx = -\frac{EA}{\ell} - \omega^2 \mu \int_0^\ell \frac{1}{\sin(\psi)} \sin\left(\frac{\psi}{\ell}x\right) \left\{1 - \frac{1}{\ell}x\right\} dx \\
 &= -\frac{EA}{\ell} - \omega^2 \mu \left\{ \frac{\ell}{\psi \sin \psi} - \frac{\ell}{\psi^2} \right\} = -\frac{EA}{\ell} - \frac{EA\ell}{EA\ell} \frac{\omega^2 \mu \ell}{\psi \sin \psi} + \frac{\omega^2 \mu \ell}{\psi^2} = -\frac{EA}{\ell} - \frac{EA}{\ell} \frac{\psi}{\sin \psi} + \frac{EA}{\ell} \\
 &= -\frac{EA}{\ell} \frac{\psi}{\sin \psi}.
 \end{aligned}$$

The entries of the elementary dynamic stiffness matrix of beam  $ij$  of length  $\ell$ , mass per unit length  $\mu$ , normal stiffness  $EA$ , and bending stiffness  $EI$  are

$$\hat{\mathbf{K}}_{ij}^{\text{loc}} = \begin{bmatrix} \frac{EA}{\ell} \psi \cot \psi & 0 & 0 & -\frac{EA}{\ell} \frac{\psi}{\sin \psi} & 0 & 0 \\ 0 & \frac{EI}{\ell^3} F_6(\lambda) & -\frac{EI}{\ell^2} F_4(\lambda) & 0 & \frac{EI}{\ell^3} F_5(\lambda) & \frac{EI}{\ell^2} F_3(\lambda) \\ 0 & -\frac{EI}{\ell^2} F_4(\lambda) & \frac{EI}{\ell} F_2(\lambda) & 0 & -\frac{EI}{\ell^2} F_3(\lambda) & \frac{EI}{\ell} F_1(\lambda) \\ -\frac{EA}{\ell} \frac{\psi}{\sin \psi} & 0 & 0 & \frac{EA}{\ell} \psi \cot \psi & 0 & 0 \\ 0 & \frac{EI}{\ell^3} F_5(\lambda) & -\frac{EI}{\ell^2} F_3(\lambda) & 0 & \frac{EI}{\ell^3} F_6(\lambda) & \frac{EI}{\ell^2} F_4(\lambda) \\ 0 & \frac{EI}{\ell^2} F_3(\lambda) & \frac{EI}{\ell} F_1(\lambda) & 0 & \frac{EI}{\ell^2} F_4(\lambda) & \frac{EI}{\ell} F_2(\lambda) \end{bmatrix}, \quad (3.73)$$

$$\begin{aligned}
 F_1(\lambda) &= \lambda \frac{\sin \lambda - \sinh \lambda}{\cos \lambda \cosh \lambda - 1}, & F_2(\lambda) &= -\lambda \frac{\cosh \lambda \sin \lambda - \sinh \lambda \cos \lambda}{\cos \lambda \cosh \lambda - 1} \\
 F_3(\lambda) &= -\lambda^2 \frac{\cosh \lambda - \cos \lambda}{\cos \lambda \cosh \lambda - 1}, & F_4(\lambda) &= \lambda^2 \frac{\sinh \lambda \sin \lambda}{\cos \lambda \cosh \lambda - 1}, \\
 F_5(\lambda) &= \lambda^3 \frac{\sinh \lambda + \sin \lambda}{\cos \lambda \cosh \lambda - 1}, & F_6(\lambda) &= -\lambda^3 \frac{\cosh \lambda \sin \lambda + \sinh \lambda \cos \lambda}{\cos \lambda \cosh \lambda - 1},
 \end{aligned}$$

$$\psi = \ell \sqrt{\frac{\omega^2 \mu}{EA}}, \quad \lambda = \ell^4 \sqrt{\frac{\omega^2 \mu}{EI}}.$$

We have to note here that if the forcing frequency  $\omega$  coincides with one of the natural circular frequencies  $\omega_{0j}$  of the longitudinal vibration of the clamped-clamped bar, then  $\psi = j\pi$ , therefore  $\psi \cot \psi$  and  $\psi/\sin \psi$  become singular. Besides, if  $\omega$  coincides with one of the natural circular frequencies  $\omega_{0i}$  of the transverse vibration of the clamped-clamped beam, then all the functions  $F_1(\lambda), F_2(\lambda), \dots, F_6(\lambda)$  become singular. Thus matrix  $\hat{\mathbf{K}}_{ij}^{\text{loc}}$  cannot be inverted in these special cases. This phenomenon is the *resonance*.

An alternative way to construct the elementary stiffness matrix purely from dynamic shape functions is given in Appendix A.4.

### 3.3 Consistent mass matrix

Construction of the elementary dynamic stiffness matrix of a member of the planar frame was discussed in the previous subsection, and an explicit formula (3.71) was derived.

The drawback of that approach is that the mass matrix (3.72) is frequency-dependent. Therefore, if someone needs to analyse a structure subjected to different loading (frequencies), they need to compile the mass matrix for *each* load frequency for the same structure. Another weak point is that the calculation of the mass matrix assumed that each nodal force has the same frequency  $\omega$ . If it is not the case, for instance when the nodal forces have different frequencies, or they are not harmonic functions of time, then there does not exist a frequency  $\omega$  which can be used for the calculation of the entries of the mass matrix. In fact, the whole procedure, assuming that the response of the structure follows the same frequency  $\omega$ , fails in those cases.

Hence, in practice, the elementary mass matrix is approximated by using purely static shape functions (which are frequency independent) instead of the dynamic ones. That estimation leads to the construction of the so-called *consistent mass matrix*

$$\mathbf{M}_{\text{cons},ij}^{\text{loc}} = \mu \int_0^{\ell} \mathbf{N}^T \mathbf{N} \, dx. \quad (3.74)$$

Since here we use the same static shape functions as for the computation of the static stiffness matrix (3.27), this composition of the mass matrix is consistent with the static stiffness matrix, therefore it is often called the stiffness consistent mass matrix.

**Problem 3.3.1** (Entry 1,1 of the consistent mass matrix). The fixed-fixed beam  $ij$  is of length  $\ell$ , normal stiffness  $EA$ , bending stiffness  $EI$ , and mass per unit length  $\mu$ . Determine entry 1,1 of its elementary consistent mass matrix!

**Solution.** Entry 1,1 is of the consistent mass matrix according to (3.74) and (3.23) is

$$M_{\text{cons},ij,11}^{\text{loc}} = \mu \int_0^{\ell} u_{ix}(x) u_{ix}(x) \, dx.$$

Here  $u_{ix}(x)$  is the deformation of the bar caused by an axial unit translation of end  $i$ . This function  $u_{ix}(x)$  was already derived in Problem 3.1.1, its is given by Eq. (3.13) as:

$$u_{ix}(x) = 1 - \frac{x}{\ell}.$$

Now we compute the entry of the consistent mass matrix

$$\begin{aligned} M_{\text{cons},ij,11}^{\text{loc}} &= \mu \int_0^{\ell} u_{ix}(x) u_{ix}(x) \, dx = \mu \int_0^{\ell} \left(1 - \frac{x}{\ell}\right)^2 \, dx = \mu \int_0^{\ell} 1 - 2\frac{x}{\ell} + \frac{x^2}{\ell^2} \, dx \\ &= \left[ x - \frac{x^2}{\ell} + \frac{x^3}{3\ell^2} \right]_0^{\ell} = \mu \frac{\ell}{3}. \end{aligned}$$



The entries of the consistent mass matrix are *independent of the loading frequency*, which is a huge advantage in the further analysis. The approximated dynamic stiffness matrix expressed with the consistent mass matrix is

$$\hat{\mathbf{K}}_{ij}^{\text{loc}}(\omega) \approx \mathbf{K}_{ij}^{\text{loc}} - \omega^2 \mathbf{M}_{\text{cons},ij}^{\text{loc}}.$$

Hereafter we leave the subscript “cons” and denote the consistent mass matrix by  $\mathbf{M}_{\text{cons}} = \mathbf{M}$ . The entries of the consistent mass matrix of a beam of length  $\ell$  and mass per unit length  $\mu$  are

$$\mathbf{M}_{\text{cons},ij}^{\text{loc}} = \mathbf{M}_{ij}^{\text{loc}} = \mu \ell \begin{bmatrix} \frac{1}{3} & 0 & 0 & \frac{1}{6} & 0 & 0 \\ 0 & \frac{13}{35} & \frac{11}{210}\ell & 0 & \frac{9}{70} & -\frac{13}{420}\ell \\ 0 & \frac{11}{210}\ell & \frac{1}{105}\ell^2 & 0 & \frac{13}{420}\ell & -\frac{1}{140}\ell^2 \\ \hline \frac{1}{6} & 0 & 0 & \frac{1}{3} & 0 & 0 \\ 0 & \frac{9}{70} & \frac{13}{420}\ell & 0 & \frac{13}{35} & -\frac{11}{210}\ell \\ 0 & -\frac{13}{420}\ell & -\frac{1}{140}\ell^2 & 0 & -\frac{11}{210}\ell & \frac{1}{105}\ell^2 \end{bmatrix}. \quad (3.75)$$

In further analysis we use the consistent mass matrix  $\mathbf{M}$ , even if the structure is subjected to a general loading (forces that are arbitrary functions of time, or harmonic forces with different frequencies).

### 3.3.1 Different end conditions of beam members

Similarly to the case of the elementary static stiffness matrix, the elementary consistent mass matrix can also be modified using dyadic decompositions.

The computation of the displacements of any point of the beam axis can be achieved using the end-of-beam displacements  $\mathbf{u}_i$  and the static shape functions  $\mathbf{N}$  of the beam:

$$\mathbf{u}(x) = \mathbf{N}_0(x)\mathbf{u}_0.$$

For an unloaded beam ( $\mathbf{q}_i = \mathbf{0}$ ) (3.34) yields

$$\mathbf{K}_0\mathbf{u}_0 = \mathbf{q}_i.$$

Multiplying it from the left by  $\mathbf{R}$  and substituting (3.35) in the right hand side we get:

$$\mathbf{R}\mathbf{K}_0\mathbf{u}_0 = \mathbf{u}_i - \mathbf{u}_0 \quad \rightarrow \quad \mathbf{u}_0 = (\mathbf{I} + \mathbf{R}\mathbf{K}_0)^{-1}\mathbf{u}_i,$$

thus

$$\mathbf{u}(x) = \mathbf{N}_0(x)(\mathbf{I} + \mathbf{R}\mathbf{K}_0)^{-1}\mathbf{u}_i,$$

which implies

$$\mathbf{N}(x) = \mathbf{N}_0(x)(\mathbf{I} + \mathbf{R}\mathbf{K}_0)^{-1}.$$

By definition the consistent mass matrix is

$$\begin{aligned} \mathbf{M} &= \mu \int_0^\ell \mathbf{N}^T \mathbf{N} \, dx = \mu \int_0^\ell (\mathbf{I} + \mathbf{R}\mathbf{K}_0)^{-T} \mathbf{N}_0^T \mathbf{N}_0 (\mathbf{I} + \mathbf{R}\mathbf{K}_0)^{-1} \, dx \\ &= (\mathbf{I} + \mathbf{R}\mathbf{K}_0)^{-T} \left\{ \mu \int_0^\ell \mathbf{N}_0^T \mathbf{N}_0 \, dx \right\} (\mathbf{I} + \mathbf{R}\mathbf{K}_0)^{-1} = (\mathbf{I} + \mathbf{R}\mathbf{K}_0)^{-T} \mathbf{M}_0 (\mathbf{I} + \mathbf{R}\mathbf{K}_0)^{-1}. \end{aligned}$$

(Note that  $\mathbf{I}$ ,  $\mathbf{R}$ , and  $\mathbf{K}_0$  are independent of  $x$ .) Here  $\mathbf{M}_0$  is the consistent mass matrix of the fixed-fixed beam.

If only one degree of freedom (the  $p$ th) of the beam ends is connected elastically to the adjacent node, then matrix  $\mathbf{R}$  can be written in the dyadic form (3.38), and

$$\mathbf{R}\mathbf{K}_0 = r_p \mathbf{e}_p \mathbf{k}_p^T,$$

According to (3.39)

$$(\mathbf{I} - r_p \mathbf{e}_p \mathbf{k}_p^T)^{-1} = \mathbf{I} - \frac{1}{k_{pp} + \frac{1}{r_p}} \mathbf{e}_p \mathbf{k}_p^T.$$

Hence

$$\begin{aligned} \mathbf{M} &= (\mathbf{I} + \mathbf{R}\mathbf{K}_0)^{-T} \mathbf{M}_0 (\mathbf{I} + \mathbf{R}\mathbf{K}_0)^{-1} = \left( \mathbf{I} - \frac{1}{k_{pp} + \frac{1}{r_p}} \mathbf{e}_p \mathbf{k}_p^T \right)^T \mathbf{M}_0 \left( \mathbf{I} - \frac{1}{k_{pp} + \frac{1}{r_p}} \mathbf{e}_p \mathbf{k}_p^T \right) \\ &= \mathbf{M}_0 - \frac{1}{k_{pp} + \frac{1}{r_p}} \{ \mathbf{k}_p \mathbf{e}_p^T \mathbf{M}_0 + \mathbf{M}_0 \mathbf{e}_p \mathbf{k}_p^T \} + \frac{1}{\left( k_{pp} + \frac{1}{r_p} \right)^2} \mathbf{k}_p \mathbf{e}_p^T \mathbf{M}_0 \mathbf{e}_p \mathbf{k}_p^T, \end{aligned}$$

which yields

$$\boxed{\mathbf{M} = \mathbf{M}_0 - \frac{1}{k_{pp} + \frac{1}{r_p}} (\mathbf{k}_p \mathbf{m}_p^T + \mathbf{m}_p \mathbf{k}_p^T) + \frac{m_{pp}}{\left( k_{pp} + \frac{1}{r_p} \right)^2} \mathbf{k}_p \mathbf{k}_p^T.} \quad (3.76)$$

**Problem 3.3.2** (Elementary consistent mass matrix of a fixed-pinned beam). The beam  $ij$  of length  $\ell$ , normal stiffness  $EA$ , bending stiffness  $EI$ , and mass per unit length  $\mu$  is fixed at end  $i$  and pinned at end  $j$ . (It is fixed-pinned.) Determine its elementary consistent mass matrix  $\mathbf{M}_{ij}^{\text{loc,fp}}$ !

**Solution.** We use Eq. (3.76) for the construction of the mass matrix. We start with the static stiffness matrix  $\mathbf{K}_{ij}^{\text{loc}}$  and the consistent mass matrix  $\mathbf{M}_{ij}^{\text{loc}}$  of the fixed-fixed beam, given by (3.28) and (3.75), respectively. Because of the rotation of end  $j$  (the sixth degree of freedom of the beam) is relaxed,  $p = 6$  and  $r_6 \rightarrow \infty$ . Thus the entries 6,6 and the 6th column of  $\mathbf{K}_{ij}^{\text{loc}}$  and  $\mathbf{M}_{ij}^{\text{loc}}$  are needed:

$$\begin{aligned} k_{66} &= \frac{4EI}{\ell}, \quad m_{66} = \frac{\mu\ell^3}{105} \\ \mathbf{k}_6^T &= \left[ 0 \quad \frac{6EI}{\ell^2} \quad \frac{2EI}{\ell} \quad 0 \quad -\frac{6EI}{\ell^2} \quad \frac{4EI}{\ell} \right] \\ \mathbf{m}_6^T &= \left[ 0 \quad -\frac{13\mu\ell^2}{420} \quad -\frac{\mu\ell^3}{140} \quad 0 \quad -\frac{11\mu\ell^2}{210} \quad \frac{\mu\ell^3}{105} \right] \end{aligned}$$

Now we apply formula (3.76) with the above input data:

$$\begin{aligned}
 \mathbf{M}_{ij}^{\text{loc,fp}} &= \mathbf{M}_{ij}^{\text{loc}} - \frac{1}{k_{66}} (\mathbf{m}_6 \mathbf{k}_6^T + \mathbf{k}_6 \mathbf{m}_6^T) + \frac{m_{66}}{k_{66}^2} \mathbf{k}_6 \mathbf{k}_6^T \\
 &= \mathbf{M}_{ij}^{\text{loc}} - \frac{1}{\frac{4EI}{\ell}} \begin{bmatrix} 0 \\ -\frac{13\mu\ell^2}{420} \\ -\frac{\mu\ell^3}{140} \\ 0 \\ -\frac{11\mu\ell^2}{210} \\ \frac{\mu\ell^3}{105} \end{bmatrix} \left[ 0 \quad \frac{6EI}{\ell^2} \quad \frac{2EI}{\ell} \mid 0 \quad -\frac{6EI}{\ell^2} \quad \frac{4EI}{\ell} \right] \\
 &\quad - \frac{1}{\frac{4EI}{\ell}} \begin{bmatrix} 0 \\ \frac{6EI}{\ell^2} \\ \frac{2EI}{\ell} \\ 0 \\ -\frac{6EI}{\ell^2} \\ \frac{4EI}{\ell} \end{bmatrix} \left[ 0 \quad -\frac{13\mu\ell^2}{420} \quad -\frac{\mu\ell^3}{140} \mid 0 \quad -\frac{11\mu\ell^2}{210} \quad \frac{\mu\ell^3}{105} \right] \\
 &\quad + \frac{\frac{\mu\ell^3}{105}}{\left(\frac{4EI}{\ell}\right)^2} \begin{bmatrix} 0 \\ \frac{6EI}{\ell^2} \\ \frac{2EI}{\ell} \\ 0 \\ -\frac{6EI}{\ell^2} \\ \frac{4EI}{\ell} \end{bmatrix} \left[ 0 \quad \frac{6EI}{\ell^2} \quad \frac{2EI}{\ell} \mid 0 \quad -\frac{6EI}{\ell^2} \quad \frac{4EI}{\ell} \right] \\
 &= \mu\ell \begin{bmatrix} \frac{1}{3} & 0 & 0 & \frac{1}{6} & 0 & 0 \\ 0 & \frac{17}{35} & \frac{3}{35}\ell & 0 & \frac{39}{280} & 0 \\ 0 & \frac{3}{35}\ell & \frac{2}{105}\ell^2 & 0 & \frac{11}{280}\ell & 0 \\ \hline \frac{1}{6} & 0 & 0 & \frac{1}{3} & 0 & 0 \\ 0 & \frac{39}{280} & \frac{11}{280}\ell & 0 & \frac{33}{140} & 0 \\ 0 & 0 & 0 & 0 & 0 & 0 \end{bmatrix}.
 \end{aligned}$$

### 3.3.2 Accuracy with the consistent mass matrix

In order to get some information about the accuracy of the stiffness matrix obtained using the consistent mass matrix, we compare the entries of the consistent matrix with the same entries of the accurate dynamic stiffness matrix.

Let us compare entries 3,6 of the accurate dynamic stiffness matrix  $\hat{\mathbf{K}}_{ij}^{\text{loc}}$  and of the approximated stiffness matrix  $\mathbf{K}_{ij}^{\text{loc}} - \omega^2 \mathbf{M}_{ij}^{\text{loc}}$ . (Here  $\mathbf{M}_{ij}^{\text{loc}}$  is the elementary consistent mass matrix.)

Entry 3,6 of  $\hat{\mathbf{K}}_{ij}^{\text{loc}}$  is

$$\hat{K}_{ij,36}^{\text{loc}} = \frac{EI}{\ell} F_1(\lambda) = \frac{EI}{\ell} \lambda \frac{\sin \lambda - \sinh \lambda}{\cos \lambda \cosh \lambda - 1}.$$

The *Taylor* expansion of the above function with respect to  $\lambda$  is

$$\hat{K}_{ij,36}^{\text{loc}} = \frac{EI}{\ell} (2 + 0.7143 \cdot 10^{-2} \lambda^4 + 0.1570 \cdot 10^{-4} \lambda^8 + 0.3182 \cdot 10^{-7} \lambda^{12} + \mathcal{O}(\lambda^{16})).$$

Entry 3,6 of  $\mathbf{K}_{ij}^{\text{loc}} - \omega^2 \mathbf{M}_{ij}^{\text{loc}}$  is

$$\hat{K}_{ij,36}^{\text{loc}} \approx K_{ij,36}^{\text{loc}} - \omega^2 M_{ij,36}^{\text{loc}} = \frac{2EI}{\ell} - \omega^2 \mu \ell \left( -\frac{1}{140} \ell^2 \right) = \frac{2EI}{\ell} + \frac{EI}{\ell} 0.7143 \cdot 10^{-2} \lambda^4.$$

Here we used the identity

$$\lambda = \ell \sqrt[4]{\frac{\omega^2 \mu}{EI}} \quad \rightarrow \quad \omega^2 \mu = EI \frac{\lambda^4}{\ell^4}.$$

The difference between the accurate and the estimate values is

$$\hat{K}_{ij,36}^{\text{loc}} - (K_{ij,36}^{\text{loc}} - \omega^2 M_{ij,36}^{\text{loc}}) = \frac{EI}{\ell} (0.1570 \cdot 10^{-4} \lambda^8 + 0.3182 \cdot 10^{-7} \lambda^{12} + \mathcal{O}(\lambda^{16})).$$

As we can see,  $\lambda$  governs the magnitude of the error: it appears on the power of higher than seven in the error. Hence, decreasing the value of  $\lambda$  makes the approximation of the dynamic stiffness matrix more accurate. Usually we cannot decrease the mass or increase the bending stiffness, because those are given parameters of the structure. What we can do in order to obtain a better accuracy is reducing the length  $\ell$  of the members, i.e. applying more nodes. It is important to note that higher forcing frequency  $\omega$  increases  $\lambda$ , thus it also increases the error, i.e. decreases the accuracy of the approximate stiffness matrix. Thus, the higher the forcing frequency is, the shorter members (i.e. more nodes) we have to use for the same accuracy. A good rule of thumb is that the approximate model built with the consistent mass matrix is usually accurate enough if the smallest natural circular frequency of the applied beam members is larger than the largest natural circular frequency of the whole model.

$$\omega_{0,\min}^{\text{members}} > \omega_{0,\max}^{\text{structure}}, \quad T_{0,\max}^{\text{members}} < T_{0,\min}^{\text{structure}}$$

### 3.3.3 Additional masses

Additional masses are often needed to be considered in structural design (furnitures, plaster-work, devices, etc.). These are modeled as continuously distributed mass, or as a concentrated (lumped) mass on a beam.

#### Continuously distributed additional mass along a beam

Let a mass per unit length  $\mu_{\text{add}}$  be distributed along the whole length of the beam. In this case one only needs to determine an *equivalent mass* per unit length

$$\mu_{\text{ekv}} = \mu + \mu_{\text{add}}$$

and use it (instead of  $\mu$ ) in the computation of the consistent mass matrix (3.75) of the beam.

### Concentrate additional mass on one node

If a mass  $m$  is placed right on a node  $p$  of the mechanical model, then the additional diagonal mass matrix

$$\mathbf{M}_{\text{add}}^{\text{glob}} = \begin{bmatrix} m & 0 & 0 \\ 0 & m & 0 \\ 0 & 0 & I_0 \end{bmatrix}$$

is to be added to the corresponding block of the total mass matrix of the structure. Here  $I_0$  is the moment of inertia of the mass with respect to the node.

### Concentrate additional mass on a beam

Let a mass  $m$  be on the beam at  $x = a$ . An additional (consistent) mass matrix can be computed as

$$\mathbf{M}_{\text{add}}^{\text{loc}} = m \mathbf{N}^T|_{x=a} \mathbf{N}|_{x=a}.$$

Then this 6-by-6 matrix  $\mathbf{M}_{\text{add}}^{\text{loc}}$  is simply added to the original elementary mass matrix of the corresponding beam member.

## 3.4 Equivalent dynamic nodal loads

If there is a dynamic, distributed load  $\mathbf{f}(x, t) = [f_x(x, t), f_y(x, t)]^T$  (whose components are given by an axial load  $f_x(x, t)$  and a transverse load  $f_y(x, t)$ ) acting on beam  $ij$  between  $x = a$  and  $x = b$ , then an *equivalent nodal load*  $\mathbf{q}_{\text{eq},ij}(t)$  must be determined for the matrix displacement method. Without going into details of the derivations, this equivalent nodal load can be approximated as

$$\mathbf{q}_{\text{eq},ij}^{\text{loc}}(t) = \int_a^b \mathbf{N}^T \mathbf{f}(x, t) dx. \quad (3.77)$$

Here vector  $\mathbf{q}_{\text{eq},ij}(t) = [\mathbf{q}_{\text{eq},i}(t), \mathbf{q}_{\text{eq},j}(t)]^T$  contains the equivalent loads on the ends  $i$  and  $j$  of the beam member. The static shape functions are collected in  $\mathbf{N}$  (see (3.23)).

In the case of a concentrated force  $\mathbf{F}(t) = [F_x(t), F_y(t)]^T$  acting at  $x = a$ , the equivalent load is estimated as

$$\mathbf{q}_{\text{eq},ij}^{\text{loc}}(t) = \mathbf{N}^T|_{x=a} \mathbf{F}(t). \quad (3.78)$$

**Problem 3.4.1** (Dynamic analysis of a simple planar frame). Let us examine the planar frame shown in Figure 3.10 (a). It consists of three beams of equal length  $\ell = 8$  m, bending stiffness  $EI = 100000$  Nm<sup>2</sup>, normal stiffness  $EA = 5000000$  N, and mass per unit length  $\mu = 200$  kg/m. The frame is loaded by a dynamic exciting force  $P \sin(\omega t) = 100000 \sin(40t)$  N at the right top node, leaning  $45^\circ$  from the horizontal, as it is shown in Figure 3.10 (a). Determine the steady-state response of the frame due to this exciting force!

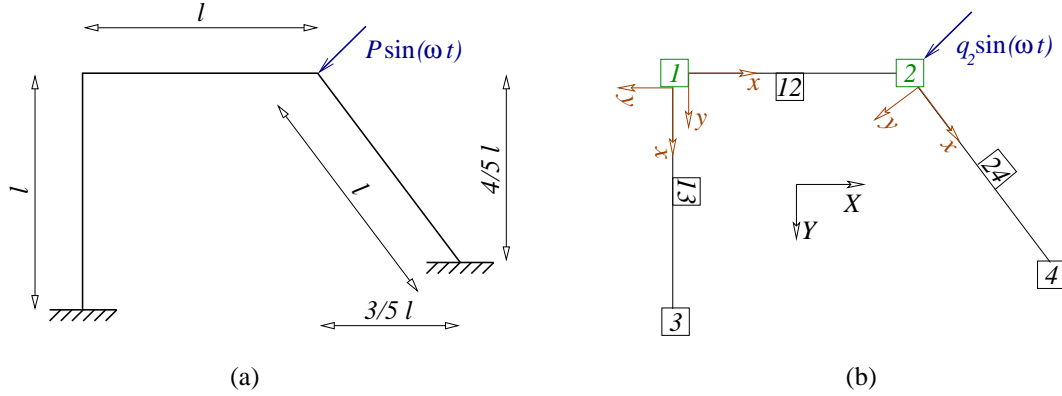


**Figure 3.10:** (a) Sketch of a simple planar frame. (b) Mechanical model for the matrix displacement method.

**Solution.** We use the total dynamic stiffness matrix  $\hat{\mathbf{K}}(\omega)$  of the frame and solve (3.48):

$$\hat{\mathbf{K}}(\omega) \mathbf{u}_{f0} = \mathbf{q}_0 \quad \rightarrow \quad \mathbf{u}_{f0} = \hat{\mathbf{K}}^{-1}(\omega) \mathbf{q}_0.$$

Here  $\mathbf{u}_{f0}$  is the amplitude of the vibration of the nodes of the structure. The steady-state vibration is then governed by

$$\mathbf{u}_f(t) = \mathbf{u}_{f0} \sin(\omega t).$$

We also compute two approximate solutions by using the consistent mass matrix  $\mathbf{M}$  and the diagonally lumped mass matrix  $\mathbf{M}_{\text{lum}}$ . With the aid of these matrices the dynamic stiffness matrix can be estimated as

$$\hat{\mathbf{K}}(\omega) \approx \mathbf{K} - \omega^2 \mathbf{M}, \quad \text{and} \quad \hat{\mathbf{K}}(\omega) \approx \mathbf{K} - \omega^2 \mathbf{M}_{\text{lum}}.$$

For these approximations we need to compile the total static stiffness matrix  $\mathbf{K}$  of the frame, too.

First we start with the nodal decomposition of the frame, then we define the local and global reference systems, and the coordinate transformations. We apply four nodes, as shown in Figure 3.10 (b). Nodes 1 and 2 are *internal nodes*, while nodes 3 and 4 are *supported nodes*. Since there is not any support motion, we exclude these external nodes from the compilation of the total (stiffness, mass, and dynamic stiffness) matrices. The global reference system is the left handed one  $XYZ$  shown in Figure 3.10 (b). There are local reference systems  $xyz$  attached to each beam member, as indicated in Figure 3.10 (b). The vector of the unknown displacements of the internal nodes 1 and 2 in the global reference system is

$$\mathbf{u}(t) = \begin{bmatrix} u_{1X}(t) \\ u_{1Y}(t) \\ \varphi_1(t) \\ u_{2X}(t) \\ u_{2Y}(t) \\ \varphi_2(t) \end{bmatrix}.$$

The force vector acting on the internal nodes 1 and 2 in the global reference system is

$$\mathbf{q}(t) = \begin{bmatrix} F_{1X}(t) \\ F_{1Y}(t) \\ M_1(t) \\ F_{2X}(t) \\ F_{2Y}(t) \\ M_2(t) \end{bmatrix} = \begin{bmatrix} 0 \\ 0 \\ 0 \\ -P/\sqrt{2} \\ P/\sqrt{2} \\ 0 \end{bmatrix} \sin(\omega t) \quad \rightarrow \quad \mathbf{q}_0 = \begin{bmatrix} 0 \\ 0 \\ 0 \\ -P/\sqrt{2} \\ P/\sqrt{2} \\ 0 \end{bmatrix}.$$

The transformations from the local reference systems of beams 12, 13, 24 into the global reference system are given by

$$\mathbf{T}_{12} = \begin{bmatrix} 1 & 0 & 0 \\ 0 & 1 & 0 \\ 0 & 0 & 1 \end{bmatrix}, \quad \mathbf{T}_{13} = \begin{bmatrix} 0 & -1 & 0 \\ 1 & 0 & 0 \\ 0 & 0 & 1 \end{bmatrix}, \quad \mathbf{T}_{24} = \begin{bmatrix} 3/5 & -4/5 & 0 \\ 4/5 & 3/5 & 0 \\ 0 & 0 & 1 \end{bmatrix}.$$

All the three beams are fixed-fixed, and they have the same geometric and material properties, which implies that they have the same *elementary* stiffness and mass matrices in the local systems.

The elementary static stiffness matrix of the beams in the local system is

$$\mathbf{K}_{12}^{\text{loc}} = \mathbf{K}_{13}^{\text{loc}} = \mathbf{K}_{24}^{\text{loc}} = \begin{bmatrix} \frac{EA}{\ell} & 0 & 0 & -\frac{EA}{\ell} & 0 & 0 \\ 0 & \frac{12EI}{\ell^3} & \frac{6EI}{\ell^2} & 0 & -\frac{12EI}{\ell^3} & \frac{6EI}{\ell^2} \\ 0 & \frac{6EI}{\ell^2} & \frac{4EI}{\ell} & 0 & -\frac{6EI}{\ell^2} & \frac{2EI}{\ell} \\ -\frac{EA}{\ell} & 0 & 0 & \frac{EA}{\ell} & 0 & 0 \\ 0 & -\frac{12EI}{\ell^3} & -\frac{6EI}{\ell^2} & 0 & \frac{12EI}{\ell^3} & -\frac{6EI}{\ell^2} \\ 0 & \frac{6EI}{\ell^2} & \frac{2EI}{\ell} & 0 & -\frac{6EI}{\ell^2} & \frac{4EI}{\ell} \end{bmatrix} = \begin{bmatrix} 625000 & 0 & 0 & -625000 & 0 & 0 \\ 0 & 2344 & 9375 & 0 & -2344 & 9375 \\ 0 & 9375 & 50000 & 0 & -9375 & 25000 \\ -625000 & 0 & 0 & 625000 & 0 & 0 \\ 0 & -2344 & -9375 & 0 & 2344 & -9375 \\ 0 & 9375 & 25000 & 0 & -9375 & 50000 \end{bmatrix}.$$

The (exact) elementary dynamic stiffness matrix of the beams in the local system comes from (3.73). The general formula of this matrix is fairly long and complicated. That is one of the drawbacks of using the (exact) dynamic stiffness matrix. Therefore we only provide the reader with the entries of the matrix *evaluated* at the given forcing frequency  $\omega = 40$  rad/s:

$$\hat{\mathbf{K}}_{12}^{\text{loc}}(\omega = 40) = \hat{\mathbf{K}}_{13}^{\text{loc}}(\omega = 40) = \hat{\mathbf{K}}_{24}^{\text{loc}}(\omega = 40) = \begin{bmatrix} -615805 & 0 & 0 & -1406846 & 0 & 0 \\ 0 & -1024410 & -587067 & 0 & -820788 & 613717 \\ 0 & -587067 & -305208 & 0 & -613717 & 458874 \\ -1406846 & 0 & 0 & -615805 & 0 & 0 \\ 0 & -820788 & -613717 & 0 & -1024410 & 587067 \\ 0 & 613717 & 458874 & 0 & 587067 & -305208 \end{bmatrix}.$$

The elementary consistent mass matrix of the all beams is constructed following (3.75):

$$\mathbf{M}_{12}^{\text{loc}} = \mathbf{M}_{13}^{\text{loc}} = \mathbf{M}_{24}^{\text{loc}} = \mu\ell \begin{bmatrix} \frac{1}{3} & 0 & 0 & \frac{1}{6} & 0 & 0 \\ 0 & \frac{13}{35} & \frac{11}{210}\ell & 0 & \frac{9}{70} & -\frac{13}{420}\ell \\ 0 & \frac{11}{210}\ell & \frac{1}{105}\ell^2 & 0 & \frac{13}{420}\ell & -\frac{1}{140}\ell^2 \\ \hline \frac{1}{6} & 0 & 0 & \frac{1}{3} & 0 & 0 \\ 0 & \frac{9}{70} & \frac{13}{420}\ell & 0 & \frac{13}{35} & -\frac{11}{210}\ell \\ 0 & -\frac{13}{420}\ell & -\frac{1}{140}\ell^2 & 0 & -\frac{11}{210}\ell & \frac{1}{105}\ell^2 \end{bmatrix}$$

$$= \begin{bmatrix} 533.3 & 0 & 0 & 266.7 & 0 & 0 \\ 0 & 594.3 & 670.5 & 0 & 205.7 & -396.2 \\ 0 & 670.5 & 975.2 & 0 & 396.2 & -731.4 \\ \hline 266.7 & 0 & 0 & 533.3 & 0 & 0 \\ 0 & 205.7 & 396.2 & 0 & 594.3 & -670.5 \\ 0 & -396.2 & -731.4 & 0 & -670.5 & 975.2 \end{bmatrix}.$$

We also compose the diagonally lumped mass matrix  $\mathbf{M}_{\text{lum}}$ . We directly construct the *total* mass matrix in the global system. Entries 1,1 and 2,2 correspond to the horizontal and vertical translations of node 1. The values of these entries thus the sum of masses of the halves of (the connecting) beams 12 and 13. Entry 3,3 corresponds to the rotation of node 1, thus it is the rotary inertia of the halves of (the connecting) beams 12 and 13. Similarly, entries 4,4 and 5,5 correspond to the translations of node 2, thus they are the sum of masses of the halves of beams 12 and 24. Entry 6,6 is the rotary inertia of the halves of beams 12 and 24. Therefore the total diagonally lumped mass matrix of the structure is

$$\mathbf{M}_{\text{lum}} = \begin{bmatrix} 2 \cdot \mu\ell/2 & 0 & 0 & 0 & 0 & 0 \\ 0 & 2 \cdot \mu\ell/2 & 0 & 0 & 0 & 0 \\ 0 & 0 & 2 \cdot \mu(\ell/2)^3/3 & 0 & 0 & 0 \\ \hline 0 & 0 & 0 & 2 \cdot \mu\ell/2 & 0 & 0 \\ 0 & 0 & 0 & 0 & 2 \cdot \mu\ell/2 & 0 \\ 0 & 0 & 0 & 0 & 0 & 2 \cdot \mu(\ell/2)^3/3 \end{bmatrix}$$

$$= \begin{bmatrix} 1600 & 0 & 0 & 0 & 0 & 0 \\ 0 & 1600 & 0 & 0 & 0 & 0 \\ 0 & 0 & 8533 & 0 & 0 & 0 \\ \hline 0 & 0 & 0 & 1600 & 0 & 0 \\ 0 & 0 & 0 & 0 & 1600 & 0 \\ 0 & 0 & 0 & 0 & 0 & 8533 \end{bmatrix}.$$

Now we compile the total dynamic stiffness matrix, the total static stiffness matrix, and the total consistent mass matrices of the structure. The block structure of the total static stiffness matrix of the frame is

$$\mathbf{K} = \begin{bmatrix} \mathbf{K}_{12}^{\text{glob},11} + \mathbf{K}_{13}^{\text{glob},11} & \mathbf{K}_{12}^{\text{glob},12} \\ \mathbf{K}_{12}^{\text{glob},21} & \mathbf{K}_{12}^{\text{glob},22} + \mathbf{K}_{24}^{\text{glob},22} \end{bmatrix}$$

Here the blocks are transformed from the local to the global system as

$$\mathbf{K}_{13}^{\text{glob},11} = \mathbf{T}_{13} \mathbf{K}_{13}^{\text{loc},11} \mathbf{T}_{13}^T, \quad \mathbf{K}_{24}^{\text{glob},22} = \mathbf{T}_{24} \mathbf{K}_{24}^{\text{loc},22} \mathbf{T}_{24}^T.$$



Blocks

$$\mathbf{K}_{12}^{\text{glob},11} = \mathbf{K}_{12}^{\text{loc},11}, \quad \mathbf{K}_{12}^{\text{glob},22} = \mathbf{K}_{12}^{\text{loc},22}, \quad \mathbf{K}_{12}^{\text{glob},12} = \mathbf{K}_{12}^{\text{glob},12}, \quad \mathbf{K}_{12}^{\text{glob},21} = \mathbf{K}_{12}^{\text{glob},21},$$

since  $\mathbf{T}_{12}$  is the identity matrix. The transformation follows the same procedure in the cases of the consistent mass matrix, and of the dynamic stiffness matrix. We just need to substitute the corresponding blocks of the elementary static stiffness matrix with the elementary consistent or with the elementary dynamic stiffness matrices.

The total stiffness matrix of the structure is

$$\mathbf{K} = \left[ \begin{array}{ccc|ccc} 627344 & 0 & -9375 & -625000 & 0 & 0 \\ 0 & 627344 & 9375 & 0 & -2344 & 9375 \\ -9375 & 9375 & 100000 & 0 & -9375 & 25000 \\ \hline -625000 & 0 & 0 & 851500 & 298875 & -7500 \\ 0 & -2344 & -9375 & 298875 & 403188 & -3750 \\ 0 & 9375 & 25000 & -7500 & -3750 & 100000 \end{array} \right],$$

while the total consistent mass matrix is

$$\mathbf{M} = \left[ \begin{array}{ccc|ccc} 1128 & 0 & -670.5 & 266.7 & 0 & 0 \\ 0 & 1128 & 670.5 & 0 & 205.7 & -396.2 \\ -670.5 & 670.5 & 1950 & 0 & 396.2 & -731.4 \\ \hline 266.7 & 0 & 0 & 1106 & -29.26 & -536.4 \\ 0 & 205.7 & 396.2 & -29.26 & 1150 & -268.2 \\ 0 & -396.2 & -731.4 & -536.4 & -268.2 & 1950 \end{array} \right].$$

The total dynamic stiffness matrix of the structure evaluated at the forcing frequency  $\omega = 40$  rad/s is

$$\hat{\mathbf{K}}(\omega = 40) = \left[ \begin{array}{ccc|ccc} -1640214 & 0 & 587067 & -1406845 & 0 & 0 \\ 0 & -1640214 & -587067 & 0 & -820787 & 613716 \\ 587067 & -587067 & -610415 & 0 & -613716 & 458873 \\ \hline -1406845 & 0 & 0 & -1493116 & 196130 & 469653 \\ 0 & -820787 & -613716 & 196130 & -1787312 & 234826 \\ 0 & 613716 & 458873 & 469653 & 234826 & -610415 \end{array} \right].$$

Approximation of this dynamic stiffness matrix can be obtained by

$$\hat{\mathbf{K}}(\omega) \approx \mathbf{K} - \omega^2 \mathbf{M} = \left[ \begin{array}{ccc|ccc} -1176847 & 0 & 1063387 & -1051667 & 0 & 0 \\ 0 & -1176847 & -1063387 & 0 & -331487 & 643280 \\ 1063387 & -1063387 & -3020762 & 0 & -643280 & 1195286 \\ \hline -1051667 & 0 & 0 & -917582 & 345686 & 850710 \\ 0 & -331487 & -643280 & 345686 & -1436112 & 425355 \\ 0 & 643280 & 1195286 & 850710 & 425355 & -3020762 \end{array} \right].$$

Another, less accurate approximation of this dynamic stiffness matrix uses the diagonally lumped mass matrix:

$$\hat{\mathbf{K}}(\omega) \approx \mathbf{K} - \omega^2 \mathbf{M}_{\text{lum}} = \left[ \begin{array}{ccc|ccc} -1932656 & 0 & -9375 & -625000 & 0 & 0 \\ 0 & -1932656 & 9375 & 0 & -2344 & 9375 \\ -9375 & 9375 & -13553333 & 0 & -9375 & 25000 \\ \hline -625000 & 0 & 0 & -1708500 & 298875 & -7500 \\ 0 & -2344 & -9375 & 298875 & -2156813 & -3750 \\ 0 & 9375 & 25000 & -7500 & -3750 & -13553333 \end{array} \right].$$

(Both approximations are evaluated at the given frequency  $\omega = 40$  rad/s.)

The first natural circular frequency of the structure, according to the exact dynamic stiffness matrix, is  $\omega_{01} = 4.499$  rad/s. In fact, there are infinitely many natural circular frequencies of the structure if we use the

exact dynamic stiffness matrix. (Remember, it contains the dynamic shape functions, which are combinations of trigonometric and hyperbolic functions.) If an approximate approach is used (i.e. we apply the consistent mass matrix, or the diagonally lumped one), then the number of natural circular frequencies of the frame structure equals to the number of total DOF of the model, which is 6 in our example. These natural circular frequencies, and the first few frequencies of the exact model are summarized in the following table.

	$\omega_{0,1}$	$\omega_{0,2}$	$\omega_{0,3}$	$\omega_{0,4}$	$\omega_{0,5}$	$\omega_{0,6}$	$\omega_{0,7}$	...
exact	1.429	4.452	7.138	7.816	7.882	15.14	18.54	...
consistent	1.437	5.320	11.25	19.88	27.16	47.47	–	–
lumped	1.310	2.964	3.825	16.81	19.80	29.87	–	–

**Table 3.1:** The first few natural circular frequencies (in rad/s) of the frame and all the six natural circular frequencies of the approximate models (with the consistent the diagonally lumped mass matrices).

In practice, the approximate model is usually accurate enough if the smallest natural frequency of the applied beam members is larger than the largest circular frequency of the model. The first natural frequency of the fixed-fixed beam members of the studied frame is [11]

$$\omega_{01}^{\text{ffbeam}} = 22.4 \sqrt{\frac{EI}{\mu \ell^4}} = 7.826 \text{ rad/s.}$$

This is far not larger than the largest natural frequency of the approximate models (see Table 3.1). Therefore, we should introduce additional internal nodes, i.e. we should divide the structure into more beam members. We do not do so, just go on with the inaccurate approximation and show what differences appear between the final results of the exact and the approximate models.

The final result, the amplitudes of the translations and rotations of nodes 1 and 2, are computed as

$$\mathbf{u}_{f0} = \hat{\mathbf{K}}^{-1} \mathbf{q}_0, \quad \mathbf{u}_{f0} \approx (\mathbf{K} - \omega^2 \mathbf{M})^{-1} \mathbf{q}_0, \quad \mathbf{u}_{f0} \approx (\mathbf{K} - \omega^2 \mathbf{M}_{\text{lum}})^{-1} \mathbf{q}_0$$

Using the exact dynamic stiffness matrix  $\hat{\mathbf{K}}$ , the amplitudes of the displacements of the nodes are

$$\mathbf{u}_{f0} = \begin{bmatrix} 0.01224 \\ 0.1352 \\ 0.5459 \\ 0.2135 \\ -0.1815 \\ 0.6408 \end{bmatrix}.$$

The application of the consistent mass matrix leads to the result

$$\mathbf{u}_{f0} \approx \begin{bmatrix} 0.06310 \\ -0.02154 \\ 0.04293 \\ -0.02720 \\ -0.07163 \\ -0.005344 \end{bmatrix},$$

while it follows from the usage of the diagonally lumped matrix that

$$\mathbf{u}_{f0} \approx \begin{bmatrix} -0.01345 \\ 0.00003283 \\ 0.00002799 \\ 0.04158 \\ -0.02702 \\ -0.00001546 \end{bmatrix}.$$

## 3.5 Support vibration of MDOF systems

In this section we deal with the support vibration of planar frame structures. Several kinematical forcing of structures comes from the motion of the underlying ground (e.g. earthquakes, ground vibration from underground and road traffic etc.). We follow a similar approach to the one presented in the statical analysis. In the upcoming subsections we analyse the effect of rigid supports on the applied model, the calculation of elastically supported structures, the harmonic support vibration, and the support vibration equal at each supported node.

### 3.5.1 Prescribed motion of DOFs

As a first step, we have to compile the static stiffness matrix  $\mathbf{K}$  the consistent mass matrix  $\mathbf{M}$ , and the vector of external load  $\mathbf{q}(t)$  reduced to the degrees-of-freedom. Here we have to take into account all  $M$  nodes of 3 degrees-of-freedom each. The unconstrained equation of motion is

$$\mathbf{M}\ddot{\mathbf{u}}(t) + \mathbf{K}\mathbf{u}(t) = \mathbf{q}(t). \quad (3.79)$$

The above equation is subjected to the constrains on the prescribed displacements of the supported nodes (prescribed values can be zeros for a rigid support or a time-dependent function for a vibrating support). Please note, that prescribing the displacement of a degree-of-freedom implies that we also prescribe its first and second derivatives with respect to time, i.e. its velocity and acceleration.

With row- and column exchanges in Eq. (3.79) we can construct a special form of it, where the equation of motion of the DOFs with prescribed values are in the last rows, and the displacements of the DOFs with prescribed values are the last entries in vector  $\mathbf{u}(t)$ . The schema of the exchange of one row and column is the same as the one in Eq. (3.45). The same must be done for the mass matrix as well.

Partitioning the matrices and vectors in this reordered form is of the following blocks:

$$\begin{bmatrix} \mathbf{M}^{II} & \mathbf{M}^{Ig} \\ \mathbf{M}^{gI} & \mathbf{M}^{gg} \end{bmatrix} \begin{bmatrix} \ddot{\mathbf{u}}^I(t) \\ \ddot{\mathbf{u}}^g(t) \end{bmatrix} + \begin{bmatrix} \mathbf{K}^{II} & \mathbf{K}^{Ig} \\ \mathbf{K}^{gI} & \mathbf{K}^{gg} \end{bmatrix} \begin{bmatrix} \mathbf{u}^I(t) \\ \mathbf{u}^g(t) \end{bmatrix} = \begin{bmatrix} \mathbf{q}^I(t) \\ \mathbf{q}^g(t) + \mathbf{r}^g(t) \end{bmatrix}. \quad (3.80)$$

Here the vector  $\mathbf{u}^g(t)$  contains the prescribed displacements (typically they are the displacements of the supports, or ground, that is why the subscript  $g$  is for), and the vector  $\mathbf{u}^I(t)$  contains the displacements of the non-supported, internal nodes. The vector  $\mathbf{q}^I(t)$  contains the forces reduced to the internal nodes, and the vector  $\mathbf{q}^g(t)$  contains the forces reduced to the supported nodes. The vector  $\mathbf{r}^g(t)$  contains the reactions in the supports. The second block of equations of (3.80) can be used to calculate the reactions once the unknown displacements of  $\mathbf{u}^I(t)$  and the accelerations of  $\ddot{\mathbf{u}}^I(t)$  are known.

The first block of equations of (3.80) can be written in the form

$$\mathbf{M}^{ii}\ddot{\mathbf{u}}^i(t) + \mathbf{K}^{ii}\mathbf{u}^i(t) = \bar{\mathbf{q}}^i(t), \quad (3.81)$$

which is the matrix-differential equation of the forced, undamped vibration of a MDOF system (see Eq. (3.47)) with the forcing vector:

$$\bar{\mathbf{q}}^i(t) = \mathbf{q}^i(t) - \mathbf{M}^{ig}\ddot{\mathbf{u}}^g(t) - \mathbf{K}^{ig}\mathbf{u}^g(t). \quad (3.82)$$

The solution of the matrix differential equation (3.81) can be obtained by any of the known solution methods.

### Fixed supports as prescribed motion

Some of the supports have prescribed zero valued displacements. The accelerations of those supports are zero as well. These are called fixed supports. The corresponding elements of vectors  $\mathbf{u}^g(t)$  and  $\ddot{\mathbf{u}}^g(t)$  are zero in Eq. (3.82), thus the corresponding columns of matrices  $\mathbf{M}^{ig}$  and  $\mathbf{K}^{ig}$  are cancelled. Non-moving supports creates no vibration of the structure, so it is easier to exclude them from the calculations.

We can follow the strategy, that we make the reduction into the form of Eq. (3.81) in two steps. In the first step, we eliminate only the fixed supports which cause no vibration of the structure. In this step the second and third terms on the right hand side of Eq. (3.82) become zero. In the second step, we eliminate the vibrating supported nodes from the previously reduced system. Here the load vector is modified by the support vibration according to Eq. (3.82).

A rigorous analysis of the above steps makes it possible to create the final matrix equation of motion in one single step. This is illustrated in Figure 3.11, where two degrees-of-freedom have the prescribed nonzero displacements  $u^{g1}(t)$  and  $u^{g2}(t)$  while one degree-of-freedom is fixed to  $u^{g0} = 0$ . The matrix block structure are shown before and after the elimination process in Figure 3.11 (a) and (b), respectively.

### Elastically supported nodes

In Subsubsection 3.1.8 we have seen, that in the fixed support model a massless supporting node is used in order to model the elastic support. The prescribed motion of a support can be applied on the supporting node. Then we can eliminate the supporting node, while its motion results in an excess load given by the last two terms of Eq. (3.82).

## 3.5.2 Harmonic support vibration

Let us analyse the situation when every supported node vibrates harmonically with the same circular frequency  $\omega$ . In this case the kinematical load vector  $\mathbf{u}^g(t)$  in Eq. (3.82) can be written as

$$\mathbf{u}^g(t) = \mathbf{u}_0^g \sin(\omega t),$$

and its second derivative with respect to time is

$$\ddot{\mathbf{u}}^g(t) = \mathbf{u}_0^g(-\omega^2) \sin(\omega t).$$

If the vector of nodal loads  $\mathbf{q}(t)$  can be neglected, then Eq. (3.81) leads to

$$\mathbf{M}^{ii} \ddot{\mathbf{u}}^i(t) + \mathbf{K}^{ii} \mathbf{u}^i(t) = -(\mathbf{K}^{ig} - \omega^2 \mathbf{M}^{ig}) \mathbf{u}_0^g \sin(\omega t). \quad (3.83)$$

(a) The block structure of the matrix equation of motion with fixed support  $u^{g_0} = 0$  and vibrating supports  $u^{g_1}(t)$  and  $u^{g_2}(t)$

$$\begin{aligned}
 & \begin{bmatrix} \mathbf{M}^{AA} & \mathbf{m}^{Ag_1} & \mathbf{M}^{AB} & \mathbf{m}^{Ag_0} & \mathbf{M}^{AC} & \mathbf{m}^{Ag_2} & \mathbf{M}^{AD} \\ \mathbf{m}^{g_1A} & m^{g_1g_1} & \mathbf{m}^{g_1B} & m^{g_1g_0} & \mathbf{m}^{g_1C} & m^{g_1g_2} & \mathbf{m}^{g_1D} \\ \mathbf{M}^{BA} & \mathbf{m}^{Bg_1} & \mathbf{M}^{BB} & \mathbf{m}^{Bg_0} & \mathbf{M}^{BC} & \mathbf{m}^{Bg_2} & \mathbf{M}^{BD} \\ \mathbf{m}^{g_0A} & m^{g_0g_1} & \mathbf{m}^{g_0B} & m^{g_0g_0} & \mathbf{m}^{g_0C} & m^{g_0g_2} & \mathbf{m}^{g_0D} \\ \mathbf{M}^{CA} & \mathbf{m}^{Cg_1} & \mathbf{M}^{CB} & \mathbf{m}^{Cg_0} & \mathbf{M}^{CC} & \mathbf{m}^{Cg_2} & \mathbf{M}^{CD} \\ \mathbf{m}^{g_2A} & m^{g_2g_1} & \mathbf{m}^{g_2B} & m^{g_2g_0} & \mathbf{m}^{g_2C} & m^{g_2g_2} & \mathbf{m}^{g_2D} \\ \mathbf{M}^{DA} & \mathbf{m}^{Dg_1} & \mathbf{M}^{DB} & \mathbf{m}^{Dg_0} & \mathbf{M}^{DC} & \mathbf{m}^{Dg_2} & \mathbf{M}^{DD} \end{bmatrix} \begin{bmatrix} \ddot{\mathbf{u}}^A(t) \\ \ddot{u}^{g_1}(t) \\ \ddot{\mathbf{u}}^B(t) \\ \ddot{u}^{g_0} \\ \ddot{\mathbf{u}}^C(t) \\ \ddot{u}^{g_2}(t) \\ \ddot{\mathbf{u}}^D(t) \end{bmatrix} \\
 + & \begin{bmatrix} \mathbf{K}^{AA} & \mathbf{k}^{Ag_1} & \mathbf{K}^{AB} & \mathbf{k}^{Ag_0} & \mathbf{K}^{AC} & \mathbf{k}^{Ag_2} & \mathbf{K}^{AD} \\ \mathbf{k}^{g_1A} & k^{g_1g_1} & \mathbf{k}^{g_1B} & k^{g_1g_0} & \mathbf{k}^{g_1C} & k^{g_1g_2} & \mathbf{k}^{g_1D} \\ \mathbf{K}^{BA} & \mathbf{k}^{Bg_1} & \mathbf{K}^{BB} & \mathbf{k}^{Bg_0} & \mathbf{K}^{BC} & \mathbf{k}^{Bg_2} & \mathbf{K}^{BD} \\ \mathbf{k}^{g_0A} & k^{g_0g_1} & \mathbf{k}^{g_0B} & k^{g_0g_0} & \mathbf{k}^{g_0C} & k^{g_0g_2} & \mathbf{k}^{g_0D} \\ \mathbf{K}^{CA} & \mathbf{k}^{Cg_1} & \mathbf{K}^{CB} & \mathbf{k}^{Cg_0} & \mathbf{K}^{CC} & \mathbf{k}^{Cg_2} & \mathbf{K}^{CD} \\ \mathbf{k}^{g_2A} & k^{g_2g_1} & \mathbf{k}^{g_2B} & k^{g_2g_0} & \mathbf{k}^{g_2C} & k^{g_2g_2} & \mathbf{k}^{g_2D} \\ \mathbf{K}^{DA} & \mathbf{k}^{Dg_1} & \mathbf{K}^{DB} & \mathbf{k}^{Dg_0} & \mathbf{K}^{DC} & \mathbf{k}^{Dg_2} & \mathbf{K}^{DD} \end{bmatrix} \begin{bmatrix} \mathbf{u}^A(t) \\ u^{g_1}(t) \\ \mathbf{u}^B(t) \\ u^{g_0} \\ \mathbf{u}^C(t) \\ u^{g_2}(t) \\ \mathbf{u}^D(t) \end{bmatrix} = \begin{bmatrix} \mathbf{q}^A(t) \\ q_1^g(t) + r_1^g(t) \\ \mathbf{q}^B(t) \\ q_0^g(t) + r_0^g(t) \\ \mathbf{q}^C(t) \\ q_2^g(t) + r_2^g(t) \\ \mathbf{q}^D(t) \end{bmatrix}
 \end{aligned}$$

(b) The block structure of the reduced matrix equation after the eliminating prescribed displacements  $u^{g_0}$ ,  $u^{g_1}$ , and  $u^{g_2}$

$$\begin{aligned}
 & \begin{bmatrix} \mathbf{M}^{AA} & \mathbf{M}^{AB} & \mathbf{M}^{AC} & \mathbf{M}^{AD} \\ \mathbf{M}^{BA} & \mathbf{M}^{BB} & \mathbf{M}^{BC} & \mathbf{M}^{BD} \\ \mathbf{M}^{CA} & \mathbf{M}^{CB} & \mathbf{M}^{CC} & \mathbf{M}^{CD} \\ \mathbf{M}^{DA} & \mathbf{M}^{DB} & \mathbf{M}^{DC} & \mathbf{M}^{DD} \end{bmatrix} \begin{bmatrix} \ddot{\mathbf{u}}^A(t) \\ \ddot{\mathbf{u}}^B(t) \\ \ddot{\mathbf{u}}^C(t) \\ \ddot{\mathbf{u}}^D(t) \end{bmatrix} + \begin{bmatrix} \mathbf{K}^{AA} & \mathbf{K}^{AB} & \mathbf{K}^{AC} & \mathbf{K}^{AD} \\ \mathbf{K}^{BA} & \mathbf{K}^{BB} & \mathbf{K}^{BC} & \mathbf{K}^{BD} \\ \mathbf{K}^{CA} & \mathbf{K}^{CB} & \mathbf{K}^{CC} & \mathbf{K}^{CD} \\ \mathbf{K}^{DA} & \mathbf{K}^{DB} & \mathbf{K}^{DC} & \mathbf{K}^{DD} \end{bmatrix} \begin{bmatrix} \mathbf{u}^A(t) \\ \mathbf{u}^B(t) \\ \mathbf{u}^C(t) \\ \mathbf{u}^D(t) \end{bmatrix} \\
 = & \begin{bmatrix} \mathbf{q}^A(t) \\ \mathbf{q}^B(t) \\ \mathbf{q}^C(t) \\ \mathbf{q}^D(t) \end{bmatrix} - \begin{bmatrix} \mathbf{m}^{Ag_1} & \mathbf{m}^{Ag_2} \\ \mathbf{m}^{Bg_1} & \mathbf{m}^{Bg_2} \\ \mathbf{m}^{Cg_1} & \mathbf{m}^{Cg_2} \\ \mathbf{m}^{Dg_1} & \mathbf{m}^{Dg_2} \end{bmatrix} \begin{bmatrix} \ddot{u}^{g_1}(t) \\ \ddot{u}^{g_2}(t) \end{bmatrix} - \begin{bmatrix} \mathbf{k}^{Ag_1} & \mathbf{k}^{Ag_2} \\ \mathbf{k}^{Bg_1} & \mathbf{k}^{Bg_2} \\ \mathbf{k}^{Cg_1} & \mathbf{k}^{Cg_2} \\ \mathbf{k}^{Dg_1} & \mathbf{k}^{Dg_2} \end{bmatrix} \begin{bmatrix} u^{g_1}(t) \\ u^{g_2}(t) \end{bmatrix}
 \end{aligned}$$

**Figure 3.11:** The change of the block structure of the matrix equation of motion during the elimination of the prescribed motion of supports.

### 3.5.3 Support motion due to earthquake

Earthquakes induce sudden changes in the shape of the earth crust. An earthquake causes discontinuity in the displacements. This discontinuity travels in the continuum with the velocity of the travelling waves. In contrast to the travelling waves shown in Subsection 2.1.1, the waves in the solid continuum have a decreasing amplitude due to their propagation along an inflating sphere. Hence the amplitude of the ground motion is affected by the distance from the location of the earthquake, too. The discontinuities travel as pressure and as shear waves. Pressure waves travel faster in the solid materials than shear waves.

In a typical engineering structure on a typical solid ground, distances between the supported nodes are small enough. Therefore the differences between the amplitudes of the support motions, and the phase differences are often neglected. So, the vector of prescribed displacements can be written as

$$\mathbf{u}^g(t) = u^g(t)\mathbf{r}^g,$$

where  $\mathbf{r}_g$  is an index vector selecting the vibrating supported nodes. Here we assume that each support vibrates in the same direction. The acceleration of the supported nodes is

$$\ddot{\mathbf{u}}^g(t) = \ddot{u}^g(t)\mathbf{r}^g.$$

The matrix equation of motion is now

$$\mathbf{M}^{ii}\ddot{\mathbf{u}}^i(t) + \mathbf{K}^{ii}\mathbf{u}^i(t) = -\mathbf{M}^{ig}\ddot{u}^g(t)\mathbf{r}^g - \mathbf{K}^{ig}u^g(t)\mathbf{r}^g. \quad (3.84)$$

We remind the reader, that the unknowns in Eq. (3.84) are displacements. These displacements are the components of vector  $\mathbf{u}^i(t)$  in the global reference system. The displacements can be written as the sum of the displacements of the supports in the direction of the support vibration ( $u^g(t)$ ) and the excess elastic deformation ( $u_{el}(t)$ ):

$$\mathbf{u}^i(t) = \mathbf{u}_{el}(t) + u^g(t)\mathbf{r}^i. \quad (3.85)$$

The *influence vector*  $\mathbf{r}^i$  in the above equation describes the displacements of the internal degrees-of-freedom if we apply a unit displacement in the direction of the support vibration. With these definitions vectors  $\mathbf{r}^i$  and  $\mathbf{r}^g$  represent a rigid body translation of the whole structure. We refer to this rigid body translation of the whole, unconstrained structure with the *total influence vector*  $\mathbf{r}$ , for short:

$$\mathbf{r} = \begin{bmatrix} \mathbf{r}^i \\ \mathbf{r}^g \end{bmatrix}.$$

We substitute the displacements (3.85) and their derivatives into Eq. (3.84) and rearrange it into

$$\mathbf{M}^{ii}\ddot{\mathbf{u}}_{el}(t) + \mathbf{K}^{ii}\mathbf{u}_{el}(t) = -\mathbf{M}^{ig}\ddot{u}^g(t)\mathbf{r}^g - \mathbf{M}^{ii}\ddot{u}^g(t)\mathbf{r}^i - \mathbf{K}^{ig}u^g(t)\mathbf{r}^g - \mathbf{K}^{ii}u^g(t)\mathbf{r}^i,$$

which is written in a block form

$$\mathbf{M}^{ii}\ddot{\mathbf{u}}_{el}(t) + \mathbf{K}^{ii}\mathbf{u}_{el}(t) = -\ddot{u}^g(t) \begin{bmatrix} \mathbf{M}^{ii} & \mathbf{M}^{ig} \end{bmatrix} \begin{bmatrix} \mathbf{r}^i \\ \mathbf{r}^g \end{bmatrix} - u^g(t) \begin{bmatrix} \mathbf{K}^{ii} & \mathbf{K}^{ig} \end{bmatrix} \begin{bmatrix} \mathbf{r}^i \\ \mathbf{r}^g \end{bmatrix}. \quad (3.86)$$

We already observed, that vectors  $\mathbf{r}^i$  and  $\mathbf{r}^g$  represent a rigid body translation of the whole structure. A rigid body motion causes no internal forces in the structure, so the last term in Eq.(3.86) is zero independently of the support vibration  $u^g(t)$ :

$$\left[ \mathbf{K}^{ii} \mid \mathbf{K}^{ig} \right] \begin{bmatrix} \mathbf{r}^i \\ \mathbf{r}^g \end{bmatrix} = \mathbf{0}.$$

Let us define the vector of forced masses  $\mathbf{m}^g$  as

$$\mathbf{m}^g = \left[ \mathbf{M}^{ii} \mid \mathbf{M}^{ig} \right] \begin{bmatrix} \mathbf{r}_i \\ \mathbf{r}_g \end{bmatrix} = \mathbf{M}^i \mathbf{r}. \quad (3.87)$$

The final matrix equation of motion in the case of earthquake is then:

$$\mathbf{M}^{ii} \ddot{\mathbf{u}}_{el}(t) + \mathbf{K}^{ii} \mathbf{u}_{el}(t) = -\ddot{u}^g(t) \mathbf{m}^g. \quad (3.88)$$

## 3.6 Real modal analysis, internal forces

In the previous section we presented how to compile the system of differential equations of an undamped planar frame structure. The elastic properties of the beams were incorporated into the stiffness matrix  $\mathbf{K}$ , while the loads were reduced to the nodal load vector  $\mathbf{q}(t)$ . The masses of the structural elements were collected into the consistent mass matrix  $\mathbf{M}$ . With these components we can write the differential equations of motion in the matrix form:

$$\mathbf{M} \ddot{\mathbf{u}}(t) + \mathbf{K} \mathbf{u}(t) = \mathbf{q}(t). \quad (3.89)$$

In this section we show how to solve the above equation in the case of an arbitrary load function  $\mathbf{q}(t)$ , and how the internal forces of the structure can be calculated.

### 3.6.1 Solution of the MDOF system with real modal analysis

We have seen in Subsection 1.3.3 that a system of differential equations like Eq. (3.89) can be solved with modal analysis in case of a harmonic load vector  $\mathbf{q}(t) = \mathbf{q}_0 \sin(\omega t)$ . There, the forced vibration of the MDOF system was reduced to vibration of independent SDOF oscillators, using the eigenvectors  $\mathbf{u}_i$  normalized to the mass matrix. A similar approach can be used for the case of general forcing, but then the answer of each SDOF oscillator is calculated using the Duhamel's integral (1.26).

The first step is the calculation of the natural circular frequencies  $\omega_{0j}$  and the corresponding modal shape vectors  $\mathbf{u}_j$  normalized to the mass matrix. These are the unique solutions of the generalized eigenvalue problem

$$(\mathbf{K} - \omega_0^2 \mathbf{M}) \mathbf{u} = \mathbf{0},$$

which is derived from the complementary equation of Eq. (3.89). (See Subsection 1.3.2 for details.)

The second step is to write the particular solution of the inhomogeneous matrix differential equation (3.89) as a linear combination of the normalized eigenvectors:

$$\mathbf{u}_f(t) = \sum_{j=1}^N \mathbf{u}_j y_j(t). \quad (3.90)$$

We collect the eigenvectors into the *modal matrix*  $\mathbf{U}$  and the modal displacements into the vector  $\mathbf{y}(t)$ :

$$\mathbf{U} = [\mathbf{u}_1 \quad \mathbf{u}_2 \quad \dots \quad \mathbf{u}_N], \quad \mathbf{y}^T(t) = [y_1(t) \quad y_2(t) \quad \dots \quad y_N(t)], \quad (3.91)$$

so Eq. (3.90) can be written in the form:

$$\mathbf{u}_f(t) = \mathbf{U}\mathbf{y}(t). \quad (3.92)$$

We substitute the particular solution (3.92) into Eq. (3.89) and multiply both sides from the left by the transpose of the modal matrix ( $\mathbf{U}^T$ ):

$$\mathbf{U}^T \mathbf{M} \mathbf{U} \ddot{\mathbf{y}}(t) + \mathbf{U}^T \mathbf{K} \mathbf{U} \mathbf{y}(t) = \mathbf{U}^T \mathbf{q}(t). \quad (3.93)$$

(Here we used the fact, that the eigenvectors, and so the modal matrix  $\mathbf{U}$  are independent of time, hence the derivative of  $\mathbf{u}(t)$  depends only on the derivative of  $\mathbf{y}(t)$ :  $\ddot{\mathbf{u}}(t) = \mathbf{U} \ddot{\mathbf{y}}(t)$ .)

The orthogonality of the eigenvectors on the mass and the stiffness matrices (see Eqns. (1.45), (1.46)) implies that  $\mathbf{U}^T \mathbf{M} \mathbf{U}$  and  $\mathbf{U}^T \mathbf{K} \mathbf{U}$  are diagonal matrices. Moreover, the matrix  $\mathbf{U}^T \mathbf{M} \mathbf{U}$  is a unit matrix, while the matrix  $\mathbf{U}^T \mathbf{K} \mathbf{U}$  contains the squares of the natural circular frequencies of the structure in its main diagonal (see Eq. (1.41)):

$$\mathbf{U}^T \mathbf{M} \mathbf{U} = \mathbf{I}, \quad \text{and} \quad \mathbf{U}^T \mathbf{K} \mathbf{U} = \langle \omega_{01}^2 \quad \omega_{02}^2 \quad \dots \quad \omega_{0N}^2 \rangle = \boldsymbol{\Omega}^2. \quad (3.94)$$

The matrix  $\boldsymbol{\Omega}$  is called the *spectral matrix*. Now we can write Eq. (3.93) as:

$$\ddot{\mathbf{y}}(t) + \boldsymbol{\Omega}^2 \mathbf{y}(t) = \mathbf{f}(t), \quad (3.95)$$

where  $\mathbf{f}(t)$  is the vector of modal forcing. Its  $j$ th entry is

$$f_j(t) = \mathbf{u}_j^T \mathbf{q}(t). \quad (3.96)$$

Due to the diagonal structure of the spectral matrix  $\boldsymbol{\Omega}^2$ , the system of differential equations (3.89) falls apart into  $N = 3M$  independent differential equations of SDOF oscillators in Eq. (3.95). The differential equation of the  $j$ th mode is:

$$\ddot{y}_j(t) + \omega_{0j}^2 y_j(t) = f_j(t). \quad (3.97)$$

The above ODE is an undamped version of Eq. (1.22) with  $m = 1$ ,  $c = 0$ , and  $k = \omega_{0j}^2$ , so we can write its solution with a Duhamel's integral:

$$y_j(t) = \int_0^t \frac{f_j(\tau)}{\omega_0} \sin(\omega_0(t - \tau)) \, d\tau. \quad (3.98)$$



This equality can be used in Eq. (3.90) with the nodal load (3.96):

$$\mathbf{u}_f(t) = \sum_{j=1}^N \mathbf{u}_j \int_0^t \frac{\mathbf{u}_j^T \mathbf{q}(\tau)}{\omega_{0j}} \sin(\omega_{0j}(t - \tau)) d\tau. \quad (3.99)$$

One can see in the formula (3.99), that the vibration of each mode is divided by the corresponding natural circular frequency. It results in a decrease of the effect of the higher modal shapes in the final sum, just like we had in the case of the harmonic excitation of MDOF systems (1.60).

**Problem 3.6.1** (Undamped planar frame with an impulse load). Let us analyse the structure already shown in Problem 3.4.1. The forcing is an impulse load acting on the first node in the horizontal direction at  $t = 0$ . We solve the problem with modal analysis.

**Solution.** We do not repeat the calculation of the system matrices, the details are in Problem 3.4.1. The total stiffness matrix is

$$\mathbf{K} = \begin{bmatrix} 627343.75 & 0 & -9375 & -625000 & 0 & 0 \\ 0 & 627343.75 & 9375 & 0 & -2343.75 & 9375 \\ -9375 & 9375 & 100000 & 0 & -9375 & 25000 \\ -625000 & 0 & 0 & 851500 & 298875 & -7500 \\ 0 & -2343.75 & -9375 & 298875 & 403187.5 & -3750 \\ 0 & 9375 & 25000 & -7500 & -3750 & 100000 \end{bmatrix},$$

and the total consistent mass matrix is

$$\mathbf{M} = \begin{bmatrix} 1128 & 0 & -670.5 & 266.7 & 0 & 0 \\ 0 & 1128 & 670.5 & 0 & 205.7 & -396.2 \\ -670.5 & 670.5 & 1950 & 0 & 396.2 & -731.4 \\ 266.7 & 0 & 0 & 1106 & -29.26 & -536.4 \\ 0 & 205.7 & 396.2 & -29.26 & 1150 & -268.2 \\ 0 & -396.2 & -731.4 & -536.4 & -268.2 & 1950 \end{bmatrix}.$$

The force vector is an impulse on the first node in the horizontal direction at time instant  $t = 0$

$$\mathbf{q}(t) = \begin{bmatrix} 1000 \\ 0 \\ 0 \\ 0 \\ 0 \\ 0 \end{bmatrix} \delta(t) = \mathbf{q}_0 \delta(t),$$

where  $\delta(t)$  is the Dirac delta function (2.74).

Solution of the generalized eigenvalue problem  $(\mathbf{K} - \omega_0^2 \mathbf{M}) \mathbf{u} = \mathbf{0}$  results in the following natural circular frequencies and corresponding (mass-normalized) modal shape vectors:

$$\begin{aligned} \omega_{01} &= 1.4365 \text{ rad/s}, & \mathbf{u}_1 &= [0.01706, -0.00006692, -0.0001327, 0.01704, -0.01271, 0.0007558]^T \\ \omega_{02} &= 5.3204 \text{ rad/s}, & \mathbf{u}_2 &= [-0.003077, -0.0006746, -0.01308, -0.003095, 0.001616, 0.01405]^T \\ \omega_{03} &= 11.253 \text{ rad/s}, & \mathbf{u}_3 &= [0.008010, 0.0006601, 0.02370, 0.008609, -0.007061, 0.02132]^T \\ \omega_{04} &= 19.882 \text{ rad/s}, & \mathbf{u}_4 &= [-0.01428, -0.005737, -0.0001224, -0.003592, -0.02463, -0.006325]^T \\ \omega_{05} &= 27.163 \text{ rad/s}, & \mathbf{u}_5 &= [0.003505, -0.03264, 0.01145, 0.005892, 0.007928, 0.0003340]^T \\ \omega_{06} &= 47.469 \text{ rad/s}, & \mathbf{u}_6 &= [0.02727, -0.01069, 0.01284, -0.02683, -0.009150, -0.006025]^T \end{aligned}$$

We can calculate the time-dependent part of integral Eq. (3.99) for every mode:

$$\int_0^t \delta(\tau) \sin(\omega_{0j}(t - \tau)) \, d\tau = \sin(\omega_{0j}t).$$

We have to calculate the modal participation factor  $p_j = \mathbf{u}_j^T \mathbf{q}_0 / \omega_{0j}$  for each node. The results are summarized in Table 3.2. It can be seen that the first mode has the biggest participation in the motion.

$j$	1	2	3	4	5	6
$\omega_{0j}$	1.4365	5.3204	11.253	19.882	27.163	47.469
$\mathbf{u}_j^T \mathbf{q}_0$	17.056	-3.0770	8.0102	-14.277	3.5051	27.266
$p_j = \mathbf{u}_j^T \mathbf{q}_0 / \omega_{0j}$	11.873	-0.5783	0.7119	-0.7181	0.1290	0.5744

**Table 3.2:** The first six natural circular frequencies of the frame, the projections of the load vector to the modal shape vectors, and the modal participation factors

Finally, the steady-state vibration of the structure caused by the impulse at  $t = 0$  is

$$\mathbf{u}_f(t) = \sum_{j=1}^N \mathbf{u}_j p_j \sin(\omega_{0j}t).$$

### 3.6.2 Calculation of internal forces

In the matrix displacement method the unknowns of our dynamical equations are the displacements (translations and rotations) of the nodes as the function of time. However, in structural engineering the magnitudes of internal forces are in interest usually. We have seen that the displacements can be calculated by the serial application of modal analysis and the Duhamel's integral.

From the global displacement vector  $\mathbf{u}_f(t)$  we can collect the displacements of the end nodes of any beam member. If we denote the  $i$ th and  $j$ th blocks of the displacement vector  $\mathbf{u}_f(t)$  by  $\mathbf{u}_{f,i}^{\text{glob}}(t)$  and  $\mathbf{u}_{f,j}^{\text{glob}}(t)$ , respectively, then the displacement vector of beam  $ij$  is

$$\mathbf{u}_{f,ij}^{\text{glob}}(t) = \begin{bmatrix} \mathbf{u}_{f,i}^{\text{glob}}(t) \\ \mathbf{u}_{f,j}^{\text{glob}}(t) \end{bmatrix}.$$

The above displacement vector consists of the displacements of the DOFs of beam  $ij$ . In order to calculate the internal forces in a beam, it is recommended to transform the displacements from the global reference system  $XYZ$  to the local reference system  $xyz$  using the transformation matrices  $\mathbf{T}_{ij}^T$  and  $\bar{\mathbf{T}}_{ij}^T$  introduced in 3.1:

$$\mathbf{u}_{f,ij}^{\text{loc}}(t) = \bar{\mathbf{T}}_{ij}^T \mathbf{u}_{f,ij}^{\text{glob}}(t) = \begin{bmatrix} \mathbf{T}_{ij}^T \mathbf{u}_{f,i}^{\text{glob}}(t) \\ \mathbf{T}_{ij}^T \mathbf{u}_{f,j}^{\text{glob}}(t) \end{bmatrix}.$$

In a static analysis one has to multiply the displacement vector by the stiffness matrix to obtain the nodal forces. These nodal forces are directly related to the end-of-beam internal

forces:

$$\mathbf{K}_{ij}^{\text{loc}} \mathbf{u}_{ij}^{\text{loc}} = \begin{bmatrix} \frac{EA}{\ell} & 0 & 0 & -\frac{EA}{\ell} & 0 & 0 \\ 0 & \frac{12EI}{\ell^3} & \frac{6EI}{\ell^2} & 0 & -\frac{12EI}{\ell^3} & \frac{6EI}{\ell^2} \\ 0 & \frac{6EI}{\ell^2} & \frac{4EI}{\ell} & 0 & -\frac{6EI}{\ell^2} & \frac{2EI}{\ell} \\ -\frac{EA}{\ell} & 0 & 0 & \frac{EA}{\ell} & 0 & 0 \\ 0 & -\frac{12EI}{\ell^3} & -\frac{6EI}{\ell^2} & 0 & \frac{12EI}{\ell^3} & -\frac{6EI}{\ell^2} \\ 0 & \frac{6EI}{\ell^2} & \frac{2EI}{\ell} & 0 & -\frac{6EI}{\ell^2} & \frac{4EI}{\ell} \end{bmatrix} \begin{bmatrix} u_{ix}^{\text{loc}} \\ u_{iy}^{\text{loc}} \\ \varphi_{iz} \\ u_{jx}^{\text{loc}} \\ u_{jy}^{\text{loc}} \\ \varphi_{jz} \end{bmatrix} = \begin{bmatrix} -N_i \\ -V_i \\ +M_i \\ +N_j \\ +V_j \\ -M_j \end{bmatrix}. \quad (3.100)$$

The internal forces along the rod are calculated from their end values and the distributed load along the beam. For further details see [8].

In a dynamical analysis of harmonically excited MDOF systems we have seen that the elementary mass matrix depends on the circular frequency of the harmonic excitation. That results in a frequency-dependent dynamic stiffness matrix  $\hat{\mathbf{K}}(\omega) = \mathbf{K} - \omega^2 \hat{\mathbf{M}}(\omega)$ . If the load vector  $\mathbf{q}(t)$  is not harmonic, i.e. there is no fixed value of  $\omega$ , then we cannot use a dynamic stiffness matrix of the above form. If we want to use the advantages of the finite DOF model, then we have to make some approximations.

There is no acceptable reason why to use any specific circular frequency  $\omega$ , so, even if we calculate the displacements with the consistent mass matrix of the structure, the approximate dynamic stiffness matrix  $\hat{\mathbf{K}}(\omega) \approx \mathbf{K} - \omega^2 \mathbf{M}$  cannot be used for the calculation of the internal forces. The only thing we can do is to use the approximation  $\hat{\mathbf{K}} \approx \mathbf{K}$ , i.e. we apply a quasi-static analysis for the calculation of the internal forces.<sup>3</sup>

To decrease the error arising from the above approximation, we have to use shorter beam members (more nodes, or a finer mesh in a finite element model). The effect of shorter beams is twofold.

- The stiffness matrix of a shorter member contains larger entries, generally speaking. From the formula (3.28) one can see that the entries of the matrix are inversely proportional to the first-to-third power of the length of the beam member.
- The mass matrix of a shorter member contains smaller entries, in general. Either using the frequency-dependent mass matrix (3.72), or the consistent mass matrix (3.74), each entry of these matrices is proportional to the first-to-third power of the length of the member.

The above statements imply that the difference between the dynamic stiffness matrix  $\hat{\mathbf{K}}$  and the applied static stiffness matrix  $\mathbf{K}$  decreases with the decrease of the member size.

We have to call the attention of the reader to the fact that the smaller the beams are, the more nodal points there are, resulting in more total DOF of the system. Thus, the solution of the generalized eigenvalue problem demands more computational capacity *in exchange* for the higher accuracy.

<sup>3</sup>If we follow a finite element approach, and calculate the internal forces from the strains of the cross-sections, which are obtained from the displacement functions approximated by the static shape functions  $\mathbf{N}(x)$ , then we still have the same problem, because without a circular frequency we cannot use the dynamic shape functions  $\hat{\mathbf{N}}(x)$  only the static shape functions  $\mathbf{N}(x)$ .

### Internal forces with the modal analysis

In the structural analysis we do not really need the internal forces at all time instant, usually we are interested in their extreme values. Using the formula (3.99) we can calculate the  $j$ th modal component of the structural response

$$y_{f,j}(t) = \int_0^t \frac{\mathbf{u}_j^T \mathbf{q}(\tau)}{\omega_{0j}} \sin(\omega_{0j}(t - \tau)) d\tau,$$

and its maximum in a given time interval, which we will denote by  $y_{j,max}$ .

The end-of-beam internal forces can be calculated from the displacements of the end nodes of any given beam. One have to transform the end-of-beam displacements into the local reference system, and then use the local displacements in Eq. (3.100). The mode shape vector  $\mathbf{u}_j$  contains the displacements of each node in the vibration with the  $j$ th natural circular frequency. We have to calculate the end-of-beam internal forces from the displacement vector  $\mathbf{u}_j$  with the above method. We denote the internal force in question by  $C_j$ , where  $j$  represents the  $j$ th mode, and  $C$  can be any of  $N_i, V_i, M_i, N_j, V_j, M_j$  in Eq. (3.100), or any internal force in any other cross-section.

During the forced vibration the maximal modal internal force in the  $j$ th mode will be the product of  $C_j$  from the modal shape and  $y_{j,max}$  from the modal load

$$C_{j,max} = C_j y_{j,max}.$$

The question arises, how should we sum up the maximal modal internal forces. We can take the *sum of absolute values* (ABSSUM):

$$C_{max} = \sum_{j=1}^N |C_{j,max}|. \quad (3.101)$$

This is on the safe side, it is very unlikely, that each maximum occurs at the same time.

If the natural circular frequencies are separated, we can take the *square root of the sum of squares* (SRSS)

$$C_{max} = \sqrt{\sum_{j=1}^N C_{j,max}^2}. \quad (3.102)$$

or we can make an emphasis on the first mode, because it is always the most important:

$$C_{max} = C_{1,max} + \sqrt{\sum_{j=2}^N C_{j,max}^2}.$$

The root square of the sum of squares can be written in matrix form:

$$C_{max} = \sqrt{\mathbf{C}_{max}^T \mathbf{I} \mathbf{C}_{max}}. \quad (3.103)$$

with the vector of maximal modal internal forces

$$\mathbf{C}_{max}^T = [ C_{1,max} \quad C_{2,max} \quad \dots \quad C_{N,max} ].$$

If there is a  $\xi$  damping in the structure, the modes are coupled. In that case one can use the *complete quadratic combination rule* (CQC)

$$C_{max} = \sqrt{\mathbf{C}_{max}^T \rho \mathbf{C}_{max}}, \quad (3.104)$$

where the correlation matrix  $\rho$  represents the coupling between the modes. Its entries are calculated by minimizing the error between the calculated responses of the structure to a random forcing with broad spectrum (*white noise*) obtained by numerical integration and by modal analysis. The entries in the correlation matrix are

$$\rho_{ij} = \frac{8\xi^2 \left(1 + \frac{\omega_{0i}}{\omega_{0j}}\right) \left(\frac{\omega_{0i}}{\omega_{0j}}\right)^{3/2}}{\left(1 - \left(\frac{\omega_{0i}}{\omega_{0j}}\right)^2\right)^2 + 4\xi^2 \left(1 + \frac{\omega_{0i}}{\omega_{0j}}\right)^2}.$$

The natural circular frequencies are well separated, when the smallest relative difference between any two frequencies is more than 10%. In an undamped system  $\rho = \mathbf{I}$ .

### 3.7 Partial solution of the generalized eigenvalue problem

We have seen in many examples about the forced vibration of MDOF systems that higher modes play a less significant role in the dynamics of the structure. This statement holds only if the natural circular frequencies of higher modes are sufficiently far from the circular frequency of the forcing. Otherwise, we have to take care of the state of resonance.

It is enough to have a look at Eqs. (1.60), (2.73), (2.76), (3.99) to realize that the natural circular frequency appears in the denominator in each formula even on higher powers, depending on the type of forcing.

Discretization of continuous structures into a finer mesh (more nodes) leads to more DOFs and, consequently, more natural circular frequencies. The more nodes we introduce, the better approximations we get for the lower modes. But the accuracy of the higher frequencies is poor. The application of the higher, inaccurate frequencies is therefore unnecessary, and pointless.

#### Reduced system of modal shape vectors

If we do not want to use the higher modes in our approximate calculations, then there is no use to calculate them at all while solving the generalized eigenvalue problem. In this case we speak about a partial solution of the generalized eigenvalue problem. For large system we do not follow the classical way of calculating the natural frequencies, i.e. we do not expand the determinant of the matrix  $\mathbf{K} - \omega_0^2 \mathbf{M}$ , because it would be numerically too expensive. Fortunately, there are existing numerical methods capable to calculate the lowest eigenvalues of the problem and the corresponding eigenvectors. We can implement one of these procedures to obtain the first  $n$  natural circular frequencies ( $\omega_{0j}$ ,  $j = 1, \dots, n$ ) and the first  $n$  modal shape vector normalized to the mass matrix ( $\mathbf{u}_j$ ,  $j = 1, \dots, n$ ). Similarly to Eq. (3.91), we introduce the *reduced modal matrix*  $\tilde{\mathbf{U}}$  as

$$\tilde{\mathbf{U}} = [\mathbf{u}_1 \quad \mathbf{u}_2 \quad \dots \quad \mathbf{u}_n], \quad (3.105)$$

and approximate the displacement with the first  $n$  modal displacements  $y_j(t)$ :

$$\tilde{\mathbf{u}}(t) = \tilde{\mathbf{U}}\mathbf{y}(t).$$

A crucial question of every iterative method is its accuracy. In this case we have to find out, what number  $n$  is sufficient to perform an accurate calculation. To analyse this, we recall the orthogonality of the mass-matrix-normalized eigenvectors to the mass matrix. Eq. (1.45) with the modal matrix  $\mathbf{U}$  is

$$\mathbf{U}^T \mathbf{M} \mathbf{U} = \mathbf{I}_N, \quad (3.106)$$

where  $\mathbf{I}_N$  is the  $N$ -by- $N$  identity matrix.  $\mathbf{U}^T$  is a quadratic matrix of linearly independent rows. It has the inverse with the property

$$\mathbf{U}^T (\mathbf{U}^T)^{-1} = \mathbf{I}_N,$$

so, we can conclude from Eq. (3.106), that

$$(\mathbf{U}^T)^{-1} = \mathbf{M} \mathbf{U},$$

and using this inverse matrix in the computation of the product  $\mathbf{M} \mathbf{U} \mathbf{U}^T$  we obtain the identity

$$\mathbf{M} \mathbf{U} \mathbf{U}^T = (\mathbf{U}^T)^{-1} \mathbf{U}^T = \mathbf{I}_N, \quad (3.107)$$

If we use the partial solution of the eigenvalue problem, the eigenvectors are still orthogonal and normalized, so

$$\tilde{\mathbf{U}}^T \mathbf{M} \tilde{\mathbf{U}} = \mathbf{I}_n,$$

where  $\mathbf{I}_n$  is a the smaller,  $n$ -by- $n$  identity matrix. Now, neither  $\tilde{\mathbf{U}}^T$  nor  $\mathbf{M} \tilde{\mathbf{U}}$  is quadratic, i.e. they cannot be inverted, but we still can calculate their product

$$\mathbf{M} \tilde{\mathbf{U}} \tilde{\mathbf{U}}^T \quad (3.108)$$

as a pseudo-unit matrix. The better the approximation is with only  $n$  modes is, the closer the above matrix is to the unit matrix.<sup>4</sup> The accuracy is analysed in accordance with the load vector and the structure.

### Accuracy of the reduced modal analysis in the case of a given load vector

In the reduced modal analysis the load vector  $\mathbf{q}(t)$  is multiplied by the transpose of the reduced modal matrix  $\tilde{\mathbf{U}}$ :

$$\tilde{\mathbf{f}}(t) = \tilde{\mathbf{U}}^T \mathbf{q}(t).$$

The effective part of the load vector is defined as:

$$\tilde{\mathbf{q}}(t) = \mathbf{M} \tilde{\mathbf{U}} \tilde{\mathbf{f}}(t) = \mathbf{M} \tilde{\mathbf{U}} \tilde{\mathbf{U}}^T \mathbf{q}(t). \quad (3.109)$$

<sup>4</sup>Here, close refers here to the result of the transformation that the matrix does. A unit-matrix transforms any vector into itself. A pseudo-unit matrix transforms a subspace of the  $N$ -space into itself.

(Note, that if all the eigenvectors are used, the  $\mathbf{MUU}^T = \mathbf{I}$ , and  $\mathbf{q}(t) = \mathbf{MUU}^T \mathbf{q}(t)$  holds evidently.) The neglected part of the load vector is the difference between the effective and the real load vector:

$$\Delta \mathbf{q}(t) = \mathbf{q}(t) - \tilde{\mathbf{q}}(t) = \mathbf{q}(t) - \mathbf{M}\tilde{\mathbf{U}}\tilde{\mathbf{U}}^T \mathbf{q}(t).$$

The magnitude of  $\Delta \mathbf{q}(t)$  compared to  $\mathbf{q}(t)$  gives an estimation of the error of the calculation with  $n$  natural mode on behalf of the load vector.

**Problem 3.7.1** (Excited vibration of a fixed-fixed beam). Let us analyse the structure shown in Figure 3.12 (a). It is a fixed-fixed beam of length  $\ell = 6$  m, bending stiffness  $EI = 18000 \text{ Nm}^2$ , mass per unit length  $\mu = 420 \text{ kg/m}$ . The beam is taken to be inextensible, so no longitudinal displacements occur. This allows us to take only two degrees-of-freedom per nodes (the vertical translation and the rotation) into account. The beam is excited by the concentrated force  $q(t)$  in its mid-span.

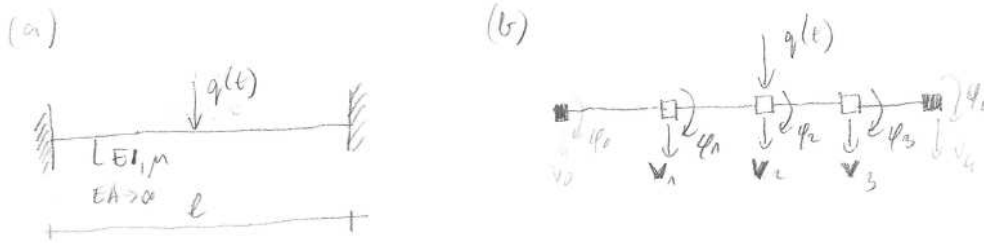


**Figure 3.12:** (a) Sketch of a fixed-fixed beam. (b) Mechanical model for the matrix displacement method (fixed support model).

Divide the structure into four equal members, and analyse the accuracy of the reduced modal analysis using various number  $n$  of eigenvectors!

**Solution.** Figure 3.12 (a) shows the beam members, and the used internal nodes. Each beam is the same and the local and global reference systems coincide. So, there is no need for the transformation between the local and global systems. We do not have displacements and forces in the horizontal directions, so the first and fourth rows and columns can be omitted from Eq. (3.28) and (3.75). Thus the elementary stiffness and consistent mass matrices are

$$\mathbf{K}_{ij}^{\text{loc}} = \mathbf{K}_{ij}^{\text{glob}} = \begin{bmatrix} \frac{12EI}{\ell^3} & \frac{6EI}{\ell^2} & -\frac{12EI}{\ell^3} & \frac{6EI}{\ell^2} \\ \frac{6EI}{\ell^2} & \frac{4EI}{\ell} & -\frac{6EI}{\ell^2} & \frac{2EI}{\ell} \\ -\frac{12EI}{\ell^3} & -\frac{6EI}{\ell^2} & \frac{12EI}{\ell^3} & -\frac{6EI}{\ell^2} \\ \frac{6EI}{\ell^2} & \frac{2EI}{\ell} & -\frac{6EI}{\ell^2} & \frac{4EI}{\ell} \end{bmatrix} = \begin{bmatrix} 64 & 48 & -64 & 48 \\ 48 & 48 & -48 & 24 \\ -64 & -48 & 64 & -48 \\ 48 & 24 & -48 & 48 \end{bmatrix} \cdot 1000,$$

$$\mathbf{M}_{ij}^{\text{loc}} = \mu \ell \begin{bmatrix} \frac{13}{35} & \frac{11}{210} \ell & \frac{9}{70} & -\frac{13}{420} \ell \\ \frac{11}{210} \ell & \frac{1}{105} \ell^2 & \frac{13}{420} \ell & -\frac{1}{140} \ell^2 \\ \frac{9}{70} & \frac{13}{420} \ell & \frac{13}{35} & -\frac{11}{210} \ell \\ -\frac{13}{420} \ell & -\frac{1}{140} \ell^2 & -\frac{11}{210} \ell & \frac{1}{105} \ell^2 \end{bmatrix} = \begin{bmatrix} 234 & 49.5 & 81 & -29.25 \\ 49.5 & 13.5 & 29.25 & -10.125 \\ 81 & 29.25 & 234 & -49.5 \\ -29.25 & -10.125 & -49.5 & 13.5 \end{bmatrix}.$$

From the above matrices we can compile the total stiffness and mass matrices of the structure. In a fixed support model we must take into account the supported nodes 0 and 4 as well. While taking the fix supports into account, we should erase the block rows and block columns from the unconstrained matrices in this case. The erase process is done on the matrices:

$$\mathbf{K} = \begin{bmatrix} \mathbf{K}^{00} & \mathbf{K}^{0i} & \mathbf{K}^{04} \\ \mathbf{K}^{i0} & \mathbf{K}^{ii} & \mathbf{K}^{i4} \\ \mathbf{K}^{40} & \mathbf{K}^{4i} & \mathbf{K}^{44} \end{bmatrix}, \quad \mathbf{M} = \begin{bmatrix} \mathbf{M}^{00} & \mathbf{M}^{0i} & \mathbf{M}^{04} \\ \mathbf{M}^{i0} & \mathbf{M}^{ii} & \mathbf{M}^{i4} \\ \mathbf{M}^{40} & \mathbf{M}^{4i} & \mathbf{M}^{44} \end{bmatrix} \quad (3.110)$$

by canceling the first and third block rows and columns. Thus, what remains is the 6-by-6 matrices  $\mathbf{K}^{ii}$  and  $\mathbf{M}^{ii}$ , which are referred to as  $\mathbf{K}$  and  $\mathbf{M}$  hereafter:

$$\mathbf{K} = \begin{bmatrix} 128000 & 0 & -64000 & 48000 & 0 & 0 \\ 0 & 96000 & -48000 & 24000 & 0 & 0 \\ \hline -64000 & -48000 & 128000 & 0 & -64000 & 48000 \\ 48000 & 24000 & 0 & 96000 & -48000 & 24000 \\ \hline 0 & 0 & -64000 & -48000 & 128000 & 0 \\ 0 & 0 & 48000 & 24000 & 0 & 96000 \end{bmatrix},$$

$$\mathbf{M} = \begin{bmatrix} 468 & 0 & 81 & -29.25 & 0 & 0 \\ 0 & 27 & 29.25 & -10.125 & 0 & 0 \\ \hline 81 & 29.25 & 468 & 0 & 81 & -29.25 \\ -29.25 & -10.125 & 0 & 27 & 29.25 & -10.125 \\ \hline 0 & 0 & 81 & 29.25 & 468 & 0 \\ 0 & 0 & -29.25 & -10.125 & 0 & 27 \end{bmatrix}.$$

The natural circular frequencies and the corresponding mass-matrix-normalized eigenvectors are:

$$\begin{aligned} \omega_{01} &= 4.0739 \text{ rad/s}, & \mathbf{u}_1^T &= [.01724, .01610, .03172, 0, .01724, -.01610] \\ \omega_{02} &= 11.319 \text{ rad/s}, & \mathbf{u}_2^T &= [.02933, .01054, 0, -.03856, -.02933, .01054] \\ \omega_{03} &= 22.456 \text{ rad/s}, & \mathbf{u}_3^T &= [-.02855, .02240, .02941, 0, -.02855, -.02240] \\ \omega_{04} &= 42.484 \text{ rad/s}, & \mathbf{u}_4^T &= [-.01350, .08587, 0, -.09601, .01350, .08587] \\ \omega_{05} &= 70.262 \text{ rad/s}, & \mathbf{u}_5^T &= [-.005953, -.1445, .02800, 0, -.005953, .1445] \\ \omega_{06} &= 113.21 \text{ rad/s}, & \mathbf{u}_6^T &= [.01655, .1413, 0, .2298, -.01655, .1413] \end{aligned} \quad (3.111)$$

We can observe, that there are reflection symmetric and antisymmetric modal shapes. The load is reflection symmetric:

$$\mathbf{q}(t) = [0 \ 0 \ | \ 1 \ 0 \ | \ 0 \ 0]^T \cdot q(t),$$

so the antisymmetric modes will not participate in the motion. The results of a calculation with the reduced mode number  $n = 2$  is equivalent with the results of  $n = 1$ . The result of the calculation carried out with  $n = 4$  eigenvector is equivalent with the results of  $n = 3$  eigenvectors. The results using  $n = 6$  eigenvectors is equivalent with  $n = 5$  eigenvectors. The effective load vector  $\tilde{\mathbf{q}}_n(t)$  for odd numbers are:

$$\tilde{\mathbf{q}}_1(t) = \begin{bmatrix} 0.3374 \\ 0.04322 \\ 0.5894 \\ 0 \\ 0.3374 \\ -0.04322 \end{bmatrix} q(t), \quad \tilde{\mathbf{q}}_3(t) = \begin{bmatrix} 0.01449 \\ 0.08631 \\ 0.8967 \\ 0 \\ 0.01449 \\ -0.08631 \end{bmatrix} q(t), \quad \tilde{\mathbf{q}}_5(t) = \begin{bmatrix} 0 \\ 0 \\ 1.0000 \\ 0 \\ 0 \\ 0 \end{bmatrix} q(t).$$

### Accuracy of the reduced modal analysis in the case of support vibration

We have seen in Subsection 3.5.3 that the support vibration can be treated as a forcing, where the excitation force is calculated from the acceleration of the supports  $\ddot{u}^g(t)$ , the mass matrix  $\mathbf{M}$ , and an influence vector  $\mathbf{r}$ . This influence vector denotes all degrees-of-freedom that are able to move in the direction of the support vibration.



Standards prescribe the use of as many natural modes, as many needed to get back 90% of the total mass in the analysed direction. To calculate the effective mass with the reduced number of eigenvectors, we can follow a similar approach to the one we used for the loads.

In the case of the full modal analysis we can conclude from Eq. (3.107) that the following identity holds:

$$\mathbf{M}\mathbf{U}\mathbf{U}^T\mathbf{M} = \mathbf{M}.$$

In the reduced modal analysis the product

$$\tilde{\mathbf{M}} = \mathbf{M}\tilde{\mathbf{U}}\tilde{\mathbf{U}}^T\mathbf{M} \quad (3.112)$$

i.e. the *reduced mass matrix*  $\tilde{\mathbf{M}}$  is different from the total mass matrix  $\mathbf{M}$  of the structure. The accuracy of the calculation with the reduced modal analysis depends in general on what fraction of the total mass matrix appears in the reduced mass matrix.

In the vibration analysis of the MDOF system the total mass of the structure appears in every admissible direction. At once we are only interested in one of these directions. Let us define the influence vector  $\mathbf{r}$  that gives the displacement of each degree-of-freedom due to the unit displacement of the supported nodes in one chosen (global) direction. So, this vector represents a rigid-body translation of the structure in that specific direction. In the case of a planar frame, the influence vector  $\mathbf{r}_X$  associated with the horizontal displacement is

$$\mathbf{r}_X^T = [1, 0, 0, 1, 0, 0, \dots, 1, 0, 0],$$

and the influence vector  $\mathbf{r}_Y$  associated with the vertical displacement is

$$\mathbf{r}_Y^T = [0, 1, 0, 0, 1, 0, \dots, 0, 1, 0].$$

The *directional mass vectors*

$$\mathbf{m}_X = \mathbf{M}\mathbf{r}_X \quad \text{and} \quad \mathbf{m}_Y = \mathbf{M}\mathbf{r}_Y \quad (3.113)$$

represent the total masses vibrating in the degrees-of-freedom along the directions  $X$  and  $Y$ , respectively. The quasi-static, rigid body translation of the structure requires the displacement of the supported nodes as well, so the influence vectors must refer to the supported degrees-of-freedom of the structure, too. Therefore, the directional mass vector must be calculated in accordance with Eq. (3.87). The further calculations are the same for both directions  $X$  and  $Y$ , so we show the upcoming steps of the calculation without those indexes.

The *modal participation* of the  $j$ th mode is the projection of the directional mass vector on the modal shape vector  $\mathbf{u}_j$ . We can collect all the products  $\mathbf{u}_j^T\mathbf{M}\mathbf{r}$  in the *modal participation vector*:

$$\mathbf{\Gamma} = \mathbf{U}^T\mathbf{M}\mathbf{r} = \mathbf{U}^T\mathbf{m}. \quad (3.114)$$

The  $j$ th entry of  $\mathbf{\Gamma}$  is related to the motion of the center of gravity of the structure in the case of the vibration of the  $j$ th mode. The square of the  $j$ th entry of  $\mathbf{\Gamma}$  is the effective mass appearing in the  $j$ th mode. This effective mass is denoted by  $m_{\text{eff},j}$ :

$$m_{\text{eff},j} = \Gamma_j^2, \quad j = 1, 2, \dots, N.$$

The sum of all effective masses corresponding to a given influence vector  $\mathbf{r}$  gives the total mass of the structure:

$$m = \sum_{j=1}^N m_{\text{eff},j} = \mathbf{\Gamma}^T \mathbf{\Gamma}.$$

If we use a partial solution of the generalized eigenvalue problem, we can calculate a reduced modal participation vector:

$$\tilde{\mathbf{\Gamma}} = \tilde{\mathbf{U}}^T \mathbf{M} \mathbf{r} = \tilde{\mathbf{U}}^T \mathbf{m}.$$

The partial solution of the generalized eigenvalue problem evidently provides the same modal shape vectors for the first  $n$  natural modes, therefore the elements of  $\tilde{\mathbf{\Gamma}}$  are the same as the first  $n$  elements of  $\mathbf{\Gamma}$ . The effective masses are calculated in the same way as in the case of the total solution of the eigenvalue problem, but for smaller number of modes:

$$\tilde{m}_{\text{eff},j} = m_{\text{eff},j} = \tilde{\Gamma}_j^2, \quad j = 1, 2, \dots, n.$$

The reduced effective mass of the structure using the reduced set of eigenvectors is

$$\tilde{m}_{\text{eff}} = \sum_{j=1}^n m_{\text{eff},j} = \tilde{\mathbf{\Gamma}}^T \tilde{\mathbf{\Gamma}}.$$

We can substitute the modal participation vector into the above formula:

$$\tilde{m}_{\text{eff}} = \left( \tilde{\mathbf{U}}^T \mathbf{M} \mathbf{r} \right)^T \left( \tilde{\mathbf{U}}^T \mathbf{M} \mathbf{r} \right) = \mathbf{r}^T \mathbf{M} \tilde{\mathbf{U}} \tilde{\mathbf{U}}^T \mathbf{M} \mathbf{r}.$$

We can conclude, that the total effective mass of the structure can be calculated using the reduced mass matrix Eq. (3.112) and the influence vector with the quadratic formula:

$$\tilde{m}_{\text{eff}} = \mathbf{r}^T \tilde{\mathbf{M}} \mathbf{r}.$$

The ratio of  $\tilde{m}_{\text{eff}}$  to the total mass  $m$  gives the estimation on the ratio of the used mass. As we mentioned earlier, this ratio must exceed 90% in the case of earthquake analysis.

**Problem 3.7.2** (Support vibration of a fixed-fixed beam). Let us analyse the reduced modal analysis for support vibration of the structure shown in Figure 3.13 (a). It is the same fixed-fixed beam of length  $\ell = 6$  m, bending stiffness  $EI = 18000 \text{ Nm}^2$ , mass per unit length  $\mu = 420 \text{ kg/m}$  as we had in Problem 3.7.1. The beam is inextensible, so no longitudinal displacements occur. This allows us to take only two degrees-of-freedom per nodes (the vertical translation and the rotation) into account. The beam is excited by support vibration  $v_g(t)$  at its both supports. Calculate the effective mass of the normal modes!

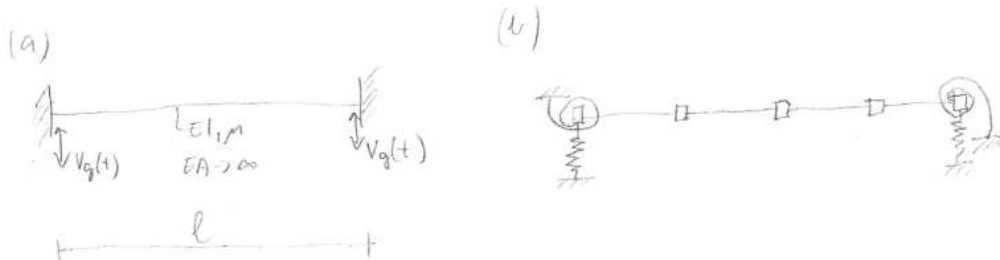


**Figure 3.13:** (a) Sketch of a fixed-fixed beam. (b) Mechanical model for the matrix displacement method (spring model).

**Solution** (Using the fixed support model). The structure has the same stiffness and mass matrices as in Problem 3.7.1, so the natural circular frequencies are the same as we have seen in Eq. (3.111).

In the influence vector  $\mathbf{r}_Y$  we must take the supported nodes 0 and 4 into account as well (see Fig.3.12 (b) for these excess nodes). Since we do not use the horizontal translations, the applied influence vector is

$$\mathbf{r}_Y^T = [1, 0, 1, 0, 1, 0, 1, 0, 1, 0].$$

We must use the mass matrix of the unconstrained structure in Eq. (3.113). In our case it is the middle block row in Eq. (3.110):  $[ \mathbf{M}^{i0} \mid \mathbf{M}^{ii} \mid \mathbf{M}^{i4} ]$ . The blocks are compiled from the elementary consistent mass matrices  $\mathbf{M}_{ij}^{\text{oc}}$  of Problem 3.7.1:

$$[ \mathbf{M}^{i0} \mid \mathbf{M}^{ii} \mid \mathbf{M}^{i4} ] = \left[ \begin{array}{cc|cc|cc|cc|cc} 81 & 29.5 & 468 & 0 & 81 & -29.25 & 0 & 0 & 0 & 0 \\ -29.25 & -10.125 & 0 & 27 & 29.25 & -10.125 & 0 & 0 & 0 & 0 \\ \hline 0 & 0 & 81 & 29.25 & 468 & 0 & 81 & -29.25 & 0 & 0 \\ 0 & 0 & -29.25 & -10.125 & 0 & 27 & 29.25 & -10.125 & 0 & 0 \\ \hline 0 & 0 & 0 & 0 & 81 & 29.25 & 468 & 0 & 81 & -29.25 \\ 0 & 0 & 0 & 0 & -29.25 & -10.125 & 0 & 27 & 29.25 & -10.125 \end{array} \right]$$

The directional mass vector is finally:

$$\mathbf{m}_Y = [ \mathbf{M}^{i0} \mid \mathbf{M}^{ii} \mid \mathbf{M}^{i4} ] \mathbf{r}_Y = \left[ \begin{array}{c} 630 \\ 0 \\ \hline 630 \\ 0 \\ \hline 630 \\ 0 \end{array} \right].$$

The modal participation vector is from Eq. (3.114):

$$\mathbf{\Gamma} = \mathbf{U}^T \mathbf{m}_Y = [ 41.71 \quad 0 \mid -17.44 \quad 0 \mid 10.14 \quad 0 ]^T.$$

It is easy to spot that the antisymmetric (odd) modal shapes contribute no mass to this support vibration. The effective modal masses are:

$$m_{\text{eff},1} = 1739 \text{ kg}, \quad m_{\text{eff},3} = 304.3 \text{ kg}, \quad m_{\text{eff},5} = 102.8 \text{ kg}, \quad m_{\text{eff},2} = m_{\text{eff},4} = m_{\text{eff},6} = 0 \text{ kg}.$$

The total mass of the structure is  $m = \mu \ell = 2520 \text{ kg}$ . The effective mass appearing in the modal analysis is:

$$m_{\text{eff}} = m_{\text{eff},1} + m_{\text{eff},3} + m_{\text{eff},5} = 2146.1 \text{ kg}.$$

It is still less than the 90% of the total mass of the structure, so there is not either a reduced or a full set of mode shapes, which would be sufficient to calculate the support vibration with modal analysis. This is caused by the large fraction of total mass reduced to the supported nodes. Dividing the beam into five members would reduce this effect. In that case the first three active modes (due to the symmetries, these are the first, the third and the fifth modes) would produce an effective mass more than 90% of the total mass.

**Solution** (Solution of the same problem with the spring support model). We show the solution steps of the same problem with the spring support model too. In that case we have to use a five-node model and connect the supported nodes with stiff springs to the support (see Fig.3.13 (b)). The elementary stiffness and mass matrices

are the same as in Problem 3.7.1, but we must compile the 10-by-10 matrices, and add large spring stiffnesses  $\rho_Y$  and  $\rho_\varphi$  to the corresponding entries in the main diagonal of the stiffness matrix. The resulting stiffness matrix is

$$\mathbf{K} = \begin{bmatrix}
 64000 + \rho_Y & 48000 & -64000 & 48000 & 0 & 0 & 0 & 0 & 0 & 0 \\
 48000 & 48000 + \rho_\varphi & -48000 & 24000 & 0 & 0 & 0 & 0 & 0 & 0 \\
 -64000 & -48000 & 128000 & 0 & -64000 & 48000 & 0 & 0 & 0 & 0 \\
 48000 & 24000 & 0 & 96000 & -48000 & 24000 & 0 & 0 & 0 & 0 \\
 0 & 0 & -64000 & -48000 & 128000 & 0 & -64000 & 48000 & 0 & 0 \\
 0 & 0 & 48000 & 24000 & 0 & 96000 & -48000 & 24000 & 0 & 0 \\
 0 & 0 & 0 & 0 & -64000 & -48000 & 128000 & 0 & -64000 & 48000 \\
 0 & 0 & 0 & 0 & 48000 & 24000 & 0 & 96000 & -48000 & 24000 \\
 0 & 0 & 0 & 0 & 0 & 0 & -64000 & -48000 & 64000 + \rho_Y & -48000 \\
 0 & 0 & 0 & 0 & 0 & 0 & 48000 & 24000 & -48000 & 48000 + \rho_\varphi
 \end{bmatrix}$$

while the mass matrix is

$$\mathbf{M} = \begin{bmatrix}
 234 & 49.5 & 81 & -29.25 & 0 & 0 & 0 & 0 & 0 & 0 \\
 49.5 & 13.5 & 29.25 & -10.125 & 0 & 0 & 0 & 0 & 0 & 0 \\
 81 & 29.25 & 468 & 0 & 81 & -29.25 & 0 & 0 & 0 & 0 \\
 -29.25 & -10.125 & 0 & 27 & 29.25 & -10.125 & 0 & 0 & 0 & 0 \\
 0 & 0 & 81 & 29.25 & 468 & 0 & 81 & -29.25 & 0 & 0 \\
 0 & 0 & -29.25 & -10.125 & 0 & 27 & 29.25 & -10.125 & 0 & 0 \\
 0 & 0 & 0 & 0 & 81 & 29.25 & 468 & 0 & 81 & -29.25 \\
 0 & 0 & 0 & 0 & -29.25 & -10.125 & 0 & 27 & 29.25 & -10.125 \\
 0 & 0 & 0 & 0 & 0 & 0 & 81 & 29.25 & 234 & -49.5 \\
 0 & 0 & 0 & 0 & 0 & 0 & -29.25 & -10.125 & -49.5 & 13.5
 \end{bmatrix}$$

The results of the solution of the generalized eigenvalue problem is summarized in Table 3.3. It worth realizing, that if the spring stiffnesses are below  $10^7$ , then the first six natural frequencies are affected. If the spring stiffnesses are equal to or larger than  $10^7$ , then there is a significant effect only on the last four natural frequencies. So, if we want to model the system with spring support, we have to take this value into account when choosing a *sufficiently* large spring stiffness.

The analysis of the efficient modal masses can be done on the actual mass matrix with the same influence vector as we used in the previous solution.

$\rho_Y = \rho_\varphi$	$\omega_{01}$	$\omega_{02}$	$\omega_{03}$	$\omega_{04}$	$\omega_{05}$	$\omega_{06}$	$\omega_{07}$	$\omega_{08}$	$\omega_{09}$	$\omega_{010}$
$10^4$	1.9480	4.2419	7.5605	14.132	24.586	43.230	67.054	102.95	178.53	193.41
$10^5$	3.4599	8.6133	14.748	22.307	31.827	50.547	77.019	115.07	282.09	292.01
$10^6$	3.9976	10.955	21.328	38.351	56.479	75.025	94.437	123.79	755.84	771.06
$10^7$	4.0661	11.281	22.343	42.109	69.183	111.12	232.66	236.59	2344.3	2387.7
$10^8$	4.0732	11.315	22.444	42.447	70.160	113.04	722.18	728.36	7398.7	7534.6
$10^9$	4.0739	11.318	22.455	42.480	70.252	113.19	2279.7	2297.9	23392.	23821.
$10^{10}$	4.0739	11.319	22.456	42.484	70.261	113.21	7207.7	7264.8	73971.	75329.

**Table 3.3:** The natural circular frequencies of the beam with elastic supports for various spring stiffnesses.

In this solution we presented the application of the spring support model for the dynamical calculation of a beam with elastic end supports.

In the fixed support model we should add two supporting nodes to the system, but the mass matrix would be zero in their block rows and block columns (the supporting springs are supposed to be massless). Therefore, we can leave out the excess nodes from the calculations. Finally, we can conclude that the stiffness and mass matrices are the same in the elastic supported case for both support models.

## 3.8 Second order effects

In this section we analyse the effects of the rotational inertia and the normal force to the dynamical stiffness matrix of the beam.

### 3.8.1 Rotational inertia

We derive the dynamical stiffness matrix of a beam member similarly to Subsection 3.2.2, using the principle of virtual displacements. The only extension we make here is that the rotary inertia of the cross-section is taken into account. As in Subsection 3.2.2, we let the beam be vibrating such that the translation of its  $i$ th end is  $v_{iy}(0, t) = 1 \cdot \sin(\omega t)$ , while all other displacements of its ends are zero (see Figure 3.14 top). The internal forces at the ends of the beam are the harmonic functions

$$\begin{aligned} N_{iy}(0, t) &= \hat{N}_{iyy} \sin(\omega t), & V_{iy}(0, t) &= \hat{V}_{iyy} \sin(\omega t), & M_{iy}(0, t) &= \hat{M}_{iyy} \sin(\omega t), \\ N_{iy}(\ell, t) &= \hat{N}_{jyy} \sin(\omega t), & V_{iy}(\ell, t) &= \hat{V}_{jyy} \sin(\omega t), & M_{iy}(\ell, t) &= \hat{M}_{jyy} \sin(\omega t). \end{aligned} \quad (3.115)$$

These internal forces and the bending moment diagram at a certain time instant are sketched at the bottom of Figure 3.14.

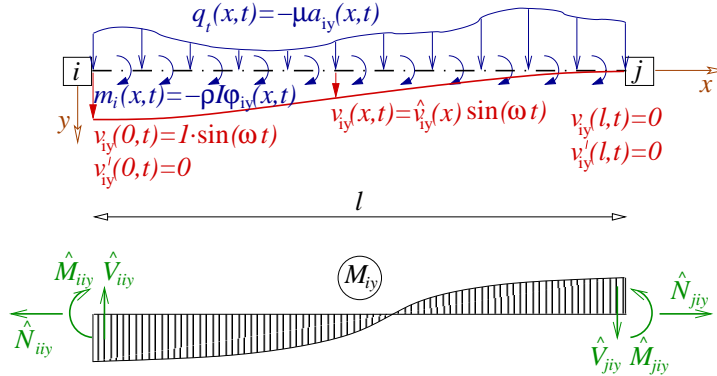


**Figure 3.14:** (top) Sketch of the deformed shape of beam  $ij$  due to a harmonic translation of unit amplitude of end  $i$  along axis  $y$ . (bottom) The corresponding bending moment diagram and the positive definition of the end-of-beam internal forces.

We need to determine the amplitudes of the internal forces  $(\hat{N}_{iyy}, \hat{V}_{iyy}, \hat{M}_{iyy}, \hat{N}_{jyy}, \hat{V}_{jyy}, \hat{M}_{jyy})$  due to a harmonic vertical translation of unit amplitude of end  $i$  with the rotational inertia of the cross-section taken into account.

The computation of the end-of-beam internal forces is based on the principle of virtual displacements. At time instant  $t$ , we apply the fictitious force system to the beam as shown in Figure 3.14. The inertia force  $q_t(x, t) = -\mu a_{iy}(x, t)$  is due to the linear momentum of the beam elements, and the fictitious inertia moment  $m_i(x, t) = -\rho I \ddot{\phi}_{iy}(x, t) = -\mu i_0^2 \ddot{\phi}_{iy}(x, t)$  arises from the angular momentum of the beam elements. Here  $i_0^2 = I/A$ .

Thus we have a statically admissible force system: the internal forces and the fictitious inertia force and moment are in equilibrium. We take the (statical) displacement system  $v_{iy}(x)$  due to a unit translation of end  $i$  (which is shown in Figure 3.4) as the virtual displacement

system. We compute the virtual work that the force system shown in Figure 3.14 does on this virtual displacement system at time instant  $t$ :

$$\begin{aligned} \delta W_{\text{ds}} = & V_{iy}(0, t) \cdot (-1) + \int_0^\ell \{-\mu a_{iy}(x, t)\} v_{iy}(x) \, dx + \int_0^\ell \{-\mu i_0^2 \ddot{\varphi}_{iy}(x, t)\} v'_{iy}(x) \, dx \\ & - \int_0^\ell M_{iy}(x, t) \kappa_{iy}(x) \, dx = 0. \end{aligned}$$

Here the first term is the work done by the shear force  $V_{iy}(0, t)$  on the translation of end  $i$ . The last term is the internal work done by the bending moment  $M_{iy}(x, t)$  on the curvature  $\kappa_{iy}(x) = M_{iy}(x)/EI$ . The second term is the work done by the (distributed) inertia force

$$-\mu a_{iy}(x, t) = -\mu \ddot{v}_{iy}(x, t) = \mu \omega^2 \hat{v}_{iy} \sin(\omega t)$$

on the translation  $v_{iy}(x)$  along the whole length of the beam. The third term is the work done by the (distributed) inertia moment

$$-\mu i_0^2 \ddot{\varphi}_{iy}(x, t) = -\mu i_0^2 \ddot{v}'_{iy}(x, t) = \mu i_0^2 \omega^2 \hat{v}'_{iy} \sin(\omega t)$$

on the rotation  $v'_{iy}(x)$  along the whole length of the beam. This, Eq. (3.49), and Eq (3.67) implies that the above work is

$$\begin{aligned} \delta W_{\text{ds}} = & \left\{ -\hat{V}_{iyy} + \mu \omega^2 \int_0^\ell \hat{v}_{iy}(x) v_{iy}(x) \, dx + \mu i_0^2 \omega^2 \int_0^\ell \hat{v}'_{iy}(x) v'_{iy}(x) \, dx \right. \\ & \left. - \int_0^\ell \hat{M}_{iy}(x) \frac{M_{iy}(x)}{EI} \, dx \right\} \sin(\omega t) = 0. \end{aligned} \quad (3.116)$$

Next, we express the virtual work that the statical force system (shown in Figure 3.4) does on the dynamical displacement system (sketched in Figure 3.14) at certain time instant  $t$ :

$$\delta W_{\text{sd}} = V_{iyy}(0) \cdot \{-1 \cdot \sin(\omega t)\} - \int_0^\ell M_{iy}(x) \frac{M_{iy}(x, t)}{EI} \, dx = 0.$$

Using Eqs. (3.115) the above work is reformulated as

$$\delta W_{\text{sd}} = \left\{ -V_{iyy} - \int_0^\ell M_{iy}(x) \frac{\hat{M}_{iy}(x)}{EI} \, dx \right\} \sin(\omega t) = 0. \quad (3.117)$$

Both Eqs. (3.116) and (3.117) have zero on the right hand side. Therefore, their left hand sides divided by  $\sin(\omega t) \neq 0$ , are equal:

$$\begin{aligned} & -\hat{V}_{iiy} + \mu\omega^2 \int_0^\ell \hat{v}_{iy}(x)v_{iy}(x) dx + \mu i_0^2 \omega^2 \int_0^\ell \hat{v}'_{iy}(x)v'_{iy}(x) dx \\ & - \int_0^\ell \hat{M}_{iy}(x) \frac{M_{iy}(x)}{EI} dx = -V_{iiy} - \int_0^\ell M_{iy}(x) \frac{\hat{M}_{iy}(x)}{EI} dx. \end{aligned}$$

Here the virtual internal works are the same:

$$\int_0^\ell \hat{M}_{iy}(x) \frac{M_{iy}(x)}{EI} dx = \int_0^\ell M_{iy}(x) \frac{\hat{M}_{iy}(x)}{EI} dx.$$

Finally, we can express the amplitude of the dynamical bending moment at end  $i$  caused by a harmonic translation of the same end. This is the entry 2,2 of the dynamical stiffness matrix  $\hat{\mathbf{K}}_{ij}^{\text{loc}}$ :

$$\begin{aligned} \hat{K}_{ij,22}^{\text{loc}} &= -\hat{V}_{iiy} = -V_{iiy} - \mu\omega^2 \int_0^\ell \hat{v}_{iy}(x)v_{iy}(x) dx - \mu i_0^2 \omega^2 \int_0^\ell \hat{v}'_{iy}(x)v'_{iy}(x) dx \\ &= K_{ij,22}^{\text{loc}} - \mu\omega^2 \int_0^\ell \hat{v}_{iy}(x)v_{iy}(x) dx - \mu i_0^2 \omega^2 \int_0^\ell \hat{v}'_{iy}(x)v'_{iy}(x) dx. \end{aligned}$$

We can derive all the internal forces at the ends of the beam due to longitudinal and transverse (harmonic) translations and (harmonic) rotations of unit amplitudes of the ends in a similar way. mass related matrix. We can construct a matrix similar to (3.23):

$$\hat{\mathbf{N}}'_\varphi = \begin{bmatrix} 0 & \hat{v}'_{iy}(x) & \hat{v}'_{i\varphi}(x) & 0 & \hat{v}'_{jy}(x) & \hat{v}'_{j\varphi}(x) \end{bmatrix}. \quad (3.118)$$

Here prime denotes derivation with respect to  $x$ . The shape function  $\hat{v}_{iy}(x)$  is due to a harmonic translation of unit amplitude of end  $i$  along  $y$ , i.e. the solution of the homogeneous part of (2.41):

$$\mu \left( \frac{\partial^2 v(x, t)}{\partial t^2} - i_0^2 \frac{\partial^4 v(x, t)}{\partial x^2 \partial t^2} \right) + EI \frac{\partial^4 v(x, t)}{\partial x^4} = 0. \quad (3.119)$$

with  $v(x, t) = \hat{v} \sin(\omega t)$  and boundary conditions (3.62). The shape function  $v_{i\varphi}(x)$  describes the deformed shape of the beam caused by a harmonic rotation of unit amplitude of end  $i$ . It is the solution of (3.119) with boundary conditions (3.63). The same holds for superscript  $j$  with the appropriate boundary conditions. It is important to note, that these shape functions are a functions of  $x$ , but they also depend on the following parameters  $\mu$ ,  $EI$ ,  $EA$ ,  $\ell$  (which are given parameters of the beam), and  $\omega$ , which is the frequency of the forcing. Therefore  $\hat{\mathbf{N}}'_\varphi$  is *frequency-dependent*!

Now we can write the elementary dynamical stiffness matrix of beam  $ij$  in the short form

$$\hat{\mathbf{K}}_{ij}^{\text{loc}}(\omega) = \mathbf{K}_{ij}^{\text{loc}} - \omega^2 \left( \hat{\mathbf{M}}_{ij}^{\text{loc}}(\omega) + \hat{\mathbf{M}}_{ij}^{\text{loc}\varphi}(\omega) \right). \quad (3.120)$$

Here  $\mathbf{K}_{ij}^{\text{loc}}$  is the elementary statical stiffness matrix of beam  $ij$ ,  $\hat{\mathbf{M}}_{ij}^{\text{loc}}(\omega)$  is the elementary mass matrix

$$\hat{\mathbf{M}}_{ij}^{\text{loc}}(\omega) = \mu \int_0^\ell \hat{\mathbf{N}}^T \mathbf{N} \, dx, \quad (3.121)$$

and  $\hat{\mathbf{M}}_{ij}^{\text{loc}\varphi}(\omega)$  is the elementary rotational mass matrix:

$$\hat{\mathbf{M}}_{ij}^{\text{loc}\varphi}(\omega) = \mu i_0^2 \int_0^\ell \hat{\mathbf{N}}_\varphi'^T \mathbf{N}'_\varphi \, dx. \quad (3.122)$$

These mass matrices depend on the circular frequency  $\omega$  of the external forcing. Concluding the results, we can say, that the dynamical elementary stiffness matrix equals to the statical elementary stiffness matrix minus the sum of the mass matrices (3.121), (3.122) times the square of the forcing frequency. This dynamical stiffness matrix is *frequency-dependent*! From Eq. (3.120) it can be verified, that the mass matrices  $\hat{\mathbf{M}}_{ij}^{\text{loc}}(\omega)$  and  $\hat{\mathbf{M}}_{ij}^{\text{loc}\varphi}(\omega)$  are *symmetric*, and so is the dynamical stiffness matrix  $\hat{\mathbf{K}}_{ij}^{\text{loc}}(\omega)$ .

Similar to the translational mass matrix, the rotational mass matrix can be approximated by a consistent rotational mass matrix, if necessary. In that case the matrix  $\hat{\mathbf{N}}'_\varphi$  is estimated by

$$\mathbf{N}'_\varphi = \begin{bmatrix} 0 & v'_{iy}(x) & v'_{i\varphi}(x) & 0 & v'_{jy}(x) & v'_{j\varphi}(x) \end{bmatrix}.$$

and the consistent rotational mass matrix becomes

$$\mathbf{M}_{\text{cons},ij}^{\text{loc}\varphi} = \mu i_0^2 \int_0^\ell \mathbf{N}'_\varphi'^T \mathbf{N}'_\varphi \, dx.$$

In this case the dynamical stiffness matrix is approximately

$$\hat{\mathbf{K}}_{ij}^{\text{loc}}(\omega) \approx \mathbf{K}_{ij}^{\text{loc}} - \omega^2 \left( \mathbf{M}_{\text{cons},ij}^{\text{loc}} + \mathbf{M}_{\text{cons},ij}^{\text{loc}\varphi} \right)$$

### 3.8.2 Static normal force

In this subsection we will incorporate the effect of constant statical normal forces on the motion of the rod using similar approach as in Subsection 3.2.2.

If the beam vibrates so that the translation of its  $i$ th end is  $v_{iy}(0, t) = 1 \cdot \sin(\omega t)$ , while all other displacements of its ends are zero (see Figure 3.14 top), then the end-of-beam internal forces are the harmonic functions

$$\begin{aligned} N_{iy}(0, t) &= \hat{N}_{iyy} \sin(\omega t), & V_{iy}(0, t) &= \hat{V}_{iyy} \sin(\omega t), & M_{iy}(0, t) &= \hat{M}_{iyy} \sin(\omega t), \\ N_{iy}(\ell, t) &= \hat{N}_{jyy} \sin(\omega t), & V_{iy}(\ell, t) &= \hat{V}_{jyy} \sin(\omega t), & M_{iy}(\ell, t) &= \hat{M}_{jyy} \sin(\omega t). \end{aligned} \quad (3.123)$$



The amplitudes of the internal forces ( $\hat{N}_{iyy}$ ,  $\hat{V}_{iyy}$ ,  $\hat{M}_{iyy}$ ,  $\hat{N}_{jyy}$ ,  $\hat{V}_{jyy}$ ,  $\hat{M}_{jyy}$ ) due to a harmonic translation of unit amplitude of end  $i$  of the beam can be determined using the principle of virtual displacements.

This time we take the moment that the normal force  $S$  exerts on the (rotated) elementary beam segment into account, which is shown in Figure 3.15. The rotation of the segment causes an eccentricity of the normal force, which indicates a distributed moment  $m_S(x, t) = -Sv'_{iy}(x, t)$ .

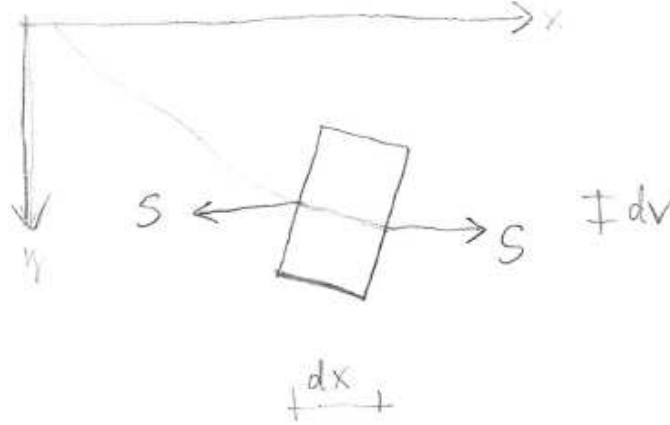


**Figure 3.15:** Demonstration of the moment caused by the normal force  $S$  on a rotated elementary segment of the beam.

At time instant  $t$ , we apply the fictitious inertia force  $q_t(x, t) = -\mu a_{iy}(x, t)$ , the fictitious inertia moment  $m_i(x, t) = -\rho I \ddot{\varphi}_{iy}(x, t) = -\mu i_0^2 \ddot{\varphi}_{iy}(x, t)$  and the distributed moment  $m_S(x, t) = -Sv'_{iy}(x, t)$  to the beam. The internal forces, the fictitious inertia force, the fictitious inertia moment and the distributed moment caused by the force  $S$  are in equilibrium. We take the (statical) displacement system  $v_{iy}(x)$  due to a unit translation of end  $i$  (which is shown in Figure 3.4) as the virtual displacement system. The virtual work that the (dynamical) force system shown in Figure 3.14 does on this (virtual) displacement system at time instant  $t$  is:

$$\begin{aligned} \delta W_{ds} = & V_{iy}(0, t) \cdot (-1) + \int_0^\ell \{-\mu a_{iy}(x, t)\} v_{iy}(x) dx + \int_0^\ell \{-\mu i_0^2 \ddot{\varphi}_{iy}(x, t)\} v'_{iy}(x) dx \\ & + \int_0^\ell \{-Sv'_{iy}(x, t)\} v'_{iy}(x) dx - \int_0^\ell M_{iy}(x, t) \kappa_{iy}(x) dx = 0. \end{aligned}$$

Here the first term is the work done by the shear force  $V_{iy}(0, t)$  on the translation of end  $i$ . The last term is the internal work done by the bending moment  $M_{iy}(x, t)$  on the curvature  $\kappa_{iy}(x) = M_{iy}(x)/EI$ . The second term is the work done by the (distributed) inertia force

$$-\mu a_{iy}(x, t) = -\mu \dot{v}_{iy}(x, t) = \mu \omega^2 \hat{v}_{iy} \sin(\omega t)$$

on the translation  $v_{iy}(x)$ . The third term is the work done by the (distributed) inertia moment

$$-\mu i_0^2 \ddot{\varphi}_{iy}(x, t) = -\mu i_0^2 \ddot{v}'_{iy}(x, t) = \mu i_0^2 \omega^2 \hat{v}'_{iy} \sin(\omega t)$$

on the rotation  $v'_{iy}(x)$  along the whole length of the beam just as before. The new, fourth term is the work done by the distributed moment from the normal force

$$-Sv'_{iy}(x, t) = -S\hat{v}'_{iy} \sin(\omega t)$$

on the rotation  $v'_{iy}(x)$ .

This, Eq. (3.49), and Eq (3.67) implies that the above work is

$$\delta W_{\text{ds}} = \left\{ -\hat{V}_{iyy} + \mu\omega^2 \int_0^\ell \hat{v}_{iy}(x)v_{iy}(x) dx + (\mu i_0^2 \omega^2 - S) \int_0^\ell \hat{v}'_{iy}(x)v'_{iy}(x) dx - \int_0^\ell \hat{M}_{iy}(x) \frac{M_{iy}(x)}{EI} dx \right\} \sin(\omega t) = 0. \quad (3.124)$$

Here, similarly to Subsection 3.2.2 and 3.8.1,

$$V_{iyy} = - \int_0^\ell \hat{M}_{iy}(x) \frac{M_{iy}(x)}{EI} dx.$$

Therefore, the amplitude of the dynamical shear force at end  $i$  caused by a harmonic translation of the same end, i.e. the entry 2,2 of the dynamical stiffness matrix  $\hat{\mathbf{K}}_{ij}^{\text{loc}}$  is

$$\begin{aligned} \hat{K}_{ij,22}^{\text{loc}} &= -\hat{V}_{iyy} = -V_{iyy} - \mu\omega^2 \int_0^\ell \hat{v}_{iy}(x)v_{iy}(x) dx - (\mu i_0^2 \omega^2 - S) \int_0^\ell \hat{v}'_{iy}(x)v'_{iy}(x) dx \\ &= K_{ij,22}^{\text{loc}} + S \int_0^\ell \hat{v}_{iy}(x)v_{iy}(x) dx - \mu\omega^2 \int_0^\ell \hat{v}_{iy}(x)v_{iy}(x) dx - \mu i_0^2 \omega^2 \int_0^\ell \hat{v}'_{iy}(x)v'_{iy}(x) dx. \end{aligned}$$

We can derive all the internal forces at the ends of the beam due to longitudinal and transverse (harmonic) translations and (harmonic) rotations of unit amplitudes of the ends in a similar way.

The elementary dynamical stiffness matrix of beam  $ij$  is

$$\boxed{\hat{\mathbf{K}}_{ij}^{\text{loc}}(\omega) = \mathbf{K}_{ij}^{\text{loc}} + \hat{\mathbf{K}}_{ij}^{\text{locG}}(\omega) - \omega^2 \left( \hat{\mathbf{M}}_{ij}^{\text{loc}}(\omega) + \hat{\mathbf{M}}_{ij}^{\text{loc}\varphi}(\omega) \right)}. \quad (3.125)$$

Here  $\mathbf{K}_{ij}^{\text{loc}}$  is the elementary statical stiffness matrix of beam  $ij$ ,  $\hat{\mathbf{K}}_{ij}^{\text{locG}}(\omega)$  is the elementary geometrical stiffness matrix and

$$\hat{\mathbf{K}}_{ij}^{\text{locG}}(\omega) = S \int_0^\ell \hat{\mathbf{N}}_\varphi'^T \mathbf{N}'_\varphi dx, \quad (3.126)$$

with the matrix of shape functions Eq. (3.118). This matrix related to the change of the geometry with respect to the straight unloaded case, and modifies the stiffness of the beam element.  $\hat{\mathbf{M}}_{ij}^{\text{loc}}(\omega)$  is the elementary mass matrix

$$\hat{\mathbf{M}}_{ij}^{\text{loc}}(\omega) = \mu \int_0^\ell \hat{\mathbf{N}}^T \mathbf{N} \, dx, \quad (3.127)$$

and  $\hat{\mathbf{M}}_{ij}^{\text{loc}\varphi}(\omega)$  is the elementary rotational mass matrix

$$\hat{\mathbf{M}}_{ij}^{\text{loc}\varphi}(\omega) = \mu i_0^2 \int_0^\ell \hat{\mathbf{N}}_\varphi'^T \mathbf{N}'_\varphi \, dx. \quad (3.128)$$

Finally we can say, that the dynamical elementary stiffness matrix equals to the statical elementary stiffness matrix plus the geometrical elementary stiffness matrix (3.126) minus the sum of the mass matrices (3.121), (3.122) times the square of the forcing frequency. This dynamical stiffness matrix is *frequency-dependent*! From Eq. (3.125) it can be verified, that the mass matrices  $\hat{\mathbf{K}}_{ij}^{\text{locG}}(\omega)$ ,  $\hat{\mathbf{M}}_{ij}^{\text{loc}}(\omega)$  and  $\hat{\mathbf{M}}_{ij}^{\text{loc}\varphi}(\omega)$  are *symmetric* and frequency dependent, and so is the dynamical stiffness matrix  $\hat{\mathbf{K}}_{ij}^{\text{loc}}(\omega)$ .

The calculation of the geometric stiffness matrix can be approximated with the static displacement functions. In this case we have to use the same matrix

$$\mathbf{N}'_\varphi = [ 0 \quad v'_{iy}(x) \quad v'_{i\varphi}(x) \quad 0 \quad v'_{jy}(x) \quad v'_{j\varphi}(x) ],$$

what we used for the calculation of the consistent rotational mass matrix: This way, the approximate geometric stiffness matrix is

$$\mathbf{K}_{\text{cons},ij}^{\text{locG}} = S \int_0^\ell \mathbf{N}'_\varphi'^T \mathbf{N}'_\varphi \, dx, \quad (3.129)$$

and the dynamical stiffness matrix can be approximated by

$$\hat{\mathbf{K}}_{ij}^{\text{loc}}(\omega) \approx (\mathbf{K}_{ij}^{\text{loc}} + \mathbf{K}_{\text{cons},ij}^{\text{locG}}) - \omega^2 (\mathbf{M}_{\text{cons},ij}^{\text{loc}} + \mathbf{M}_{\text{cons},ij}^{\text{loc}\varphi}).$$

Here we have to call the attention of the reader, that in the absence of harmonic forcing (i.e.  $\omega = 0$ ) the above stiffness matrix simplifies to

$$\hat{\mathbf{K}}_{ij}^{\text{loc}}(\omega) = (\mathbf{K}_{ij}^{\text{loc}} + \mathbf{K}_{\text{cons},ij}^{\text{locG}}),$$

which can be used for (statical) stability analysis of the structure. Eq. (3.129) provides the exact geometric stiffness matrix (however it requires the normal force  $S$  for its calculation which leads to an iterative solution in some cases). This sum of statical and geometric stiffness matrices allows stability analysis of a structure.

## Chapter 4

# Damping in structural dynamics

In real structures the energy of the vibrating system dissipates through various mechanisms, such as thermal effects of cyclic loading, internal friction of the body, friction at connections, opening and closing of microcracks, etc. [3]. It is very difficult to model all of these effects. Instead, in practice, a so-called *equivalent viscous damping* is often used, which stands for all the important energy dissipating components while remains still fairly easy to handle (see [3] for further details). In the case of viscous dampings, the energy dissipation is proportional to the loading frequency. However, laboratory cyclic loading experiments on structural metals, and vibration tests of real structures within the usual range of loading frequency show that the energy dissipation is essentially independent of the loading frequency. This observation has led to the development of *rate-independent (linear) damping* in structural design. (This damping is also called as structural damping, solid damping, or hysteretic damping.) Rate-independent damping is mainly associated with static hysteresis, which can arise from plastic strain, localized plastic deformations within the global elastic limit of the structure, for example [3]. Apart from the internal energy dissipation properties of the material, the friction of connections, etc., there can be real dashpots built in or attached to the structure. Even the surrounding soil has damping effects, which are often worth considering [6].

In this chapter we introduce some important concepts regarding the effects of damping on the vibrations of structures. We show how the steady-state vibration of a harmonically excited, damped MDOF system can be obtained by direct solution techniques. The idea of mass- and stiffness-proportional damping is introduced, which makes real modal analysis of the structure possible. Rate-independent damping is originated directly from the results of the real modal analysis of proportionally damped systems. Later on the damping effects of soil and the phenomenon of radiation damping is revealed. Finally, a widely used numerical procedure, the *Newmark* method is discussed.

## 4.1 Steady-state vibration of viscously damped systems

The system of differential equations of a (linearly) damped, forced MDOF system is given in the matrix form

$$\boxed{\mathbf{M}\ddot{\mathbf{u}}(t) + \mathbf{C}\dot{\mathbf{u}}(t) + \mathbf{K}\mathbf{u}(t) = \mathbf{q}(t)}. \quad (4.1)$$

Here  $\mathbf{M}$ ,  $\mathbf{C}$ , and  $\mathbf{K}$  are the mass, (linear, viscous) damping, and stiffness matrices of the system, respectively, while  $\mathbf{u}(t)$  contains the unknown displacements of the degrees of freedom. In the next subsection the direct solution of the above equation is given for harmonic loadings.

### 4.1.1 Harmonic excitation of damped MDOF systems

If the forcing varies harmonically with time, then the load in Eq. (4.1) is either  $\mathbf{q}(t) = \mathbf{q}_0 \sin(\omega t)$ , or  $\mathbf{q}(t) = \mathbf{q}_0 \cos(\omega t)$ , or a combination of sine and cosine functions with different amplitudes.

#### Sinusoidal excitation

First let us determine the particular solution of the sinusoidally forced mechanical model described by the second order matrix differential equation

$$\mathbf{M}\ddot{\mathbf{u}}(t) + \mathbf{C}\dot{\mathbf{u}}(t) + \mathbf{K}\mathbf{u}(t) = \mathbf{q}_0 \sin(\omega t). \quad (4.2)$$

The solution is searched for in the separated form

$$\mathbf{u}_f(t) = \mathbf{u}_{f1} \sin(\omega t) + \mathbf{u}_{f2} \cos(\omega t), \quad (4.3)$$

i.e. as a linear combination of sine and cosine functions with the same frequency  $\omega$  as the forcing. If we substitute the trial function (4.3) into Eq. (4.2), then we get

$$\begin{aligned} & -\omega^2 \mathbf{M} (\mathbf{u}_{f1} \sin(\omega t) + \mathbf{u}_{f2} \cos(\omega t)) + \omega \mathbf{C} (\mathbf{u}_{f1} \cos(\omega t) - \mathbf{u}_{f2} \sin(\omega t)) \\ & + \mathbf{K} (\mathbf{u}_{f1} \sin(\omega t) + \mathbf{u}_{f2} \cos(\omega t)) = \mathbf{q}_0 \sin(\omega t). \end{aligned} \quad (4.4)$$

Collecting the coefficients of sine and cosine in both sides we can obtain the following two equations:

$$\begin{aligned} & (-\omega^2 \mathbf{M} \mathbf{u}_{f1} - \omega \mathbf{C} \mathbf{u}_{f2} + \mathbf{K} \mathbf{u}_{f1}) \sin(\omega t) = \mathbf{q}_0 \sin(\omega t) \\ & (-\omega^2 \mathbf{M} \mathbf{u}_{f2} + \omega \mathbf{C} \mathbf{u}_{f1} + \mathbf{K} \mathbf{u}_{f2}) \cos(\omega t) = \mathbf{0}. \end{aligned}$$

The latter equation can be solved for  $\mathbf{u}_{f2}$ , and it is substituted back into the former one:

$$\begin{aligned} \mathbf{u}_{f2} &= -\omega (\mathbf{K} - \omega^2 \mathbf{M})^{-1} \mathbf{C} \mathbf{u}_{f1}, \\ (\mathbf{K} - \omega^2 \mathbf{M} + \omega^2 \mathbf{C} (\mathbf{K} - \omega^2 \mathbf{M})^{-1} \mathbf{C}) \mathbf{u}_{f1} &= \mathbf{q}_0 \\ \rightarrow \mathbf{u}_{f1} &= (\mathbf{K} - \omega^2 \mathbf{M} + \omega^2 \mathbf{C} (\mathbf{K} - \omega^2 \mathbf{M})^{-1} \mathbf{C})^{-1} \mathbf{q}_0. \end{aligned}$$

Therefore, the particular solution of this forced vibration is:

$$\begin{aligned} \mathbf{u}_f(t) = & \left( \mathbf{K} - \omega^2 \mathbf{M} + \omega^2 \mathbf{C} (\mathbf{K} - \omega^2 \mathbf{M})^{-1} \mathbf{C} \right)^{-1} \mathbf{q}_0 \sin(\omega t) \\ & - \omega (\mathbf{K} - \omega^2 \mathbf{M})^{-1} \mathbf{C} \left( \mathbf{K} - \omega^2 \mathbf{M} + \omega^2 \mathbf{C} (\mathbf{K} - \omega^2 \mathbf{M})^{-1} \mathbf{C} \right)^{-1} \mathbf{q}_0 \cos(\omega t). \end{aligned} \quad (4.5)$$

### Cosinusoidal excitation

The determination of the particular solution of the cosinusoidally forced mechanical model described by the second order matrix differential equation

$$\mathbf{M}\ddot{\mathbf{u}}(t) + \mathbf{C}\dot{\mathbf{u}}(t) + \mathbf{K}\mathbf{u}(t) = \mathbf{q}_0 \cos(\omega t) \quad (4.6)$$

goes in a very similar way. The solution is searched for in the separated form

$$\mathbf{u}_f(t) = \mathbf{u}_{f1} \sin(\omega t) + \mathbf{u}_{f2} \cos(\omega t) \quad (4.7)$$

again. We substitute the trial function (4.7) into Eq. (4.6):

$$\begin{aligned} -\omega^2 \mathbf{M} (\mathbf{u}_{f1} \sin(\omega t) + \mathbf{u}_{f2} \cos(\omega t)) + \omega \mathbf{C} (\mathbf{u}_{f1} \cos(\omega t) - \mathbf{u}_{f2} \sin(\omega t)) \\ + \mathbf{K} (\mathbf{u}_{f1} \sin(\omega t) + \mathbf{u}_{f2} \cos(\omega t)) = \mathbf{q}_0 \cos(\omega t). \end{aligned} \quad (4.8)$$

Collecting the coefficients of sine and cosine in both sides we can write the equations:

$$\begin{aligned} (-\omega^2 \mathbf{M} \mathbf{u}_{f1} - \omega \mathbf{C} \mathbf{u}_{f2} + \mathbf{K} \mathbf{u}_{f1}) \sin(\omega t) &= \mathbf{0} \\ (-\omega^2 \mathbf{M} \mathbf{u}_{f2} + \omega \mathbf{C} \mathbf{u}_{f1} + \mathbf{K} \mathbf{u}_{f2}) \cos(\omega t) &= \mathbf{q}_0 \cos(\omega t). \end{aligned}$$

The former equation can be solved for  $\mathbf{u}_{f1}$ , and it is substituted back into the latter one. Thus

$$\begin{aligned} \mathbf{u}_{f1} &= \omega (\mathbf{K} - \omega^2 \mathbf{M})^{-1} \mathbf{C} \mathbf{u}_{f2}, \\ \left( \mathbf{K} - \omega^2 \mathbf{M} + \omega^2 \mathbf{C} (\mathbf{K} - \omega^2 \mathbf{M})^{-1} \mathbf{C} \right) \mathbf{u}_{f2} &= \mathbf{q}_0 \\ \rightarrow \mathbf{u}_{f2} &= \left( \mathbf{K} - \omega^2 \mathbf{M} + \omega^2 \mathbf{C} (\mathbf{K} - \omega^2 \mathbf{M})^{-1} \mathbf{C} \right)^{-1} \mathbf{q}_0. \end{aligned}$$

Therefore, the particular solution of this forced vibration is:

$$\begin{aligned} \mathbf{u}_f(t) = & \omega (\mathbf{K} - \omega^2 \mathbf{M})^{-1} \mathbf{C} \left( \mathbf{K} - \omega^2 \mathbf{M} + \omega^2 \mathbf{C} (\mathbf{K} - \omega^2 \mathbf{M})^{-1} \mathbf{C} \right)^{-1} \mathbf{q}_0 \sin(\omega t) \\ & + \left( \mathbf{K} - \omega^2 \mathbf{M} + \omega^2 \mathbf{C} (\mathbf{K} - \omega^2 \mathbf{M})^{-1} \mathbf{C} \right)^{-1} \mathbf{q}_0 \cos(\omega t). \end{aligned} \quad (4.9)$$

### Sine and cosine forcing handled together

In order to handle both the sinusoidal and the cosinusoidal forcing together, we cannot avoid using complex functions. We write the force in the form of:

$$\mathbf{q}(t) = \mathbf{q}_0 \{ \cos(\omega t) + i \sin(\omega t) \} = \mathbf{q}_0 e^{i\omega t}.$$

Here  $i$  is the imaginary unit, satisfying  $i^2 = -1$ . The matrix differential equation of motion in this case is

$$\mathbf{M}\ddot{\tilde{\mathbf{u}}}(t) + \mathbf{C}\dot{\tilde{\mathbf{u}}}(t) + \mathbf{K}\tilde{\mathbf{u}}(t) = \mathbf{q}_0 e^{i\omega t}. \quad (4.10)$$

Notice, that now the vector of unknown displacements  $\tilde{\mathbf{u}}(t)$  can be complex, that is the reason why it is distinguished by a tilde from the previous, real vectors.

The particular solution is searched for in the separated form

$$\tilde{\mathbf{u}}_f(t) = \tilde{\mathbf{u}}_{f0} e^{i\omega t}. \quad (4.11)$$

We substitute the trial function (4.11) into Eq. (4.10):

$$(-\omega^2 \mathbf{M} + i\omega \mathbf{C} + \mathbf{K}) \tilde{\mathbf{u}}_{f0} e^{i\omega t} = \mathbf{q}_0 e^{i\omega t}. \quad (4.12)$$

Now the coefficient of the trial function (4.11) can be obtained by inversion:

$$\tilde{\mathbf{u}}_{f0} = (-\omega^2 \mathbf{M} + i\omega \mathbf{C} + \mathbf{K})^{-1} \mathbf{q}_0. \quad (4.13)$$

The final result is

$$\tilde{\mathbf{u}}_f(t) = \tilde{\mathbf{K}}^{-1} \mathbf{q}_0 e^{i\omega t}, \quad (4.14)$$

where

$$\tilde{\mathbf{K}} = \mathbf{K} - \omega^2 \mathbf{M} + i\omega \mathbf{C}$$

is the complex dynamic stiffness matrix of the damped system. The *real* and *imaginary parts* of solution (4.14) correspond to the *cosine* and *sine forcing*, respectively. This abstract approach leads to a simple formalism, therefore we prefer using it hereafter. However, we have to note that a complex matrix must be inverted in Eq. (4.13), thus the computation is not easier than in the previous cases when sine and cosine forcing were separately studied. If the reader is further interested in how to invert a complex matrix and whether these results really coincide with the previous ones, then they may read Appendix A.8.

As a conclusion, we can state that using complex functions leads to simpler formalism, but requires us to be familiar with complex algebra. In these cases, the complex algebra appeared because of the damping: the first derivative of the trial function (4.11) introduced the imaginary unit  $i$  into (4.10). We hardly need to say now that damping makes structural dynamics calculations much more difficult in general.

However, if the damping matrix is special, then both the homogeneous and the particular solutions of the forced system can be obtained using the mass-matrix-normalized modal shape vectors of the same system without damping. A special damping matrix means that it is proportional to the mass and/or stiffness matrices. In the following subsection we demonstrate the physical origin of this proportionality.

## 4.2 Mass- and stiffness-proportional damping

### 4.2.1 The *Kelvin-Voigt* material

If the material is such that it can be described by the *Kelvin-Voigt* model, then the stress  $\sigma$ , the strain  $\varepsilon$ , and its derivative with respect to time  $t$  are related by

$$\sigma = E\varepsilon + \alpha E\dot{\varepsilon}.$$

Here  $\alpha$  is a material parameter, and  $\alpha E$  is the (internal) viscous damping of the material. This equation can also be applied to shear stresses. However, our beams are unsharable, so we only deal with the normal stresses.

Normal stresses are associated with normal force and bending moment in planar frame members. Thus the above constitutive law implies that the (internal) normal force and bending moment are

$$\boxed{N(x, t) = EA\varepsilon(x, t) + \alpha EA\dot{\varepsilon}(x, t), \quad M(x, t) = EI\kappa(x, t) + \alpha EI\dot{\kappa}(x, t)}. \quad (4.15)$$

### 4.2.2 Stiffness of a damped beam made of *Kelvin-Voigt* material

Let us examine a beam that is made of *Kelvin-Voigt* material, and that is further damped by a continuously distributed (external) viscous damping, which is constant along the length of the beam. This damping is denoted by  $\zeta$ . We derive the dynamic stiffness matrix of the beam member using the principle of virtual displacements. We use the same steps as in Section 3.2, but with the damping considered. We show how to obtain one entry, namely entry 2,2 of the dynamic stiffness matrix. Here the first index is the “place”, thus we need the shear force at end  $i$ , while the second index is the “cause”, which is the translation of end  $i$  along  $y$ . Therefore we need to compute the shear force of end  $i$  of a beam that vibrates so that the translation of its end  $i$  is  $v_{iy}(0, t) = 1 \cdot e^{i\omega t}$ , while all other displacements of its ends are zero <sup>1</sup> (see Figure 4.1 top).

We assume that the vibration of the beam can be written as a function of separated variables  $x$  and  $t$ :

$$v_{iy}(x, t) = \tilde{v}_{iy}(x) e^{i\omega t}.$$

The dynamic shape function  $\tilde{v}_{iy}(x)$  can be complex in the presence of damping. It is distinguished with an overtilde from the real-valued dynamic shape function of the undamped case (for which a hat was used instead). The end-of-beam internal forces can also be written in separated forms:

$$\begin{aligned} N_{iy}(0, t) &= \tilde{N}_{iiy} e^{i\omega t}, & V_{iy}(0, t) &= \tilde{V}_{iiy} e^{i\omega t}, & M_{iy}(0, t) &= \tilde{M}_{iiy} e^{i\omega t}, \\ N_{iy}(\ell, t) &= \tilde{N}_{jiy} e^{i\omega t}, & V_{iy}(\ell, t) &= \tilde{V}_{jiy} e^{i\omega t}, & M_{iy}(\ell, t) &= \tilde{M}_{jiy} e^{i\omega t}. \end{aligned} \quad (4.16)$$

These end-of-beam forces and the bending moment diagram at a certain time instant  $t$  are sketched at the bottom of Figure 4.1.

<sup>1</sup>Note that upright  $i$  denotes the *imaginary unit*, while italic subscript  $i$  refers to end  $i$  of the beam.



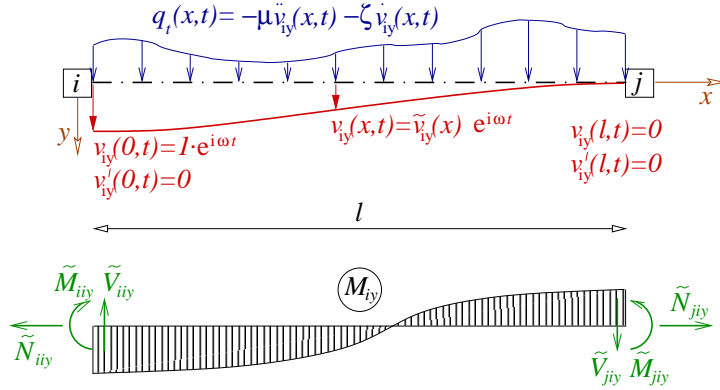


**Figure 4.1:** (top) Sketch of the deformed shape of a beam due to a dynamic vibration of end  $i$  along axis  $y$ . The beam is continuously damped with a viscous damping of coefficient  $\zeta$ . (bottom) The corresponding bending moment diagram and the positive definition of the internal forces at the ends of the beam.

The computation of the end-of-beam shear force  $\tilde{V}_{iyy}$  is based on the principle of virtual displacements. At time instant  $t$ , we apply the fictitious force

$$q_t(x, t) = -\mu\ddot{v}_{iy}(x, t) - \zeta\dot{v}_{iy}(x, t)$$

originated from the inertial mass and the damping, as shown in Figure 4.1. Thus we have a statically admissible force system: the internal forces and the fictitious force are in equilibrium. We take the (static) displacement system  $v_{iy}(x)$  caused by a unit translation of end  $i$  (shown in Figure 3.4) as the virtual displacement system. We compute the virtual work that the force system shown in Figure 4.1 does on this (virtual) displacement system at time instant  $t$ :

$$\delta W_{\text{ds}} = V_{iy}(0, t) \cdot (-1) + \int_0^\ell \{-\mu\ddot{v}_{iy}(x, t) - \zeta\dot{v}_{iy}(x, t)\}v_{iy}(x) dx - \int_0^\ell M_{iy}(x, t)\kappa_{iy}(x) dx = 0.$$

Here the first term is the work done by the shear force  $V_{iy}(0, t)$  on the virtual translation of end  $i$ . The last term is the internal work done by the bending moment  $M_{iy}(x, t) = EI\kappa_{iy}(x, t) + \alpha EI\dot{\kappa}_{iy}(x, t) = -EI\{1 + i\omega\alpha\}\tilde{v}_{iy}''(x)e^{i\omega t}$  on the virtual curvature  $\kappa_{iy}(x) = -v_{iy}''(x)$ . The second term is the work done by the (distributed) fictitious force

$$q_t(x, t) = -\mu\ddot{v}_{iy}(x, t) - \zeta\dot{v}_{iy}(x, t) = \mu\omega^2\tilde{v}_{iy}(x)e^{i\omega t} - i\omega\zeta\tilde{v}_{iy}(x)e^{i\omega t}$$

on the virtual translation  $v_{iy}(x)$  along the whole length of the beam. Thus, the above work can be written as

$$\delta W_{\text{ds}} = \left\{ -\tilde{V}_{iyy} + \mu\omega^2 \int_0^\ell \tilde{v}_{iy}(x)v_{iy}(x) dx - i\zeta\omega \int_0^\ell \tilde{v}_{iy}(x)v_{iy}(x) dx - EI \int_0^\ell \tilde{v}_{iy}''(x)v_{iy}''(x) dx - i\alpha\omega EI \int_0^\ell \tilde{v}_{iy}''(x)v_{iy}''(x) dx \right\} e^{i\omega t} = 0. \quad (4.17)$$

Finally, we can express the amplitude of the dynamic shear force at end  $i$  caused by the vibration  $e^{i\omega t}$  of end  $i$ . Due to the positive definition of the end-of-beam internal forces, and of the entries of the elementary stiffness matrix (see (3.66)), this shear force is the opposite of entry 2,2 of the dynamic stiffness matrix:

$$\begin{aligned} \tilde{K}_{ij,22}^{\text{loc}} = -\tilde{V}_{iiy} = & EI \int_0^\ell \tilde{v}_{iy}''(x)v_{iy}''(x) dx - \mu\omega^2 \int_0^\ell \tilde{v}_{iy}(x)v_{iy}(x) dx \\ & + i\alpha\omega EI \int_0^\ell \tilde{v}_{iy}''(x)v_{iy}''(x) dx + i\zeta\omega \int_0^\ell \tilde{v}_{iy}(x)v_{iy}(x) dx. \end{aligned}$$

As we can see, the dynamic stiffness is complex, which originates from the damping effects. That is the reason why we distinguish the elementary dynamic stiffness matrix by an overtilde for the damped case.

Similarly to (3.70), we can collect the (damped) dynamic shape functions into the matrix

$$\tilde{\mathbf{N}} = \begin{bmatrix} \tilde{u}_{ix}(x) & 0 & 0 & \tilde{u}_{jx}(x) & 0 & 0 \\ 0 & \tilde{v}_{iy}(x) & \tilde{v}_{i\varphi}(x) & 0 & \tilde{v}_{jy}(x) & \tilde{v}_{j\varphi}(x) \end{bmatrix}. \quad (4.18)$$

Following the earlier used definitions (3.23)–(3.27) and the notation  $\tilde{\mathbf{B}} = \mathbf{L}\tilde{\mathbf{N}}$ , the whole elementary dynamic stiffness matrix of beam  $ij$  is

$$\tilde{\mathbf{K}}_{ij}^{\text{loc}}(\omega) = (1 + i\alpha\omega) \int_0^\ell \tilde{\mathbf{B}}^T \mathbf{D} \mathbf{B} dx - (\omega^2 - i\beta\omega)\mu \int_0^\ell \tilde{\mathbf{N}}^T \mathbf{N} dx, \quad (4.19)$$

where

$$\beta = \zeta/\mu.$$

We can substitute the (damped) dynamic shape functions with the static ones in order to approximate the stiffness matrix as

$$\tilde{\mathbf{K}}_{ij}^{\text{loc}}(\omega) \approx (1 + i\alpha\omega)\mathbf{K}_{ij}^{\text{loc}} - (\omega^2 - i\beta\omega)\mathbf{M}_{\text{cons},ij}^{\text{loc}}. \quad (4.20)$$

Here  $\mathbf{K}_{ij}^{\text{loc}}$  and  $\mathbf{M}_{\text{cons},ij}^{\text{loc}}$  are the static stiffness and the consistent mass matrices of the beam, respectively. The complex part of the approximate stiffness matrix is the (approximate) elementary damping matrix

$$\mathbf{C}_{ij}^{\text{loc}} = \alpha\mathbf{K}_{ij}^{\text{loc}} + \beta\mathbf{M}_{\text{cons},ij}^{\text{loc}}. \quad (4.21)$$

Since this (approximate) damping matrix is proportional both to the static stiffness matrix (3.27) and to the consistent mass matrix (3.74), it is often called the *mass- and stiffness-proportional damping matrix*. If this approximate version of the dynamic stiffness matrix is applied, then we have to use beam members short enough to estimate the dynamic behaviour of the structure accurately. If the structure is not subjected to harmonic excitation, but to an arbitrary forcing, we can still use the approximate, (stiffness) consistent mass matrix, the static

stiffness matrix, and the proportional damping matrix (4.21) with sufficiently short beam members.

Finally, it is worth noting that the stiffness-proportional damping is originated from the material behaviour, while the mass-proportional damping is due to external viscous damping. The mass-proportional damping appears for example when the structure is in viscous fluid (in water, for instance).

If all the frame members are of the same (*Kelvin-Voigt*) material (thus  $\alpha$  is the same for each beam), and the external damping is also the same for each member (therefore  $\beta$  is also the same for all of the members), then the total damping matrix of the structure is proportional to both the total stiffness and mass matrices of the structure. In this special case, the system of equations of motion (4.1) is simplified to the form

$$\boxed{\mathbf{M}\ddot{\mathbf{u}}(t) + (\alpha\mathbf{K} + \beta\mathbf{M})\dot{\mathbf{u}}(t) + \mathbf{K}\mathbf{u}(t) = \mathbf{q}(t)}. \quad (4.22)$$

The advantage of this formulation is that it can be solved with (real) modal analysis, as shortly reviewed in the next subsection.

### 4.2.3 Real modal analysis of proportionally damped systems

#### Free vibration

Let us consider the homogeneous part of Eq. (4.22):

$$\mathbf{M}\ddot{\mathbf{u}}_h(t) + (\alpha\mathbf{K} + \beta\mathbf{M})\dot{\mathbf{u}}_h(t) + \mathbf{K}\mathbf{u}_h(t) = \mathbf{0}. \quad (4.23)$$

We recall the results of Subsection 3.6.1. There is a new variable  $\mathbf{y}_h(t) = [y_{h1}(t) \ y_{h2}(t) \ \dots \ y_{hN}(t)]^T$  introduced as

$$\mathbf{u}_h(t) = \mathbf{U}\mathbf{y}_h(t).$$

Here  $\mathbf{U}$  is the modal matrix, that contains the mass-matrix-normalized eigenvectors of the same, but undamped system. See Eq. (3.91). Using this new variable in the homogeneous equation (4.23), and multiplying it by the transpose of  $\mathbf{U}$  from the left we get:

$$\mathbf{U}^T\mathbf{M}\mathbf{U}\ddot{\mathbf{y}}_h(t) + (\alpha\mathbf{U}^T\mathbf{K}\mathbf{U} + \beta\mathbf{U}^T\mathbf{M}\mathbf{U})\dot{\mathbf{y}}_h(t) + \mathbf{U}^T\mathbf{K}\mathbf{U}\mathbf{y}_h(t) = \mathbf{U}^T\mathbf{0}.$$

According to the orthogonality of  $\mathbf{U}$  to  $\mathbf{M}\mathbf{U}$  and  $\mathbf{K}\mathbf{U}$  (see Eq. (3.94)), the above system of equations splits into  $N$  independent homogeneous equations of motion:

$$\ddot{y}_{hj}(t) + (\alpha\omega_{0j}^2 + \beta)\dot{y}_{hj}(t) + \omega_{0j}^2 y_{hj}(t) = 0, \quad j = 1, 2, \dots, N.$$

These SDOF, damped, free vibrations can be solved for  $y_{hj}(t)$ . If the damping is small for every  $j$ , then the previously derived solution of each damped SDOF system (repeated from Eq. (1.7))

$$y_h(t) = e^{-\xi\omega_0 t} \{A \cos(\omega_0^* t) + B \sin(\omega_0^* t)\}$$

can be used with the substitutions

$$m = 1, \quad c = \alpha\omega_{0j}^2 + \beta, \quad k = \omega_{0j}^2, \\ \xi = \frac{c_j}{2\sqrt{k_j m_j}} = \frac{\alpha\omega_{0j}^2 + \beta}{2\omega_{0j}}, \quad \omega_0^* = \omega_{0j}\sqrt{1 - \xi_j^2} = \omega_{0j}\sqrt{1 - \left(\frac{\alpha\omega_{0j}^2 + \beta}{2\omega_{0j}}\right)^2}. \quad (4.24)$$

Thus the free vibrations in the modal space (if all the modal oscillators are underdamped, i.e.  $\xi_j < 1$ ) is:

$$y_{hj}(t) = e^{-\frac{\alpha\omega_{0j}^2 + \beta}{2}t} \left\{ A_j \cos \left( \omega_{0j}\sqrt{1 - \left(\frac{\alpha\omega_{0j}^2 + \beta}{2\omega_{0j}}\right)^2} t \right) \right. \\ \left. + B_j \sin \left( \omega_{0j}\sqrt{1 - \left(\frac{\alpha\omega_{0j}^2 + \beta}{2\omega_{0j}}\right)^2} t \right) \right\}. \quad (4.25)$$

We note here that the  $j$ th logarithmic decrement (1.1.2) is

$$\vartheta_j = \ln \frac{y_{hj}(t)}{y_{hj}(t + T_{0j}^*)} = 2\pi \frac{\xi_j}{\sqrt{1 - \xi_j^2}} = \pi \frac{\alpha\omega_{0j}^2 + \beta}{\omega_{0j}\sqrt{1 - \left(\frac{\alpha\omega_{0j}^2 + \beta}{2\omega_{0j}}\right)^2}}. \quad (4.26)$$

Finally, the solution for  $\mathbf{u}_h(t)$  is obtained by transforming back  $\mathbf{y}_h(t)$  from the modal space:

$$\mathbf{u}_h(t) = \mathbf{U}\mathbf{y}_h(t).$$

The free parameters  $A_j$  and  $B_j$  ( $j = 1, 2, \dots, N$ ) can be determined from the initial values of  $\mathbf{u}_h(0)$  and  $\dot{\mathbf{u}}_h(0)$ .

We have to emphasize that the final results given here (and also the logarithmic decrement) is for the case of *small modal damping*. If there are some large modal damping coefficients, then we have to modify (4.25) for some  $j$ .

### Forced vibration

The particular solution of the forced vibration (4.22) can also be derived using the modal matrix  $\mathbf{U}$  of the same, but undamped system. Substituting  $\mathbf{u}(t) = \mathbf{U}\mathbf{y}_f(t)$  into (4.22) and multiplying it by  $\mathbf{U}^T$  from the left yields

$$\mathbf{U}^T \mathbf{M} \mathbf{U} \ddot{\mathbf{y}}_f(t) + (\alpha \mathbf{U}^T \mathbf{K} \mathbf{U} + \beta \mathbf{U}^T \mathbf{M} \mathbf{U}) \dot{\mathbf{y}}_f(t) + \mathbf{U}^T \mathbf{K} \mathbf{U} \mathbf{y}_f(t) = \mathbf{U}^T \mathbf{q}(t).$$

The mass-matrix-normalized eigenvectors of the undamped system  $\mathbf{U} = [\mathbf{u}_1 \ \mathbf{u}_2 \ \dots \ \mathbf{u}_N]$  are orthogonal to  $\mathbf{M}\mathbf{U}$  and  $\mathbf{K}\mathbf{U}$  (see Eq. (3.94)). Therefore, the above system of equations splits into independent equations of motion:

$$\ddot{y}_{fj}(t) + (\alpha\omega_{0j}^2 + \beta) \dot{y}_{fj}(t) + \omega_{0j}^2 y_{fj}(t) = \mathbf{u}_j^T \mathbf{q}(t) = f_j(t), \quad j = 1, 2, \dots, N. \quad (4.27)$$

**Arbitrary forcing** If the load  $\mathbf{q}(t)$  is an arbitrary function of time, then each of the equations (4.27) can be solved separately by using the *Duhamel's* integral (1.26)

$$y_{fj}(t) = \frac{1}{m_j \omega_{0j}^*} \int_0^t f_j(\tau) e^{-\xi_j \omega_{0j} \{t-\tau\}} \sin(\omega_{0j}^* \{t-\tau\}) d\tau$$

with the substitutions (4.24) and  $f_j(t) = \mathbf{u}_j^T \mathbf{q}(t)$ . Thus

$$y_{fj}(t) = \frac{1}{\omega_{0j} \sqrt{1 - \left(\frac{\alpha \omega_{0j}^2 + \beta}{2\omega_{0j}}\right)^2}} \times \int_0^t \mathbf{u}_j^T \mathbf{q}(\tau) e^{\frac{-\alpha \omega_{0j}^2 - \beta}{2} \{t-\tau\}} \sin\left(\omega_{0j} \sqrt{1 - \left(\frac{\alpha \omega_{0j}^2 + \beta}{2\omega_{0j}}\right)^2} \{t-\tau\}\right) d\tau. \quad (4.28)$$

**Harmonic forcing** If the loading  $\mathbf{q}(t)$  in Eq. (4.27) is harmonic, for instance if

$$\mathbf{q}(t) = \mathbf{q}_0 \sin(\omega t),$$

then Eq. (4.27) becomes

$$\ddot{y}_{fj}(t) + (\alpha \omega_{0j}^2 + \beta) \dot{y}_{fj}(t) + \omega_{0j}^2 y_{fj}(t) = \mathbf{u}_j^T \mathbf{q}_0 \sin(\omega t), \quad j = 1, 2, \dots, N.$$

According to (1.13) and (4.24), the solution for  $y_{fj}(t)$  in the case of this harmonic forcing is

$$y_{fj}(t) = \frac{\mathbf{u}_j^T \mathbf{q}_0}{k_j} \frac{1}{\sqrt{\left(1 - \frac{\omega^2}{\omega_{0j}^2}\right)^2 + \left(2\xi_j \frac{\omega}{\omega_{0j}}\right)^2}} \sin\left(\omega t - \operatorname{arccot} \frac{1 - \frac{\omega^2}{\omega_{0j}^2}}{2\xi_j \frac{\omega}{\omega_{0j}}}\right) \\ = \frac{\mathbf{u}_j^T \mathbf{q}_0}{\omega_{0j}^2} \frac{1}{\sqrt{\left(1 - \frac{\omega^2}{\omega_{0j}^2}\right)^2 + \left(\alpha \omega + \beta \frac{\omega}{\omega_{0j}^2}\right)^2}} \sin\left(\omega t - \operatorname{arccot} \frac{1 - \frac{\omega^2}{\omega_{0j}^2}}{\alpha \omega + \beta \frac{\omega}{\omega_{0j}^2}}\right) \quad (4.29)$$

If we have solved Eq. (4.27) for a given load, then the particular solution of the original system of equations (4.22) is obtained simply by transforming the results back from the modal space:

$$\mathbf{u}_f(t) = \mathbf{U} \mathbf{y}_f(t).$$

If one needs to take initial conditions into account, then the sum of the homogeneous and particular solutions are needed, and the initial conditions should be used to determine the free parameters of the homogeneous solution. (Modal analysis is the recommended tool for this.)

### 4.3 Rate-independent damping

Damping of structural materials are considered to be small and frequency independent according to experiments. Laboratory tests and on-site measurements recorded that the logarithmic decrement (the rate of the vibration amplitude decaying) is *frequency independent*. For example, the same logarithmic decrement,  $\vartheta \approx 0.01$ , is measured in case of steel beams of different natural circular frequencies (i.e. different lengths and cross-sections). For standard structural materials it is around  $\vartheta = 0.01 \dots 0.1$ .

Previously we assumed that the damping is proportional to the mass and stiffness matrices. This led to *frequency-dependent* logarithmic decrement (4.26) for each vibration component in the modal space. If we want to take our result closer to the reality, first we set  $\beta = 0$ , since the mass-proportional damping was originated from external dampers, and now we are interested in the damping properties of the building material. If  $\beta = 0$ , then the logarithmic decrement (4.26) simplifies to

$$\vartheta_j = \frac{\alpha \omega_{0j}}{\sqrt{1 - \left(\frac{\alpha \omega_{0j}}{2}\right)^2}} \pi.$$

Second, we *formally set*

$$\alpha := \frac{2\bar{\xi}}{\omega_{0j}}. \quad (4.30)$$

(This is a rude step, it should be thought of as if the frequency dependency of the logarithmic decrement were “penalized”.) With these assumptions the logarithmic decrement really becomes *frequency independent*:

$$\vartheta_j = \frac{2\bar{\xi}\pi}{\sqrt{1 - \bar{\xi}^2}}.$$

Here  $\bar{\xi}$  is called the *structural damping coefficient*. It depends only on the material type. It has *small* values for building materials (it is around 0.01 for reinforced concrete, for example). Therefore, we can approximate  $\sqrt{1 - \bar{\xi}^2} \approx 1$ , and we can estimate  $\bar{\xi}$  from the measured logarithmic decrement as

$$\bar{\xi} \approx \frac{\vartheta_j}{2\pi}.$$

(Note that in BSc Dynamics we used  $\gamma := \vartheta_j/\pi \approx 2\bar{\xi}$  as structural damping coefficient.)

#### 4.3.1 Real modal analysis in case of rate-independent damping

Rate-independent damping is a special proportional damping with  $\beta = 0$  and  $\alpha = 2\bar{\xi}/\omega_{0j}$ . Therefore the results of proportionally damped systems can be directly applied, we only need to substitute  $\beta = 0$  and  $\alpha = 2\bar{\xi}/\omega_{0j}$  into the final results of Subsection 4.2.3.

The free vibration of a rate-independently damped MDOF system is given by the homogeneous solution (4.25) of (4.23) with  $\beta = 0$  and  $\alpha = 2\bar{\xi}/\omega_{0j}$ :

$$y_{hj}(t) = e^{-\bar{\xi}\omega_{0j}t} \{A_j \cos(\omega_{0j}^*t) + B_j \sin(\omega_{0j}^*t)\},$$

where

$$\omega_{0j}^* = \omega_{0j} \sqrt{1 - \bar{\xi}^2}.$$

The particular solution of the arbitrary forced system with rate-independent damping is (4.28) with  $\beta = 0$  and  $\alpha = 2\bar{\xi}/\omega_{0j}$

$$y_{fj}(t) = \frac{1}{\omega_{0j}^*} \int_0^t \mathbf{u}_j^T \mathbf{q}(\tau) e^{-\bar{\xi}\omega_{0j}(t-\tau)} \sin(\omega_{0j}^* \{t - \tau\}) d\tau,$$

while the particular solution of the rate-independently damped, sinusoidally excited system ((4.22) with  $\mathbf{q}(t) = \mathbf{q}_0 \sin(\omega t)$ ) is from (4.29)

$$y_{fj}(t) = \frac{\mathbf{u}_j^T \mathbf{q}_0}{\omega_{0j}^2} \frac{1}{\sqrt{\left(1 - \frac{\omega^2}{\omega_{0j}^2}\right)^2 + \left(2\bar{\xi} \frac{\omega}{\omega_{0j}}\right)^2}} \sin\left(\omega t - \operatorname{arccot} \frac{1 - \frac{\omega^2}{\omega_{0j}^2}}{2\bar{\xi} \frac{\omega}{\omega_{0j}}}\right).$$

### 4.3.2 Direct solution of rate-independently damped systems

We search for the particular solution of the stiffness-proportionally damped, harmonically excited system

$$\mathbf{M}\ddot{\tilde{\mathbf{u}}}(t) + \alpha\mathbf{K}\dot{\tilde{\mathbf{u}}}(t) + \mathbf{K}\tilde{\mathbf{u}}(t) = \mathbf{q}_0 (\cos(\omega t) + i \sin(\omega t)) = \mathbf{q}_0 e^{i\omega t} \quad (4.31)$$

in the complex form

$$\tilde{\mathbf{u}}_f(t) = \tilde{\mathbf{u}}_{f0} e^{i\omega t}. \quad (4.32)$$

Substituting the above trial function into (4.31) yields

$$(-\omega^2 \mathbf{M} + i\alpha\omega \mathbf{K} + \mathbf{K}) \tilde{\mathbf{u}}_{f0} e^{i\omega t} = \mathbf{q}_0 e^{i\omega t}.$$

We can turn the damping associated term  $i\alpha\omega \mathbf{K}$  into frequency independent by setting

$$\alpha := \frac{2\bar{\xi}}{\omega},$$

where  $\bar{\xi}$  is the previously introduced structural damping coefficient.

With that choice the complex, linear system of equation to solve for the unknown coefficient  $\tilde{\mathbf{u}}_{f0}$  of the trial function (4.32) is

$$\left(\tilde{\mathbf{K}}_{\text{st}} - \omega^2 \mathbf{M}\right) \tilde{\mathbf{u}}_{f0} = \mathbf{q}_0,$$

where

$$\tilde{\mathbf{K}}_{\text{st}} = (1 + i 2\bar{\xi})\mathbf{K} \quad (4.33)$$

is the *complex (static) stiffness matrix*. Finally, the particular solution of (4.31) is

$$\tilde{\mathbf{u}}_f(t) = \left( \tilde{\mathbf{K}}_{\text{st}} - \omega^2 \mathbf{M} \right)^{-1} \mathbf{q}_0 e^{i\omega t},$$

the real part of which corresponds to the cosine excitation  $\mathbf{q}_0 \cos(\omega t)$ , while the imaginary part is due to the sine excitation  $\mathbf{q}_0 \sin(\omega t)$ . As we can see, a complex, frequency-dependent matrix has to be inverted in order to obtain the solution. The complex part of this matrix is originated from damping, while the frequency-dependence is purely from the inertial effects.

The damping now is not a linear, viscous one, but a special, proportional one: the rate-independent (or structural) damping. In this special case, the damping and stiffness matrices can be combined into the complex stiffness matrix (4.33). With the aid of this complex matrix, the equations of motion of the forced system can be written in a short form:

$$\mathbf{M}\ddot{\tilde{\mathbf{u}}}(t) + \tilde{\mathbf{K}}_{\text{st}}\tilde{\mathbf{u}}(t) = \tilde{\mathbf{q}}(t). \quad (4.34)$$

Notice that there is not any velocity vector and damping matrix in the above equation formally. But damping is present, it is built in the complex, frequency-independent static stiffness matrix  $\tilde{\mathbf{K}}_{\text{st}}$ .

## 4.4 Equivalent rate-independent damping

In the case of mass- and stiffness-proportional damping, the matrix differential equation of the structure can be written as (4.22) only if all the structural elements have the same damping properties. If that is not the case, then the elementary damping matrix of a frame member is still proportional to its elementary stiffness and mass matrices, but the compiled, total damping matrix of the structure is not proportional to the total mass and stiffness matrices.

The direct solution given in Subsection 4.1.1 still works for this case, but inverting a large matrix requires very high computational capacities, and for a large number of DOF it is not always technically feasible. The problem with structures not having uniform elementary damping mechanisms is that the matrix differential equation they lead to cannot be solved by real modal analysis. In these cases the much more difficult complex modal analysis should be used, but the discussion of this method is beyond the scope of this textbook. For large systems the reduced (complex) modal analysis, numerical time integration techniques, or Fast *Fourier* Transformations can be applied.

However, we show an *approximate method*, which is often used for cases when the damping is proportional to the (elementary) stiffness matrices. This technique is based on the determination of *equivalent structural damping coefficients*, which can be later used in real modal analysis. The equivalent damping coefficient for the  $r$ th mode can be computed as [6]

$$\bar{\xi}_{\text{eq},r} = \frac{\sum_{ij} \bar{\xi}_{ij} \mathbf{u}_{r,ij}^T \mathbf{K}_{ij} \mathbf{u}_{r,ij}}{\sum_{ij} \mathbf{u}_{r,ij}^T \mathbf{K}_{ij} \mathbf{u}_{r,ij}}. \quad (4.35)$$

Here  $\mathbf{K}_{ij}$  is the elementary stiffness matrix of beam  $ij$ ,  $\bar{\xi}_{ij}$  is the structural damping coefficient of beam  $ij$ . The vector  $\mathbf{u}_r$  is the  $r$ th eigenvector of the structure without damping, and  $\mathbf{u}_{r,ij}$  contains its entries corresponding to the end nodes of beam  $ij$ .



### 4.4.1 Quasi-modal analysis for equivalent rate-independent damping

The results of Subsection 4.3.1 can be directly applied for structures which are not made of the same building material, but for each material rate-independent damping holds. We only need to replace  $\bar{\xi}$  with the equivalent structural damping coefficient (4.35) of the corresponding mode. We have to emphasize that this gives an *estimate result*, which can be quite inaccurate. It is also important that the applicable value of equivalent rate-independent damping is maximized by building codes for structural design.

## 4.5 Dynamics of soil, the equivalent soil bar

In this chapter we introduce an estimate method to model the vibration of soils. Instead of investigating the stress and strain distribution in an elastic half-space, we assume that the normal stress distribution is constant in a given depth and it propagates within an exponential envelope in the vertical direction, as it was suggested by Wolf [13]. This simplified, planar soil bar model is shown in Figure 4.2.

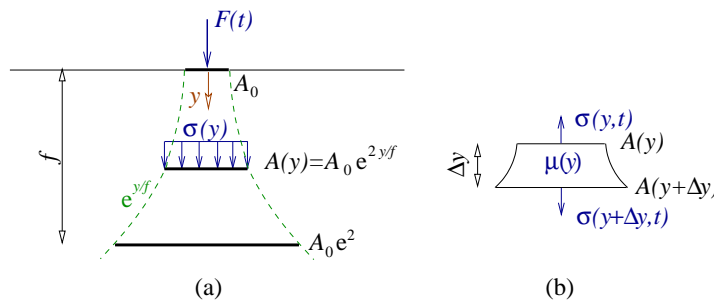


**Figure 4.2:** (a) Assumed stress propagation in the equivalent soil bar and (b) the free-body diagram of a slice of the bar

On the ground level there is rigid disk of area  $A_0 = R^2\pi$ , where  $R$  is the radius. If there is a constant vertical force  $F_0$  on the top of this plate, then the normal stress on the top level is  $\sigma_0 = F_0/A_0$ . It is supposed that at depth  $y$  the normal stress is constant within the envelope, i.e. it is constant on the circular area

$$A(y) = (R e^{y/f})^2\pi = A_0 e^{2y/f}, \quad (4.36)$$

and zero outside of it. Here  $f$  denotes the characteristic depth of the soil bar. It is computed from the condition that the static stiffness of the model is the same as the static stiffness obtained from the solution of the classical problem of elasticity: a disk lying on an elastic half-space. The model is called the *equivalent soil bar*.

First we derive the differential equation of motion of the equivalent soil bar. Then we calibrate our model by fitting its static stiffness to the *Boussinesq* solution through the characteristic depth  $f$ . Finally, the normal force on the top due to a harmonic vibration of unit amplitude of the top is computed from the equation of motion, leading to the *dynamic stiffness of the soil bar* by definition.

### 4.5.1 Differential equation of the equivalent soil bar

#### Free vibration of the soil model

We cut the soil model with two horizontal plane being  $\Delta y$  apart from each other. *Newton's* second law of motion is written for this piece of the soil bar:

$$-\sigma(y, t)A(y) + \sigma(y + \Delta y, t)A(y + \Delta y) = \rho A(y)\Delta y \frac{\partial^2 v(y, t)}{\partial t^2}. \quad (4.37)$$

Here  $\mu(y) = \rho A(y)$  is the mass distribution of the model. The mass of the cut was approximated by  $\mu(y)\Delta y$  in the previous equation (which is accurate if  $\Delta y \rightarrow 0$ ). The *Taylor* expansions of  $\sigma(y, t)$  and  $A(y)$  with respect to  $y$  are:

$$\begin{aligned} \sigma(y + \Delta y, t) &= \sigma(y, t) + \frac{\partial \sigma(y, t)}{\partial y} \Delta y + \mathcal{O}(\Delta y^2), \\ A(y + \Delta y) &= A(y) + \frac{dA(y)}{dy} \Delta y + \mathcal{O}(\Delta y^2). \end{aligned}$$

Substituting these equalities in Eq. (4.37), dividing it by  $\Delta y$  and tending  $\Delta y \rightarrow 0$  yields

$$\sigma(y, t) \frac{dA(y)}{dy} + \frac{\partial \sigma(y, t)}{\partial y} A(y) = \rho A(y) \frac{\partial^2 v(y, t)}{\partial t^2}. \quad (4.38)$$

The constitutive law is

$$\sigma(y, t) = E_c \frac{\partial v(y, t)}{\partial y},$$

where  $E_c$  is the *constrained modulus*

$$E_c = \frac{1 - \nu}{(1 + \nu)(1 - 2\nu)} E \quad (4.39)$$

corresponding to the general spatial stress state. Here  $E$  is the *Young's* modulus, and  $\nu$  is the *Poisson's* ratio of the soil. <sup>2</sup> This equation is substituted in Eq. (4.38):

$$E_c \frac{\partial v(y, t)}{\partial y} \frac{dA(y)}{dy} + E_c \frac{\partial^2 v(y, t)}{\partial y^2} A(y) = \rho A(y) \frac{\partial^2 v(y, t)}{\partial t^2}.$$

Now we divide the above expression by  $E_c A(y)$  and introduce  $c_n = \sqrt{E_c/\rho}$ :

$$\frac{\partial^2 v(y, t)}{\partial y^2} + \frac{\partial v(y, t)}{\partial y} \frac{dA(y)}{dy} \frac{1}{A(y)} = \frac{1}{c_n^2} \frac{\partial^2 v(y, t)}{\partial t^2}.$$

<sup>2</sup>Note that the shear modulus  $G$ , the *Young's* modulus  $E$ , and the *Poisson's* ratio  $\nu$  are not independent:  $G = 1/2/(1 + \nu)E$ .

The term  $dA(y)/dy$  can be determined from the derivative of Eq. (4.36):

$$\frac{dA(y)}{dy} = \frac{d}{dy} (A_0 e^{2y/f}) = \frac{2}{f} A_0 e^{2y/f} = \frac{2}{f} A(y).$$

With this equality the partial differential equation of motion of the unloaded soil bar is

$$\boxed{\frac{\partial^2 v(y, t)}{\partial y^2} + \frac{2}{f} \frac{\partial v(y, t)}{\partial y} - \frac{1}{c_n^2} \frac{\partial^2 v(y, t)}{\partial t^2} = 0}. \quad (4.40)$$

### 4.5.2 Static stiffness of the soil model

In the static case there is no vibration, i.e.  $\frac{\partial^2 v(y, t)}{\partial t^2} = 0$  and (4.40) yields

$$\boxed{\frac{d^2 v(y)}{dy^2} + \frac{2}{f} \frac{dv(y)}{dy} = 0}. \quad (4.41)$$

The solution is searched for as

$$v(y) = A e^{\lambda y},$$

leading to the characteristic polynomial

$$\lambda^2 + \frac{2}{f} \lambda = \lambda \left( \lambda + \frac{2}{f} \right) = 0 \quad \rightarrow \quad \lambda_1 = 0, \quad \lambda_2 = -\frac{2}{f}.$$

From these roots the solutions for  $v(y)$  is the linear combination

$$v(y) = A_1 + A_2 e^{-\frac{2}{f}y}.$$

Here the coefficients  $A_1$  and  $A_2$  are computed from two boundary conditions.

If we are interested in the static stiffness of the soil bar, then we need to compute the normal force on the top due to a unit translation of the top. Thus the first boundary condition is

$$v(y) \Big|_{y=0} = 1.$$

The second boundary condition should correspond to the other end of the bar. Since analytical solutions for the stiffness of the elastic half space are available, we study a *semi-infinite soil bar*. We assume that the other end is in the infinity and its displacement is zero:

$$v(y) \Big|_{y \rightarrow \infty} = 0.$$

Using the above two boundary conditions we obtain  $A_1 = 0$  and  $A_2 = 1$ , thus the static shape function of the semi-infinite soil bar due to the unit translation of its top is:

$$v(y) = e^{-\frac{2}{f}y}.$$

The normal force on the top of the bar due to its unit translation is the opposite of the static stiffness:

$$k_{\text{soil}}^{\text{static}} = -N(0) = -E_c A_0 \left. \frac{dv(y)}{dy} \right|_{y=0} \rightarrow \boxed{k_{\text{soil}}^{\text{static}} = \frac{2E_c A_0}{f} = 2E_c R \frac{R\pi}{f}}. \quad (4.42)$$

From the classical (*Boussinesq*) solution for the static problem of a disc lying on an elastic half space the static stiffness is [14]:

$$k_{\text{soil}}^{\text{exact}} = 4GR \frac{1}{1-\nu} = 2E_c R \frac{1-2\nu}{(1-\nu)^2}$$

Finally, we can equate the above two stiffness values and express the characteristic depth  $f$  as:

$$\boxed{f = R\pi \frac{(1-\nu)^2}{1-2\nu}}. \quad (4.43)$$

### 4.5.3 Dynamic stiffness of the soil model

Now we investigate the case when the disc vibrates harmonically in time with a unit amplitude, described by the complex, harmonic displacement function

$$v(0, t) = 1 \cdot e^{i\omega t}. \quad (4.44)$$

We separate the variables  $y$  and  $t$  in  $v(y, t)$ , assuming that the vibration of the soil model at any depth  $y$  is also harmonic in time:

$$v(y, t) = \tilde{v}(y) e^{i\omega t}. \quad (4.45)$$

This separated form of  $v(y, t)$  is substituted in (4.40) yielding:

$$\left\{ \frac{d^2 \tilde{v}(y)}{dy^2} + \frac{2}{f} \frac{d\tilde{v}(y)}{dy} + \frac{\omega^2}{c_n^2} \tilde{v}(y) \right\} e^{i\omega t} = 0.$$

The above identity holds for any time instant  $t$  if

$$\boxed{\frac{d^2 \tilde{v}(y)}{dy^2} + \frac{2}{f} \frac{d\tilde{v}(y)}{dy} + \frac{\omega^2}{c_n^2} \tilde{v}(y) = 0}. \quad (4.46)$$

We search for the solution of Eq. (4.46) in the exponential form:

$$\tilde{v}(y) = B e^{\lambda y}. \quad (4.47)$$

(Here both  $B$  and  $\lambda$  can be complex.) Substituting (4.47) in (4.46) we get

$$\left( \lambda^2 + \frac{2}{f} \lambda + \frac{\omega^2}{c_n^2} \right) e^{\lambda y} = 0.$$

The roots of the above quadratic polynomial are

$$\lambda_{1,2} = -\frac{1}{f} \pm \sqrt{\left(\frac{1}{f}\right)^2 - \left(\frac{\omega}{c_n}\right)^2},$$

thus the solution of Eq. (4.46) is the linear combination

$$\tilde{v}(y) = B_1 e^{\left\{-\frac{1}{f} + \sqrt{\left(\frac{1}{f}\right)^2 - \left(\frac{\omega}{c_n}\right)^2}\right\}y} + B_2 e^{\left\{-\frac{1}{f} - \sqrt{\left(\frac{1}{f}\right)^2 - \left(\frac{\omega}{c_n}\right)^2}\right\}y}. \quad (4.48)$$

Coefficients  $B_1$  and  $B_2$  are computed from two prescribed boundary conditions.

Note that if

$$\omega < \frac{c_n}{f}, \quad (4.49)$$

then the solution  $\tilde{v}(y)$  is *real*, but if

$$\omega > \frac{c_n}{f}, \quad (4.50)$$

then  $\tilde{v}(y)$  is *complex*. These two different cases imply different soil stiffness characteristics. We start with the discussion of the complex case.

### The case of higher forcing frequencies

If  $\omega > \frac{c_n}{f}$ , then the term in the square roots of (4.48) is negative, and  $\tilde{v}(y)$  is complex. First we write

$$\sqrt{\left(\frac{1}{f}\right)^2 - \left(\frac{\omega}{c_n}\right)^2} = i \omega \sqrt{\left(\frac{1}{c_n}\right)^2 - \left(\frac{1}{f\omega}\right)^2}.$$

Then by introducing

$$\frac{1}{c_{sd}} = \sqrt{\left(\frac{1}{c_n}\right)^2 - \left(\frac{1}{f\omega}\right)^2}, \quad (4.51)$$

(4.48) becomes

$$\tilde{v}(y) = B_1 e^{\left\{-\frac{1}{f} + i \frac{\omega}{c_{sd}}\right\}y} + B_2 e^{\left\{-\frac{1}{f} - i \frac{\omega}{c_{sd}}\right\}y},$$

and (4.45) finally yields

$$\begin{aligned} v(y, t) &= B_1 e^{-\frac{y}{f}} e^{i \frac{\omega}{c_{sd}}(y+c_{sd}t)} + B_2 e^{-\frac{y}{f}} e^{-i \frac{\omega}{c_{sd}}(y-c_{sd}t)} \\ &= B_1 e^{-\frac{y}{f}} \left[ \cos\left(\frac{\omega}{c_{sd}}\{y+c_{sd}t\}\right) + i \sin\left(\frac{\omega}{c_{sd}}\{y+c_{sd}t\}\right) \right] \\ &\quad + B_2 e^{-\frac{y}{f}} \left[ \cos\left(\frac{\omega}{c_{sd}}\{y-c_{sd}t\}\right) - i \sin\left(\frac{\omega}{c_{sd}}\{y-c_{sd}t\}\right) \right]. \end{aligned} \quad (4.52)$$

From this form it can be recognized that there are *travelling waves* in the soil model due to the harmonic vibration of the top. If time  $t$  is changed by  $\Delta t$  ( $t = t + \Delta t$ ), while  $y$  is *increased* by  $c_{sd}\Delta t$  ( $y = y + c_{sd}\Delta t$ ), then the argument  $y - c_{sd}t$  does not change. Thus the terms multiplied by  $B_2$  represent mechanical waves travelling *downwards* at a constant speed  $c_{sd}$ . Similarly, if time is changed by  $\Delta t$ , while  $y$  is *decreased* by  $c_{sd}\Delta t$ , then  $y + c_{sd}t$  does not change. Hence the terms multiplied by  $B_1$  are the mechanical waves travelling *upwards* at a constant speed  $c_{sd}$ .

However, if a *semi-infinite* soil bar is excited at the top, and the soil is assumed to be homogeneous, then only the waves that travel downwards exist. The reason of this is that the excitation of the top induces waves travelling downwards, and these waves do not reflected from any material discontinuity, which would be one source of waves travelling upwards. The bottom of the bar can also reflect downward-travelling waves, as the other source of the upward-travelling waves, but the bottom is in the infinity now, so this source does not exist either. Therefore, for the specific case of the *homogeneous, semi-infinite soil bar* we keep only

$$\tilde{v}(y) = B_2 e^{\left\{-\frac{1}{f} - i\frac{\omega}{c_{sd}}\right\}y}. \quad (4.53)$$

The boundary condition at the top implies that

$$\tilde{v}(y)\Big|_{y=0} = B_2 e^{\left\{-\frac{1}{f} - i\frac{\omega}{c_{sd}}\right\}0} = 1 \quad \rightarrow \quad B_2 = 1.$$

The normal force on the top due to the harmonic vibration of the top is:

$$N(0) = -E_c A_0 \frac{d\tilde{v}(y)}{dy}\Big|_{y=0} = -E_c A_0 \left( \frac{1}{f} + i\omega \frac{1}{c_{sd}} \right),$$

which is the opposite of the dynamic stiffness of the homogeneous, semi-infinite soil bar:

$$\tilde{k}_{\text{soil}} = \frac{E_c A_0}{f} + i\omega \frac{E_c A_0}{c_{sd}}. \quad (4.54)$$

As we can see, the stiffness of the soil bar is complex, which means that besides an elastic spring of stiffness  $E_c A_0 / f$ , there is also a viscous damper of coefficient  $E_c A_0 / c_{sd}$  in our system, even though no internal (material) damping is considered in the constitutive law. The origin of this energy dissipation mechanism of the soil is that the downward-travelling waves are not reflected back and so radiate energy from the system. This damping phenomenon is called *radiation damping*.

### The case of lower forcing frequencies

If  $\omega < \frac{c_n}{f}$ , then the term in the square roots of (4.48) is positive, and  $\tilde{v}(y)$  is real. Instead of deriving the stiffness of the soil starting from Eq. (4.48), we simply make use of the previously derived complex dynamic stiffness (4.54). We have to take into account that now (4.51) is

complex and we have to reformulate (4.54) as

$$\begin{aligned} \frac{E_c A_0}{f} + i\omega \frac{E_c A_0}{c_{sd}} &= E_c A_0 \left\{ \frac{1}{f} + i\omega \sqrt{\left(\frac{1}{c_n}\right)^2 - \left(\frac{1}{f\omega}\right)^2} \right\} \\ &= E_c A_0 \left\{ \frac{1}{f} + \sqrt{(-1) \left(\frac{\omega^2}{c_n^2} - \frac{1}{f^2}\right)} \right\}. \end{aligned}$$

Thus the dynamic stiffness of the soil in the case of low forcing frequency is:

$$\boxed{\hat{k}_{\text{soil}} = E_c A_0 \left\{ \frac{1}{f} + \sqrt{\frac{1}{f^2} - \frac{\omega^2}{c_n^2}} \right\}}. \quad (4.55)$$

And the real dynamic shape function is:

$$\hat{v}(y) = e^{\left\{ -\frac{1}{f} - \sqrt{\frac{1}{f^2} - \frac{\omega^2}{c_n^2}} \right\} y}.$$

We can verify this result by comparing it to the static stiffness (4.42), which is the limit case  $\omega \rightarrow 0$ :

$$\hat{k}_{\text{soil}} \Big|_{\omega \rightarrow 0} = \frac{2E_c A_0}{f} = k_{\text{soil}}^{\text{static}} \quad \checkmark$$

The other limit case is  $\omega \rightarrow c_n/f$ , when

$$\hat{k}_{\text{soil}} \Big|_{\omega \rightarrow c_n/f} = \frac{E_c A_0}{f} = \frac{1}{2} k_{\text{soil}}^{\text{static}},$$

which equals the real part of the complex dynamic stiffness (4.54).

As a conclusion we can state that the soil can be modeled by an elastic spring and a dashpot if the forcing frequency is high enough, and by a single elastic spring if the forcing frequency is sufficiently low. Table 4.1 summarizes the results obtained for the equivalent spring constant  $k_{\text{soil}}^{\text{eq}}$  and damping coefficient  $c_{\text{soil}}^{\text{eq}}$  depending on the forcing frequency  $\omega$  and soil parameters.

Finally, we mention that internal damping of the soil material itself can also be taken into account by replacing  $E$  with the complex elastic modulus

$$\tilde{E} = (1 + i 2\bar{\xi}_{\text{soil}}) E$$

in the previous derivations. (Here  $\bar{\xi}_{\text{soil}}$  is the structural damping coefficient of the soil.) In this case there can be two types of damping in the model. One originates from the internal damping, which is rate-independent, thus appears at any loading frequency. The other one is due to the radiation damping, and it only appears at higher forcing frequencies. We note that the stiffness of the soil due to horizontal translation and to rotation of the rigid disk can be computed in a similar way.

Forcing frequency	$\omega < \frac{c_n}{f}$	$\omega > \frac{c_n}{f}$
Spring stiffness	$\frac{1}{2}k_{\text{soil}}^{\text{static}} < k_{\text{soil}}^{\text{eq}} < k_{\text{soil}}^{\text{static}}$	$k_{\text{soil}}^{\text{eq}} = \frac{1}{2}k_{\text{soil}}^{\text{static}}$
Damping coefficient	$c_{\text{soil}}^{\text{eq}} = 0$	$c_{\text{soil}}^{\text{eq}} = \frac{E_c A_0}{c_{\text{sd}}}$

**Table 4.1:** Equivalent spring stiffness  $k_{\text{soil}}^{\text{eq}}$  and damping coefficient  $c_{\text{soil}}^{\text{eq}}$  of the soil, assuming a homogeneous elastic half space, corresponding to “low” and “high” forcing frequency  $\omega$ . Here  $E_c$  is the constrained modulus of the soil,  $A_0$  is the area of the rigid plate on the soil surface,  $c_n = \sqrt{E_c/\varrho}$  with  $\varrho$  being the mass density of the soil, while the characteristic depth  $f$  is given by (4.43) for a disk. The velocity of the travelling wave  $c_{\text{sd}}$  is computed according to (4.51)

**Problem 4.5.1** (Modelling the soil under a machine foundation). There is a machine that exerts a periodic force  $q(t) = q_0 \sin(\omega t)$  on its foundation which can be regarded as a rigid disk of diameter  $D = 2$  m. The circular frequency of the force is  $\omega = 50 \frac{1}{\text{s}}$ . The underlying soil is sand with *Young’s* modulus  $E = 30 \text{ MPa} = 30 \cdot 10^6 \text{ N/m}^2$ , *Poisson’s* ratio  $\nu = 0.4$ , and mass density  $\varrho = 2 \text{ t/m}^3 = 2 \cdot 10^3 \text{ kg/m}^3$ . Determine the equivalent soil parameters for the dynamical calculation!

**Solution.** First we compute the constrained modulus  $E_c$  and the characteristic depth  $f$ , from Eqs. (4.39) and (4.43):

$$E_c = \frac{1 - \nu}{(1 + \nu)(1 - 2\nu)} E = \frac{0.6}{(1.4)(0.2)} 30 \cdot 10^6 = 64.28 \cdot 10^6 \text{ N/m}^2,$$

$$f = R\pi \frac{(1 - \nu)^2}{1 - 2\nu} = \pi \frac{(0.6)^2}{0.2} = 1.8\pi \text{ m}.$$

We also need  $c_n = \sqrt{E_c/\varrho}$ :

$$c_n = \sqrt{\frac{64.28 \cdot 10^6}{2 \cdot 10^3}} = 179.28 \frac{\text{m}}{\text{s}}.$$

Now we can compare the circular frequency  $\omega$  of the forcing to  $c_n/f$ :

$$\omega = 50 \frac{1}{\text{s}}, \quad \frac{c_n}{f} = \frac{179.28}{1.8\pi} = 31.70 \frac{1}{\text{s}}, \quad \rightarrow \quad \omega > \frac{c_n}{f},$$

thus the forcing frequency is high enough to induce travelling waves which radiates in the soil. Hence we need an elastic spring and a viscous damper, too, to model the soil. The velocity  $c_{\text{sd}}$  of the travelling waves is computed from (4.51)

$$\frac{1}{c_{\text{sd}}} = \sqrt{\left(\frac{1}{c_n}\right)^2 - \left(\frac{1}{f\omega}\right)^2} = \sqrt{\left(\frac{1}{179.28}\right)^2 - \left(\frac{1}{1.8\pi \cdot 50}\right)^2} = 4.313 \cdot 10^{-3} \frac{\text{s}}{\text{m}}, \quad \rightarrow \quad c_{\text{sd}} = 231.84 \frac{\text{m}}{\text{s}}.$$

Finally, the equivalent stiffness and damping parameters  $k_{\text{soil}}^{\text{eq}}$  and  $c_{\text{soil}}^{\text{eq}}$  of the soil are calculated from (4.54):

$$k_{\text{soil}}^{\text{eq}} = \frac{E_c A_0}{f} = \frac{64.28 \cdot 10^6 \cdot \pi}{1.8\pi} = 35.71 \cdot 10^6 \frac{\text{N}}{\text{m}},$$

$$c_{\text{soil}}^{\text{eq}} = \frac{E_c A_0}{c_{\text{sd}}} = \frac{64.28 \cdot 10^6 \cdot \pi}{231.84} = 87.10 \cdot 10^4 \frac{\text{Ns}}{\text{m}}.$$



**Problem 4.5.2** (Vibration of a prismatic soil bar). Study the vibration of a prismatic soil bar!

**Solution.** We can simply take  $\frac{1}{f} = 0$  in the previous analysis to obtain the differential equation of the longitudinal vibration of a prismatic (cylindrical) bar. The differential equation of motion is from (4.40):

$$\frac{\partial^2 v(y, t)}{\partial y^2} - \frac{1}{c_n^2} \frac{\partial^2 v(y, t)}{\partial t^2} = 0.$$

(Compare it to (2.6)!) If the top is vibrating by a unit amplitude, then the particular solution is written in the separated form (4.45) leading to the ordinary differential equation for the shape function

$$\frac{d^2 \tilde{v}(y)}{dy^2} + \frac{\omega^2}{c_n^2} \tilde{v}(y) = 0.$$

Using the Ansatz

$$\tilde{v}(y) = B e^{\lambda y}$$

the roots for  $\lambda$  are

$$\lambda_{1,2} = \pm \sqrt{-\left(\frac{\omega}{c_n}\right)^2} = \pm i \frac{\omega}{c_n}.$$

Thus

$$\tilde{v}(y) = B_1 e^{i \frac{\omega}{c_n} y} + B_2 e^{-i \frac{\omega}{c_n} y}.$$

We can observe travelling waves in this solution, too, but the amplitude of the vibration does not decrease with depth. The constants  $B_1$  and  $B_2$  can be determined from boundary conditions.

If we study an semi-infinite bar with a harmonically vibrating top, using  $B_1 + B_2 = 1$  and  $B_1 = 0$  as before, then the vibration of the prismatic soil bar is given by

$$v(y, t) = B_2 e^{-i \frac{\omega}{c_n} (y - c_n t)} = B_2 \left[ \cos\left(\frac{\omega}{c_n} \{y - c_n t\}\right) - i \sin\left(\frac{\omega}{c_n} \{y - c_n t\}\right) \right],$$

yielding the stiffness

$$\tilde{k}_{\text{soil}}^{\text{prism}} = -N(0) = -E_c A_0 \left. \frac{dv(y)}{dy} \right|_{y=0} = i\omega \frac{E_c A_0}{c_n}.$$

*Damping* (the complex part of the stiffness) is present due to the lack of the upward-travelling waves, but the static stiffness (the elastic resistance, the real part of the stiffness) is *zero* due to the infinite depth of the bar. It seems strange, but based on our previous studies of strength of materials we can check what the stiffness of a stretched semi-infinite bar of normal stiffness  $EA$  and length  $\ell \rightarrow \infty$  is:

$$k_{\text{bar}}^{\ell \infty} = \left. \frac{EA}{\ell} \right|_{\ell \rightarrow \infty} = 0.$$

**Problem 4.5.3** (Complex dynamic shape function of a prismatic bar). Using the complex differential equation of motion of a prismatic soil bar determine its dynamic shape function corresponding to the end conditions  $v(0, t) = 1 \cdot e^{i\omega t}$  and  $v(\ell, t) = 0$ .

**Solution.** The bar is free from force load. As in the previous problem we set  $\frac{1}{f} = 0$  in (4.40) to obtain the differential equation of motion of a prismatic bar:

$$\frac{\partial^2 v(y, t)}{\partial y^2} - \frac{1}{c_n^2} \frac{\partial^2 v(y, t)}{\partial t^2} = 0.$$

The spatial and temporal variables are separated as

$$v(y, t) = \tilde{v}(y) e^{i\omega t}.$$

Similarly to the previous problem, the shape function  $\tilde{v}(y)$  satisfies the ordinary differential equation

$$\frac{d^2 \tilde{v}(y)}{dy^2} + \frac{\omega^2}{c_n^2} \tilde{v}(y) = 0,$$

leading to

$$\tilde{v}(y) = B_1 e^{i\frac{\omega}{c_n} y} + B_2 e^{-i\frac{\omega}{c_n} y}.$$

The boundary conditions that must be fulfilled by  $\tilde{v}(y)$  are

$$\tilde{v}(y) \Big|_{y=0} = 1, \quad \tilde{v}(y) \Big|_{y=\ell} = 0,$$

yielding

$$\begin{aligned} B_1 + B_2 &= 1, \\ B_1 e^{i\frac{\omega}{c_n} \ell} + B_2 e^{-i\frac{\omega}{c_n} \ell} &= 0 \end{aligned}$$

Solving the above equations we get

$$\begin{aligned} B_1 &= \frac{-e^{-i\frac{\omega}{c_n} \ell}}{e^{i\frac{\omega}{c_n} \ell} - e^{-i\frac{\omega}{c_n} \ell}} = \frac{-1}{2i \sin\left(\frac{\omega}{c_n} \ell\right)} e^{-i\frac{\omega}{c_n} \ell} = \frac{i}{2 \sin\left(\frac{\omega}{c_n} \ell\right)} e^{-i\frac{\omega}{c_n} \ell}, \\ B_2 &= \frac{e^{i\frac{\omega}{c_n} \ell}}{e^{i\frac{\omega}{c_n} \ell} - e^{-i\frac{\omega}{c_n} \ell}} = \frac{1}{2i \sin\left(\frac{\omega}{c_n} \ell\right)} e^{i\frac{\omega}{c_n} \ell} = \frac{-i}{2 \sin\left(\frac{\omega}{c_n} \ell\right)} e^{i\frac{\omega}{c_n} \ell}. \end{aligned}$$

Thus the complex dynamic shape function is:

$$\begin{aligned} \tilde{v}(y) &= \frac{i}{2 \sin\left(\frac{\omega}{c_n} \ell\right)} e^{-i\frac{\omega}{c_n} \ell} e^{i\frac{\omega}{c_n} y} + \frac{-i}{2 \sin\left(\frac{\omega}{c_n} \ell\right)} e^{i\frac{\omega}{c_n} \ell} e^{-i\frac{\omega}{c_n} y} \\ &= \frac{i}{2 \sin\left(\frac{\omega}{c_n} \ell\right)} e^{i\frac{\omega}{c_n} (y-\ell)} + \frac{-i}{2 \sin\left(\frac{\omega}{c_n} \ell\right)} e^{-i\frac{\omega}{c_n} (y-\ell)}, \end{aligned}$$

In order to compute the stiffness of the bar we need to differentiate the shape function with respect to  $y$ :

$$\begin{aligned} \frac{d\tilde{v}(y)}{dy} &= \frac{i \cdot i\frac{\omega}{c_n}}{2 \sin\left(\frac{\omega}{c_n} \ell\right)} e^{i\frac{\omega}{c_n} (y-\ell)} + \frac{-i \cdot (-i)\frac{\omega}{c_n}}{2 \sin\left(\frac{\omega}{c_n} \ell\right)} e^{-i\frac{\omega}{c_n} (y-\ell)} \\ &= -\frac{\omega}{c_n} \frac{1}{2 \sin\left(\frac{\omega}{c_n} \ell\right)} e^{i\frac{\omega}{c_n} (y-\ell)} - \frac{\omega}{c_n} \frac{1}{2 \sin\left(\frac{\omega}{c_n} \ell\right)} e^{-i\frac{\omega}{c_n} (y-\ell)}. \end{aligned}$$

For the bar stiffnesses  $\tilde{K}_{11}$  and  $\tilde{K}_{41}$  we calculate the above derivative at the ends of the bar, multiply it by the normal stiffness  $EA$  of the bar, and apply the appropriate sign rule, similarly to Eq. (3.11) and (3.12):

$$\begin{aligned}\tilde{K}_{11} &= -EA \frac{d\tilde{v}(y)}{dy} \Big|_{y=0} = EA \frac{\omega}{c_n} \frac{1}{2 \sin\left(\frac{\omega}{c_n} \ell\right)} \left[ e^{-i\frac{\omega}{c_n} \ell} + e^{i\frac{\omega}{c_n} \ell} \right] \\ &= EA \frac{\omega}{c_n} \frac{1}{2 \sin\left(\frac{\omega}{c_n} \ell\right)} \left[ \cos\left(\frac{\omega}{c_n} \ell\right) - i \sin\left(\frac{\omega}{c_n} \ell\right) + \cos\left(\frac{\omega}{c_n} \ell\right) + i \sin\left(\frac{\omega}{c_n} \ell\right) \right] \\ &= EA \frac{\omega}{c_n} \cot\left(\frac{\omega}{c_n} \ell\right), \\ \tilde{K}_{41} &= EA \frac{d\tilde{v}(y)}{dy} \Big|_{y=\ell} = -EA \frac{\omega}{c_n} \frac{1}{2 \sin\left(\frac{\omega}{c_n} \ell\right)} \left[ e^{i\frac{\omega}{c_n} 0} + e^{-i\frac{\omega}{c_n} 0} \right] = -EA \frac{\omega}{c_n} \frac{1}{\sin\left(\frac{\omega}{c_n} \ell\right)}\end{aligned}$$

The bar has *real*-valued stiffnesses, since there is no internal (structural, or material) damping and all the travelling waves can be reflected back and forth from the ends of the bar. Note that the above values identical to the corresponding entries of (3.73).

Finally, let us compile the particular solution of the partial differential equation:

$$\begin{aligned}v(y, t) &= \tilde{v}(y) e^{i\omega t} = \frac{i}{2 \sin\left(\frac{\omega}{c_n} \ell\right)} e^{i\frac{\omega}{c_n}(y-\ell+c_nt)} + \frac{-i}{2 \sin\left(\frac{\omega}{c_n} \ell\right)} e^{-i\frac{\omega}{c_n}(y-\ell-c_nt)} \\ &= \frac{i}{2 \sin\left(\frac{\omega}{c_n} \ell\right)} \left[ \cos\left\{\frac{\omega}{c_n}(y-\ell+c_nt)\right\} + i \sin\left\{\frac{\omega}{c_n}(y-\ell+c_nt)\right\} \right] \\ &\quad - \frac{i}{2 \sin\left(\frac{\omega}{c_n} \ell\right)} \left[ \cos\left\{\frac{\omega}{c_n}(y-\ell-c_nt)\right\} - i \sin\left\{\frac{\omega}{c_n}(y-\ell-c_nt)\right\} \right].\end{aligned}$$

Now we use the trigonometric identity

$$\frac{1}{\sin^2\left(\frac{\omega}{c_n} \ell\right)} = 1 + \cot^2\left(\frac{\omega}{c_n} \ell\right) \quad \rightarrow \quad \frac{1}{2 \sin\left(\frac{\omega}{c_n} \ell\right)} = \frac{\sqrt{1 + \cot^2\left(\frac{\omega}{c_n} \ell\right)}}{2}$$

and expand the *real part* of (4.5.3):

$$\operatorname{Re}(v(y, t)) = \frac{\sqrt{1 + \cot^2\left(\frac{\omega}{c_n} \ell\right)}}{2} \left[ -\sin\left\{\frac{\omega}{c_n}(y-\ell+c_nt)\right\} - \sin\left\{\frac{\omega}{c_n}(y-\ell-c_nt)\right\} \right].$$

It is important to understand that the above result is the solution corresponding to the vibration  $\cos(\omega t)$  of the starting end of the bar, and so identical with (2.13).

Similarly, the complex part of (4.5.3) is

$$\operatorname{Im}(v(y, t)) = \frac{\sqrt{1 + \cot^2\left(\frac{\omega}{c_n} \ell\right)}}{2} \left[ \cos\left\{\frac{\omega}{c_n}(y-\ell+c_nt)\right\} - \cos\left\{\frac{\omega}{c_n}(y-\ell-c_nt)\right\} \right],$$

which is the solution corresponding to the vibration  $\sin(\omega t)$  of the starting end, and so the same as (2.15).

## 4.6 Numerical solution of the matrix differential equation of damped MDOF systems

In this section we will analyse possible solution methods of the matrix differential equation (4.1). These methods are required when the damping is non-proportional, and the modal analysis cannot be used, but we restrict our analysis to real damping matrix  $\mathbf{C}$ .

As we have seen earlier for SDOF systems in Section 1.2, the numerical integration of the equation of motion provides the displacement of the system at discrete time steps. From the displacements one can recover the motion of the system, and compute the internal forces as well.

Explicit methods calculate the next points of the solution by satisfying the differential equation in the starting point. Implicit methods calculate the next points of the solution such that they satisfy the differential equation in that point. For further details see [12].

### 4.6.1 Newmark method

At a given time  $t_i$  the vectors of displacement, velocity and acceleration are known:

$$\mathbf{u}_i = \mathbf{u}(t_i), \quad \dot{\mathbf{u}}_i = \dot{\mathbf{u}}(t_i), \quad \ddot{\mathbf{u}}_i = \ddot{\mathbf{u}}(t_i).$$

We want to derive a formula for the calculation of these vectors at the time  $t_{i+1} = t_i + \Delta t$ :

$$\mathbf{u}_{i+1} = \mathbf{u}(t_i + \Delta t), \quad \dot{\mathbf{u}}_{i+1} = \dot{\mathbf{u}}(t_i + \Delta t), \quad \ddot{\mathbf{u}}_{i+1} = \ddot{\mathbf{u}}(t_i + \Delta t).$$

Let us assume, that the continuous change of the acceleration between time steps  $t_i$  and  $t_{i+1}$  can be described by the scalar valued function  $f(\tau)$ :

$$\ddot{\mathbf{u}}(t_i + \tau\Delta t) = \ddot{\mathbf{u}}_i + f(\tau) (\ddot{\mathbf{u}}_{i+1} - \ddot{\mathbf{u}}_i). \quad (4.56)$$

Here  $\tau$  is a nondimensional time. One can conclude from the above formula, that  $f(0) = 0$  and  $f(1) = 1$ . Integrating the acceleration with respect to time provides the velocity function<sup>3</sup> (similar to the formula  $v(t) = v(0) + \int_0^t a(\tau) d\tau$ ):

$$\dot{\mathbf{u}}(t_i + \tau\Delta t) = \dot{\mathbf{u}}(t_i) + \Delta t \left( \int_0^\tau \ddot{\mathbf{u}}_i + f(T) (\ddot{\mathbf{u}}_{i+1} - \ddot{\mathbf{u}}_i) dT \right).$$

We expand the argument of the above integral

$$\dot{\mathbf{u}}(t_i + \tau\Delta t) = \dot{\mathbf{u}}_i + \ddot{\mathbf{u}}_i\tau\Delta t + (\ddot{\mathbf{u}}_{i+1} - \ddot{\mathbf{u}}_i) \Delta t \int_0^\tau f(T) dT. \quad (4.57)$$

<sup>3</sup>In the integral formula  $\int_{t_i}^{t_i+\Delta t\tau} \ddot{\mathbf{u}} dt$  we must substitute the absolute time  $t$  as the product of the time step and the nondimensional time:  $\Delta t\tau$ . The elementary time will be then  $dt = \Delta t d\tau$ . Using this exchange of variables the integral becomes  $\int_0^\tau \ddot{\mathbf{u}}\Delta t dT$ .

Let us introduce the parameter  $\alpha = \int_0^1 f(T) dT$ , and write the velocity at the  $(i + 1)$ th time instant (i.e. at  $\tau = 1$ ):

$$\dot{\mathbf{u}}_{i+1} = \dot{\mathbf{u}}_i + \ddot{\mathbf{u}}_i \Delta t + (\ddot{\mathbf{u}}_{i+1} - \ddot{\mathbf{u}}_i) \Delta t \alpha,$$

or in a more elegant form:

$$\dot{\mathbf{u}}_{i+1} = \dot{\mathbf{u}}_i + [(1 - \alpha) \ddot{\mathbf{u}}_i + \alpha \ddot{\mathbf{u}}_{i+1}] \Delta t. \quad (4.58)$$

Next, we introduce the function  $g(\tau) = \int_0^\tau f(T) dT$  into Eq. (4.57) and integrate it in order to get the displacement vector:

$$\mathbf{u}(t_i + \tau \Delta t) = \mathbf{u}(t_i) + \Delta t \left( \int_0^\tau \dot{\mathbf{u}}_i + \ddot{\mathbf{u}}_i T \Delta t + (\ddot{\mathbf{u}}_{i+1} - \ddot{\mathbf{u}}_i) \Delta t g(T) dT \right)$$

We expand the argument of the integral:

$$\mathbf{u}(t_i + \tau \Delta t) = \mathbf{u}_i + \tau \Delta t \dot{\mathbf{u}}_i + \frac{\Delta t^2 \tau^2}{2} \ddot{\mathbf{u}}_i + \Delta t^2 (\ddot{\mathbf{u}}_{i+1} - \ddot{\mathbf{u}}_i) \int_0^\tau g(T) dT. \quad (4.59)$$

We define the parameter  $\beta = \int_0^1 g(T) dT$ , and write the above displacement at the  $(i + 1)$ th time instant (i.e. when  $\tau = 1$ ):

$$\mathbf{u}_{i+1} = \mathbf{u}_i + \Delta t \dot{\mathbf{u}}_i + \frac{\Delta t^2}{2} \ddot{\mathbf{u}}_i + \Delta t^2 (\ddot{\mathbf{u}}_{i+1} - \ddot{\mathbf{u}}_i) \beta,$$

or, in a more elegant form:

$$\mathbf{u}_{i+1} = \mathbf{u}_i + \dot{\mathbf{u}}_i \Delta t + \left[ \left( \frac{1}{2} - \beta \right) \ddot{\mathbf{u}}_i + \beta \ddot{\mathbf{u}}_{i+1} \right] \Delta t^2. \quad (4.60)$$

We solve Eq. (4.60) for the acceleration

$$\ddot{\mathbf{u}}_{i+1} = \frac{1}{\beta \Delta t^2} (\mathbf{u}_{i+1} - \mathbf{u}_i - \dot{\mathbf{u}}_i \Delta t) - \left( \frac{1}{2\beta} - 1 \right) \ddot{\mathbf{u}}_i, \quad (4.61)$$

substitute the acceleration into Eq. (4.58), and solve it for the velocity:

$$\begin{aligned} \dot{\mathbf{u}}_{i+1} &= \dot{\mathbf{u}}_i + (1 - \alpha) \ddot{\mathbf{u}}_i \Delta t + \frac{\alpha}{\beta \Delta t} (\mathbf{u}_{i+1} - \mathbf{u}_i - \dot{\mathbf{u}}_i \Delta t) - \alpha \left( \frac{1}{2\beta} - 1 \right) \ddot{\mathbf{u}}_i \Delta t \\ &= \frac{\alpha}{\beta \Delta t} (\mathbf{u}_{i+1} - \mathbf{u}_i) + \left( 1 - \frac{\alpha}{\beta} \right) \dot{\mathbf{u}}_i + \left( 1 - \frac{\alpha}{2\beta} \right) \Delta t \ddot{\mathbf{u}}_i. \end{aligned}$$

We substitute the acceleration and the velocity into the matrix differential equation (4.1)

$$\begin{aligned} & \mathbf{M} \left[ \frac{1}{\beta \Delta t^2} (\mathbf{u}_{i+1} - \mathbf{u}_i - \dot{\mathbf{u}}_i \Delta t) - \left( \frac{1}{2\beta} - 1 \right) \ddot{\mathbf{u}}_i \right] + \\ & \mathbf{C} \left[ \frac{\alpha}{\beta \Delta t} (\mathbf{u}_{i+1} - \mathbf{u}_i) + \left( 1 - \frac{\alpha}{\beta} \right) \dot{\mathbf{u}}_i + \left( 1 - \frac{\alpha}{2\beta} \right) \Delta t \ddot{\mathbf{u}}_i \right] + \mathbf{K} \mathbf{u}_{i+1} = \mathbf{q}_{i+1}. \end{aligned} \quad (4.62)$$

Let us define the effective stiffness matrix  $\mathbf{K}^{\text{eff}}$  as

$$\mathbf{K}^{\text{eff}} = \mathbf{K} + \frac{\alpha}{\beta \Delta t} \mathbf{C} + \frac{1}{\beta \Delta t^2} \mathbf{M},$$

and the effective load vector  $\mathbf{q}_{i+1}^{\text{eff}}$  as:

$$\begin{aligned} \mathbf{q}_{i+1}^{\text{eff}} = \mathbf{q}_{i+1} + \mathbf{M} & \left[ \frac{1}{\beta \Delta t^2} \mathbf{u}_i + \frac{1}{\beta \Delta t} \dot{\mathbf{u}}_i + \left( \frac{1}{2\beta} - 1 \right) \ddot{\mathbf{u}}_i \right] \\ & + \mathbf{C} \left[ \frac{\alpha}{\beta \Delta t} \mathbf{u}_i + \left( \frac{\alpha}{\beta} - 1 \right) \dot{\mathbf{u}}_i + \left( \frac{\alpha}{2\beta} - 1 \right) \Delta t \ddot{\mathbf{u}}_i \right]. \end{aligned}$$

Then, the iteration formula for the calculation of the displacements in the time instant  $t_{i+1}$  can be written in the short form:

$$\boxed{\mathbf{K}^{\text{eff}} \mathbf{u}_{i+1} = \mathbf{q}_{i+1}^{\text{eff}}}. \quad (4.63)$$

In a linear system the effective stiffness matrix is constant during the computation, so it is sufficient to calculate its inverse only once. The effective load vector depends on the load at the next step, and the current state of the system, thus it is recalculated at every time step.

### Special cases of the function $f(\tau)$

The parameters  $\alpha$  and  $\beta$  depend on the shape of the assumed change of the acceleration during the analysed time step  $\Delta t$ .

In a simple case we can assume, that the acceleration is the average of  $\ddot{\mathbf{u}}_i$  and  $\ddot{\mathbf{u}}_{i+1}$ . This corresponds to  $f(\tau) = 0.5$ ,  $g(\tau) = 0.5\tau$ , which leads to  $\alpha = 0.5$  and  $\beta = 0.25$ .

The next case assumes a linearly varying acceleration with  $f(\tau) = \tau$  and  $g(\tau) = \tau^2/2$ . The numerical parameters are then  $\alpha = 0.5$  and  $\beta = 1/6$ .

# Chapter 5

## Earthquake analysis

The most significant horizontal load of structures was the wind load for many years of standardized design. Change in applied materials emerged the importance of earthquake as a load case. In this chapter we go through the basic mechanics of earthquake engineering, as a preparation for the specific subject devoted to it. We introduce the mechanical aspects of earthquakes, and their propagation as waves. Then the elements of elastic analysis of single- and multi-DOF structures, and some notes about the advanced methods are presented. We do not focus here on the standards but on the mechanical concepts and theories which are reflected in the prescriptions of building codes, for example in Eurocode 8 [4].

### 5.1 Introduction to earthquakes

The structure of Earth in a very simplified description consists of a *core* (divided usually into an inner and an outer core), surrounded by the *mantle* and covered by the *crust*. The core is mostly composed of iron and nickel. The inner core is solid with a radius of 1220 km, while the outer core is liquid with a thickness of 2270 km. The mantle consists of a highly viscous solid material with a thickness of 2850 km. The solid crust has a varying thickness between 5 km (oceanic crust) and 70 km (continental crust).

The crust consists of *tectonic plates* floating on the surface of the mantle. Convection in the mantle results in a continuous motion of the plates. Neighbouring plates are in contact, and due to the friction between the plates there are stresses accumulating in those region. When the stress exceeds its ultimate value somewhere, a sudden motion occurs between the plates and a huge amount of energy is released. This rupture is the cause of most *earthquakes*. (Further causes are volcanic activities, mine blasts, landslides, etc.) The location, where the rupture happens is called the *hypocenter* or *focus*. The point on the ground level right above the hypocenter is the *epicenter*.

The dislocation travels through the solid soil as a wave. Two types of travelling waves are distinguished.

- In *P-waves* the particles are moving parallel to the travel direction of the wave. They are called pressure waves, or primary waves. The velocity of P-waves is

$$c_p = \sqrt{\frac{M}{\rho}},$$

where  $M$  is the *elastic P-wave modulus*:

$$M = \frac{(1 - \nu)E}{(1 + \nu)(1 - 2\nu)}.$$

Here  $E$ ,  $\nu$  and  $\rho$  are the elastic modulus, the Poisson ratio and the density of the solid material, respectively. The typical velocity of P-waves in soil is in the range 5 – 13 km/h.

- In *S-waves* the particles are moving transverse to the travel direction of the wave. They are called shear waves, or secondary waves. The velocity of S-waves is

$$c_s = \sqrt{\frac{G}{\rho}},$$

where  $G$  is the *elastic shear modulus* of the solid. The typical velocity of S-waves is smaller than that of the P-waves in the same material, it is in the range 4 – 5 km/h. In liquid material (like the outer core) the S-waves do not propagate.

The difference between the velocities of P- and S-waves makes it possible to calculate the distances of the hypocenter from seismic measurement sites, and to determine the location of the hypocenter.

On interfaces between various materials both P- and S- waves can exhibit four types of behaviour. They can be reflected (back, into the same side of the interface zone) or refracted (by entering the other side of the interface zone) into a P- or an S-wave. This property helped to analyse the inner structure of Earth.

On the ground level both P- and S-waves cause displacements. Their superposition results in *surface waves*. Pressure waves and the vertical shear waves (also called as SV-waves) result in elliptic motion of the particles. These waves are the Rayleigh waves or R-waves. The horizontal shear waves (also called as SH-waves) are reflected from the surface and from interfaces between various materials near the surface. This results in another type of surface waves, which are called the Love waves, or Q-waves. The above mentioned solid and surface waves are drawn in Figure 5.1.

Far from the epicenter typically the horizontal displacements are dominant, and they may result in large excessive internal forces. Therefore earthquake analysis of engineering structures typically focus on the lateral motions.

Historical earthquakes were qualified by the caused damage or the human feelings. These qualifications incorporate many architectural and sociological factors as well, but unaware of the distance of the place of perception from the epicenter. Scientifically exact classification requires the energy released during the earthquake, and the location of the epicenter. The most



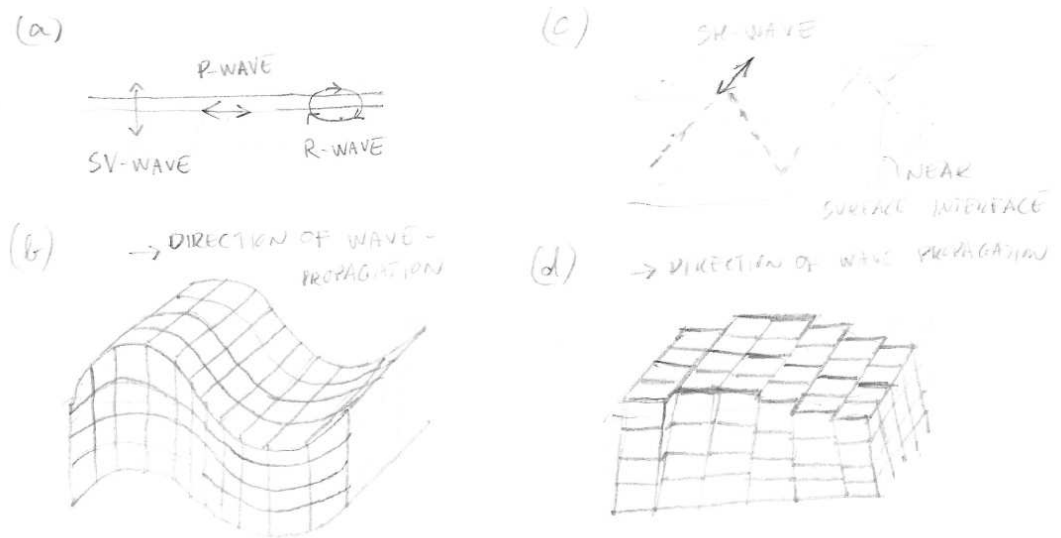


**Figure 5.1:** (a) Motion of a soil particle from vertical shear (SH), pressure (P) and Rayleigh (R) waves. (b) Deformed shape of a soil block, caused by the Rayleigh waves. (c) Motion of a soil particle from horizontal shear (SH) wave and the reflection of SH-waves on the material interfaces. (d) Deformed shape of a solid block, caused by the Love (Q) waves of the surface.

frequently used scale is the Richter magnitude scale. The Richter scale is a logarithmic scale, two units higher magnitude on the scale represents 1000 times more released energy.

It is also worth to mention, that formation of earthquakes caused by the continuous motion of the tectonic plates. As long there is no earthquake occurs in a exposed region, more and more energy accumulates thus the next earthquake has usually higher magnitude. This theory is justified by statistical analysis too.

In a specific location the earthquake is represented by the ground motion  $u_g(t)$ . This geometric load can be used as a load, allowing the solution of the differential equation of motion. Technically it is much easier to record the acceleration of the ground instead of the displacement. The tool is called an *accelerometer*. In an analog accelerometer a supported mass moves a pencil on a moving paper. We call the recorded function  $\ddot{u}_g(t)$  as a time history function, it can be used later for modelling the ground motion.

## 5.2 Response spectrum of SDOF systems

### 5.2.1 Response functions

Let us analyse a single degree-of-freedom system of mass  $m$ , viscous damping  $c$ , spring stiffness  $k$ , and general forcing  $q(t)$ . The ODE of the system is:

$$m\ddot{u}(t) + c\dot{u}(t) + ku(t) = q(t). \quad (5.1)$$

Here  $u(t)$  is the elongation of the spring (or the deformation of the elastic structure) The *response* of a SDOF system depends only on the natural circular frequency and the damping

ratio. The displacement can be calculated from the solution of the Eq. (5.1) (see the Duhamel's integral in Subsection 1.2.1 for one possible solution).

Once the displacement function  $u(t)$  is obtained we can calculate the spring force

$$f_S(t) = ku(t),$$

or we can apply this force to the structure to calculate other internal forces. We can express the spring stiffness  $k$  in terms of the mass and the undamped natural circular frequency  $\omega_0$ :

$$f_S(t) = m\omega_0^2 u(t).$$

Here  $\omega_0^2 u(t)$  is an acceleration-like quantity, which can be used to describe the current state of the motion of the analysed SDOF structure. Because it is not a real acceleration, it is called *pseudo-acceleration response* of the structure and denoted by  $a_P(t)$ :

$$a_P(t) = \omega_0^2 u(t). \quad (5.2)$$

Then, the spring force can be calculated as:

$$f_S(t) = ma_P(t).$$

Please notice the difference between the actual acceleration  $\ddot{u}(t)$  and the pseudo-acceleration  $a_P(t) = \omega_0^2 u(t)$ .

Similarly to the above concept, we define the *pseudo-velocity response* of the structure as

$$v_P(t) = \omega_0 u(t),$$

which differs from the actual velocity  $\dot{u}(t)$ .

In an undamped system the elastic displacement can be written as

$$u(t) = \frac{1}{m\omega_0} \int_0^t q(\tau) \sin(\omega_0(t - \tau)) \, d\tau.$$

Thus the pseudo-acceleration response of the undamped system is

$$a_P(t) = \omega_0^2 u(t) = \frac{\omega_0}{m} \int_0^t q(\tau) \sin(\omega_0(t - \tau)) \, d\tau.$$

**Problem 5.2.1** (Calculation of response functions). A damped, single DOF system is characterized by the mass  $m = 1$  kg, viscous damping  $c = 0.5$  Ns/m and spring stiffness  $k = 10$  N/m. The system is forced by an impulse load shown in Figure 5.2 (a). Calculate the displacement, velocity, and acceleration response functions and the pseudo-velocity and pseudo-acceleration diagrams!

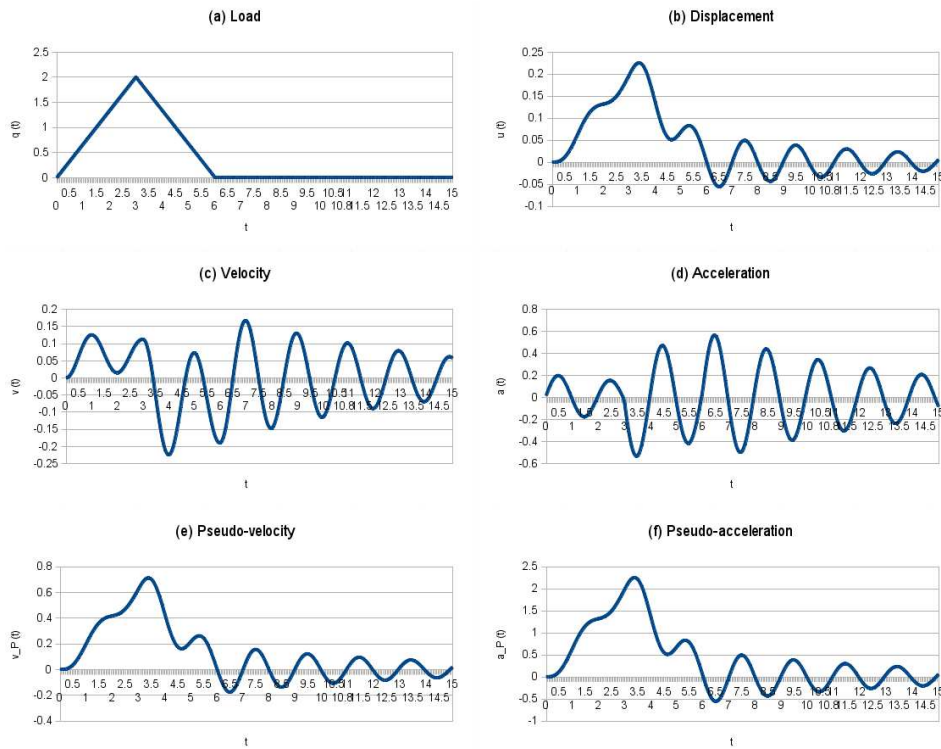


**Figure 5.2:** (a) The load function. (b) Displacement response function. (c) Velocity response function. (d) Acceleration response function. (e) Pseudo-velocity response diagram. (f) Pseudo-acceleration response diagram.

**Solution.** The calculation was carried out with the Cauchy-Euler method. The results are shown in Figure 5.2 (b-f).

### Response functions due to support vibration

We have seen in Subsection 1.1.4 that support vibration  $u_g(t)$  can be treated as a forced vibration with load  $q(t) = -m\ddot{u}_g(t)$ . In this model the unknown displacement  $u(t)$  represents the elastic deformation of the structure.

One can substitute the above load vector into the Duhamel's integral (1.26):

$$u(t) = \int_0^t \frac{-\ddot{u}_g(\tau)}{\omega_0^*} e^{-\xi\omega_0(t-\tau)} \sin(\omega_0^*(t-\tau)) d\tau.$$

The pseudo-acceleration response of a damped SDOF system due to support vibration is then:

$$a_P(t) = \omega_0^2 \int_0^t \frac{-\ddot{u}_g(\tau)}{\omega_0^*} e^{-\xi\omega_0(t-\tau)} \sin(\omega_0^*(t-\tau)) d\tau, \quad (5.3)$$

and the equivalent spring force can be calculated as above,  $f_S(t) = ma_P(t)$ .

As we have seen, the computation of the response functions is of the same steps technically both for an external loading and for support vibration. In the latter case the mass times ground acceleration is used as an equivalent external forcing. (The equivalent load is directly, the response is inversely proportional to the mass, so these two effects cancel each other.) In the further analysis we focus on earthquake analysis, so we deal only with support-vibration-type excitations.

### 5.2.2 Response spectrum

A central concept in elastic earthquake engineering is the concept of *response spectrum*. For a given structure the most important quantity is the maximal displacement and the maximal spring force. The response spectrum is the collection of these maximal values for a given load. We must calculate the peak values of the response functions for structures with different natural circular frequencies but with the same damping ratio  $\xi$ . Then we plot the natural circular frequencies versus the maximums of the response function for various structures in a common coordinate system. This diagram is called the response spectrum. It is constructed for several damping ratios. It depends on the load, the damping ratio, and the natural circular frequency. Once we have the diagram of the response spectrum based on the calculation of sufficiently large number of structures with different natural frequencies, we can find the value for any natural frequency from interpolation between two neighbouring known points. Depending on what kind of peak values are drawn, we can talk about various response spectra. For example, *displacement response spectrum* (denoted by  $s_u(\xi, \omega_0)$ ) collects the maximums of displacement responses, while *acceleration response spectrum* (denoted by  $s_a(\xi, \omega_0)$ ) collects the maximums of acceleration responses.

We note here that the *pseudo-acceleration response spectrum* (denoted by  $s_{Pa}(\xi, \omega_0)$ ) can be easily calculated from the displacement response spectrum based on the definition of the pseudo-acceleration response (5.2):

$$s_{Pa}(\xi, \omega_0) = \omega_0^2 s_u(\xi, \omega_0).$$

In engineering practice the response spectrum is often given as the function of the natural period  $T_0 = 2\pi/\omega_0$  of the structure. We note here, that every above response spectrum corresponds to one given load (here one ground-motion  $\ddot{u}_g(t)$ ), and one structural damping coefficient  $\xi$ .

**Problem 5.2.2** (Calculation of response spectrum). An undamped, single DOF system is characterized by the mass  $m = 1$  kg, and spring stiffness  $k = 10$  N/m. The system is forced by an impulse already shown in Figure 5.2 (a) Calculate the displacement- and pseudo-acceleration response spectra!

**Solution.** The calculation were carried out with Cauchy-Euler method. Three examples of the response functions are shown in 5.3 (a) with the peak values highlighted. The resulting spectra are shown in Figure 5.3 (b-c).

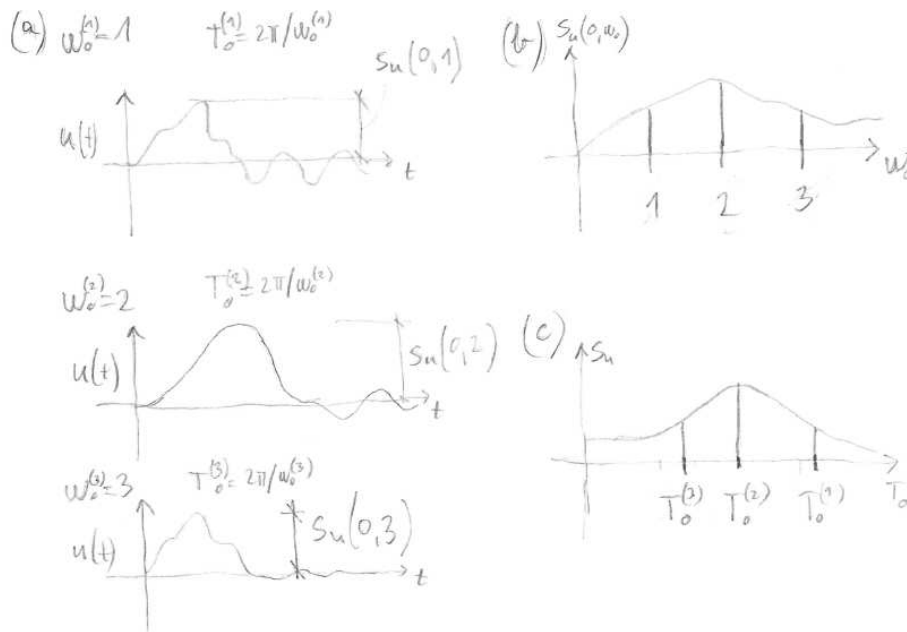


**Figure 5.3:** (a) Example diagrams of the displacement response function of structures with various loading. (b) Displacement response spectrum vs. the natural circular frequency. (c) Displacement response spectrum vs. the natural period.

### Spectral characteristics of structures

For structures with large natural circular frequencies (i.e. small natural period) the mass is connected to the ground with a very stiff spring. Therefore the deformations are small, and the (peak) value of the pseudo acceleration approaches the (peak) acceleration of the ground. This type of structures are called *acceleration sensitive* structures.

For structures with small natural circular frequencies (i.e. large natural period) the mass is connected to the ground with a very soft spring. Therefore the displacements of the mass are small, and the (peak) value of the deformation approaches the (peak) displacements of the ground. This type of structures are called *displacement sensitive* structures.

In the region between the above two types, structures are called *velocity sensitive*, because the structural response appears to be related to the velocity mainly.

### 5.2.3 Design spectrum

The peak structural response to a given load can be calculated from the response spectrum of that given load.

For design purposes the application of the response spectrum calculated from the support motion is still not a good choice. First, there may be steep jumps in the spectrum, where the analysed structure would exhibit a small peak response, but the real structure would exhibit a much larger response. Second, different earthquakes have different time history and different

response spectra. It is because of the difference in the location of the hypocenter, and in the strength of the earthquakes.

Because of the above reasons we want to create a *design spectrum*, which represents the typical earthquakes based on the response spectra of past measurements, and avoids sharp jumps. So, the design spectrum is defined as a smoothed hull above a lot of recorded response spectra.

Design spectrum is given in standards [4] for various damping coefficients  $\xi$ . In most cases they are given as the pseudo-acceleration versus the natural period:  $S_e(T_0)$ . To separate various effects,  $S_e(T_0)$  is given as:

$$S_e(T_0) = \gamma_I a_{gR} S \beta(T_0),$$

where  $\gamma_I$  is an importance factor representing the damage caused by the collapse of the structure,  $a_{gR}$  is the reference value of the ground acceleration on solid rock,  $S$  is a soil coefficient representing that soft soils increase the effect of earthquakes, and  $\beta(T_0)$  describes qualitatively the pseudo-acceleration. A typical shape of the diagram  $\beta(T_0)$  is shown in Figure 5.4.

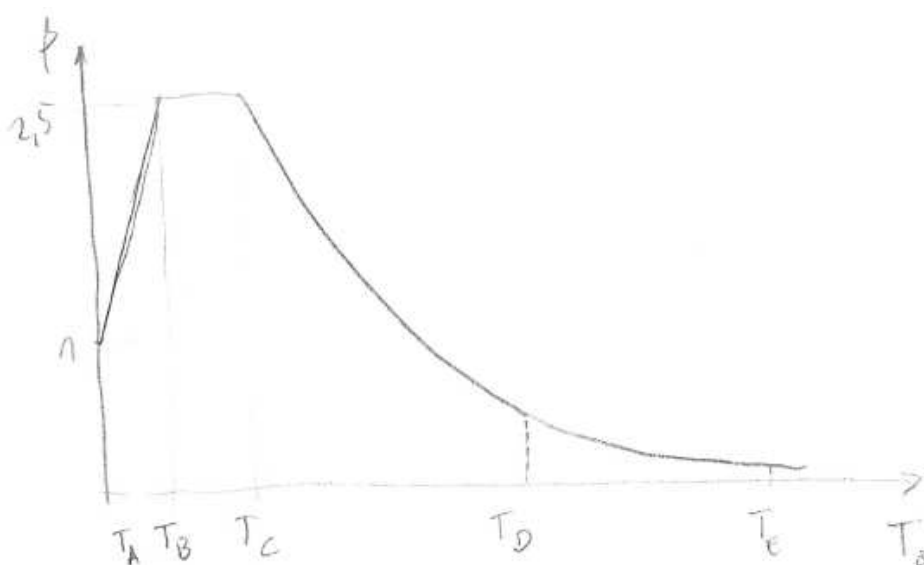


**Figure 5.4:** The function  $\beta(T_0)$  of the pseudo-acceleration response versus the natural period.

The function  $\beta(T_0)$  depends on the structural damping  $\xi$  via a correction factor  $\eta = \max(0.55, \sqrt{10/(5 + \xi)})$ . The function  $\beta(T_0)$  consists of a linear segment in the zone  $T_0 < T_B$

$$\beta(T_0) = \left( 1 + \frac{T_0}{T_B} (2.5\eta - 1) \right)$$

and a constant coefficient in the zone  $T_B < T_0 < T_C$

$$\beta(T_0) = 2.5\eta - 1.$$

In these zones there are the acceleration-sensitive structures. Velocity-sensitive structures have constant pseudo velocity, therefore the curve  $\beta(T_0)$  is inversely proportional to the natural period in the zone  $T_C < T_0 < T_D$

$$\beta(T_0) = 2.5\eta \left( \frac{T_C}{T_0} \right).$$

Displacement-sensitive structures are in the region  $T_D < T_0$  with a decaying  $\beta$ -function.

$$\beta(T_0) = 2.5\eta \left( \frac{T_C T_D}{T_0^2} \right).$$

The periods  $T_B$ ,  $T_C$ , and  $T_D$  depend on the type of the soil.

### 5.3 Response spectrum of MDOF systems

Earthquake analysis of MDOF systems can be carried out via integration of the matrix differential equation of motion with proper support vibrations as forcing. We have seen in the case of SDOF systems, that time history of earthquakes varies, so this type of analysis would require proper (real or artificial) earthquake records.

#### 5.3.1 Modal analysis

Another way of the computation is based on the modal analysis. We have seen in Section 4.2, that it requires proportional damping. We can calculate the *design modal displacement* from the design response spectrum, and calculate the modal response for each natural mode of the structure.

We repeat the important, applied equations here. The differential equation of motion

$$\mathbf{M}\ddot{\mathbf{u}}(t) + \mathbf{C}\dot{\mathbf{u}}(t) + \mathbf{K}\mathbf{u}(t) = \mathbf{q}(t) \quad (5.4)$$

is reduced to the modal equations of motion

$$\ddot{y}_j(t) + 2\xi\omega_{0j}\dot{y}_j(t) + \omega_{0j}^2 y_j(t) = \mathbf{u}_j^T \mathbf{q}(t) = f_j(t), \quad j = 1, \dots, N. \quad (5.5)$$

In the case of earthquake the load vector is

$$\mathbf{q}(t) = -\ddot{u}^g(t)\mathbf{m}^g = -\ddot{u}^g(t)\mathbf{M}^i \mathbf{r}. \quad (5.6)$$

(Here  $\mathbf{M}^i$  is the rows corresponding to the internal nodes in the unconstrained mass matrix of the structure,  $\mathbf{r}$  is the total influence vector. See Subsection 3.5.3.) The modal response can be calculated with the Duhamel's integral

$$y_j(t) = \int_0^t \frac{f_j(\tau)}{1 \cdot \omega_{0j}^*} e^{-\xi\omega_{0j}(t-\tau)} \sin(\omega_{0j}^*(t-\tau)) d\tau. \quad (5.7)$$



We can substitute the modal load given by Eqs. (5.5) and (5.6) into (5.7)

$$\begin{aligned} y_j(t) &= \int_0^t \frac{\mathbf{u}_j^T(-\ddot{u}^g(\tau))\mathbf{m}^g}{\omega_{0j}^*} e^{-\xi\omega_{0j}(t-\tau)} \sin(\omega_{0j}^*(t-\tau)) d\tau \\ &= \mathbf{u}_j^T \mathbf{m}^g \int_0^t \frac{-\ddot{u}^g(\tau)}{1 \cdot \omega_{0j}^*} e^{-\xi\omega_{0j}(t-\tau)} \sin(\omega_{0j}^*(t-\tau)) d\tau. \end{aligned}$$

The integral in the above formula is the  $j$ th modal displacement response to the support vibration  $\ddot{u}^g(t)$ . During the design process we do not have support vibration functions (since we do not know the time histories of upcoming earthquakes), but a design response spectrum. Therefore, instead of the calculation of the integral, we should read the response spectrum value at  $\omega_{0j}^*$  for the structural damping ratio  $\xi$ . However, usually we do not have the displacement response spectrum either, but the pseudo acceleration design spectrum. In this case we have to divide this pseudo-acceleration  $S_e(\xi, \omega_{0j})$  by  $\omega_{0j}^2$ . The maximal modal displacement is then

$$y_j^{\max} = \mathbf{u}_j^T \mathbf{m}^g \frac{S_e(\xi, \omega_{0j}^*)}{\omega_{0j}^2}.$$

The design values of displacements of the structure due to this modal displacement of the  $j$ th mode is:

$$\mathbf{u}_{j,\max} = \mathbf{u}_j \mathbf{u}_j^T \mathbf{m}^g \frac{S_e(\xi, \omega_{0j}^*)}{\omega_{0j}^2}. \quad (5.8)$$

We can use this displacement vector to calculate the internal forces of the members belonging to the  $j$ th mode.

**Note:** The quasi-static nodal force system that results in the above displacement system can be calculated with the stiffness matrix as

$$\mathbf{f}_{Sj,\max} = \mathbf{K}\mathbf{u}_{j,\max}.$$

One can apply the above fictitious force on the nodes to calculate the equivalent static response of the  $j$ th mode. <sup>1</sup> If we write the nodal forces with Eq. (5.8)

$$\mathbf{f}_{Sj,\max} = \mathbf{K}\mathbf{u}_j \mathbf{u}_j^T \mathbf{m}^g \frac{S_e(\xi, \omega_{0j}^*)}{\omega_{0j}^2}$$

one can realize, that  $\mathbf{K}\mathbf{u}_j = \omega_{0j}^2 \mathbf{M}\mathbf{u}_j$  results in the simplified formula

$$\mathbf{f}_{Sj,\max} = \mathbf{M}\mathbf{u}_j \Gamma_j S_e(\xi, \omega_{0j}^*)$$

with the modal participation  $\Gamma_j = \mathbf{u}_j^T \mathbf{m}^g$  introduced in Eq. (3.114).

<sup>1</sup>Apparently, that analysis would start with the solution of the classical static equation  $\mathbf{K}\mathbf{u} = \mathbf{q}$  with  $\mathbf{q} = \mathbf{f}_{Sj,\max}$ . It should not be a surprise, that the solution will be  $\mathbf{u}_{j,\max}$ .



### Summation of modal responses

With the previously presented method we can calculate a designed peak value for every mode, from which a peak value of the modal internal force can be obtained. Let us denote the designed peak of the internal force  $C$  in the  $j$ th mode by  $C_{j,\max}$ .

The question arises, how we should sum up the maximal modal internal forces?

- We can take the *sum of absolute values* (ABSSUM):

$$C_{\max} = \sum_{j=1}^N |C_{j,\max}|. \quad (5.9)$$

This is on the safe side, it is very unlikely, that each maximum occurs at the same time.

- If the natural circular frequencies are well separated <sup>2</sup>, we can take the *square root of the sum of squares* (SRSS)

$$C_{\max} = \sqrt{\sum_{j=1}^N C_{j,\max}^2}. \quad (5.10)$$

This method emphasizes the modes with larger responses. The root square of the sum of squares can be written in matrix form too:

$$C_{\max} = \sqrt{\mathbf{C}_{\max}^T \mathbf{I} \mathbf{C}_{\max}}. \quad (5.11)$$

with the vector of maximal modal internal forces

$$\mathbf{C}_{\max}^T = [ C_{1,\max} \quad C_{2,\max} \quad \dots \quad C_{N,\max} ].$$

- The first natural mode is often the most important. We can consider this in the SRSS method emphasizing the first mode:

$$C_{\max} = C_{1,\max} + \sqrt{\sum_{j=2}^N C_{j,\max}^2}.$$

- If there is a damping  $\xi$  in the structure, the modes are coupled. In that case one can use the *complete quadratic combination rule* (CQC)

$$C_{\max} = \sqrt{\mathbf{C}_{\max}^T \boldsymbol{\rho} \mathbf{C}_{\max}}, \quad (5.12)$$

where the correlation matrix  $\boldsymbol{\rho}$  represents the coupling between the modes. Its entries are computed from minimizing the error between the responses of the structure to a

<sup>2</sup> The natural circular frequencies are well separated, when the smallest relative difference between any two frequencies is more than 10%.

random forcing with broad spectrum (*white noise*) obtained by numerical integration and by modal analysis. The entries in the correlation matrix are

$$\rho_{ij} = \frac{8\xi^2 \left(1 + \frac{\omega_{0i}}{\omega_{0j}}\right) \left(\frac{\omega_{0i}}{\omega_{0j}}\right)^{3/2}}{\left(1 - \left(\frac{\omega_{0i}}{\omega_{0j}}\right)^2\right)^2 + 4\xi^2 \left(1 + \frac{\omega_{0i}}{\omega_{0j}}\right)^2}.$$

In an undamped system  $\rho = \mathbf{I}$ .

## 5.4 Various questions about earthquake analysis

### 5.4.1 Inelastic response of structure

Large earthquakes usually belong to the ultimate load cases. Structures are expected not to collapse under the ultimate loads, however, some plastic deformation is allowed. If we want to take the plastic deformation into account during our analysis, we have to implement it in the constitutive law.

For example, a simple bilinear model, the linear elastic-plastic material can be used. The spring behaves linearly up to a yield force  $F_y$ . When the spring force reaches this yield force, the displacements grow further without any change in the force. If the spring is unloaded when it is already in the plastic state, then it behaves elastic again, but a residual strain remains, which equals to the plastic deformation. (See Figure 5.5 (a).)

Numerical results of the response spectrum of linear elastic-plastic structures shows, that for large natural periods (small natural frequencies, soft, heavy structures) the response spectrum is not far from the results of the linear elastic analysis: the structure avoids the large displacements through its plastic deformations. However, the elastic-plastic materials require a certain *ductility*  $\mu_d$ , i.e. it must bear the plastic deformations beyond the yielding point, which is represented by the ratio of the maximal deformation  $u_{max}$ , and the deformation at yielding  $u_y$ :

$$\mu_d = \frac{u_{max}}{u_y}.$$

The numerical simulations suggest that the necessary ductility equals approximately to the ratio of the spring force from the elastic calculation and the yielding force.

### Inelastic response spectrum

We can take the ductility of a structure into account in the design phase, by using design response spectrum. We introduce an equivalent elastic structure that has the same initial stiffness as the elastic-plastic structure in the elastic regime (see Figure 5.5 (b)). Then we calculate the loads from the earthquake with the design response spectrum on the equivalent elastic structure. We decrease the load because of the ductility and do the analysis with the decreased load on the elastic-plastic structure. In standards the above process is implemented such that the

*design response spectrum* is defined to be the elastic design response spectrum divided by the behavioral coefficient  $q$ :

$$S_d(T_0) = \frac{S_e(T_0)}{q}.$$

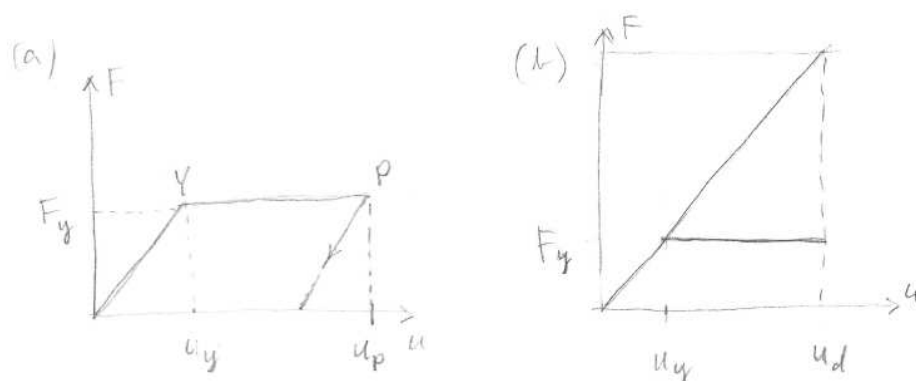


**Figure 5.5:** (a) Force-deformation diagram of the linear elastic-plastic material model: loading, reaching the yield point  $Y$ , further loading (plastic deformation), unloading at point  $P$ . Notice, that there is a residual plastic deformation  $u_p - u_y$  in the unloaded state. (b) Force-deformation diagram of the linear elastic-plastic and the equivalent elastic structures.

## 5.4.2 Time history analysis

Numerical solution of the differential equation of motion was presented in Section 4.6. It can be used to calculate the structural response for any given support motion. Using real time histories of previous earthquakes makes it possible to compute the response of a structure. In this case, the stiffnesses and masses of the structure must be determined correctly to achieve a given accuracy. For safety reason, these analysis must be performed for various earthquake records.

Another advantage of the time history analysis is that the material and geometrical nonlinear behaviour of the structure can be considered in the calculation, only the stiffness matrix must reflect the nonlinearity in Eq. (4.63).

### Artificial time-history functions

Existing earthquake records are not suitable to be used in design process. That is because there are only a few of these records, with various intensity, and they do not cover a wide range of the design spectrum. Because of that we want a procedure, that uses either the elastic, or the design response spectra in time history analysis. We must generate artificial earthquake records, which have a response spectrum close to the design response spectrum. The assumed form of the artificial earthquake record is

$$u^g(t) = I(t) \sum_{i=1}^M A_i \cos(\omega_i t + \varphi_i),$$

where  $\omega_i$  is a chosen circular frequency,  $\varphi_i$  is the corresponding phase angle chosen randomly, and  $A_i$ , ( $i = 1, \dots, M$ ) are the unknown amplitudes of each harmonic component. The function  $I(t)$  is an envelope function representing the typical behavior of earthquakes. That envelope function usually starts with an initial part where the intensity increases, followed by the strong quake, and finished by a decaying intensity. Typical envelope functions are presented in Figure 5.6.

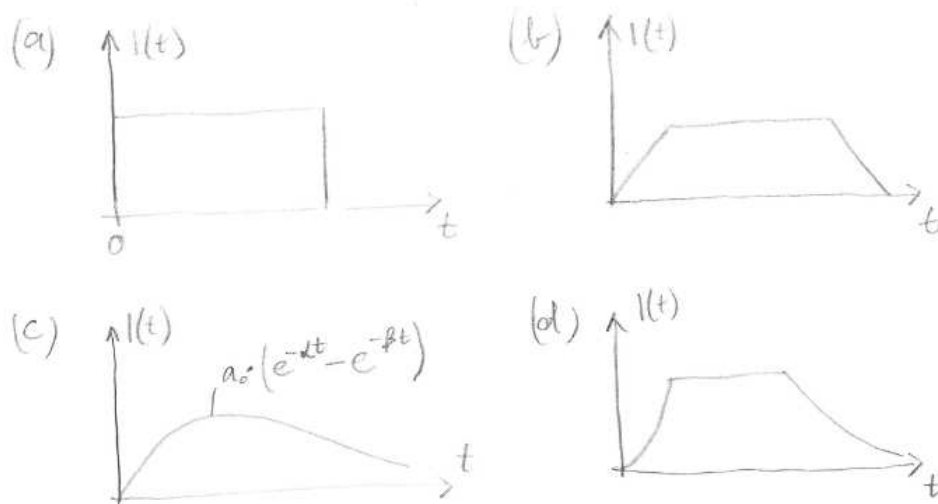


**Figure 5.6:** Typical envelope functions of artificial earthquake records. (a) boxcar: constant value as long the earthquake lasts. (b) trapezoid: linear increasing and decaying part, with a constant strong quake. (c) exponential: the sum of two exponential function. (d) compound: quadratic increasing part, constant strong quake, and exponentially decaying part.

The amplitudes  $A_i$  are iterated so that the elastic response spectrum of  $u^g(t)$  calculated from Eq. (5.3) be the closest to the elastic design spectrum. Technically, in  $M$  points, e.g. in the points  $\omega_i$  we can fit the response spectrum and the design spectrum. This is done in an iterative process, hence the change of an amplitude  $A_i$  changes all computed response spectrum values. When the amplitudes  $A_i$  do not change significantly anymore, we stop the iteration, and analyse the response of the structure to the support motion  $u^g(t)$ .

This procedure must be repeated for various phase angle sets. During the calculation, the actual deformations and internal forces can be determined.

## Bibliography

- [1] VI Arnold. *Ordinary Differential Equations*. The MIT Press, Cambridge, 1973.
- [2] FP Beer, ER Johnston Jr, JT DeWolf, and DF Mazurek. *Mechanics of Materials*. McGraw-Hill, New York, 2009.
- [3] AK Chopra. *Dynamics of Structures*. Prentice Hall, New Jersey, 1995.
- [4] EN 1998 Eurocode 8: Design of structures for earthquake resistance, 1998.
- [5] L Frýba. *Vibration of Solids and Structures under Moving Loads*. Thomas Telford, Prague, 1999.
- [6] J Györgyi. *Szerkezetek Dinamikája*. Műegyetemi Kiadó, Budapest, 2006. (In Hungarian).
- [7] M Kurutz and I Bojtár. *Lecture Notes on Strength of Materials*. Budapest University of Technology and Economics. [www.me.bme.hu/en/course/strength-materials](http://www.me.bme.hu/en/course/strength-materials).
- [8] A Lengyel and F Kovács. *Lecture Notes on Structural Analysis Theory*. Budapest University of Technology and Economics. [www.me.bme.hu/en/course/structural-analysis-theory](http://www.me.bme.hu/en/course/structural-analysis-theory).
- [9] T Tarnai. *Structural Stability in Engineering Practice (L Kollár Ed.)*, chapter Summation theorems concerning critical loads of bifurcation, pages 23–58. E & FN Spon, London, 1999.
- [10] S Timoshenko and JN Goodier. *Theory of Elasticity*. McGraw-Hill, New York, 1951.
- [11] S Timoshenko, DH Young, and W Weaver Jr. *Vibration Problems in Engineering*. John Wiley & Sons, New York, 1974.
- [12] EL Wilson. *Three-Dimensional Static and Dynamic Analysis of Structures*. Computers and Structures, Inc., Berkeley, 2002.
- [13] JP Wolf. *Dynamic Soil-Structure Interaction*. Prentice-Hall, Inc., New Jersey, 1985.
- [14] JP Wolf and A J Deeks. *Foundation Vibration Analysis: a strength-of-material approach*. Elsevier, Oxford, 2004.

# Appendix A

## Additional derivations and notes

### A.1 Travelling-wave solution for the free vibration of a prismatic bar

Instead of assuming a solution  $u(x, t)$  of Eq. (2.6) as a standing wave (Eq. (2.7)) we can search the solution as the sum of two travelling waves:

$$u(x, t) = u_1(x_1) + u_2(x_2). \quad (\text{A.1})$$

In the above equation  $x_1 = x - c_n t$  and  $x_2 = x + c_n t$  are the *phases* of a forward and a backward travelling wave, respectively. The functions  $u_1(x_1)$  and  $u_2(x_2)$  are the current shapes of those waves travelling with the velocity  $c_n$  forward and backward, respectively. At  $t = 0$  both phases are zero ( $x_1 = x_2 = x$ ), so the  $u_1(x)$  and  $u_2(x)$  functions describe the shapes of the waves at a frozen time instant.

The wave functions  $u_1(x_1)$  and  $u_2(x_2)$  are single variable functions. In the assumed form Eq. (A.1) the arguments of the wave functions are internal functions of  $x$  and  $t$ , so for the derivatives we have to use the chain rule. In the following formulas  $u_1'(x_1)$  denote the derivative of the wave function  $u_1(x_1)$  with respect to  $x_1$ , and  $u_2'(x_2)$  denote the derivative of the wave function  $u_2(x_2)$  with respect to  $x_2$ . For the partial derivatives with respect to the coordinate  $x$  we will have:

$$\frac{\partial u_1(x_1)}{\partial x} = u_1'(x_1) \frac{\partial(x - c_n t)}{\partial x} = u_1'(x_1), \quad \frac{\partial^2 u_1(x_1)}{\partial x^2} = u_1''(x_1).$$

For the partial derivatives with respect to time we have:

$$\begin{aligned} \frac{\partial u_1(x_1)}{\partial t} &= u_1'(x_1) \frac{\partial(x - c_n t)}{\partial t} = -c_n u_1'(x_1), \\ \frac{\partial^2 u_1(x_1)}{\partial t^2} &= -c_n u_1''(x_1) \frac{\partial(x - c_n t)}{\partial t} = c_n^2 u_1''(x_1). \end{aligned}$$

The same can be used for the wave function  $u_2$  of the backward travelling wave:

$$\frac{\partial u_2(x_2)}{\partial x} = u_2'(x_2) \frac{\partial(x + c_n t)}{\partial x} = u_2'(x_2), \quad \frac{\partial^2 u_2(x_2)}{\partial x^2} = u_2''(x_2).$$

For the partial derivatives with respect to time we have:

$$\begin{aligned}\frac{\partial u_2(x_2)}{\partial t} &= u_2'(x_2) \frac{\partial(x + c_n t)}{\partial t} = c_n u_2'(x_2), \\ \frac{\partial^2 u_2(x_2)}{\partial t^2} &= c_n u_2''(x_2) \frac{\partial(x + c_n t)}{\partial t} = c_n^2 u_2''(x_2).\end{aligned}$$

If we substitute the sum of the above second derivatives into Eq. (2.6) we get:

$$(c_n^2 u_1''(x - c_n t) + c_n^2 u_2''(x + c_n t)) - c_n^2 (u_1''(x - c_n t) + u_2''(x + c_n t)) = 0,$$

which is an identity, so the assumption Eq. (A.1) is correct, and  $c_n$  is indeed the velocity of travelling waves.

To find the wave functions  $u_1(x_1)$  and  $u_2(x_2)$  we have to use the initial conditions. Let us assume, that the displacement and the velocity at  $t = 0$  are given functions:

$$u(x, 0) = u_0(x), \quad \dot{u}(x, 0) = v_0(x). \quad (\text{A.2})$$

We substitute the sum of the travelling waves  $u_1(x - c_n 0)$  and  $u_2(x + c_n 0)$ , and the sum of their derivatives with respect to time  $-c_n u_1'(x - c_n 0)$  and  $c_n u_2'(x + c_n 0)$  into the initial conditions (A.2):

$$u_1(x - c_n 0) + u_2(x + c_n 0) = u_0(x), \quad (\text{A.3})$$

$$-c_n u_1'(x - c_n 0) + c_n u_2'(x + c_n 0) = v_0(x). \quad (\text{A.4})$$

We differentiate Eq. (A.3) with respect to  $x$ , and divide both sides of Eq. (A.4) by  $c_n$ , and leave behind the  $c_n 0$  terms:

$$\begin{aligned}u_1'(x) + u_2'(x) &= u_0'(x), \\ -u_1'(x) + u_2'(x) &= \frac{v_0(x)}{c_n}.\end{aligned} \quad (\text{A.5})$$

The system of differential equations (A.5) can be simplified, if we take the half of the difference of the equations and the half of the sum of the equations:

$$\begin{aligned}u_1'(x) &= \frac{1}{2} \left( u_0'(x) - \frac{v_0(x)}{c_n} \right), \\ u_2'(x) &= \frac{1}{2} \left( u_0'(x) + \frac{v_0(x)}{c_n} \right).\end{aligned} \quad (\text{A.6})$$

The ordinary differential equations of Eq. (A.6) can be solved by integration with respect to  $x$ :

$$\begin{aligned}u_1(x) &= \frac{1}{2} \int_0^x \left( u_0'(\xi) - \frac{v_0(\xi)}{c_n} \right) d\xi + C_1, \\ u_2(x) &= \frac{1}{2} \int_0^x \left( u_0'(\xi) + \frac{v_0(\xi)}{c_n} \right) d\xi + C_2.\end{aligned}$$

Since the whole solution is constructed from the sum of the above two functions translated, their constant terms will be added at any given time, in any given point, so, instead of them we have to take only one as a parameter, which must be determined from the boundary conditions. So, a simpler form of the shape functions will be:

$$\begin{aligned}
 u_1(x) &= \frac{u_0(x)}{2} - \frac{\int_0^x v_0(\xi) d\xi}{2c_n} + C, \\
 u_2(x) &= \frac{u_0(x)}{2} + \frac{\int_0^x v_0(\xi) d\xi}{2c_n}.
 \end{aligned}
 \tag{A.7}$$

And the final solution with varying time will be:

$$u_0(x, t) = \frac{u_0(x - c_n t) + u_0(x + c_n t)}{2} - \frac{\int_0^{x - c_n t} v_0(\xi) d\xi}{2c_n} + \frac{\int_0^{x + c_n t} v_0(\xi) d\xi}{2c_n} + C.$$

Figure A.1 (a) shows a simple application of the above result, where a bar with fixed-free ends is released from rest at  $t = 0$ , but the point  $B$  has an initial displacement, while points  $A$  and  $C$  are held in their original position. So, the function  $u_0(x)$  can be constructed from linear segments. Using Eq. (A.7) and the initial zero velocities the shape functions  $u_1$  and  $u_2$  will be half of the initial displacement  $u_0$  travelling forward and backward, respectively (see Fig. A.1 (b)). However, we need special care with the shape functions  $u_1$  and  $u_2$  because of the boundary conditions.

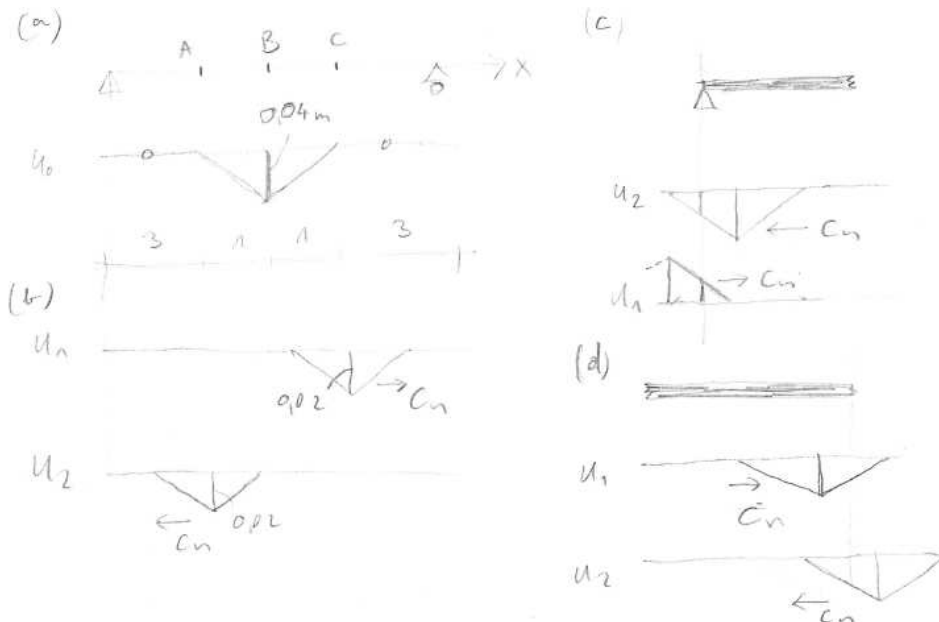


**Figure A.1:** (a) Rod with fixed-free ends with an initial displacement. (b) The forward and the backward travelling waves. (c) Bouncing back of the travelling wave from the fixed end. (d) Bouncing back of the travelling wave from the free end.

Figure A.1 (c) shows the fixed end, as the backward travelling wave  $u_2$  goes through it. But the boundary condition  $u(0, t) = 0$  requires  $u_1$  to enter the bar at the same time with



the opposite sign. (This part of the  $u_1(x)$  function was out of the bar in the beginning of the motion!) One can see, that the wave reaching a fixed end bounces back with the opposite sign and the opposite shape. Figure A.1 (d) shows the free end, as the forward travelling wave  $u_1$  goes through it. Here the boundary condition  $u'(0, t) = 0$  requires  $u_2$  to enter the bar at the same time with the same sign. (This part of the function  $u_2(x)$  was out of the bar in the beginning of the motion!) One can see, that the wave reaching a free end bounces back with the same sign and the opposite shape. Of course, the new parts of  $u_1$  and  $u_2$  entering one end of the bar, will reach the other end, "bouncing back" again, bringing new and new segments of  $u_2$  and  $u_1$  into the observable part of the bar.

## A.2 Static shape functions

The static shape functions of a beam member are collected in the matrix

$$\mathbf{N} = \left[ \begin{array}{c|c|c|c|c|c} u_i(x) & 0 & 0 & u_j(x) & 0 & 0 \\ \hline 0 & v_{iy}(x) & v_{i\varphi}(x) & 0 & v_{jy}(x) & v_{j\varphi}(x) \end{array} \right].$$

The strain matrix of a beam member is collected in

$$\mathbf{B} = \mathbf{LN} = \left[ \begin{array}{c|c|c|c|c|c} u'_i(x) & 0 & 0 & u'_j(x) & 0 & 0 \\ \hline 0 & -v''_{iy}(x) & -v''_{i\varphi}(x) & 0 & -v''_{jy}(x) & -v''_{j\varphi}(x) \end{array} \right].$$

In the case of a fixed-fixed beam, the entries of matrix  $\mathbf{N}$  are:

$$\mathbf{N}^{\text{ff}} = \left[ \begin{array}{c|c|c|c|c|c} 1 - \frac{x}{\ell} & 0 & 0 & \frac{x}{\ell} & 0 & 0 \\ \hline 0 & 2\frac{x^3}{\ell^3} - 3\frac{x^2}{\ell^2} + 1 & \frac{x^3}{\ell^2} - 2\frac{x^2}{\ell} + x & 0 & -2\frac{x^3}{\ell^3} + 3\frac{x^2}{\ell^2} & \frac{x^3}{\ell^2} - \frac{x^2}{\ell} \end{array} \right],$$

or, using  $\xi = x/\ell$ :

$$\mathbf{N}^{\text{ff}} = \left[ \begin{array}{c|c|c|c|c|c} 1 - \xi & 0 & 0 & \xi & 0 & 0 \\ \hline 0 & 2\xi^3 - 3\xi^2 + 1 & \ell(\xi^3 - 2\xi^2 + \xi) & 0 & -2\xi^3 + 3\xi^2 & \ell(\xi^3 - \xi^2) \end{array} \right].$$

The entries of the strain matrix are:

$$\mathbf{B}^{\text{ff}} = \left[ \begin{array}{c|c|c|c|c|c} \frac{1}{\ell} & 0 & 0 & -\frac{1}{\ell} & 0 & 0 \\ \hline 0 & -12\frac{x}{\ell^3} + 6\frac{1}{\ell^2} & -6\frac{x}{\ell^2} + 4\frac{1}{\ell} & 0 & 12\frac{x}{\ell^3} - 6\frac{1}{\ell^2} & -6\frac{x}{\ell^2} + 2\frac{1}{\ell} \end{array} \right],$$

or, using  $\xi = x/\ell$ :

$$\mathbf{B}^{\text{ff}} = \left[ \begin{array}{c|c|c|c|c|c} \frac{1}{\ell} & 0 & 0 & -\frac{1}{\ell} & 0 & 0 \\ \hline 0 & -\frac{12}{\ell^2}\xi + \frac{6}{\ell^2} & -\frac{6}{\ell}\xi + \frac{4}{\ell} & 0 & \frac{12}{\ell^2}\xi - \frac{6}{\ell^2} & -\frac{6}{\ell}\xi + \frac{2}{\ell} \end{array} \right].$$

In the case of a fixed-pinned beam, the entries of matrix  $\mathbf{N}$  are:

$$\mathbf{N}^{\text{fp}} = \left[ \begin{array}{c|c|c|c|c|c} 1 - \frac{x}{\ell} & 0 & 0 & \frac{x}{\ell} & 0 & 0 \\ \hline 0 & 1 + \frac{1}{2} \frac{x^3}{\ell^3} - \frac{3}{2} \frac{x^2}{\ell^2} & \frac{1}{2} \frac{x^3}{\ell^2} - \frac{3}{2} \frac{x^2}{\ell} + x & 0 & -\frac{1}{2} \frac{x^3}{\ell^3} + \frac{3}{2} \frac{x^2}{\ell^2} & 0 \end{array} \right].$$

For a pinned-fixed beam the entries of matrix  $\mathbf{N}$  are:

$$\mathbf{N}^{\text{pf}} = \left[ \begin{array}{c|c|c|c|c|c} 1 - \frac{x}{\ell} & 0 & 0 & \frac{x}{\ell} & 0 & 0 \\ \hline 0 & 1 + \frac{1}{2} \frac{x^3}{\ell^3} - \frac{3}{2} \frac{x}{\ell} & 0 & 0 & -\frac{1}{2} \frac{x^3}{\ell^3} + \frac{3}{2} \frac{x}{\ell} & \frac{1}{2} \frac{x^3}{\ell^2} - \frac{1}{2} x \end{array} \right].$$

For a pinned-pinned beam the entries of matrix  $\mathbf{N}$  are:

$$\mathbf{N}^{\text{pf}} = \left[ \begin{array}{c|c|c|c|c|c} 1 - \frac{x}{\ell} & 0 & 0 & \frac{x}{\ell} & 0 & 0 \\ \hline 0 & 1 - \frac{x}{\ell} & 0 & 0 & \frac{x}{\ell} & 0 \end{array} \right].$$

### A.3 Stiffness matrices of beam members

Elementary stiffness matrix of the fixed-fixed beam:

$$\mathbf{K}_{ij}^{\text{loc,ff}} = \left[ \begin{array}{ccc|ccc} \frac{EA}{\ell} & 0 & 0 & -\frac{EA}{\ell} & 0 & 0 \\ 0 & \frac{12EI}{\ell^3} & \frac{6EI}{\ell^2} & 0 & -\frac{12EI}{\ell^3} & \frac{6EI}{\ell^2} \\ 0 & \frac{6EI}{\ell^2} & \frac{4EI}{\ell} & 0 & -\frac{6EI}{\ell^2} & \frac{2EI}{\ell} \\ \hline -\frac{EA}{\ell} & 0 & 0 & \frac{EA}{\ell} & 0 & 0 \\ 0 & -\frac{12EI}{\ell^3} & -\frac{6EI}{\ell^2} & 0 & \frac{12EI}{\ell^3} & -\frac{6EI}{\ell^2} \\ 0 & \frac{6EI}{\ell^2} & \frac{2EI}{\ell} & 0 & -\frac{6EI}{\ell^2} & \frac{4EI}{\ell} \end{array} \right].$$

Elementary stiffness matrix of the fixed-pinned beam:

$$\mathbf{K}_{ij}^{\text{loc,fp}} = \begin{bmatrix} \frac{EA}{\ell} & 0 & 0 & -\frac{EA}{\ell} & 0 & 0 \\ 0 & \frac{3EI}{\ell^3} & \frac{3EI}{\ell^2} & 0 & -\frac{3EI}{\ell^3} & 0 \\ 0 & \frac{3EI}{\ell^2} & \frac{3EI}{\ell} & 0 & -\frac{3EI}{\ell^2} & 0 \\ \hline -\frac{EA}{\ell} & 0 & 0 & \frac{EA}{\ell} & 0 & 0 \\ 0 & -\frac{3EI}{\ell^3} & -\frac{3EI}{\ell^2} & 0 & \frac{3EI}{\ell^3} & 0 \\ 0 & 0 & 0 & 0 & 0 & 0 \end{bmatrix}$$

Elementary stiffness matrix of the pinned-fixed beam:

$$\mathbf{K}_{ij}^{\text{loc,pf}} = \begin{bmatrix} \frac{EA}{\ell} & 0 & 0 & -\frac{EA}{\ell} & 0 & 0 \\ 0 & \frac{3EI}{\ell^3} & 0 & 0 & -\frac{3EI}{\ell^3} & \frac{3EI}{\ell^2} \\ 0 & 0 & 0 & 0 & 0 & 0 \\ \hline -\frac{EA}{\ell} & 0 & 0 & \frac{EA}{\ell} & 0 & 0 \\ 0 & -\frac{3EI}{\ell^3} & 0 & 0 & \frac{3EI}{\ell^3} & -\frac{3EI}{\ell^2} \\ 0 & \frac{3EI}{\ell^2} & 0 & 0 & -\frac{3EI}{\ell^2} & \frac{3EI}{\ell} \end{bmatrix}$$

## A.4 Elementary dynamical stiffness matrix using purely dynamical shape functions

As an alternative method to that of shown in Section 3.2.2, we can formulate the elementary dynamical stiffness matrix using only dynamical shape functions. For that we write the virtual work of the force system shown in Figure 3.9 on the *same* displacement system:

$$\begin{aligned} \delta W_{\text{dd}} &= \left\{ \hat{V}_{iyy} + \mu\omega^2 \int_0^\ell \hat{v}_{iy}(x)\hat{v}_{iy}(x) dx - \int_0^\ell \hat{M}_{iy}(x)\hat{\kappa}_{iy}(x) dx \right\} \sin^2(\omega t) \\ &= \left\{ \hat{V}_{iyy} + \mu\omega^2 \int_0^\ell \hat{v}_{iy}(x)\hat{v}_{iy}(x) dx - EI \int_0^\ell \{\hat{v}_{iy}''(x)\}^2 dx \right\} \sin^2(\omega t) = 0. \end{aligned}$$

Expressing  $\hat{V}_{iyy}$ , the entry 2,2 of the dynamical stiffness matrix  $\hat{\mathbf{K}}_{ij}^{\text{loc}}$ , we get:

$$\hat{K}_{ij,22}^{\text{loc}} = \hat{V}_{iyy} = EI \int_0^\ell \{\hat{v}_{iy}''(x)\}^2 dx - \mu\omega^2 \int_0^\ell \{\hat{v}_{iy}(x)\}^2 dx.$$

If we denote the product of matrices  $\mathbf{L}$  (3.24) and  $\hat{\mathbf{N}}$  (3.70) as

$$\hat{\mathbf{B}} = \mathbf{L}\hat{\mathbf{N}},$$

then with matrices  $\hat{\mathbf{B}}$ , and with matrices  $\mathbf{D}$  (3.26) and  $\hat{\mathbf{N}}$  (3.70) we can shortly write

$$\hat{\mathbf{K}}_{ij}^{\text{loc}} = \int_0^\ell \hat{\mathbf{B}}^T \mathbf{D} \hat{\mathbf{B}} dx - \omega^2 \mu \int_0^\ell \hat{\mathbf{N}}^T \hat{\mathbf{N}} dx. \quad (\text{A.8})$$

It makes no difference whether we use (3.71) or (A.8), the final result  $\hat{\mathbf{K}}_{ij}^{\text{loc}}$  will be the same.

## A.5 Consistent mass matrices of beam members

Elementary consistent mass matrix of the fixed-fixed beam:

$$\mathbf{M}_{ij}^{\text{loc,ff}} = \mu \ell \begin{bmatrix} \frac{1}{3} & 0 & 0 & \frac{1}{6} & 0 & 0 \\ 0 & \frac{13}{35} & \frac{11}{210}\ell & 0 & \frac{9}{70} & -\frac{13}{420}\ell \\ 0 & \frac{11}{210}\ell & \frac{1}{105}\ell^2 & 0 & \frac{13}{420}\ell & -\frac{1}{140}\ell^2 \\ \hline \frac{1}{6} & 0 & 0 & \frac{1}{3} & 0 & 0 \\ 0 & \frac{9}{70} & \frac{13}{420}\ell & 0 & \frac{13}{35} & -\frac{11}{210}\ell \\ 0 & -\frac{13}{420}\ell & -\frac{1}{140}\ell^2 & 0 & -\frac{11}{210}\ell & \frac{1}{105}\ell^2 \end{bmatrix}.$$

Elementary consistent mass matrix of the fixed-pinned beam:

$$\mathbf{M}_{ij}^{\text{loc,fp}} = \mu \ell \begin{bmatrix} \frac{1}{3} & 0 & 0 & \frac{1}{6} & 0 & 0 \\ 0 & \frac{17}{35} & \frac{3}{35}\ell & 0 & \frac{39}{280} & 0 \\ 0 & \frac{3}{35}\ell & \frac{2}{105}\ell^2 & 0 & \frac{11}{280}\ell & 0 \\ \hline \frac{1}{6} & 0 & 0 & \frac{1}{3} & 0 & 0 \\ 0 & \frac{39}{280} & \frac{11}{280}\ell & 0 & \frac{33}{140} & 0 \\ 0 & 0 & 0 & 0 & 0 & 0 \end{bmatrix}.$$

Elementary consistent mass matrix of the pinned-fixed beam:

$$\mathbf{M}_{ij}^{\text{loc,pf}} = \mu \ell \begin{bmatrix} \frac{1}{3} & 0 & 0 & \frac{1}{6} & 0 & 0 \\ 0 & \frac{33}{140} & 0 & 0 & \frac{39}{280} & -\frac{11}{280}\ell \\ 0 & 0 & 0 & 0 & 0 & 0 \\ \hline \frac{1}{6} & 0 & 0 & \frac{1}{3} & 0 & 0 \\ 0 & \frac{39}{280} & 0 & 0 & \frac{17}{35} & -\frac{3}{35}\ell \\ 0 & -\frac{11}{280}\ell & 0 & 0 & -\frac{3}{35}\ell & \frac{2}{105}\ell^2 \end{bmatrix}.$$

Elementary consistent mass matrix of the pinned-pinned beam:

$$\mathbf{M}_{ij}^{\text{loc,pp}} = \mu \ell \begin{bmatrix} \frac{1}{3} & 0 & 0 & \frac{1}{6} & 0 & 0 \\ 0 & \frac{1}{3} & 0 & 0 & \frac{1}{6} & 0 \\ 0 & 0 & 0 & 0 & 0 & 0 \\ \hline \frac{1}{6} & 0 & 0 & \frac{1}{3} & 0 & 0 \\ 0 & \frac{1}{6} & 0 & 0 & \frac{1}{3} & 0 \\ 0 & 0 & 0 & 0 & 0 & 0 \end{bmatrix}.$$

## A.6 Few trigonometric identities

Here we derive two identities which are used in the particular solutions of damped, harmonically excited systems.

Let us start with the trigonometric identity

$$R \cos(\omega t - \varphi) = R \cos(\omega t) \cos(\varphi) + R \sin(\omega t) \sin(\varphi).$$

This is reformulated as

$$\begin{aligned} R \cos(\omega t - \varphi) &= (R \cos(\varphi)) \cos(\omega t) + (R \sin(\varphi)) \sin(\omega t) \\ &= a \cos(\omega t) + b \sin(\omega t), \quad \text{where} \\ a &= R \cos(\varphi), \\ b &= R \sin(\varphi) \end{aligned}$$

Here  $a$ ,  $b$ , and  $\varphi$  are computed from

$$\begin{aligned} a^2 + b^2 &= R^2(\sin^2(\varphi) + \cos^2(\varphi)) = R^2 \quad \rightarrow \quad R = \sqrt{a^2 + b^2}, \\ \frac{a}{b} &= \cot(\varphi) \quad \rightarrow \quad \varphi = \operatorname{arccot}\left(\frac{a}{b}\right). \end{aligned} \tag{A.9}$$

Therefore

$$\boxed{a \cos(\omega t) + b \sin(\omega t) = \sqrt{a^2 + b^2} \cos\left(\omega t - \operatorname{arccot}\left(\frac{a}{b}\right)\right)}. \tag{A.10}$$

Similarly, from the trigonometric identity

$$R \sin(\omega t - \varphi) = R \sin(\omega t) \cos(\varphi) - R \cos(\omega t) \sin(\varphi)$$

we can formally write

$$\begin{aligned} R \sin(\omega t - \varphi) &= (R \cos(\varphi)) \sin(\omega t) - (R \sin(\varphi)) \cos(\omega t) \\ &= a \sin(\omega t) - b \cos(\omega t), \quad \text{with} \\ a &= R \cos(\varphi), \\ b &= R \sin(\varphi) \end{aligned}$$

Here  $a$ ,  $b$ , and  $\varphi$  are computed again as (A.9). Thus

$$\boxed{a \sin(\omega t) - b \cos(\omega t) = \sqrt{a^2 + b^2} \sin\left(\omega t - \operatorname{arccot}\left(\frac{a}{b}\right)\right)}. \tag{A.11}$$

## A.7 Damped SDOF system solved with a different approach

We have shown the solution of the equation of motion of a damped, harmonically excited SDOF system. Here we recall these results. First we give the solution if the exciting force is a sine function. Then we go on with a cosine excitation. Next we show an approach that can handle both sine and cosine excitation in one hand, but as a drawback, this analysis requires complex functions. Finally we study cases when the load is a combination of harmonic functions, or it is a *Fourier* series.

### A.7.1 Sine

We have seen that the damped, harmonically excited SDOF

$$m\ddot{u}(t) + c\dot{u}(t) + ku(t) = F_0 \sin(\omega t)$$

has a homogeneous and a particular solutions. The latter one was assumed to be  $u_f(t) = u_{f0} \sin(\omega t - \varphi)$  intuitively.

The usual mathematical way is to search for the solutions as

$$u_f(t) = C_1 \sin(\omega t) + C_2 \cos(\omega t).$$

If this form is substituted back into the equation of motion, then

$$\begin{aligned} -m\omega^2 \{C_1 \sin(\omega t) + C_2 \cos(\omega t)\} + c\omega \{C_1 \cos(\omega t) - C_2 \sin(\omega t)\} \\ + k \{C_1 \sin(\omega t) + C_2 \cos(\omega t)\} = F_0 \sin(\omega t). \end{aligned}$$

Collecting the terms multiplied by  $\cos(\omega t)$  and  $\sin(\omega t)$ , respectively, we can write two equations for the coefficients  $C_1$  and  $C_2$

$$\begin{aligned} -m\omega^2 C_2 + c\omega C_1 + kC_2 = 0 & \rightarrow C_2 = -C_1 \frac{c\omega}{k - m\omega^2}, \\ -m\omega^2 C_1 - c\omega C_2 + kC_1 = F_0. \end{aligned}$$

Thus  $C_1$  and  $C_2$  are

$$\begin{aligned} C_1 &= F_0 \frac{k - m\omega^2}{(k - m\omega^2)^2 + c^2\omega^2}, \\ C_2 &= -F_0 \frac{c\omega}{(k - m\omega^2)^2 + c^2\omega^2}, \end{aligned}$$

and the solution of the equation of motion is

$$u_f(t) = F_0 \frac{k - m\omega^2}{(k - m\omega^2)^2 + c^2\omega^2} \sin(\omega t) - F_0 \frac{c\omega}{(k - m\omega^2)^2 + c^2\omega^2} \cos(\omega t).$$



This form of the solution, however, can be reformulated according to (A.11) as

$$\begin{aligned}
 u_f(t) &= F_0 \sqrt{\frac{(k - m\omega^2)^2 + c^2\omega^2}{\{(k - m\omega^2)^2 + c^2\omega^2\}^2}} \sin\left(\omega t - \operatorname{arccot}\left(\frac{k - m\omega^2}{c\omega}\right)\right) \\
 &= \frac{F_0}{k} \frac{1}{\sqrt{\left(1 - \frac{\omega^2}{\omega_0^2}\right)^2 + \omega^2 \frac{c^2}{k^2}}} \sin\left(\omega t - \operatorname{arccot}\left(\frac{1 - \frac{\omega^2}{\omega_0^2}}{\frac{c}{\omega \frac{k}{k}}}\right)\right).
 \end{aligned}$$

### A.7.2 Cosine

If the load is described by a harmonic cosine function, then the equation of motion is

$$\boxed{m\ddot{u}(t) + c\dot{u}(t) + ku(t) = F_0 \cos(\omega t)}.$$

The particular solution is again searched for as

$$u_f(t) = C_1 \sin(\omega t) + C_2 \cos(\omega t).$$

This form is substituted back into the equation of motion:

$$\begin{aligned}
 &-m\omega^2 \{C_1 \sin(\omega t) + C_2 \cos(\omega t)\} + c\omega \{C_1 \cos(\omega t) - C_2 \sin(\omega t)\} \\
 &+ k \{C_1 \sin(\omega t) + C_2 \cos(\omega t)\} = F_0 \cos(\omega t).
 \end{aligned}$$

Collecting the terms multiplied by  $\cos(\omega t)$  and  $\sin(\omega t)$ , respectively, we can write two equations for the coefficients  $C_1$  and  $C_2$

$$\begin{aligned}
 &-m\omega^2 C_2 + c\omega C_1 + kC_2 = F_0, \\
 &-m\omega^2 C_1 - c\omega C_2 + kC_1 = 0 \quad \rightarrow \quad C_1 = C_2 \frac{c\omega}{k - m\omega^2}.
 \end{aligned}$$

Thus  $C_1$  and  $C_2$  are

$$\begin{aligned}
 C_1 &= F_0 \frac{c\omega}{(k - m\omega^2)^2 + c^2\omega^2}, \\
 C_2 &= F_0 \frac{k - m\omega^2}{(k - m\omega^2)^2 + c^2\omega^2},
 \end{aligned}$$

and the solution of the equation of motion is

$$u_f(t) = F_0 \frac{c\omega}{(k - m\omega^2)^2 + c^2\omega^2} \sin(\omega t) + F_0 \frac{k - m\omega^2}{(k - m\omega^2)^2 + c^2\omega^2} \cos(\omega t).$$

This form of the solution can be reformulated according to (A.10) as

$$\begin{aligned}
 u_f(t) &= F_0 \sqrt{\frac{(k - m\omega^2)^2 + c^2\omega^2}{\{(k - m\omega^2)^2 + c^2\omega^2\}^2}} \cos\left(\omega t - \operatorname{arccot}\left(\frac{k - m\omega^2}{c\omega}\right)\right) \\
 &= \frac{F_0}{k} \frac{1}{\sqrt{\left(1 - \frac{\omega^2}{\omega_0^2}\right)^2 + \omega^2 \frac{c^2}{k^2}}} \cos\left(\omega t - \operatorname{arccot}\left(\frac{1 - \frac{\omega^2}{\omega_0^2}}{\frac{c}{\omega \frac{k}{m}}}\right)\right).
 \end{aligned}$$

### A.7.3 Sine and cosine

The approach introduced here can handle both sine and cosine loadings. In the equation of motion the loading is given as a special complex (harmonic) function:

$$m\ddot{\tilde{u}}(t) + c\dot{\tilde{u}}(t) + k\tilde{u}(t) = F_0 \{\cos(\omega t) + i \sin(\omega t)\} = F_0 e^{i\omega t}.$$

Here tilde distinguishes the complex unknown function  $\tilde{u}(t)$  from the previous real ones. Now the particular solution is searched for in the form

$$\tilde{u}_f(t) = \tilde{u}_{f0} e^{i\omega t}.$$

Substituting the above form back into the equation of motion we get:

$$(-m\omega^2 + i\omega c + k)\tilde{u}_{f0} e^{i\omega t} = F_0 e^{i\omega t}.$$

The complex coefficient  $\tilde{u}_{f0}$  is expressed as

$$\tilde{u}_{f0} = F_0 \frac{1}{-m\omega^2 + i\omega c + k} = \frac{F_0}{k} \frac{1}{\left(1 - \frac{\omega^2}{\omega_0^2}\right) + i\frac{\omega c}{k}}.$$

Now both the nominator and the denominator are multiplied with the conjugate of the denominator

$$\tilde{u}_{f0} = \frac{F_0}{k} \frac{1}{\left(1 - \frac{\omega^2}{\omega_0^2}\right) + i\frac{\omega c}{k}} \cdot \frac{\left(1 - \frac{\omega^2}{\omega_0^2}\right) - i\frac{\omega c}{k}}{\left(1 - \frac{\omega^2}{\omega_0^2}\right) - i\frac{\omega c}{k}} = \frac{F_0}{k} \frac{\left(1 - \frac{\omega^2}{\omega_0^2}\right) - i\frac{\omega c}{k}}{\left(1 - \frac{\omega^2}{\omega_0^2}\right)^2 + \frac{\omega^2 c^2}{k^2}}$$

The whole particular solution is then

$$\begin{aligned}\tilde{u}_f(t) &= \tilde{u}_{f0} e^{i\omega t} = \frac{F_0}{k} \frac{\left(1 - \frac{\omega^2}{\omega_0^2}\right) - i \frac{\omega c}{k}}{\left(1 - \frac{\omega^2}{\omega_0^2}\right)^2 + \frac{\omega^2 c^2}{k^2}} \{\cos(\omega t) + i \sin(\omega t)\} \\ &= \frac{F_0}{k} \left\{ \frac{\left(1 - \frac{\omega^2}{\omega_0^2}\right)}{\left(1 - \frac{\omega^2}{\omega_0^2}\right)^2 + \frac{\omega^2 c^2}{k^2}} \cos(\omega t) + \frac{\frac{\omega c}{k}}{\left(1 - \frac{\omega^2}{\omega_0^2}\right)^2 + \frac{\omega^2 c^2}{k^2}} \sin(\omega t) \right\} \\ &\quad + i \frac{F_0}{k} \left\{ \frac{\left(1 - \frac{\omega^2}{\omega_0^2}\right)}{\left(1 - \frac{\omega^2}{\omega_0^2}\right)^2 + \frac{\omega^2 c^2}{k^2}} \sin(\omega t) - \frac{\frac{\omega c}{k}}{\left(1 - \frac{\omega^2}{\omega_0^2}\right)^2 + \frac{\omega^2 c^2}{k^2}} \cos(\omega t) \right\}.\end{aligned}$$

This long formula can be shortened using Eqs. (A.10), (A.11):

$$\begin{aligned}\tilde{u}_f(t) &= \frac{F_0}{k} \frac{1}{\sqrt{\left(1 - \frac{\omega^2}{\omega_0^2}\right)^2 + \omega^2 \frac{c^2}{k^2}}} \cos \left( \omega t - \operatorname{arccot} \left( \frac{1 - \frac{\omega^2}{\omega_0^2}}{\omega \frac{c}{k}} \right) \right) \\ &\quad + i \frac{F_0}{k} \frac{1}{\sqrt{\left(1 - \frac{\omega^2}{\omega_0^2}\right)^2 + \omega^2 \frac{c^2}{k^2}}} \sin \left( \omega t - \operatorname{arccot} \left( \frac{1 - \frac{\omega^2}{\omega_0^2}}{\omega \frac{c}{k}} \right) \right)\end{aligned}$$

The real part of the above solution (i.e. the first term) is corresponded to the cosine excitation function, while the imaginary part (the second term) is used when the loading is given by a sine function. The main advantage of this abstract approach is that it handles both harmonic excitation modes in one formula, and that it prepares the reader for the even more abstract *Fourier* transform.

#### A.7.4 Quasi-periodic loading

It is rarely the case that the load is a harmonic function. In MDOF systems, it is even less likely, that all the loadings are governed by the same harmonic function. It is more general, that a loading is given as a combination of harmonic functions. This is also the case if the loading is turned into a *Fourier* series.

The particular solution of such a problem is simply just the sum of the particular solutions of the same system with one of the harmonic loadings. For instance, if we have a SDOF system

$$m\ddot{u}(t) + c\dot{u}(t) + ku(t) = F_1 \sin(\omega_1 t) + F_2 \cos(\omega_2 t) + F_3 \sin(\omega_3 t),$$

then the *particular* solution is

$$\begin{aligned}
 u_f(t) = & \frac{F_1}{k} \frac{1}{\sqrt{\left(1 - \frac{\omega_1^2}{\omega_0^2}\right)^2 + \omega_1^2 \frac{c^2}{k^2}}} \sin \left( \omega_1 t - \operatorname{arccot} \left( \frac{1 - \frac{\omega_1^2}{\omega_0^2}}{\omega_1 \frac{c}{k}} \right) \right) \\
 & + \frac{F_2}{k} \frac{1}{\sqrt{\left(1 - \frac{\omega_2^2}{\omega_0^2}\right)^2 + \omega_2^2 \frac{c^2}{k^2}}} \cos \left( \omega_2 t - \operatorname{arccot} \left( \frac{1 - \frac{\omega_2^2}{\omega_0^2}}{\omega_2 \frac{c}{k}} \right) \right) \\
 & + \frac{F_3}{k} \frac{1}{\sqrt{\left(1 - \frac{\omega_3^2}{\omega_0^2}\right)^2 + \omega_3^2 \frac{c^2}{k^2}}} \sin \left( \omega_3 t - \operatorname{arccot} \left( \frac{1 - \frac{\omega_3^2}{\omega_0^2}}{\omega_3 \frac{c}{k}} \right) \right).
 \end{aligned}$$

## A.8 Damped MDOF systems solved using complex algebra

### A.8.1 Inverse of a complex square matrix

Let us have a complex matrix  $\tilde{\mathbf{A}}$  of size  $N$  by  $N$ . The inverse of this matrix is denoted by  $\tilde{\mathbf{B}} = \tilde{\mathbf{A}}^{-1}$ . This matrix is searched for.

Matrices  $\tilde{\mathbf{A}}$  and  $\tilde{\mathbf{B}}$  are decomposed into real and imaginary parts:

$$\begin{aligned}\tilde{\mathbf{A}} &= \mathbf{A}_R + i\mathbf{A}_I, \\ \tilde{\mathbf{A}}^{-1} = \tilde{\mathbf{B}} &= \mathbf{B}_R + i\mathbf{B}_I.\end{aligned}$$

We compile the  $2N$ -by- $2N$  real matrix

$$\mathbf{A}_{2N} = \left[ \begin{array}{c|c} \mathbf{A}_R & \mathbf{A}_I \\ \hline -\mathbf{A}_I & \mathbf{A}_R \end{array} \right]. \quad (\text{A.12})$$

A mathematical statement says that the inverse of the above real matrix equals to

$$\mathbf{A}_{2N}^{-1} = \left[ \begin{array}{c|c} \mathbf{A}_R & \mathbf{A}_I \\ \hline -\mathbf{A}_I & \mathbf{A}_R \end{array} \right]^{-1} = \left[ \begin{array}{c|c} \mathbf{B}_R & \mathbf{B}_I \\ \hline -\mathbf{B}_I & \mathbf{B}_R \end{array} \right]. \quad (\text{A.13})$$

Thus the real part  $\mathbf{B}_R$  of the inverse of the complex matrix  $\tilde{\mathbf{A}}$  is the upper left  $N$ -by- $N$  block matrix of the inverse of the real matrix  $\mathbf{A}_{2N}$ . The imaginary part  $\mathbf{B}_I$  of complex matrix  $\tilde{\mathbf{A}}$  is the upper right  $N$ -by- $N$  block matrix of the inverse of real matrix  $\mathbf{A}_{2N}$ . Consequently, the inversion of a squared complex matrix can be traced back for the inversion of a double-sized real matrix.

The definition of the inverse matrix implies that  $\mathbf{A}_{2N}^{-1}\mathbf{A}_{2N} = \mathbf{A}_{2N}\mathbf{A}_{2N}^{-1} = \mathbf{I}_{2N}$ , where  $\mathbf{I}_{2N}$  is the  $2N$ -by- $2N$  identity matrix. With the above notations this identity is expressed:

$$\mathbf{A}_{2N}\mathbf{A}_{2N}^{-1} = \left[ \begin{array}{c|c} \mathbf{A}_R & \mathbf{A}_I \\ \hline -\mathbf{A}_I & \mathbf{A}_R \end{array} \right] \cdot \left[ \begin{array}{c|c} \mathbf{B}_R & \mathbf{B}_I \\ \hline -\mathbf{B}_I & \mathbf{B}_R \end{array} \right] = \left[ \begin{array}{c|c} \mathbf{I}_N & \mathbf{0}_N \\ \hline \mathbf{0}_N & \mathbf{I}_N \end{array} \right].$$

Here  $\mathbf{I}_N$  is the  $N$ -by- $N$  identity matrix, and  $\mathbf{0}_N$  is the  $N$ -by- $N$  zero (valued) matrix. If we execute this matrix multiplication for the blocks we get

$$\begin{aligned}\mathbf{A}_R\mathbf{B}_R - \mathbf{A}_I\mathbf{B}_I &= \mathbf{I}_N, \\ \mathbf{A}_R\mathbf{B}_I + \mathbf{A}_I\mathbf{B}_R &= \mathbf{0}_N, \\ -\mathbf{A}_I\mathbf{B}_R - \mathbf{A}_R\mathbf{B}_I &= \mathbf{0}_N, \\ -\mathbf{A}_I\mathbf{B}_I + \mathbf{A}_R\mathbf{B}_R &= \mathbf{I}_N.\end{aligned}$$

Only the first two of these equations are linearly independent. We extract  $\mathbf{B}_I$  from the second equation,  $\mathbf{B}_I = -\mathbf{A}_R^{-1}\mathbf{A}_I\mathbf{B}_R$ , and substitute it back into the first equation:

$$\mathbf{B}_R = (\mathbf{A}_R + \mathbf{A}_I\mathbf{A}_R^{-1}\mathbf{A}_I)^{-1}. \quad (\text{A.14})$$

That is the *real part* of the inverse of the complex matrix  $\tilde{\mathbf{A}}$ . Finally, from back substitution of this into the expression of  $\mathbf{B}_I$  we get the *imaginary part* of the inverse of the complex matrix  $\tilde{\mathbf{A}}$ :

$$\mathbf{B}_I = -\mathbf{A}_R^{-1}\mathbf{A}_I(\mathbf{A}_R + \mathbf{A}_I\mathbf{A}_R^{-1}\mathbf{A}_I)^{-1}. \quad (\text{A.15})$$

### A.8.2 Application forced MDOF systems

We copy here the solution (4.14) of the harmonically excited, damped MDOF system:

$$\tilde{\mathbf{u}}_f(t) = (-\omega^2 \mathbf{M} + i\omega \mathbf{C} + \mathbf{K})^{-1} \mathbf{q}_0 e^{i\omega t}.$$

We have to invert a complex matrix, then multiply it with a complex function, and separate the real and the imaginary parts of the solution. The real part becomes the particular solution, the steady-state vibration of the system due to a cosinusoidal forcing with frequency  $\omega$  and amplitudes  $\mathbf{q}_0$ . The imaginary part is governs the steady-state vibration of the system due to a sinusoidal forcing with the same frequency and amplitudes. Using the definitions introduced in the previous subsection, the matrix to invert is

$$\tilde{\mathbf{K}} = \mathbf{K} - \omega^2 \mathbf{M} + i\omega \mathbf{C},$$

i.e. the (complex) dynamical stiffness matrix. Its real and imaginary parts are

$$\operatorname{Re}(\tilde{\mathbf{K}}) = \mathbf{K} - \omega^2 \mathbf{M}, \quad \operatorname{Im}(\tilde{\mathbf{K}}) = \omega \mathbf{C}.$$

Using these parts, and following the definition (A.12), the block structure of the  $2N$ -by- $2N$  real matrix is

$$\mathbf{K}_{2N} = \left[ \begin{array}{c|c} \mathbf{K} - \omega^2 \mathbf{M} & \omega \mathbf{C} \\ \hline -\omega \mathbf{C} & \mathbf{K} - \omega^2 \mathbf{M} \end{array} \right].$$

According to the derived formula (A.15) and (A.14), the real part of the inverse of  $\tilde{\mathbf{K}}$  is

$$\operatorname{Re}(\tilde{\mathbf{K}}^{-1}) = \left( \mathbf{K} - \omega^2 \mathbf{M} + \omega^2 \mathbf{C} (\mathbf{K} - \omega^2 \mathbf{M})^{-1} \mathbf{C} \right)^{-1}, \quad (\text{A.16})$$

while the imaginary part of the inverse of  $\tilde{\mathbf{K}} = \mathbf{K} - \omega^2 \mathbf{M} + i\omega \mathbf{C}$  is

$$\operatorname{Im}(\tilde{\mathbf{K}}^{-1}) = -\omega (\mathbf{K} - \omega^2 \mathbf{M})^{-1} \mathbf{C} \left( \mathbf{K} - \omega^2 \mathbf{M} + \omega^2 \mathbf{C} (\mathbf{K} - \omega^2 \mathbf{M})^{-1} \mathbf{C} \right)^{-1}. \quad (\text{A.17})$$

The final solution (4.14) is then

$$\begin{aligned} \tilde{\mathbf{u}}_f(t) &= \left\{ \operatorname{Re}(\tilde{\mathbf{K}}^{-1}) + i \cdot \operatorname{Im}(\tilde{\mathbf{K}}^{-1}) \right\} \mathbf{q}_0 e^{i\omega t} \\ &= \left\{ \operatorname{Re}(\tilde{\mathbf{K}}^{-1}) + i \cdot \operatorname{Im}(\tilde{\mathbf{K}}^{-1}) \right\} \mathbf{q}_0 \{ \cos(\omega t) + i \sin(\omega t) \} \\ &= \left\{ \operatorname{Re}(\tilde{\mathbf{K}}^{-1}) \mathbf{q}_0 \cos(\omega t) - \operatorname{Im}(\tilde{\mathbf{K}}^{-1}) \mathbf{q}_0 \sin(\omega t) \right\} \\ &\quad + i \left\{ \operatorname{Re}(\tilde{\mathbf{K}}^{-1}) \mathbf{q}_0 \sin(\omega t) + \operatorname{Im}(\tilde{\mathbf{K}}^{-1}) \mathbf{q}_0 \cos(\omega t) \right\}. \end{aligned}$$

It can be checked, that the real part of the above expression is the same as (4.9), i.e. the steady-state vibration due to a cosinusoidal excitation with frequency  $\omega$  and amplitudes  $\mathbf{q}_0$ . Besides, the imaginary part of the above expression is identical to (4.5), which is the steady-state vibration of the model subjected to a sinusoidal forcing.